REPORT

Contract Number NAS 9-4174

30 June 1966

for

National Aeronautics and Space Agency

Manned Spacecraft Center

Prepared by R. S. Brazil
R. S. Brazil, Project Leader

Approved by C. R. Bitter
C. R. Bitter, Section Head
Antenna Section

C. R. Bitter for
T. E. Tice, Chief Engineer
Antenna and Microwave Group

[redacted]

FINAL REPORT

ON

[redacted]E SUIT COMMUNICATION

ANTENNA SYSTEM

MOTOROLA INC.
Military Electronics Division
WESTERN CENTER
8201 EAST McDOWELL ROAD, SCOTTSDALE, ARIZONA


SSC Antenna

ABSTRACT

This report documents and summarizes the results of the work performed under NASA Contract Number NAS 9-4174, Apollo Space Suit Communication Antenna System. The contract objective was to develop an antenna system for use with the Apollo astronaut communication and telemetry system that would satisfy the electrical performance requirements, be compatible with the mechanical interface requirements, and be able to withstand the lunar environment. Descriptions of several antenna configurations are given together with performance data for various antenna mounting schemes. Conclusions and recommendations based on the results obtained are given.

The report serves as the program final report and as the materials report. Conclusions and recommendations are given for the direction of any further work in this area based upon the information obtained during this investigation.

TABLE OF CONTENTS

LIST OF ILLUSTRATIONS

LIST OF ILLUSTRATIONS (cont)

LIST OF ILLUSTRATIONS (cont)

1. INTRODUCTION

This report describes a program whose objective was to develop an optimum antenna configuration for the Space Suit Communications (SSC) Antenna System for NASA-MSC under Contract NAS 9-4174. The antenna electrical performance requirements and mechanical interface requirements are reviewed. An analysis of the astronaut - LEM communication link used as a guide in determining the antenna parameters is given in Appendix A. Several antenna types were studied and evaluated for this application and the results are discussed. Some of the larger antenna structures considered require a stowage-well in the Portable Life Support System (backpack) or helmet to enable the antenna to be retracted when not in use. This requires an erection-retraction mechanism and several of these devices are discussed. As a result of the study and evaluation, the low profile dual frequency transmission line antenna best satisfies the requirements of the antenna system and a further, more detailed evaluation of this antenna was made and the results are presented in Section 3.6, Detailed Evaluation of the Transmission Line Antenna. Three flight-qualifiable antennas of the final design were fabricated and the results of the evaluation of their performance are presented.

2. PROGRAM DEFINITION

The purpose for this program was to develop an optimum antenna configuration for the Space Suit Communication (SSC) Antenna System. The SSC will provide communications between an astronaut and a spacecraft or between two astronauts. The activity includes both a study and fabrication effort. The study consists of a comprehensive investigation of antenna types which may find application, an analysis of erection/retraction techniques when applicable, and an evaluation of the relative merits of each type with respect to this program. As a result of the study, fixed and erectable/retractable types of antennas that best satisfy the antenna system requirements when located on both the Portable Life Support System (PLSS) and the helmet are selected for design and fabrication and their performance evaluated. A single antenna design representing the best of the designs considered will then be selected for detailed evaluation. Finally, three flight-qualifiable models of this design will be fabricated and tested.

3. TECHNICAL DISCUSSION

3.1 ANTENNA PERFORMANCE REQUIREMENTS

The performance requirements are based in part upon the results of an analysis of the astronaut - LEM communication link performed by Motorola. This analysis is attached as Appendix A to this report. The more important performance requirements are given below.

Radiation from the antenna must not be more than 3 dB below the level of a perfect isotropic radiator for at least 90 percent of the coverage defined by elevation angles between -20° and +20° with respect to the antenna horizon and all azimuth angles at a frequency of 259.7 Mc and not more than 5 dB below an isotropic at a frequency of 296.8 Mc. The nulls in the azimuth plane must not be more than 6 dB below the level of an isotropic radiator at each of the above frequencies.

Design goals for the antenna include pattern nulls in the azimuth plane no lower than 3 dB below the level of an isotropic radiator. The VSWR should not exceed 1.2 at 259.7 Mc and 2.0 at 296.8 Mc. Radiation of the antenna must have predominant vertical polarization. The antenna system must be capable of transmitting at least 75 millivolts average RF power.

Antenna types to be considered include both fixed and erectable-retractable types. Antenna locations include both the upper surface of the PLSS and the helmet. Electrical tests are to be performed on an appropriate mockup of the space suit and/or helmet. This mockup is an approximate electrical equivalent of the actual SSC space suit. The nominal impedance of the telemetry communications system is 50 ohms. Visors located on the helmet assembly are assumed to be electrically (RF) bonded and of electrically conductive material.

3.2 INTERFACE PARAMETERS

An electrical/mechanical interface exists between the antenna and the EMU thermal garmet. These are as follows: The PLSS is a parallelepiped 15 inches wide by 8 inches deep by 25 inches high. The top of the PLSS is 2 to 3 inches above the shoulder in the operational configuration. The top, rear, and

sides of the PLSS are covered with a removable fiberglass shell. A small tubular configuration can be retracted directly into the PLSS envelope. No alteration of the PLSS envelope is allowed for an erectable/retractable system. In any case, alteration of this envelope must be minimized. In no case are protrusions allowed near the rear corners.

The thermal garmet is a loose fitting coverall tailored to enclose the PLSS, helmet, and space suit. It is composed of multiple layers of aluminized mylar. It is assumed there is good RF bonding between separate thermal garmets (less than 0. 1 ohm) and between the SSC and PLSS cover. The helmet surface is of a plastic material.

The antenna is to be with the helmet and the PLSS both of which are covered by a thermal garmet. The antenna design must avoid the possibility of puncture to the thermal garmet or space suit. The erection/retraction mechanism must be positive and lock in either position. The opening in the thermal garment, when applicable, must be minimuzed. The erection/retraction mechanism must be operated from the front of the astronaut and require no assistance to him. Erection and retraction must be effected by the performance of a single motion, cranking, pulling, twisting, etc., and without visual inspection of the effecting device. The system must be capable of complete retraction after sustaining slight damage. The weight of the antenna should not exceed 10 ounces including an erection/retraction mechanism. The thermal input to the spacesuit as a result of the addition of the antenna system is not to exceed 4 watts.

3.3 INVESTIGATION OF ANTENNA TYPES

The following sections describe several antenna types that were considered for the Apollo astronaut communication antenna system. Relative mechanical and electrical characteristics and their trade-offs are discussed.

3.3.1 Transmission Line Antenna

One structure offering the best performance with the least height is a form of a transmission line antenna. [1*] The basic design has been modified

*See Bibliography, Section 10.

and improved by Motorola and is directly applicable to the NASA program. Multiple frequency or multi-resonant structures of low profile and minimum volume have been devised.

The basic concept of the transmission-line antenna is that of a small monopole (much less than a quarter-wavelength high) made self-resonant by transmission-line top-loading. In order for a small monopole to radiate, large currents must flow up and down the post, so that a place must be provided on top of the post for charge to accumulate. A large disc might be used to resonate the antenna except that the disc diameter becomes excessively large for small antennas. Reducing the disc to a more desirable size requires that lumped inductance must then be used to tune the antenna, resulting in loss of efficiency due to energy dissipation in the inductance. A much more efficient method of top-loading may be achieved by attaching a quarter-wavelength of transmission line to the top of the vertical post, with an open circuit at the opposite end; this provides a low impedance path to ground for displacement currents, thus enabling large conduction currents to flow on the post. The resulting vertical current element and its image in the ground plane produce radiated fields. The currents in the horizontal transmission line are opposed by those in its image in the ground plane; the fields resulting from these two currents are effectively cancelled in the far field. As defined in the conventional sense, radiation resistance of this antenna is low and is proportional to the square of the post height; but with the proper design and care in fabrication, this antenna can be made nearly as efficient as a quarter-wavelength monopole. The impedance from the antenna to ground at any point on the post or line is real and rises rapidly from the grounded end of the post. Shunt feeding thus allows any real input impedance to be selected simply by adjusting the feed point on the antenna.

Dual frequency operation can be obtained by attaching two spiraled transmission lines to the same post. Each transmission line accepts large currents only at its resonant frequency. Thus, efficient radiation occurs at two frequencies, determined by the lengths of the two transmission lines.

For this study the dual frequency structure was selected to provide the proper performance at both 259.7 Mc and 296.8 Mc. The configuration was selected to provide a good balance between efficiency and antenna volume. This structure was designed, fabricated, and tested on a ground plane to evaluate its performance. This antenna is shown in Figure 1. The fiberglass protective cover and the polyurethane foam potting material have been partly removed to show the antenna structure. The electrical performance of the antenna of Figure 1 with both polyurethane foam and fiberglass cover complete and in place and located on a circular ground plane approximately 3/4-wavelength in diameter is given below:

Pattern:	approximately equivalent to a small dipole
Polarization:	linear vertical
Gain:	255 Mc, 0.4 dB 295 Mc, 1.4 dB
VSWR:	255 Mc, less than 1.24 295 Mc, less than 1.24

The above and all following gain figures in this report are referenced to isotropic gain and are measured by the substitution method. It should be noticed that the measurement frequencies differ slightly from the desired frequencies of operation set forth in the NASA Work Statement. This is the result of optimizing the efficiency of the study; that is, the data are sufficient and accurate and represent essentially the data for the same antenna at 259.7 Mc and 296.8 Mc, the design frequencies, without consuming time to adjust the test antenna exactly to the design frequency. The final form of this antenna will incorporate a small adjusting screw to trim the resonant frequency. This adjustment need only be made once at the time of manufacture, and the screw position can be locked in place. This technique has been tried with great success on an engineering model of a spiral transmission line antenna.

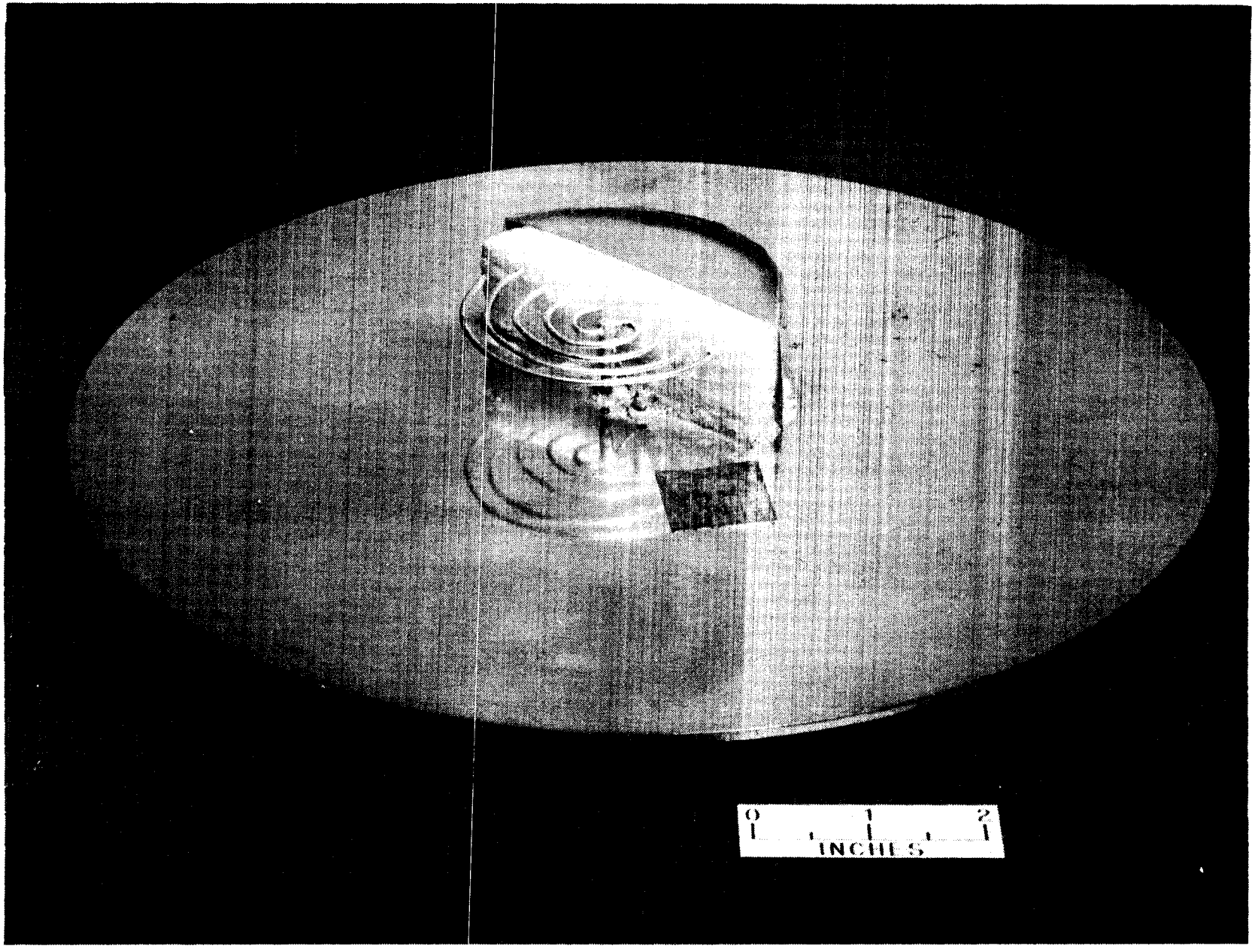

FIGURE 1

DUAL FREQUENCY SPIRAL ANTENNA
WITH COVER AND FOAM CUT BACK

It was determined experimentally that potting this antenna, as described, results in approximately 1.5 dB loss in gain.

An alternate approach to the dual frequency transmission line antenna is to use a pair of single frequency antennas. To determine the feasibility of this approach, two modified quarter-wavelength spiral antennas were mounted on a single ground plane; and the results of measurements on this antenna system are given below:

Configuration:	Spirals wound with opposite sense; 1 1/4" diameter spaced 1/2" between spiral edges; wire diameter 3/32"; height, 3/4 inch; antennas not foamed.
Coupling:	255 Mc, 6.5 dB 295 Mc, 10 dB
VSWR:	255 Mc, less than 1.24 295 Mc, less than 1.24
Gain:	255 Mc, 0 dB 295 Mc, 1.3 dB

The isolation from antenna terminal to antenna terminal can be greatly improved from the above figures by increasing the separation between the antennas; and it is felt, as a result of a study of current flow directions and mutual coupling effects, the isolation can also be increased by a change in the individual antenna configuration. Because of the increased antenna size the dual frequency antenna is more desirable and consequently initial effort was expended in that area.

Measurements were made on a mockup of the space suit to gain information on the relative merits of the PLSS location and the helmet location. The results of these initial measurements are presented below.

3.3.1.1 Transmission Line Antenna on PLSS

This is a fixed antenna mounted on the Portable Life Support System (PLSS). The antenna described in Section 3.3.1 is reduced in overall size by spiraling the transmission lines compactly around the vertical radiating element. An improved version of this antenna includes larger elements for the vertical

and horizontal members. This reduces the conductor losses and thus raises the overall efficiency and therefore the gain. A further improvement separates the resonant transmission line members vertically by one-half inch. By providing the elements with the vertical separation, a half-wavelength mode is avoided at the higher frequency. This half-wavelength mode exists when currents are not restricted to the proper quarter-wavelength arm, but also flow through the entire antenna structure. Energy converted to this mode is dissipated as heat, thus reducing the overall efficiency and hence gain of the antenna. When the half-wavelength mode is suppressed, the gain is raised to a level commensurate with the low frequency gain.

This antenna is made of 3/32-inch diameter brass rod formed to the spiraled antenna configuration. The antenna is placed on a small four-inch square ground plane 1/16-inch thick. Exact frequency tuning is achieved by the movement of a threaded extension on the end of each spiraled element. The entire assembly is silver flashed as a means of increasing the antenna's efficiency. Figure 2 shows the antenna without the tuning elements and protective cover.

Protection is provided by encapsulating the spiraled elements in a polyurethane foam material. The entire assembly is then covered with 1/16-inch thick epoxy fiberglass formed into a dome configuration. This covering is made to completely conceal the frequency tuning control screws at the end of each spiral element. The entire assembly measures approximately 3" diameter by 1 1/2 inches high.

Preliminary measurements revealed three possible antenna locations on the PLSS. Figure 3 identifies each of these positions.

Position 1 -- on the top-rear-center of the backpack.

Position 2 -- four inches to the left (or right of Position 1. These are located on the top of the PLSS in accordance with the conditions specified in the Third Supplemental Agreement to the contract.

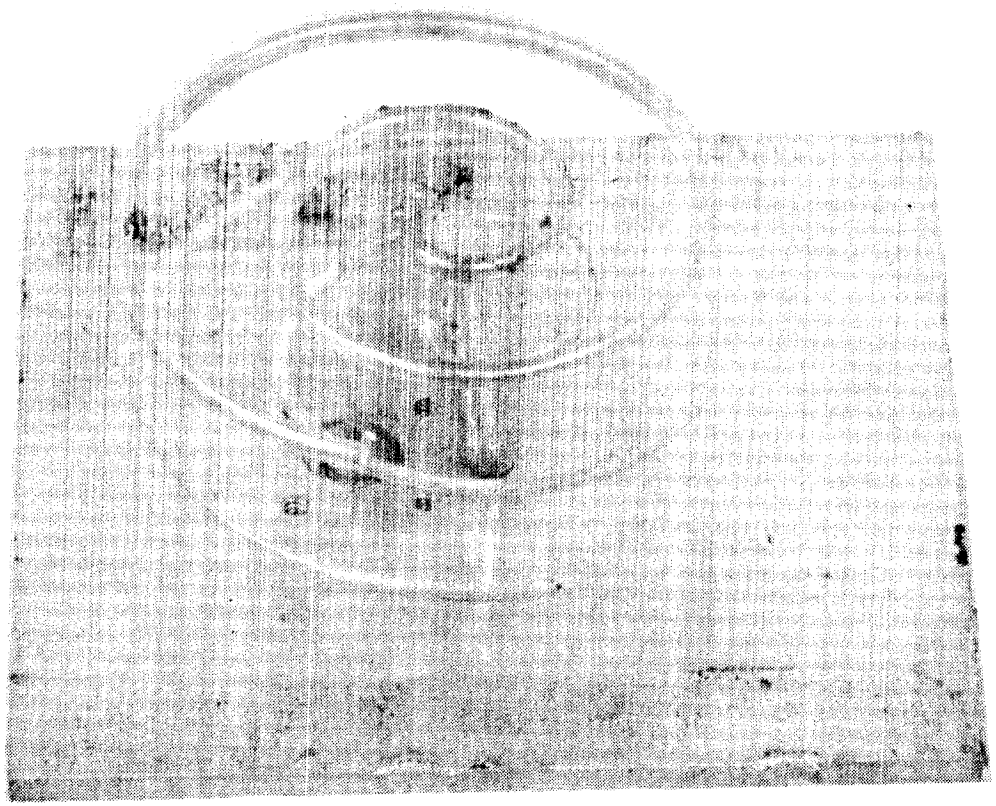

Dual Frequency Transmission Line Antenna
Showing Vertically Stacked Resonant Members

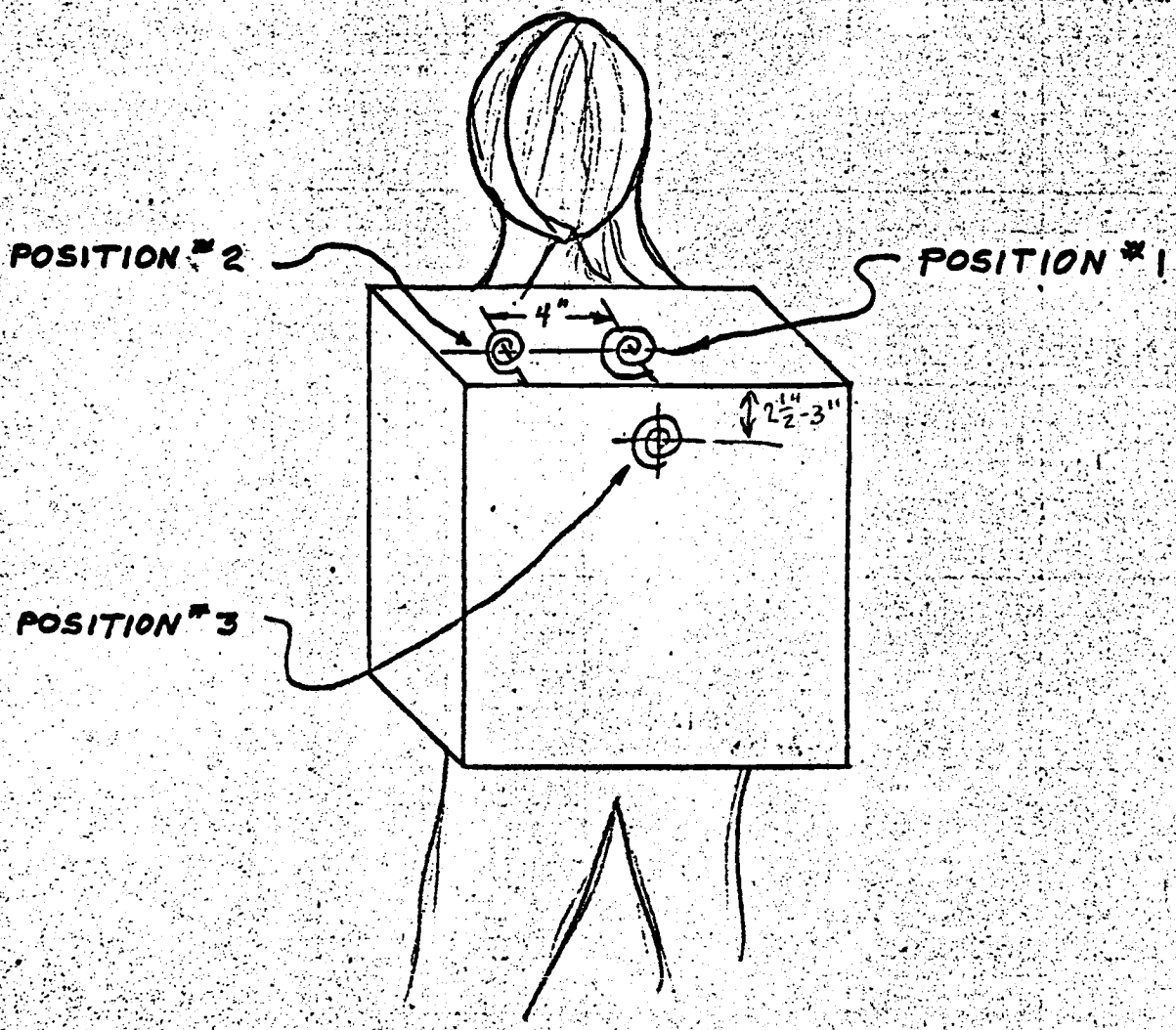

Figure 3

Dual Frequency Transmission Line Antenna

Mounting Locations on the PLSS

Position 3 -- the back surface of the PLSS at the top center. This position demonstrates somewhat more satisfactory results than those obtained at either Position 1 or 2.

The antenna complete with polyurethane foam-in-place material and fiberglass radome cover is placed on a four-inch square ground plane. Connection to the transmission line is through a coaxial connector on the ground plane. The assembly is placed on the thermal garmet at the various PLSS locations.

Performance of the antenna is shown for each of the PLSS locations in the radiation patterns of Figures 4 through 9. These conical "azimuth" patterns show the radiation level meeting the minimum requirements of -3 dB and -5 dB only when viewed from behind the space suit mockup. Radiation levels off the forward sector (face) drop to about -15 dB at the minima. This is caused by the blocking effects of the helmet.

The measured VSWR for this antenna is 1.1 and 1.3 at 259.7 Mc and 296.8 Mc respectively.

3.3.1.2 Transmission Line Antenna on the Helmet

Electrically, this location shown in Figure 10b is best for a low profile antenna. The disadvantages of this location are the increase in height of the helmet/visor protector assembly (less than 2 inches), the length of cable required to connect it to the PLSS which contains the communications package, and the necessity to complete the antenna connection when the antenna and visor protector are donned. The diameter of the antenna is within that which can be mounted to the visor protector. The thermal loading on the space suit air conditioning unit will be within the acceptable maximum (4 watts). This may be controlled by applying a proper surface coating to the exposed area of the radome (such as a white epoxy coating with a high gloss and by mounting the antenna on standoffs on the visor protector to avoid compressing the thermal suit. Meeting this requirement should not be difficult because of the

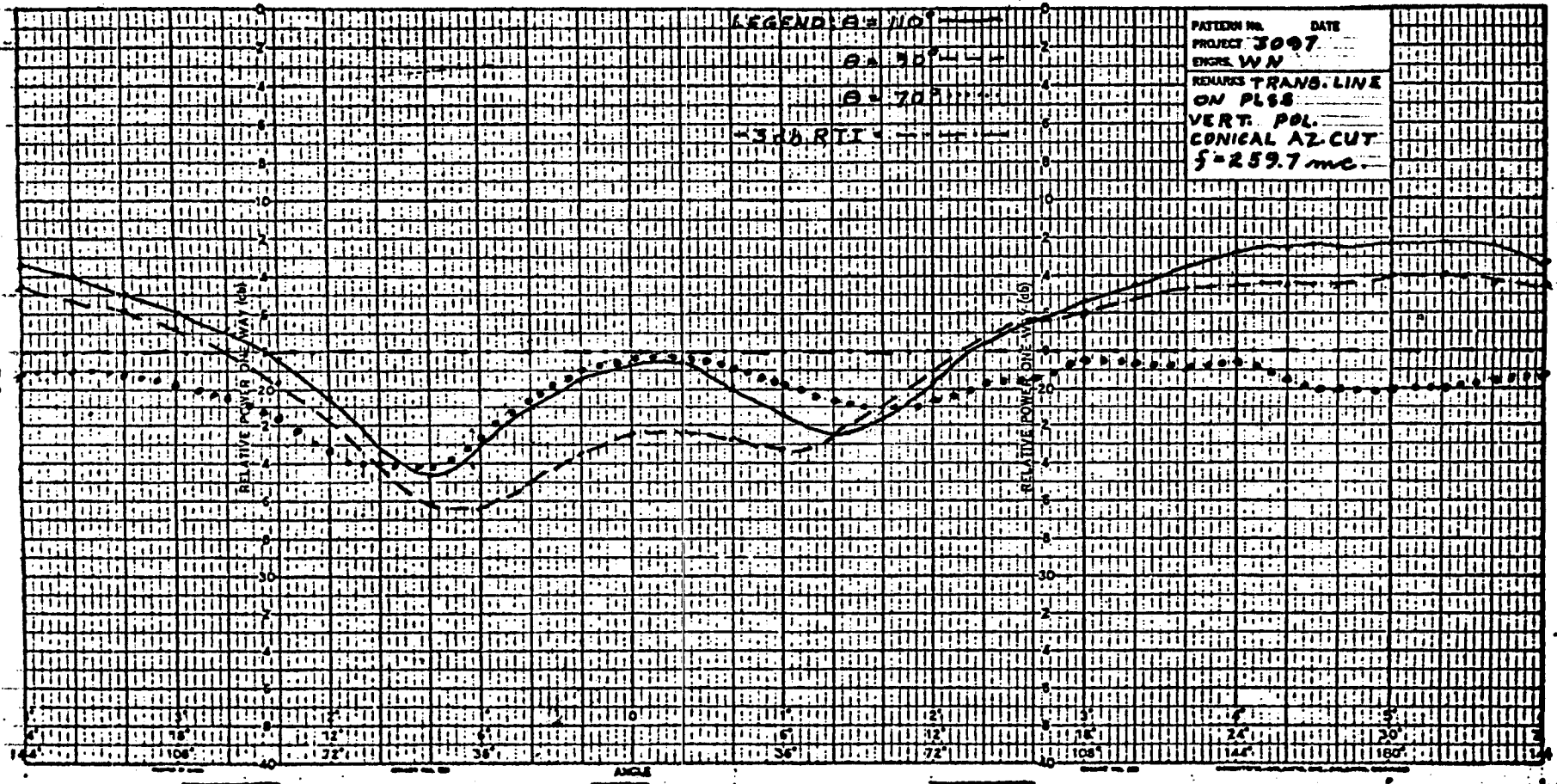

Figure 4 Radiation Pattern of Transmission Line Antenna Mounted at Position # 1 of PLSS; Frequency = 259.7 mc

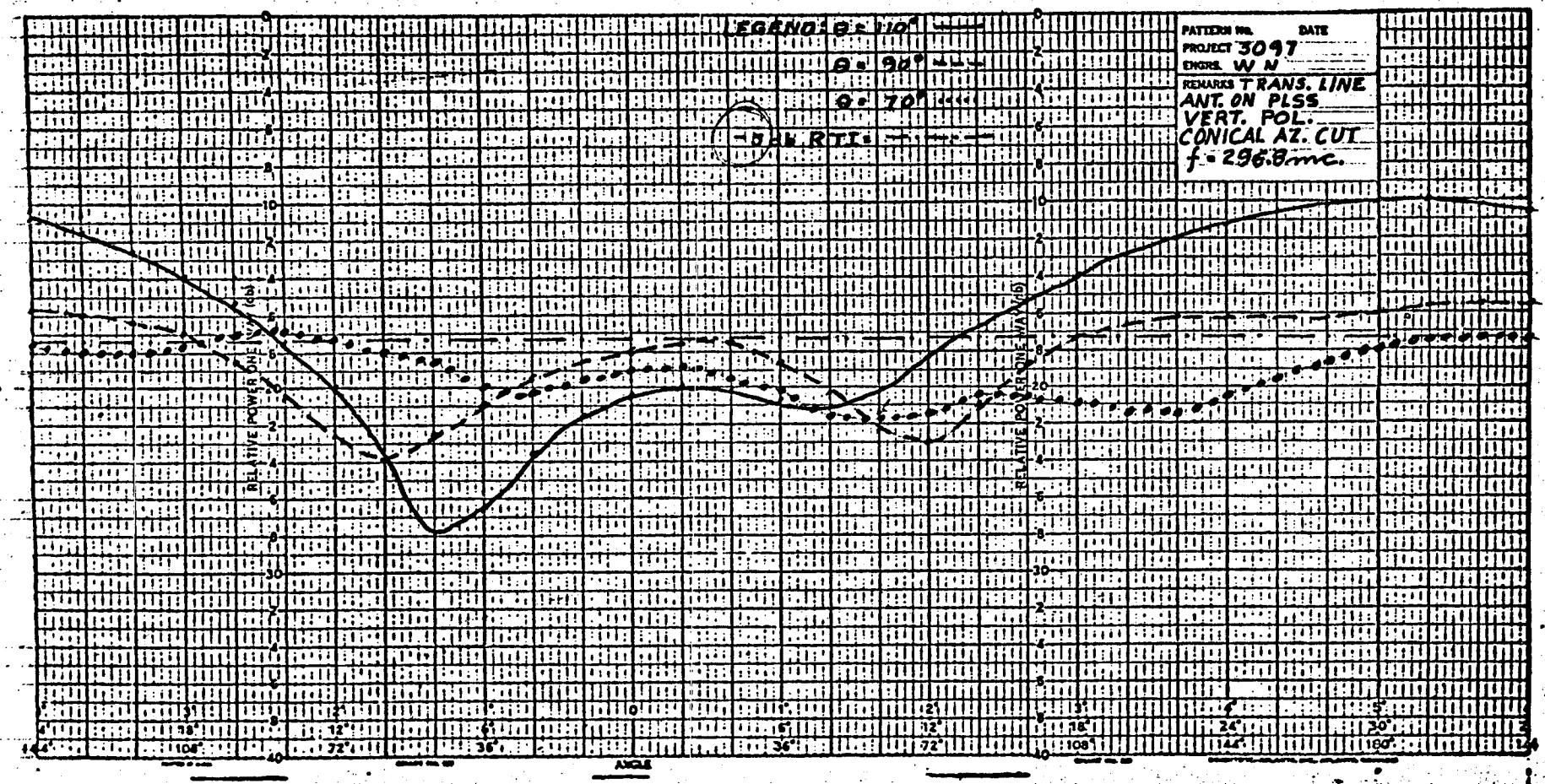

Figure 5. Radiation Pattern of Transmission Line Antenna Mounted at Position # 1 of PLSS; Frequency = 296.8 mc

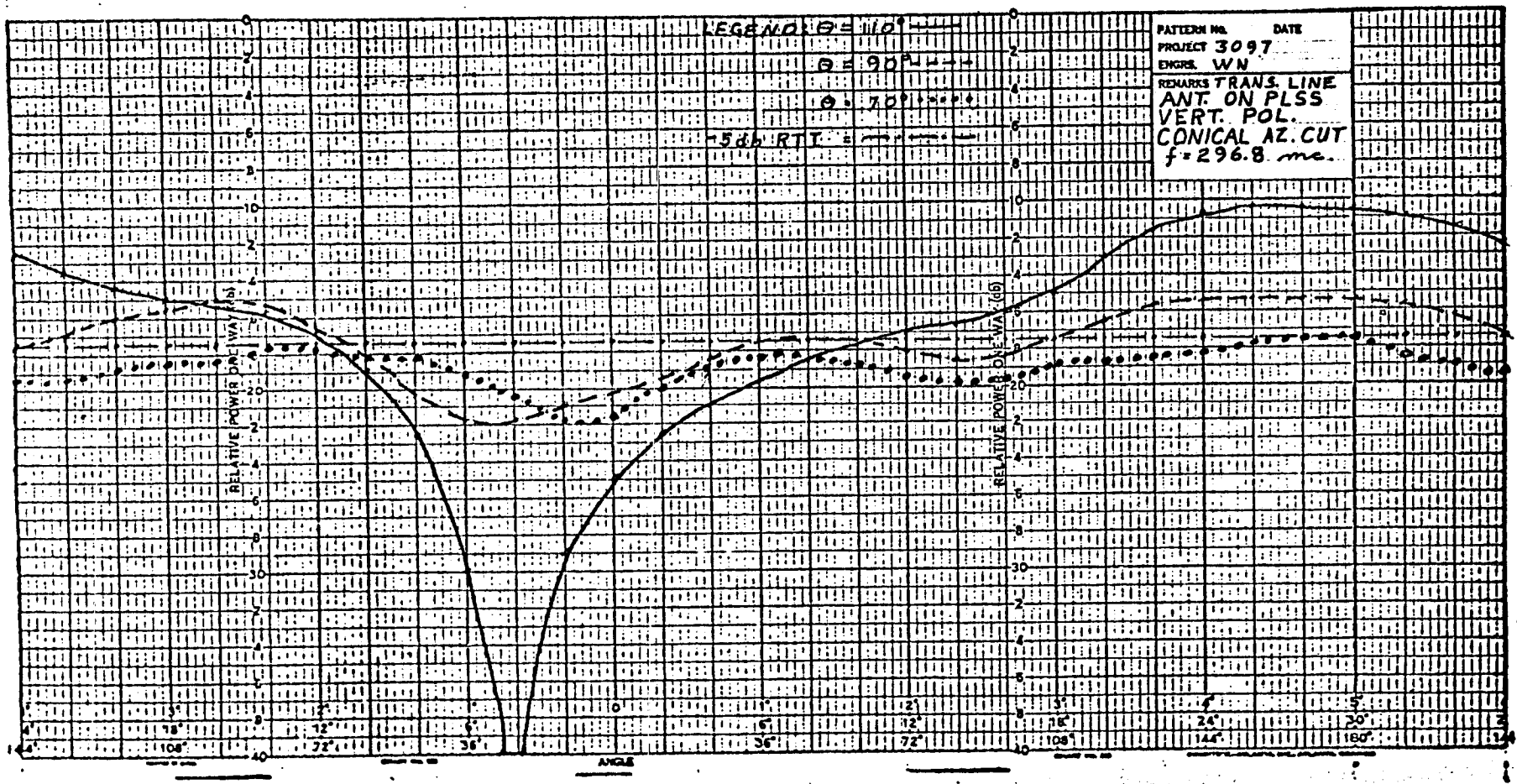

Figure 6. Radiation Pattern of Transmission Line Antenna Mounted at Position # 2 of PLSS; Frequency = 296.8 mc

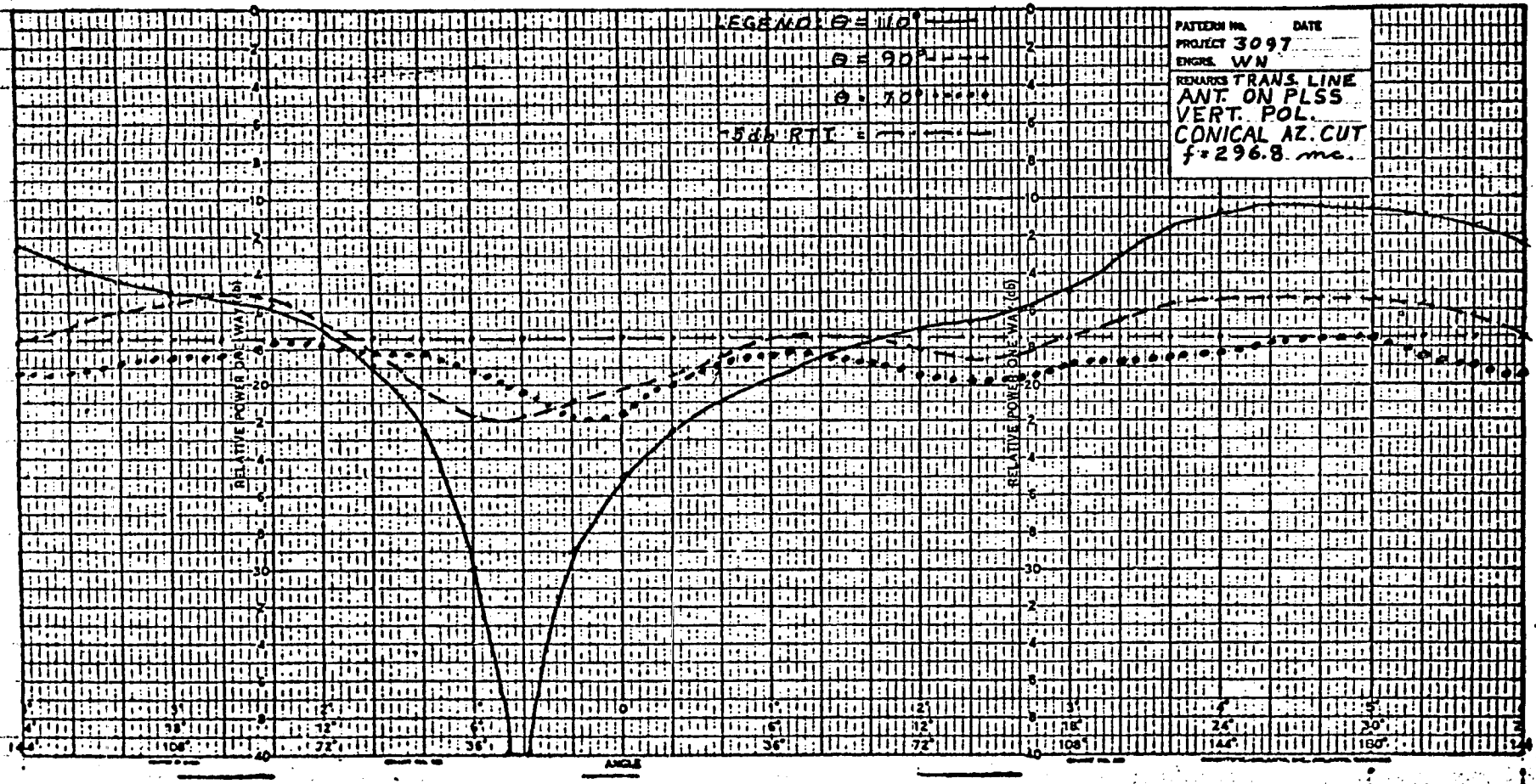

Figure 7. Radiation Pattern of Transmission Line Antenna Mounted at Position # 2 of PLSS; Frequency = 296.8 mc

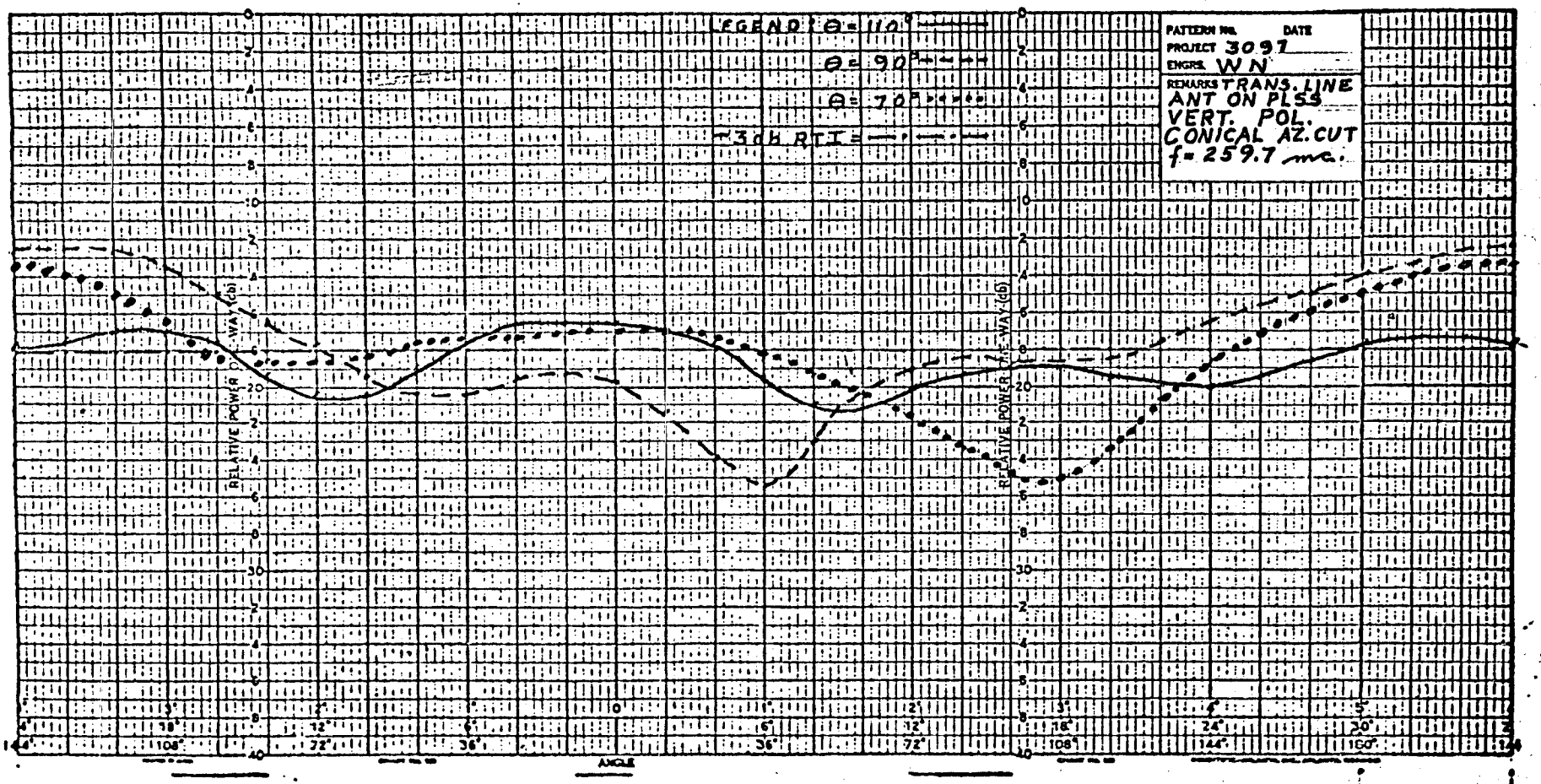

Figure 8. Radiation Pattern of Transmission Line Antenna Mounted at Position # 3 of PLSS; Frequency = 259.7 mc

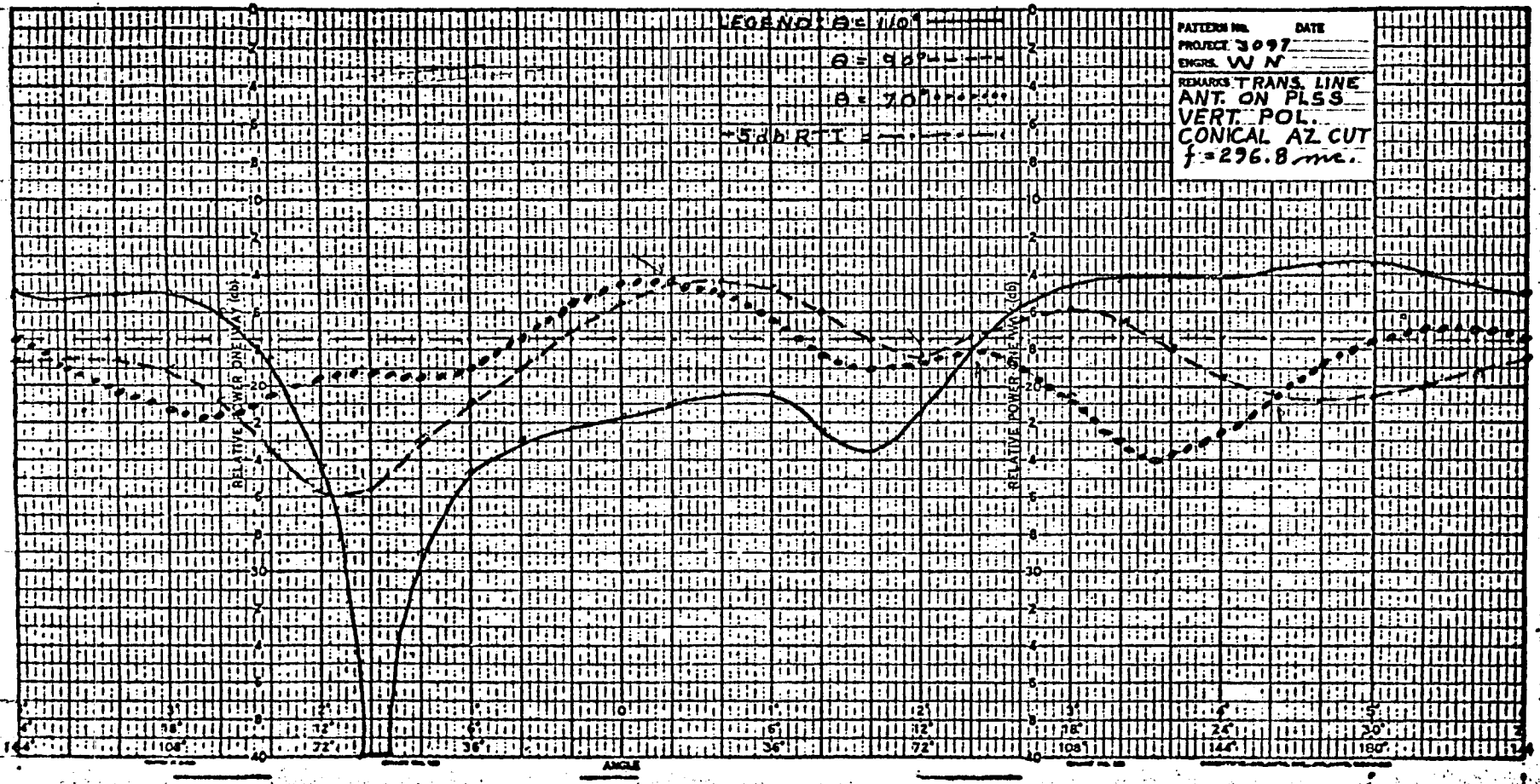

Figure 9. Radiation Pattern of Transmission Line Antenna Mounted at Position # 3 of PLSS; Frequency = 296.8 mc

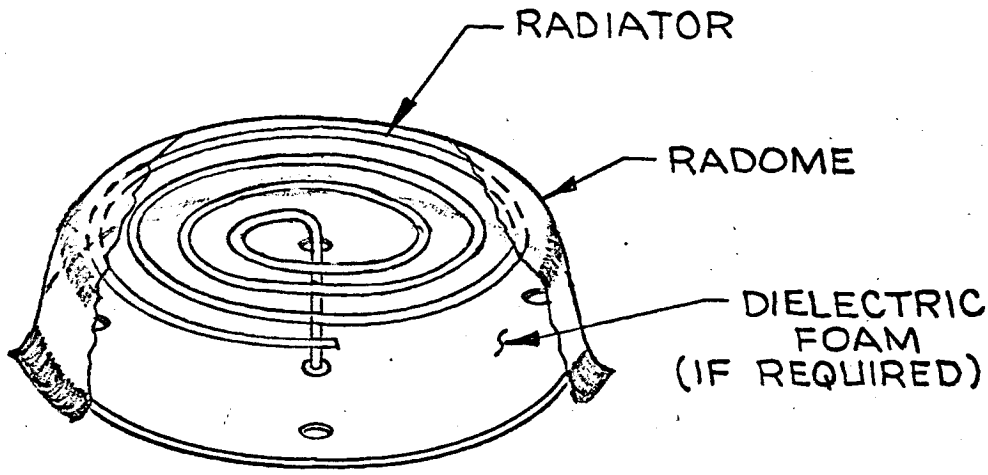

a- ANTENNA

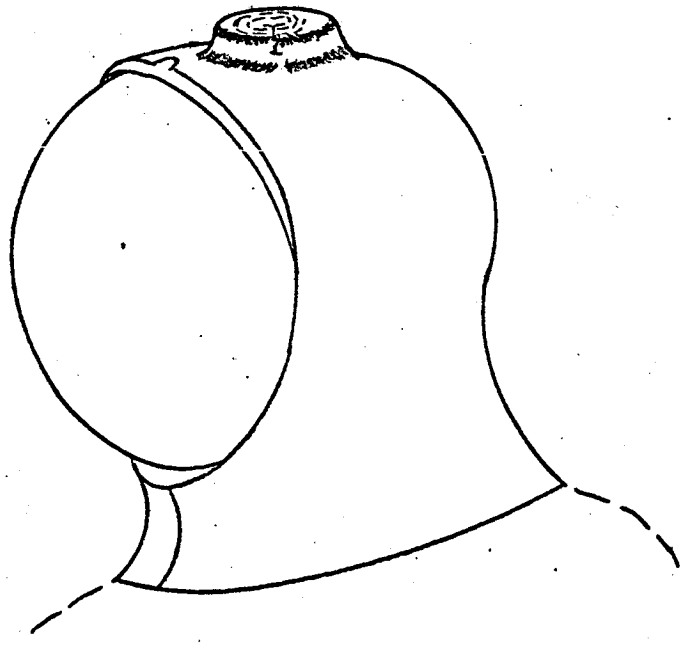

b- HELMET MOUNTING

FIGURE 10
LOW PROFILE TRANSMISSION LINE ANTENNA

long and devious thermal route of the antenna into the space suit. The length of the cable run is not so long as to give excessive loss between the antenna and the communication package.

Patterns obtained from the low profile transmission line antenna mounted on the top of the helmet gave much superior patterns than those obtained for an antenna on the PLSS. The maximum excursions of the gain in the azimuth plane were typically ± 3.5 dB. This variation in gain is attributed to the asymmetries of the space suit; the dielectric face plate and the PLSS are among the most obvious. It is thus felt that much superior antenna performance can be obtained from the helmet location.

It is felt that the pattern asymmetries that do exist can be minimized by the addition of a choke section on the antenna ground plane. This choke could take the form of a partial hood consisting of three layers of aluminized mylar that would drape over the sides and rear of the helmet in a fashion similar to the present thermal garment. This extension need only be approximately 6 to 8 inches larger than the antenna ground plane.

A change in the space suit concept resulted in the conductive thermal garment being removed from the helmet. Consequently effort was dropped on the helmet location and was devoted toward improving the transmission line antenna in the PLSS location.

The results of the above preliminary measurements encouraged further evaluation of the transmission line antenna on the PLSS. This is described in detail in Section 3.5, Detailed Evaluation of the Transmission Line Antenna.

3.3.2 Quarter wavelength whip

One of the most basic structures is the quarter wavelength monopole, or whip.

This monopole, or whip, consists of a vertical radiating element standing above a horizontal conducting ground plane. It may be driven by an unbalanced line, such as coaxial cable, with the outer conductor connected to the ground plane, and the inner conductor connected to the base of the radiating element. A simple monopole is shown in Figure 11.

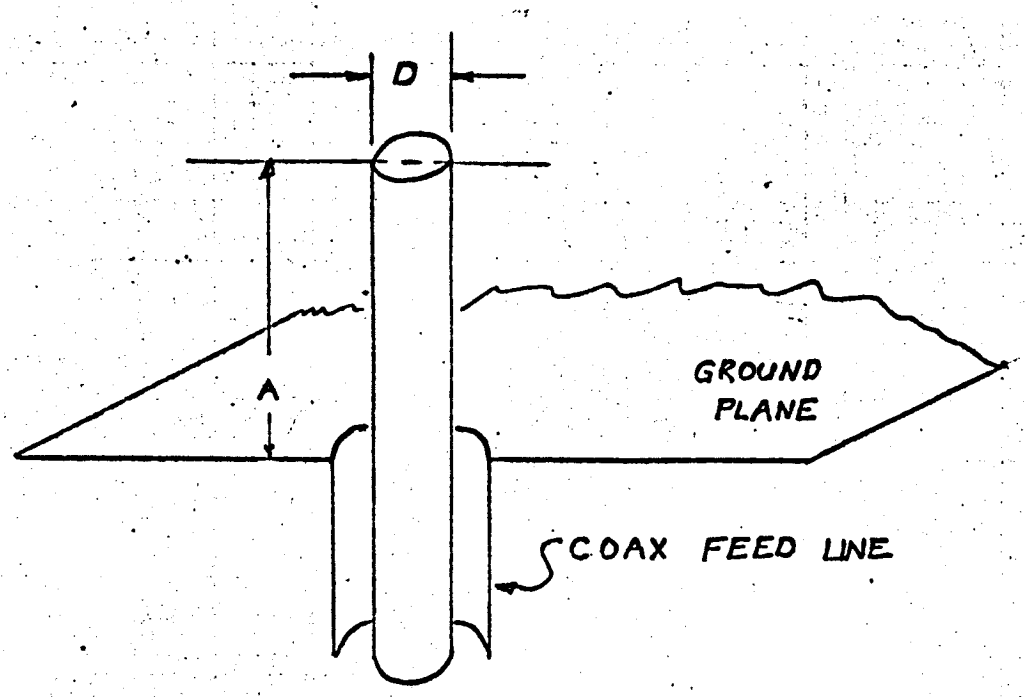

BASIC MONOPOLE, AS DESCRIBED BY BROWN AND WOODWARD

(a)

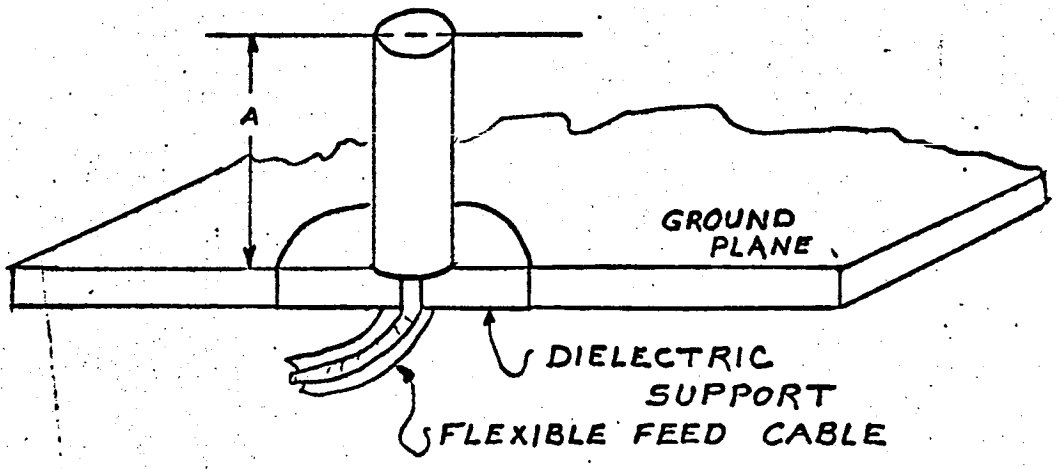

TYPICAL MONOPOLE DESIGN (b)

FIGURE 11

QUARTER WAVELENGTH MONOPOLES

Extensive analysis of monopoles have been done only for the case of radiating elements with circular cross section. However, the electrical characteristics are not very shape dependent, and an "effective" diameter, somewhat smaller than the maximum cross-sectional dimension, can be used for elements with non-circular cross sections.

The impedance presented to the coaxial line by a monopole is frequency dependent. Generally, the first resonance occurs when the height of the radiating element is about 0.22 wavelengths, and a second resonance is obtained for a somewhat larger height. The antenna resistance at the first resonance is 35 to 40 ohms, depending on the height-to-diameter ratio (L/D). The bandwidth increases with a decreasing L/D.

In order to design a monopole for a particular frequency band, one must use graphs of the impedance vs. height of the antenna for various L/D ratios. Such curves have been calculated theoretically, but the most satisfactory are the experimental curves of Brown and Woodward.[3] The impedance and reactance curves corresponding to the configurations of Figure 11 are reproduced in Figures 12 and 13.

To design an antenna to match a 50-ohm line, one must find a value of L/D for which the resistance is near 50 ohms, and simultaneously, limit the reactance to about ± 25 ohms to maintain a good match. If a large bandwidth is desired, these conditions must be met for a range of values of antenna length, since the antenna length in electrical degrees is directly proportional to frequency.

Most monopoles do not conform to the simple configuration of Figure 11(a), but have some more complicated feed point condition, such as shown in Figure 11(b). The additional feed point capacitance of this configuration changes the impedance characteristics. To account for this, the larger base capacitance can be added to the impedance in the diagram, and a new impedance plot can be constructed; or one can simply choose a promising antenna from the curves, and then measure the effect of the chosen feed point characteristics when added to the antenna impedance.

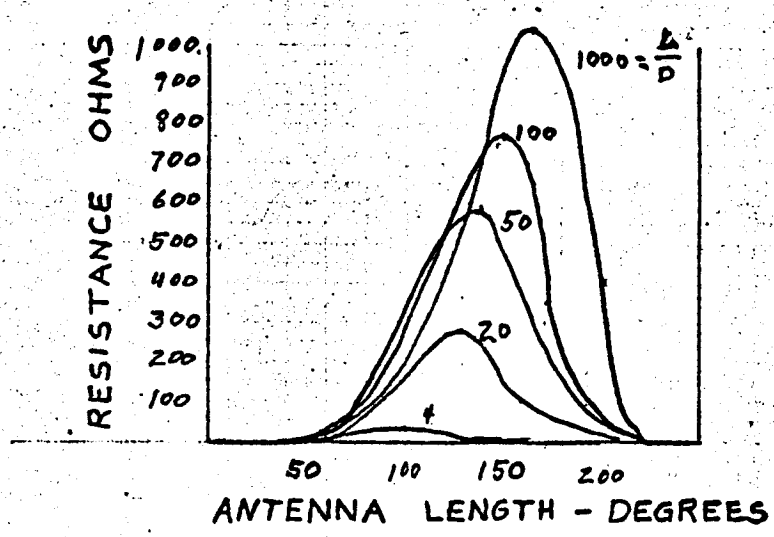

FIGURE 12 ANTENNA RESISTANCE VS ANTENNA LENGTH "L" $\frac{L}{D}$ IS A PARAMETER, "D" IS THE DIAMETER

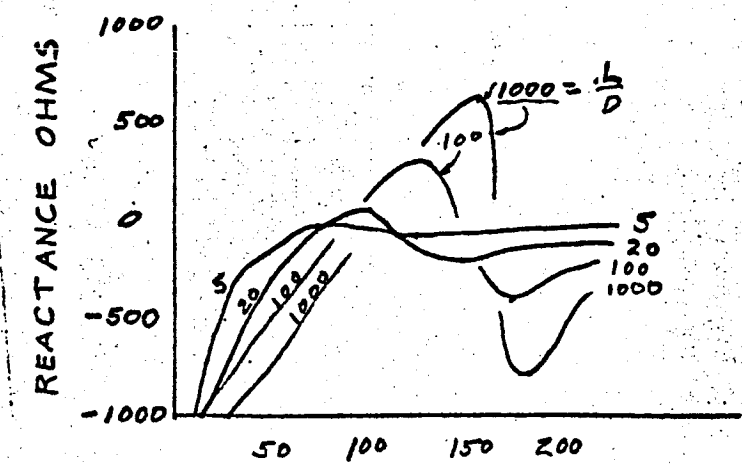

REACTANCE CURVES CORRESPONDING TO RESISTANCE CURVES ABOVE

FIGURE 13 FEED POINT RESISTANCE AND REACTANCE FOR VARIABLE L/D (DIAMETER OF OUTER CONDUCTOR OF THE FEED LINE = 2.8D)

The advantages of the quarter-wavelength monopole or whip are, that it offers good patterns and efficiency with a simple structure. Its main disadvantages are its length (approximately 10 inches at 300 Mc) and, for this application, its narrow band of operation. For very thin whips, such as would be made from spring steel wire, the input VSWR's of the antenna at 260 Mc and 300 Mc would range theoretically from approximately 2.6 to over 5.0. This antenna can be made more broadband by increasing the diameter of the whip. The input VSWR can be reduced to approximately 2.0 at both 260 Mc and 300 Mc for a whip diameter of 1/3 to 1/2 inch. To reduce the VSWR much below this value required a correspondingly much larger whip diameter.

3.3.2.1 Quarter-Wavelength Whip Antenna on Helmet

This is an erectable/retractable antenna which is placed on the top of the space suit helmet. The radiating element consists of a 0.35-inch wide strip of thin beryllium copper shaped into the arc of a circle and then heat treated to hold its shape. The resulting tape is then perforated along its center for operation in the erect/retract mechanism. The element is base-fed from a coaxial line. The antenna and its erect/retract mechanism are placed over a spherical cap ground plane which is placed on the thermal garmet over the space suit helmet.

Tests show that optimum performance is obtained when the antenna is located approximately 5 inches behind the leading edge of the thermal garment. Radiation patterns showing conical "azimuth" cuts at various elevation angles are given in Figures 14 and 15 for 259.7 Mc and 296.8 Mc respectively. These patterns shown the antenna gain to be greater than the specified minima of -3 dB and -5 dB.

The VSWR of this antenna measures 2.0 and 1.4 at 259.7 Mc and 296.8 Mc, respectively.

3.3.2.2 Quarter-Wavelength Whip Antenna on PLSS

This antenna consisted of a 0.032-inch diameter brass rod attached to an RF connector mounted on a 4 inch diameter ground plane. Radiation patterns

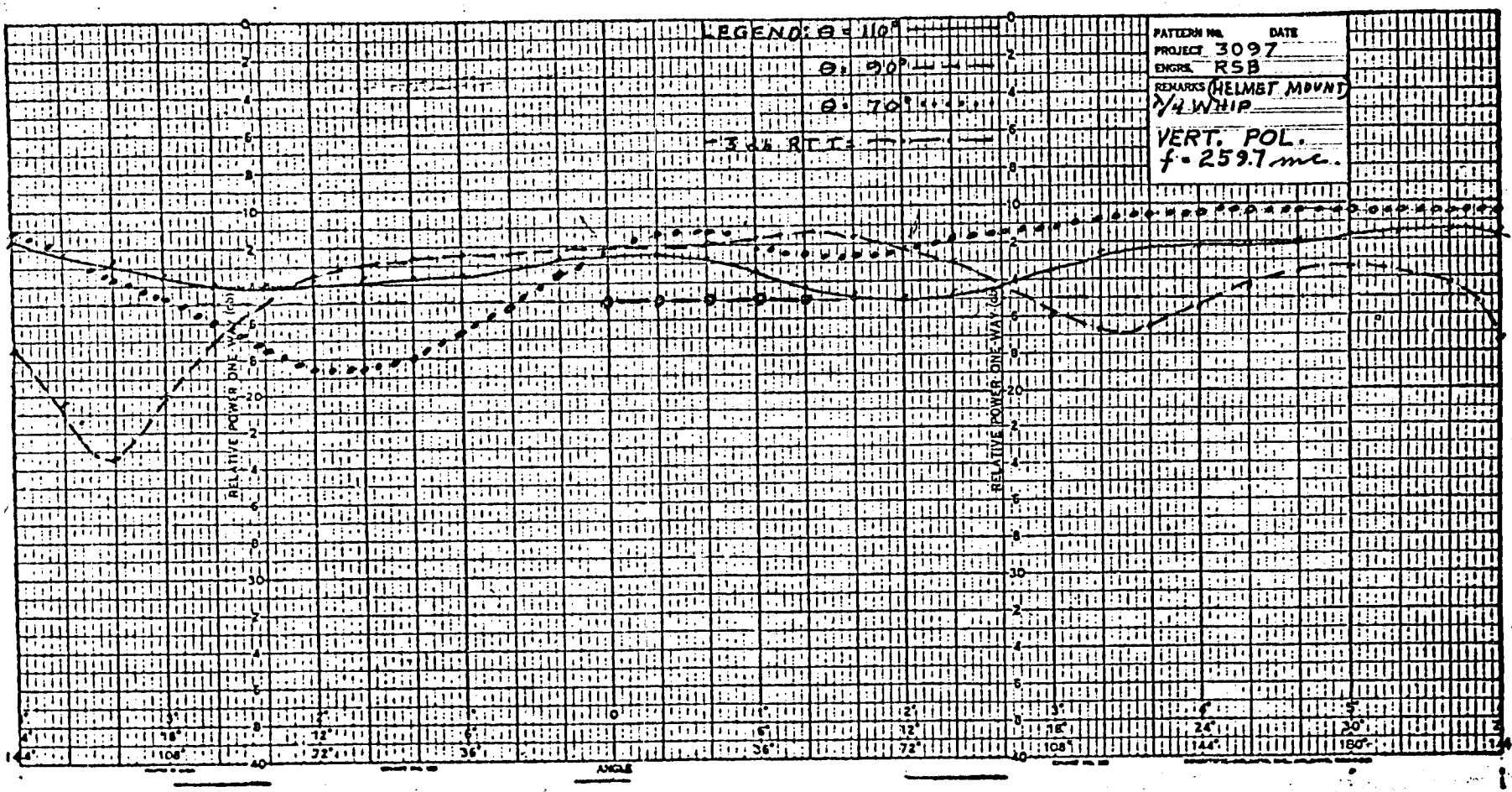

Figure 14. Radiation Patterns of Quarter-Wavelength Whip Antenna Mounted on Helmet; Frequency = 259.7 mc

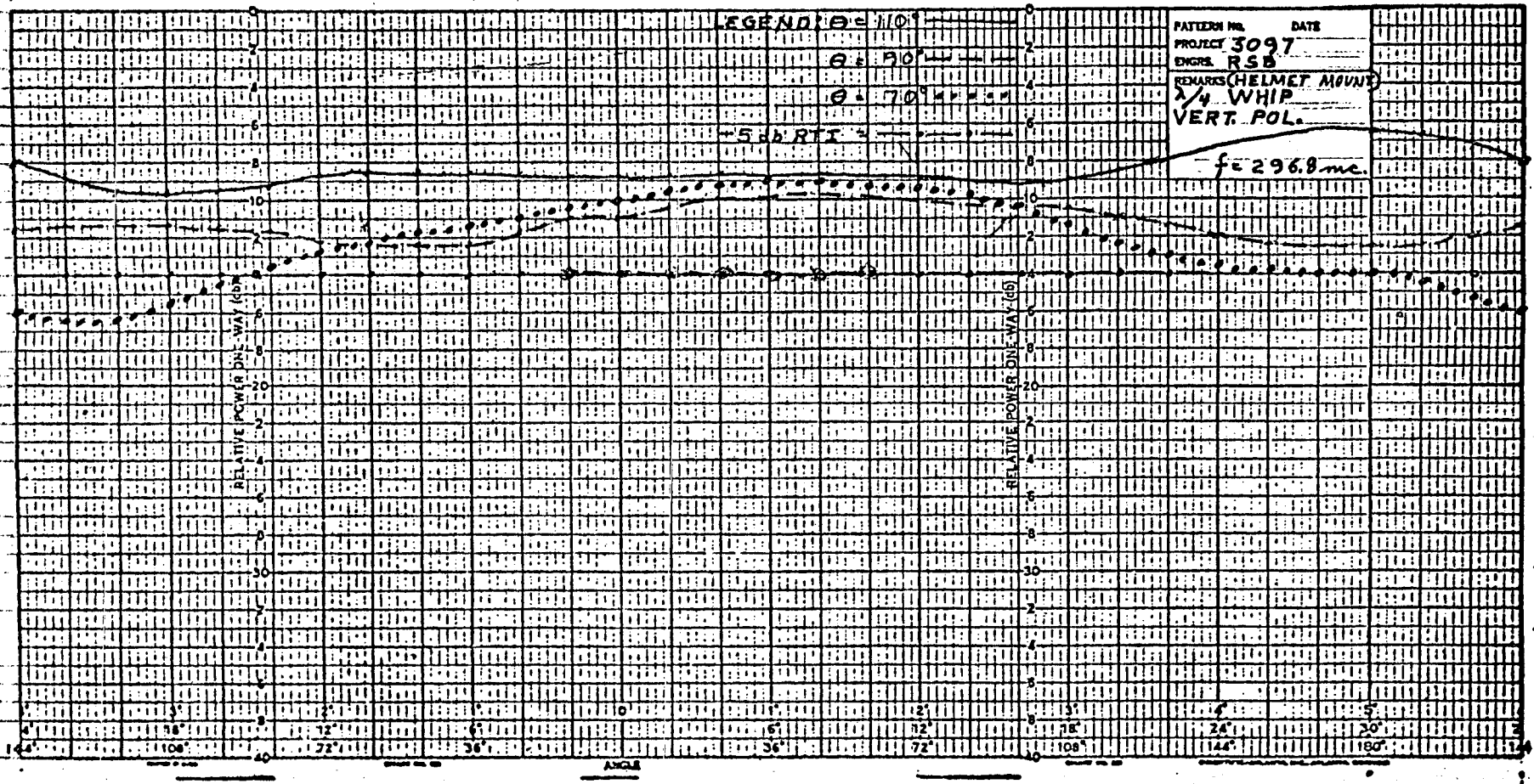

Figure 15. Radiation Patterns of Quarter-Wavelength Whip Antenna Mounted on Helmet; Frequency = 296.8 mc

were measured on this antenna while mounted on the approximate top center of the PLSS. These patterns have been reduced to the contour plots of Figures 16 and 17 showing radiated power relative to an isotropic radiator. The contours shown are for radiation power levels lying between +2 and -12 dB at 2 dB increments. The percentage of the total area covered by the respective 2 dB increments is shown in the lower left hand corner of each figure.

3.3.3 Helical Antenna

3.3.3.1 Helical Whip

The helical whip is a normal mode helix with the parameters adjusted to give essentially a vertically polarized pattern. The pattern is comparable to a quarter-wavelength monopole, and a helix winding allows a shorter structure to be realized. Several of these antennas are shown in Figure 18 along with a conventional quarter-wavelength whip. Size reduction is approximately 33 percent in length. As a result of the inductive loading, the passband is narrower than a whip and thus has higher VSWR's. Patterns are comparable to those of the whip. Measurements of VSWR with the antennas placed on an 11-inch circular ground plane are 260 Mc, 3.0; 300 Mc, 3.5. These values may be reduced with an appropriate matching network. Gain is within 0.5 dB of the gain of the quarter-wavelength whip.

3.3.3.2 Dielectric Rod Helical Whip

The size of the helical whip antenna can be further reduced by dielectric loading of the helix. During fabrication, the helix is imbedded in a dielectric rod that is coaxial with the helix and slightly larger than the helix. Size reductions of up to 50 percent are not unusual, and the pattern remains essentially unchanged. The input impedance is somewhat affected by the dielectric loading.

3.3.4 Sleeve Monopole Antennas

For a conventional monopole, signal is applied between the base of the monopole and the ground plane, but the impedance of such a monopole is usually less than 50 ohms, at the first resonance.

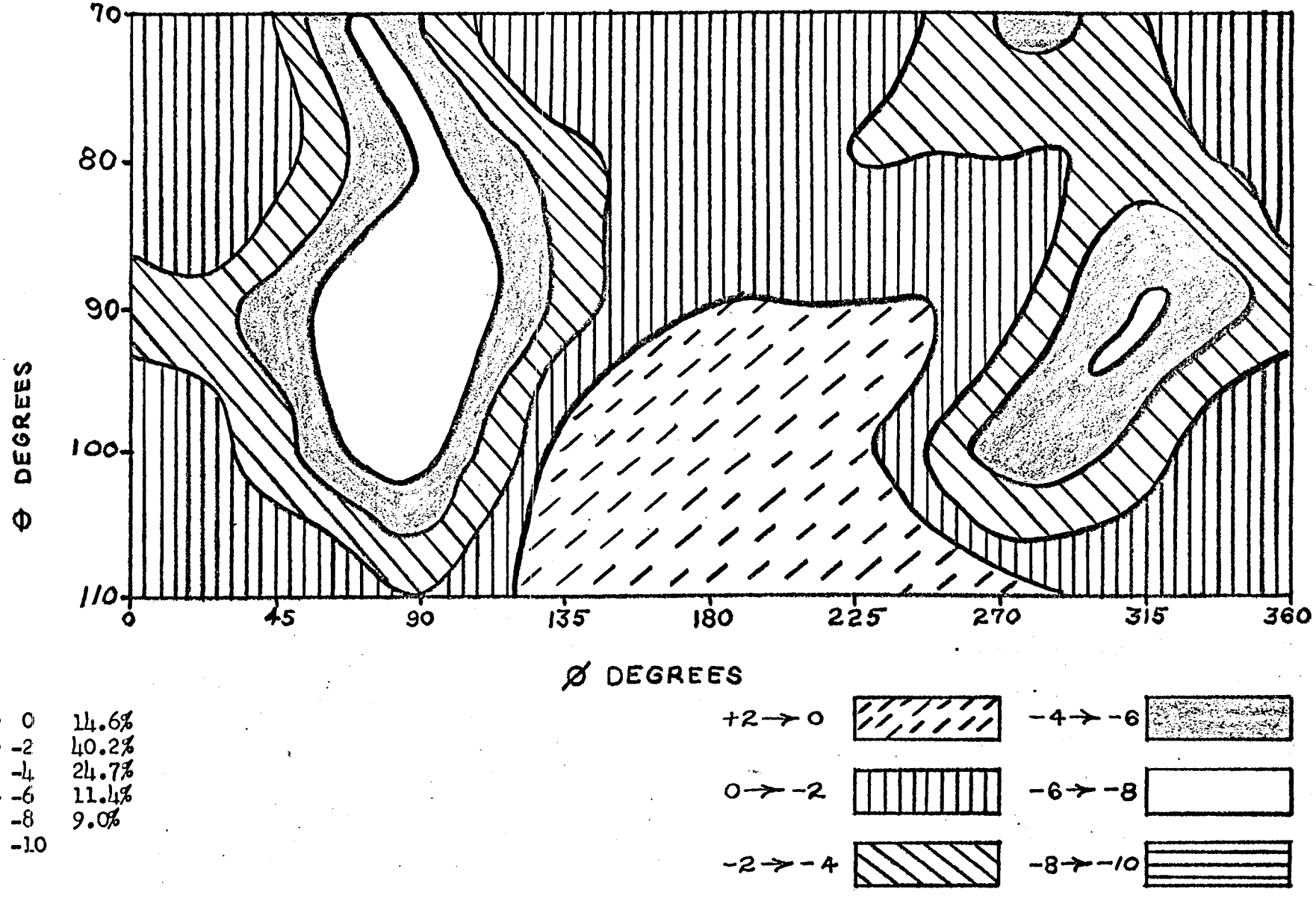

Figure 16. Contour plot showing radiation power levels (in dB) of quarter wavelength whip antenna over ± 20° of the horizon for all angles of azimuth. Frequency = 296.8 Mc.

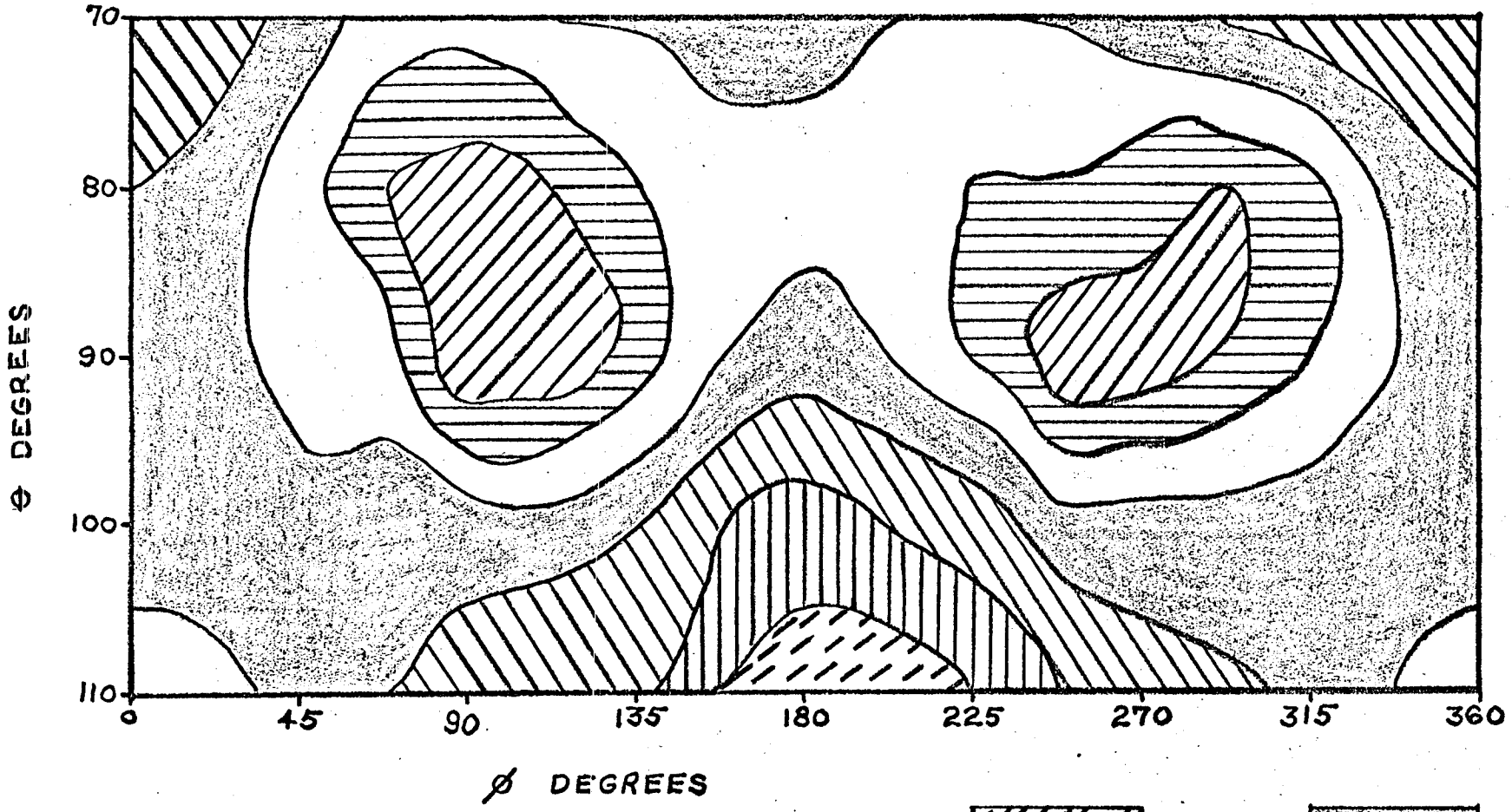

2 → 0	1.6%
0 → -2	4.6%
-2 → -4	12.2%
-4 → -6	33.0%
-6 → -8	26.9%
-8 → -10	13.5%
-10	7.9%

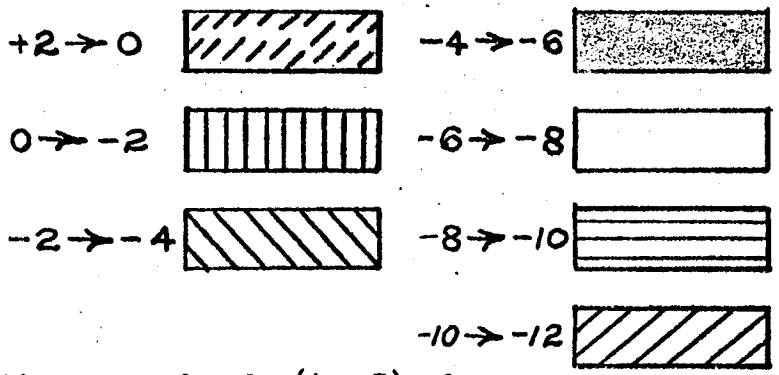

Figure 17. Contour plot showing radiation power levels (in dB) of quarter wavelength whip antenna over ± 20° of the horizon for all angles of azimuth. Frequency = 258.08 Mc.

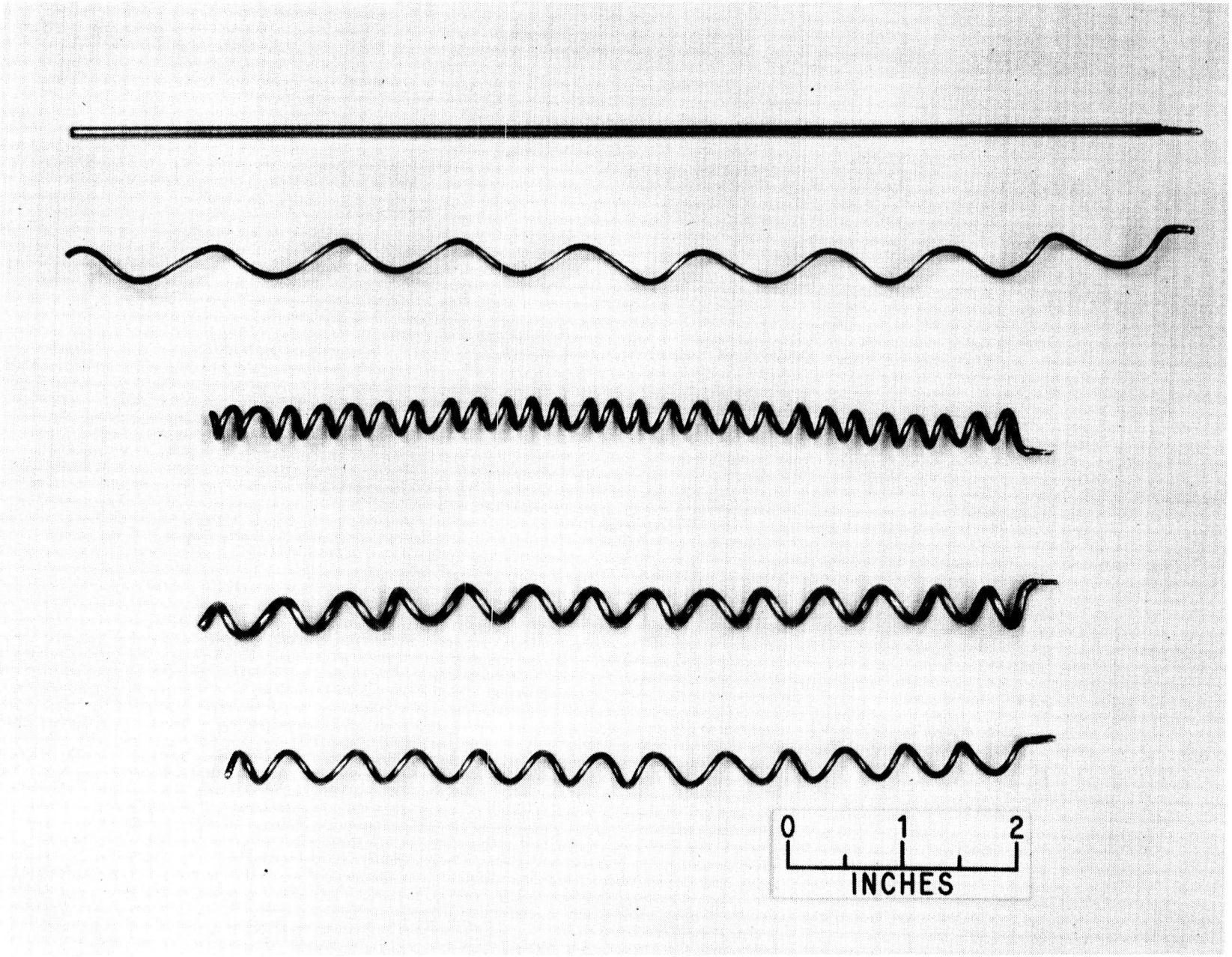

HELICAL WHIP ANTENNAS

The reactance of a monopole can be lowered by increasing the diameter, and its radiation resistance can be increased by raising the feed point. The sleeve monopole configuration accomplishes both of these objectives by making the lower part of the monopole the outer conductor of a coaxial transmission line; the inner conductor being connected to the upper part of the monopole (which may be of a different diameter). The outer conductor of the coax is, of course, the "sleeve".

The sleeve monopole, described by Figure 19, is a broadband form of the quarter-wavelength monopole. The input impedance (and hence VSWR) is a function of the ratios $\frac{\ell}{L}$ and $\frac{ID}{d}$ where ℓ, L, ID, and d are defined as in Figure 19. One model with $\frac{\ell}{L} = 2.5$ and D = 0.5 inch has a VSWR of less than 2 at both 260 Mc and 300 Mc. This figure can be improved if D (and also d) are allowed to assume larger values. Pattern and polarization are equivalent to a quarter-wavelength monopole.

Theoretical calculations of the characteristics of sleeve monopoles have not been carried out to any large extent, so one must rely on empirical data. One good source is the extensive experimental investigations of Norgorden and Walters.[2] This reference gives the impedances of sleeve monopoles of total length 30 inches in the configuration shown in Figure 20, for different sleeve diameters, different radiator-to-sleeve length ratios, and different radiator diameters. Typical resistance and reactance curves are shown in Figure 21. For these curves, the sleeve diameter is one inch and the radiator-to-sleeve length ratio is 0.5.

It is clear from the reactance curves that a good match to 50 ohms occurs when the reactance curves approach zero, as they do between 250 Mc and 310 Mc. The resistance matches 50 ohms at about 270 Mc.

These curves were taken on a very large ground plane, and the impedances on a small ground plane are quite different. Therefore, it is necessary to experimentally check the effect on the impedance of the ground configuration actually used.

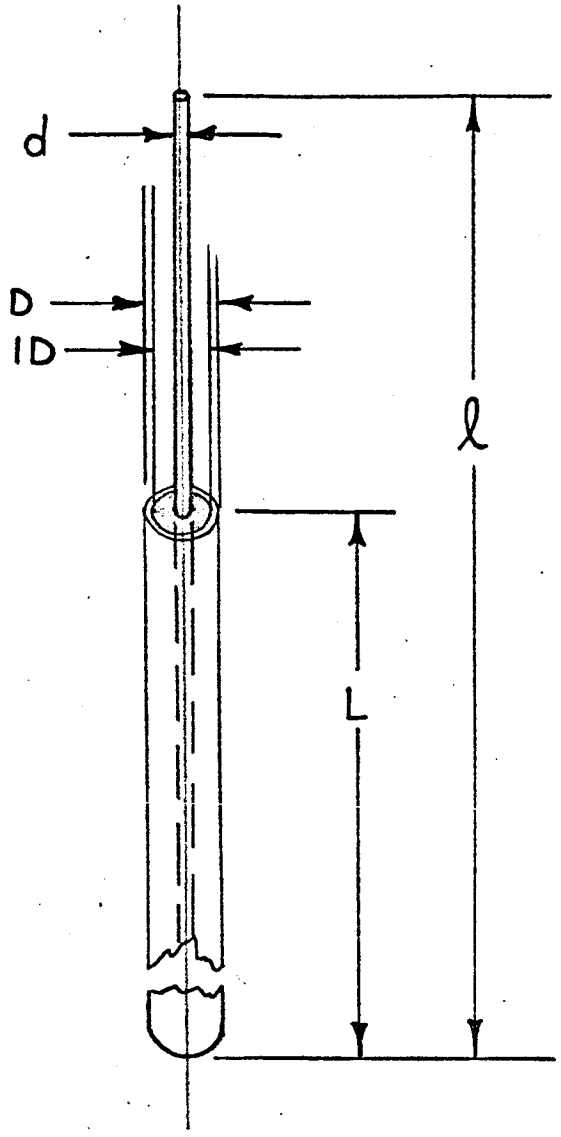

FIGURE 19
SLEEVE MONOPOLE ANTENNA

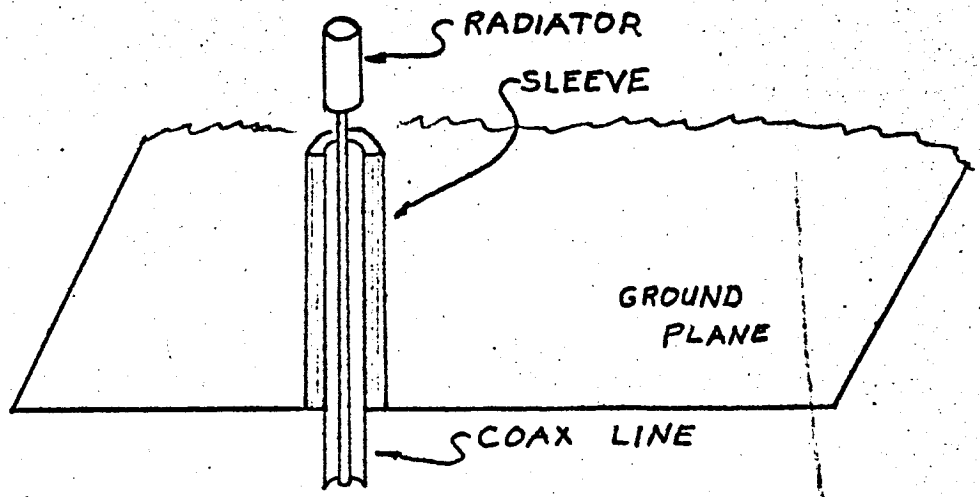

FIGURE 20. SLEEVE MONOPOLE AS DESCRIBED BY NORGORDEN AND WALTERS

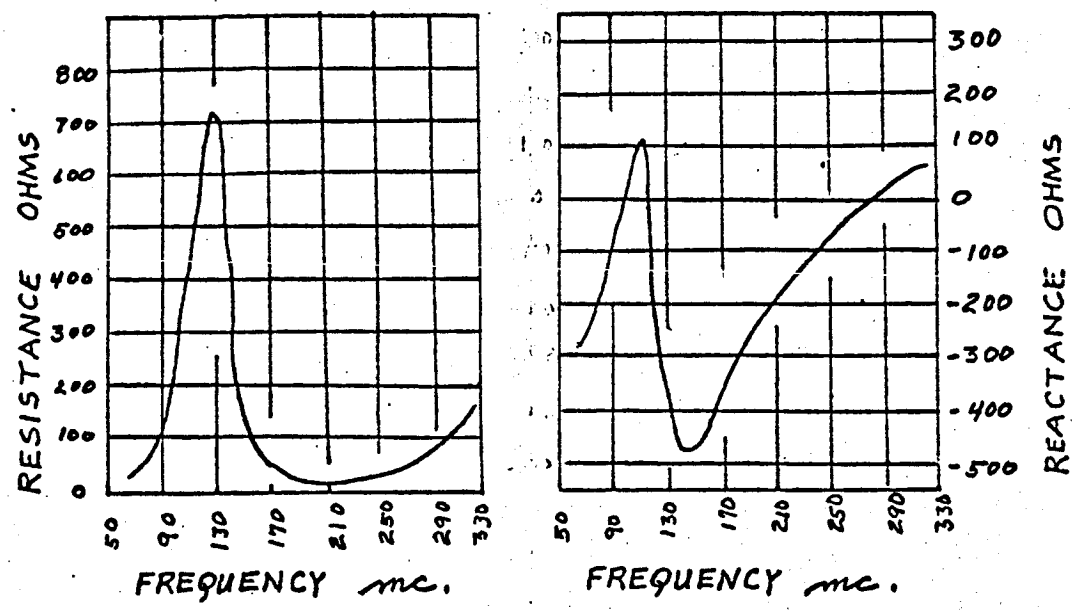

FIGURE 21. TERMINAL RESISTANCE AND REACTANCE VS. FREQUENCY FOR A 30 INCH SLEEVE MONOPOLE

3.3.4.1 Sleeve Antenna on PLSS

This is a fixed antenna mounted on the PLSS. It is considered in this study as a candidate for an erectable/retractable antenna system. It consists of a 20" long, 1" diameter sleeve, with a 1/2" diameter inner conductor, terminated in a 10" monopole element with a 1/4" diameter. Protective covering is not needed as all exposed parts are metallic.

As the antenna is designed, it has particular merit in the category of erectable/retractable antennas and, as will be seen in Section 3.4.2, it can be used with a deployment system similar to that used for the discone antenna.

Tests were performed with the antenna mounted on the front center of the PLSS, with the feed point 20" above the top surface of the PLSS, and with the bottom of the sleeve grounded to it. Reactive currents flowing down the sleeve and over the thermal garment deteriorated the performance at both frequencies. Figure 23 shows the installation and indicates the probable current paths on the thermal garment.

In order to restrict currents to the antenna proper, two concentric quarter-wave chokes are added, one for each of the operating frequencies. Figure 22 shows the antenna and its choke sections. These chokes are installed around the sleeve and adjusted for optimum patterns. The best performance is obtained when the combined length of the choke section and the monopole is approximately one half-wavelength and the feed point is 20 inches above the center of the back edge of the PLSS.

This design yields relatively smooth radiation patterns at each of the desired frequencies. The antenna gain measures better than -3 dB over a major part of the volume of interest. The VSWR is less than 1.2 at each frequency. Figures 24 and 25 show typical radiation patterns.

3.3.5 Spring Supported Monopole Antenna on Helmet

This antenna shown in Figure 26 is mounted on the top of the space suit helmet and includes an erect/retract mechanism described in Section 3.4.1. The electrical design of the antenna is strongly influenced by the mechanical

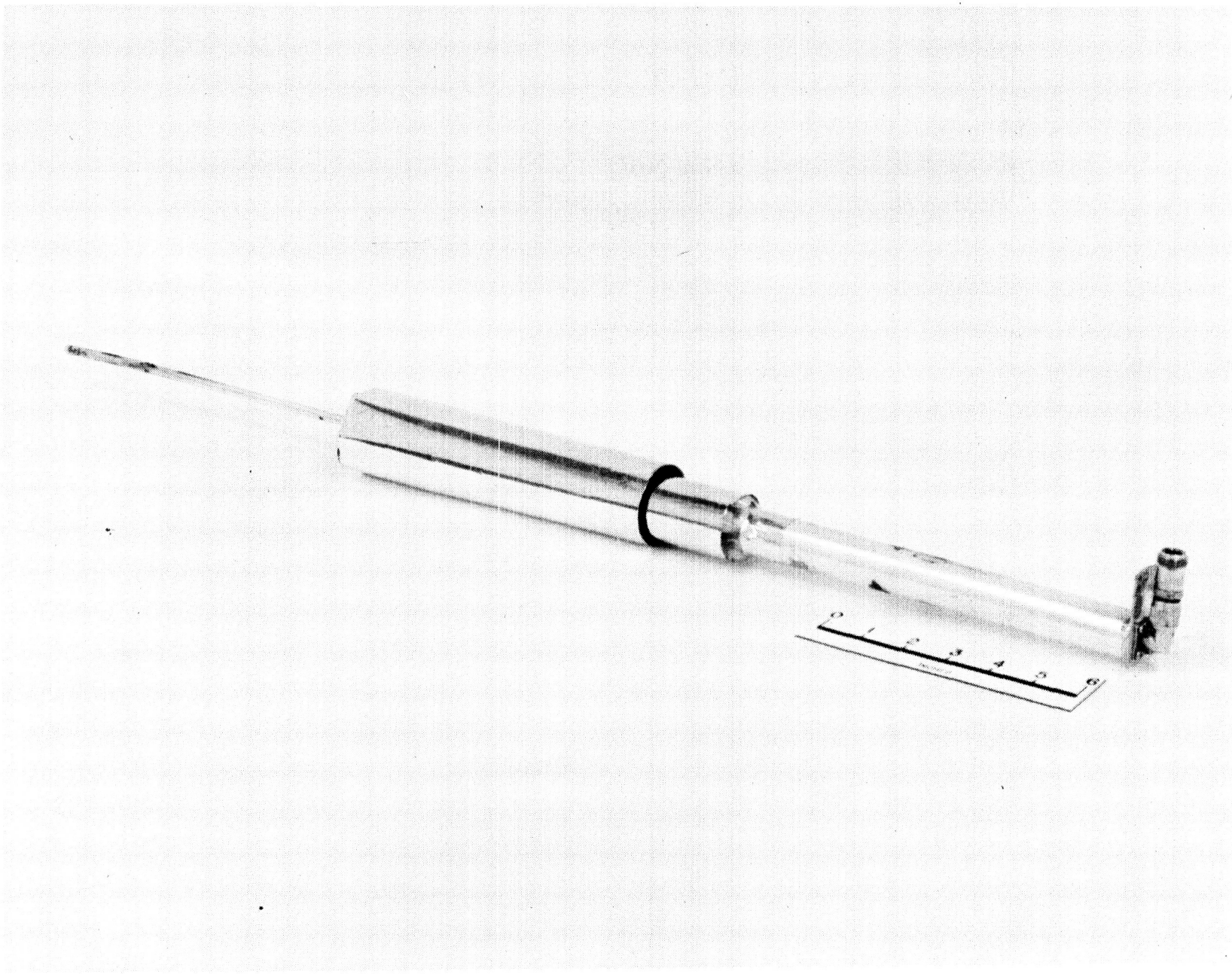

Sleeve Monopole With Quarter
Wavelength Choke Sections

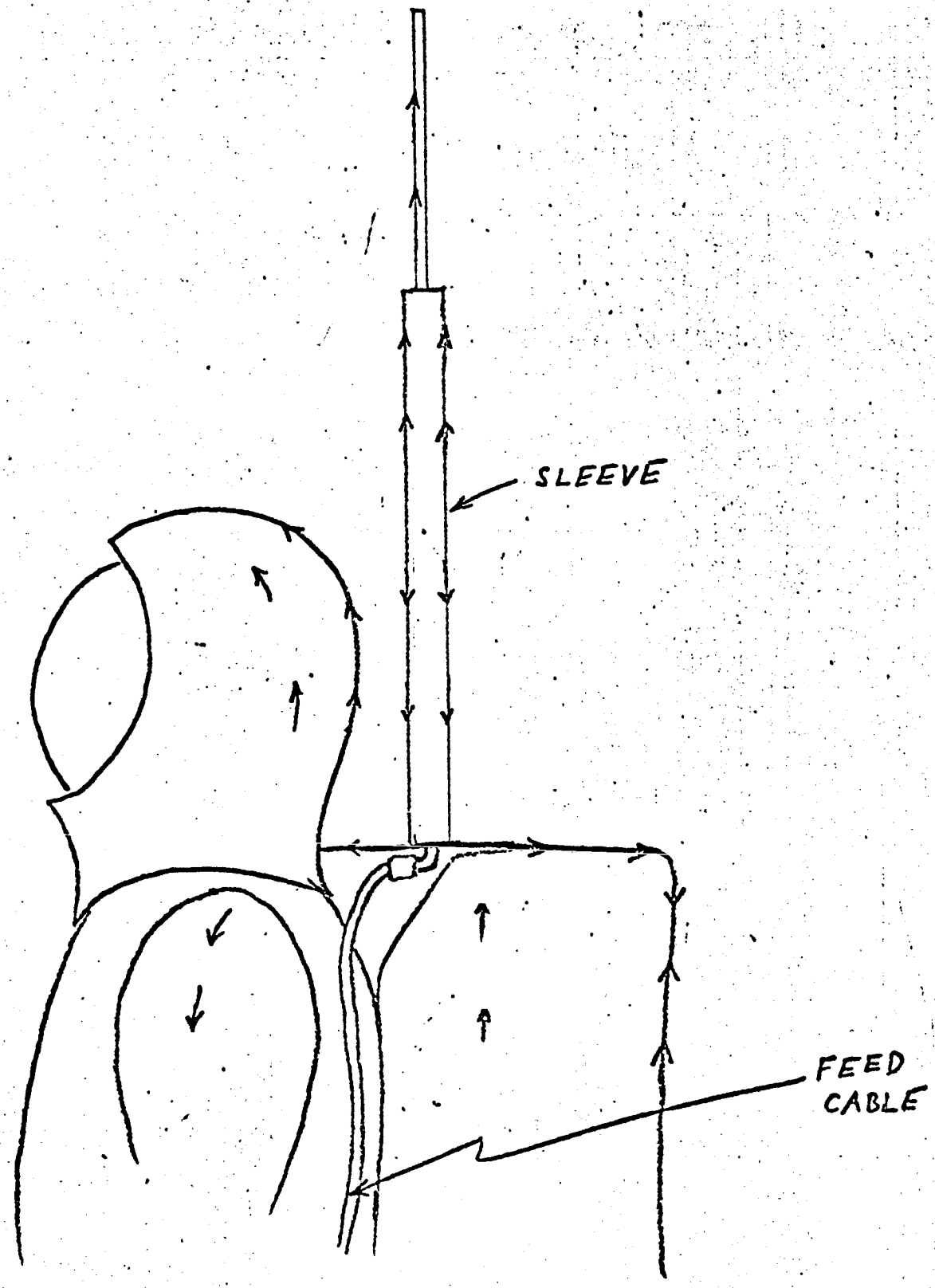

FIGURE 23. SPACE SUIT MOCKUP SHOWING SLEEVE MONOPOLE MOUNTED ON PLSS WITH ESTIMATED INDUCED CURRENTS

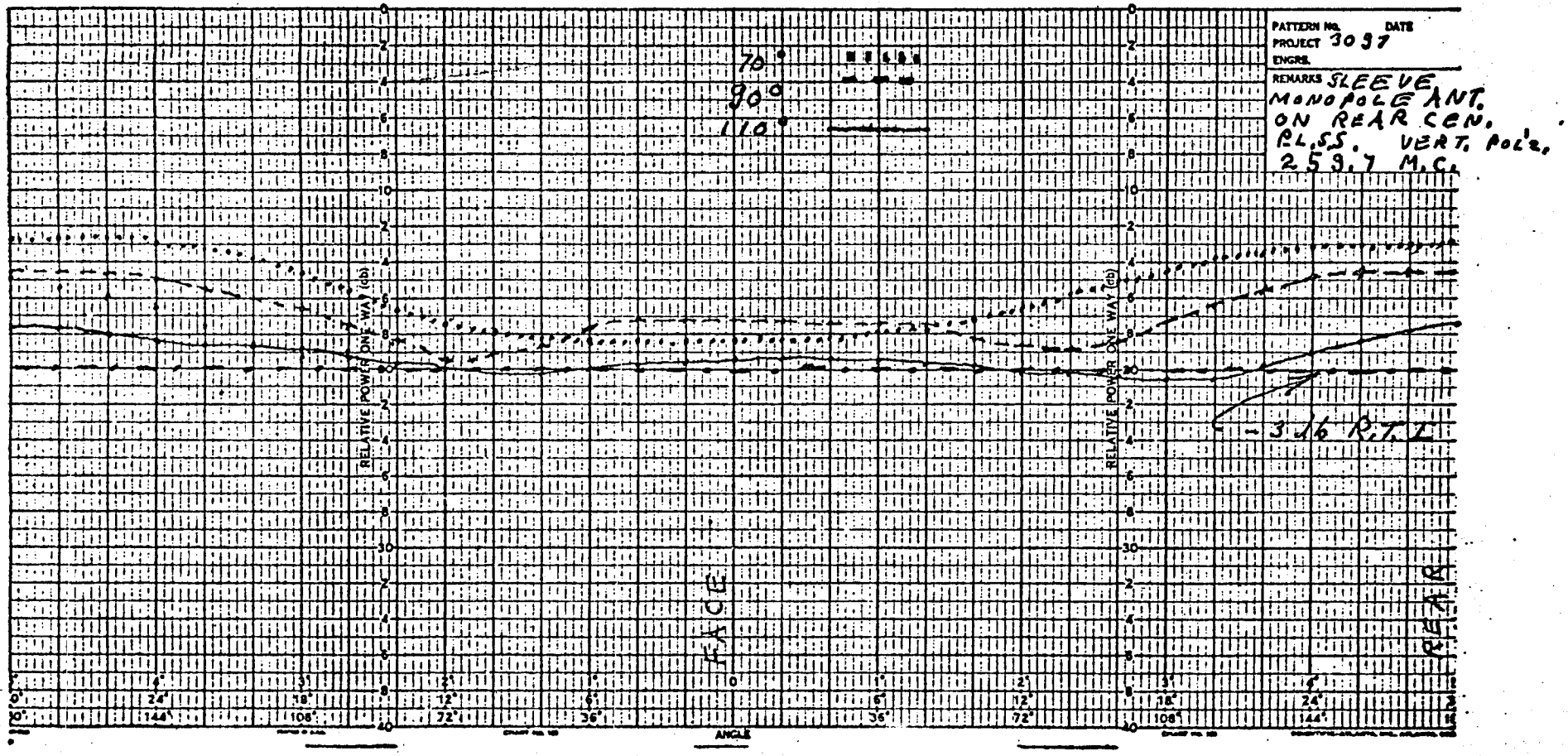

Figure 24. Radiation Pattern of Sleeve Monopole Antenna Mounted with the Feed at a Point 20 Inches over Rear-Center of PLSS. Frequency = 259.7 mc

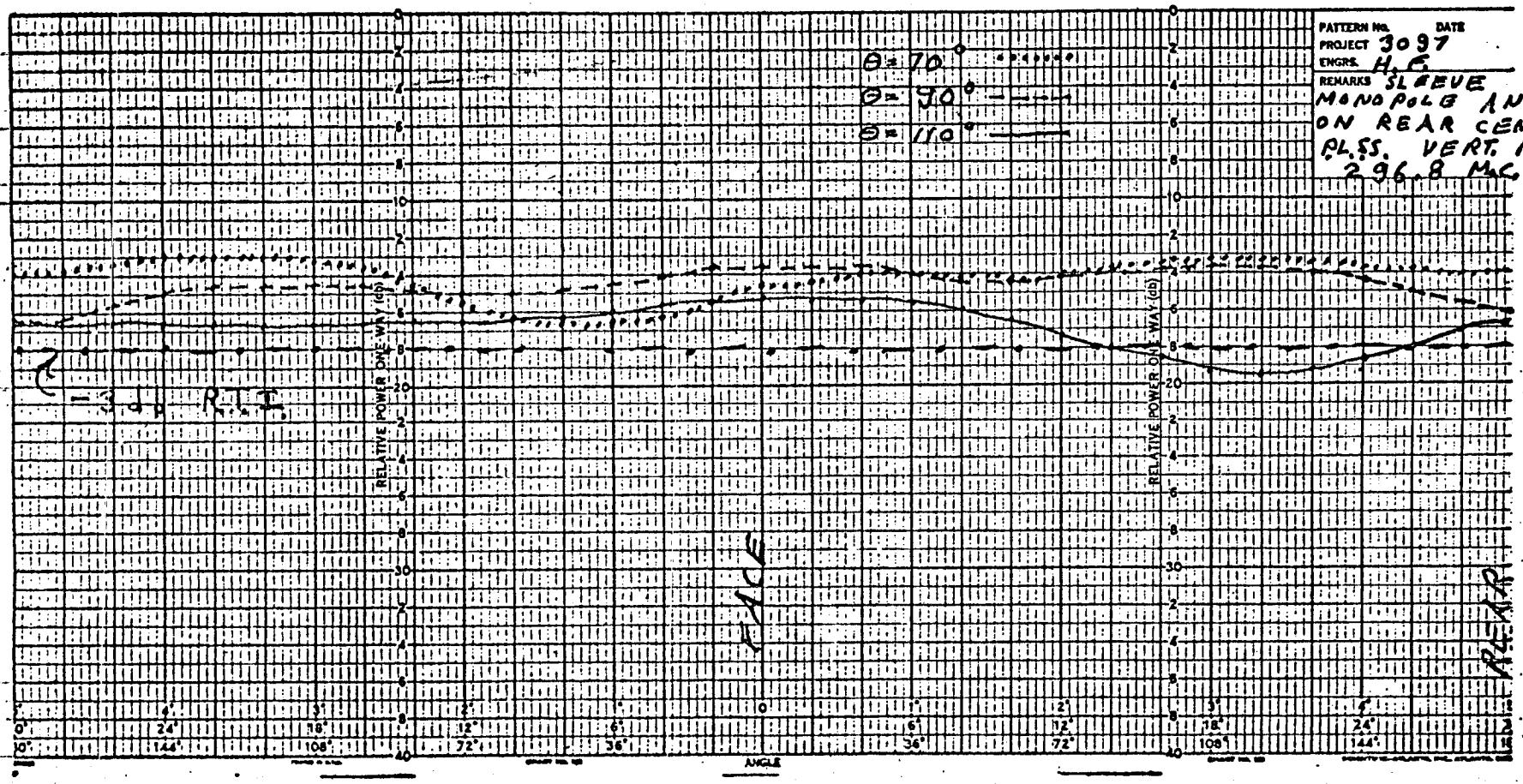

Figure 25. Radiation Pattern of Sleeve Monopole Antenna Mounted with the Feed at a Point 20 Inches over Rear-Center of PLSS. Frequency = 296.8 mc

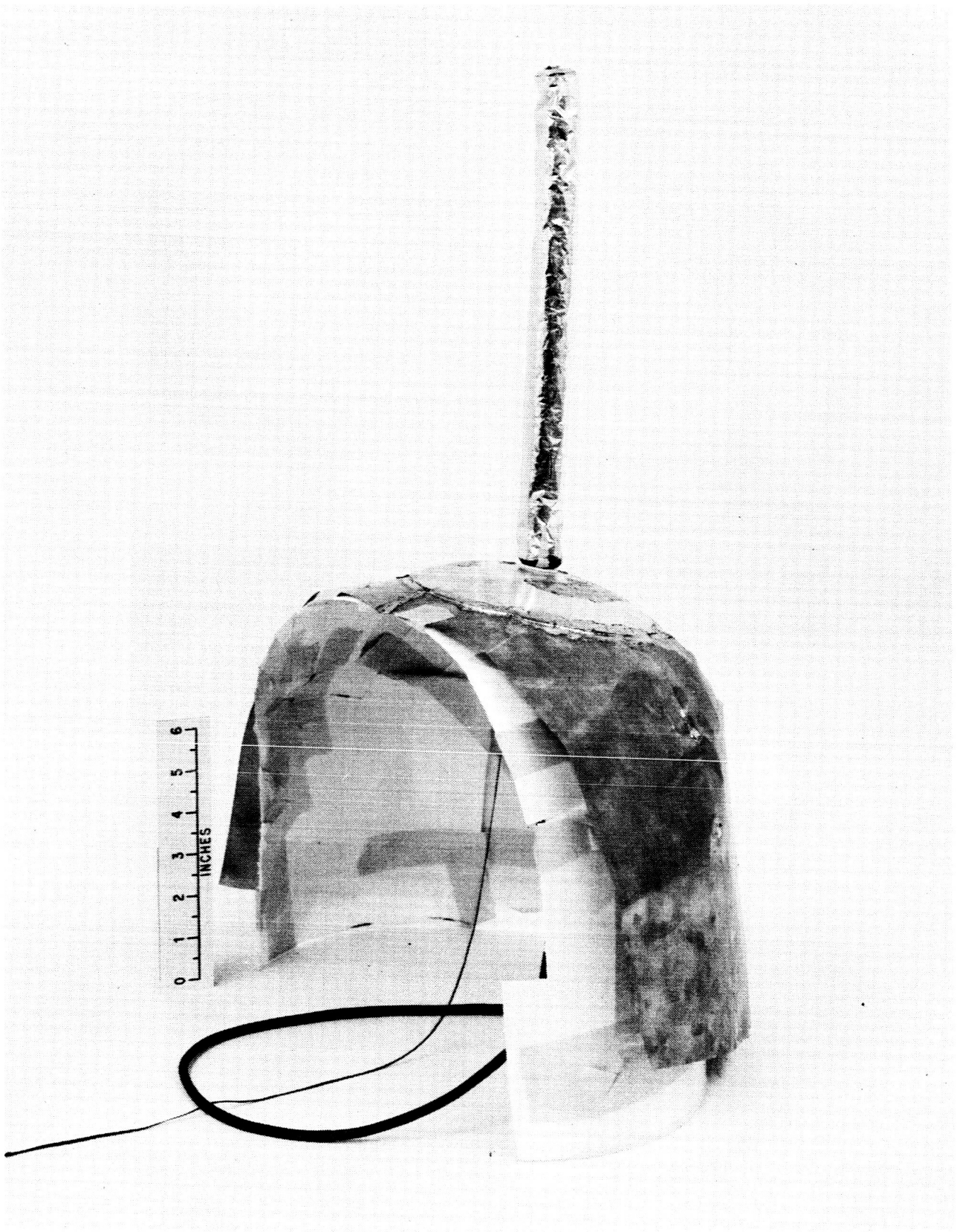

Spring Supported Monopole Antenna With
Resonant Ground Plane Mounted On A
Dielectric Covering

requirements of the erection mechanism but follows in principal the design described in Section 3.3.2.

For this antenna's erection mechanism a large diameter spring is used to support a cylinder of flexible conductive material. Because the antenna is a monopole over a ground plane, the cylinder is made a quarter-wavelength long. The large diameter of the spring causes the antenna to have a small length-to-diameter ratio (L/D = 20) which results in a broadband characteristic. The element is placed over a spherical cap ground plane which covers the top of the space suit helmet. The element is connected to a coaxial connector through the base. The entire assembly is placed directly over the thermal garment.

Tests show that optimum radiation patterns are obtained when the antenna is located approximately 5 inches behind the leading edge of the thermal garment. Patterns taken of the prototype antenna in this location are shown in Figures 27 and 28. These patterns show the antenna gain to be greater than the -3 dB and -5 dB minimum (for 259.7 and 296.8 Mc, respectively), over the principal amount of each conical sector. An exception is seen at $\theta = 90^{o}$ for the 259.7 Mc pattern, where θ is the angle measured from the zenith to the elevation angle of interest.

Measured VSWR on this antenna is less than 1.3 across the band.

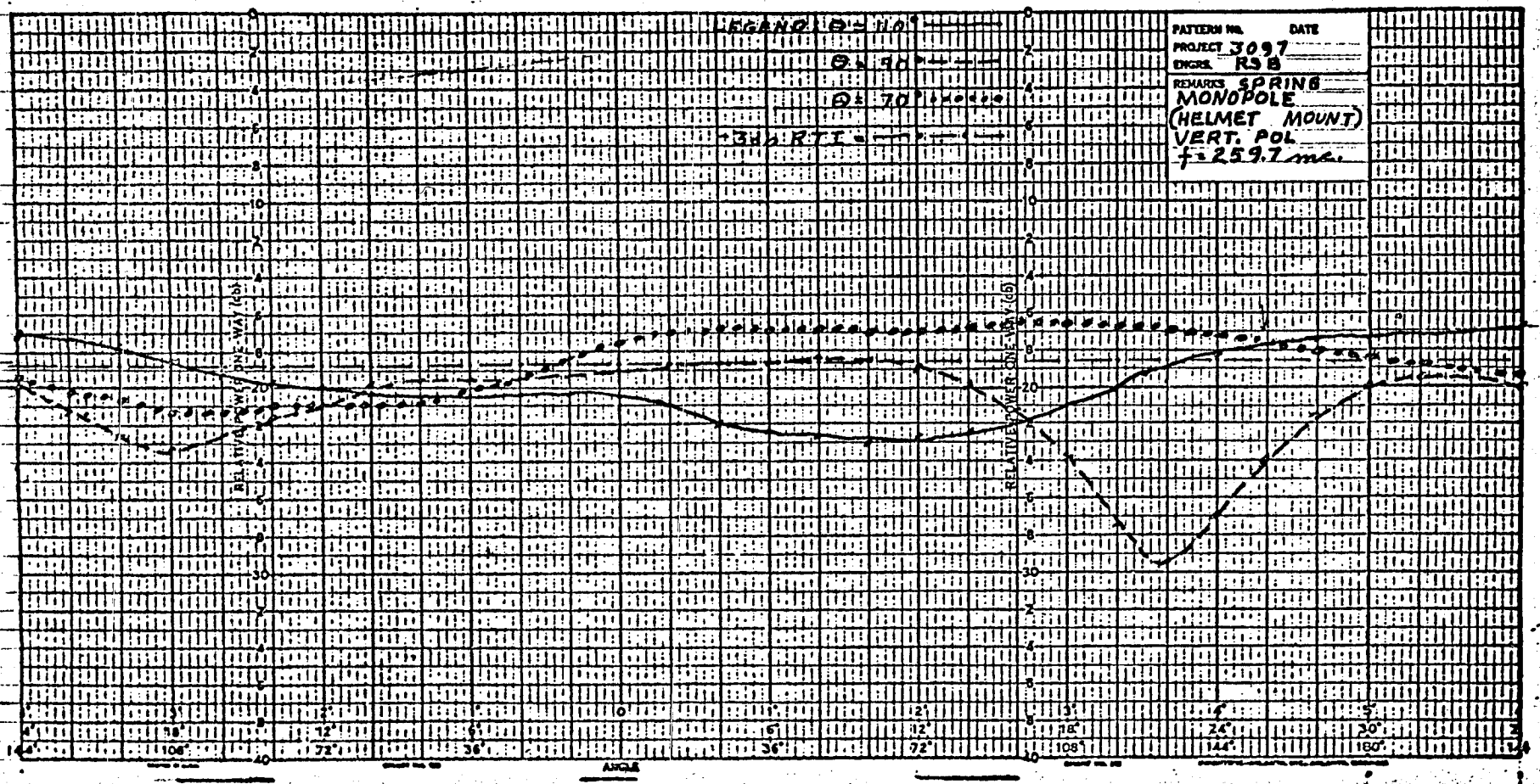

Figure 27. Radiation Patterns of Spring-Supported Monopole Antenna Mounted on Helmet; Frequency = 259.7 mc

3.3.6 Loaded Monopoles

3.3.6.1. Folded Monopole

If a monopole were folded as shown in Figure 29, the bandwidth can be increased somewhat over a standard whip. The amount of bandwidth increase is dependent on the particular design parameters. The folded monopole is as long as a quarter-wavelength whip, and the input impedance can be adjusted by controlling the ratio of the diameters of the two arms composing the antenna and the separation of the arms. Polarization, pattern, and gain are comparable to the quarter-wavelength monopole. Since the arm separation must be controlled, the structure can be flexible in one plane only, that is, the vertical plane normal to the plane defined by the two arms of the folded monopole. Also, since one of the arms of the antenna must be grounded, it is not as easily adapted to an erectable/retractable technique as the single arm monople such as the whip and the sleeve antennas.

3.3.6.2 Capacitively Loaded Monopole

The folded monopole can be reduced in height by capacitive loading. One antenna utilizing this technique is described in this section. The antenna pictured in Figure 30 is referenced to as a "top hat" antenna. It is composed of a capacitively top loaded folded monopole. The diameter ratio of the two vertical posts and the post separation determine the input impedance. This allows the input impedance to be adjusted independently of the other antenna electrical parameters. The pattern of this antenna is similar to that of a quarter-wavelength monopole on a ground plane. The bandwidth of this antenna can be made greater than that of a quarter-wavelength monopole thus permitting a better input VSWR to be realized at the two design frequencies. Typical dimensions of this radiator are four inches high and a top hat diameter of three inches. The antenna height can be reduced to as little as two inches (with a five inch diameter top hat) with a bandwidth one-third as large. While this would result in VSWR's greater than 2 at the design frequencies, the lower profile may be sufficiently attractive to offset this disadvantage.

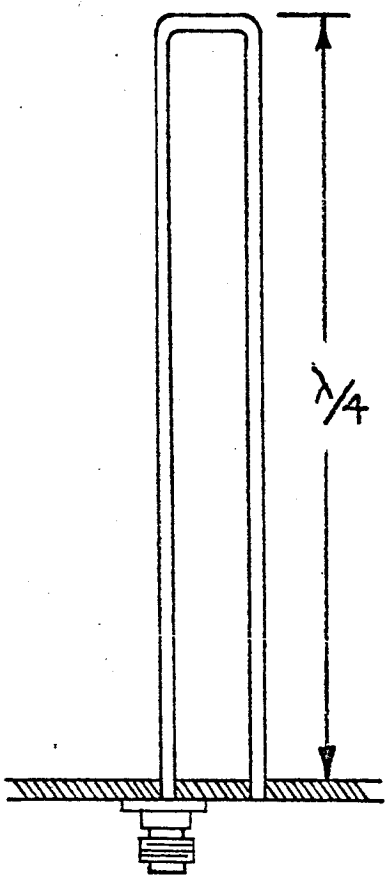

FIGURE 29
FOLDED MONOPOLE ANTENNA

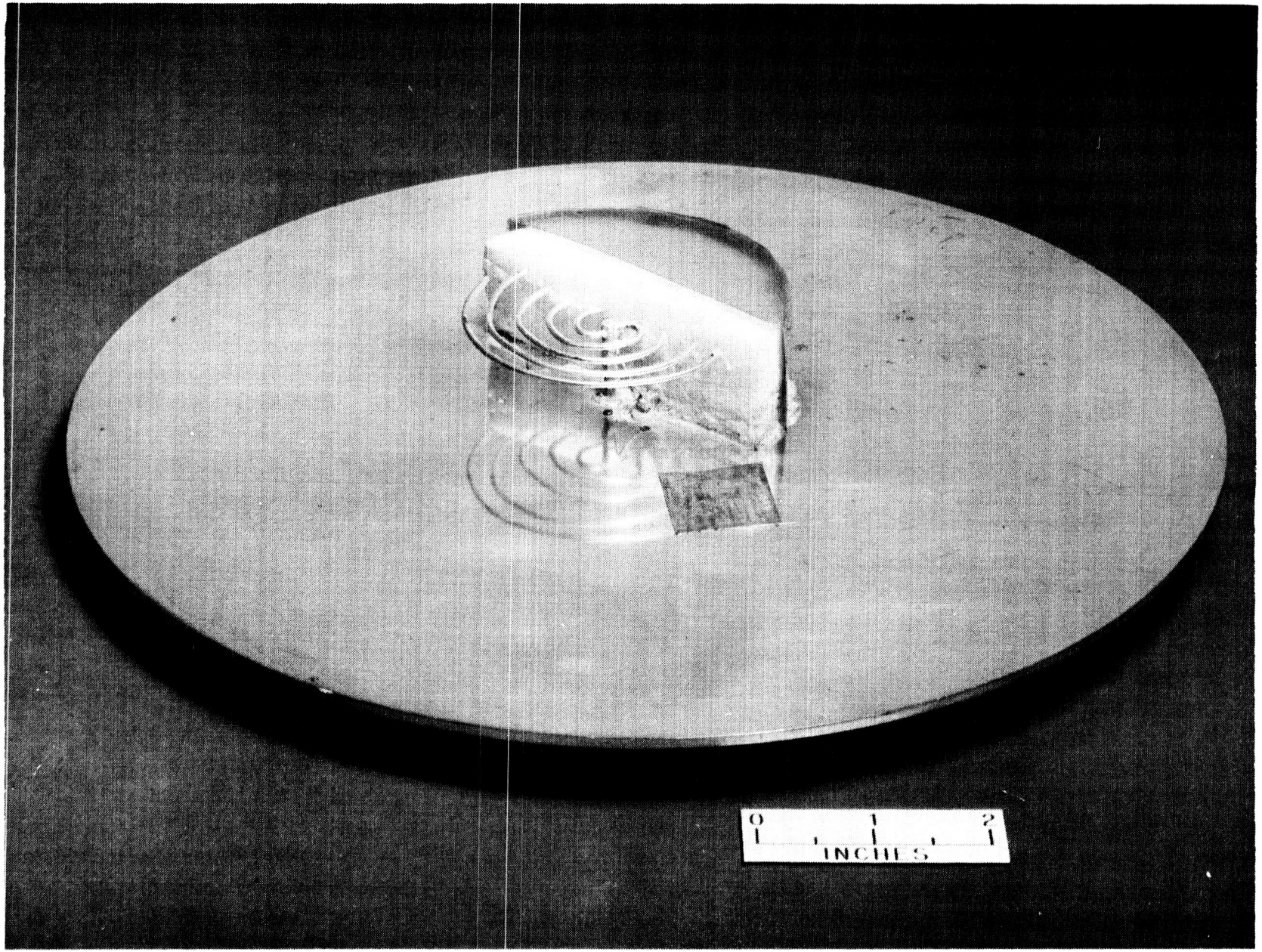

FIGURE 1

DUAL FREQUENCY SPIRAL ANTENNA
WITH COVER AND FOAM CUT BACK

3.3.6.3 Inductively Loaded Monopole

The height of a folded monopole can also be reduced by inductive loading as described below. An alternate design approach to reduce the folded monopole height uses a loading inductor in each of the folded arms. In this case, the tops of the two vertical arms are simply joined by a short horizontal conductor as in the simple folded monopole. The disadvantage of eliminating the top cap by inductive loading rather than by capacitive loading must be weighed by the loss in gain due to the addition of the inductors to the arms, from 1 dB to 2dB, depending on the degree of height reduction.

3.3.6.4 Ferrite Loaded Antennas

Ferrite antennas are not normally considered for transmitting antennas. The high values of fields appearing across the ferrite material saturates it, reducing the effective relative permeability to a low level. This in turn destroys the effectiveness of the ferrite loading; thus, ferrite loaded antennas are not of significant value for this application.

3.3.7 Discone Antennas

A wideband antenna offering good patterns, VSWR's, and gains at both frequencies is the discone antenna.

The inverted discone antenna used in this investigation can be considered to be composed of a broadband monopole (cone) mounted on a small circular ground plane (disc). The structure is fed by a coaxial line with the center conductor attached to the cone and the outer conductor attached to the disc. The solid surfaces of the disc and cone can be approximated with success by ribs, or radicals. To get the radiation pattern maximum at low elevation angles, say on the horizon, the radials comprising the disc can be drooped to form an inverted cone. Such a model is shown in Figure 31. In appearance, and to some extent in performance, it is similar to a biconical antenna.

The impedance characteristics of a discone antenna can be related to the theoretical results for a biconical antenna, and extensive experimental re-

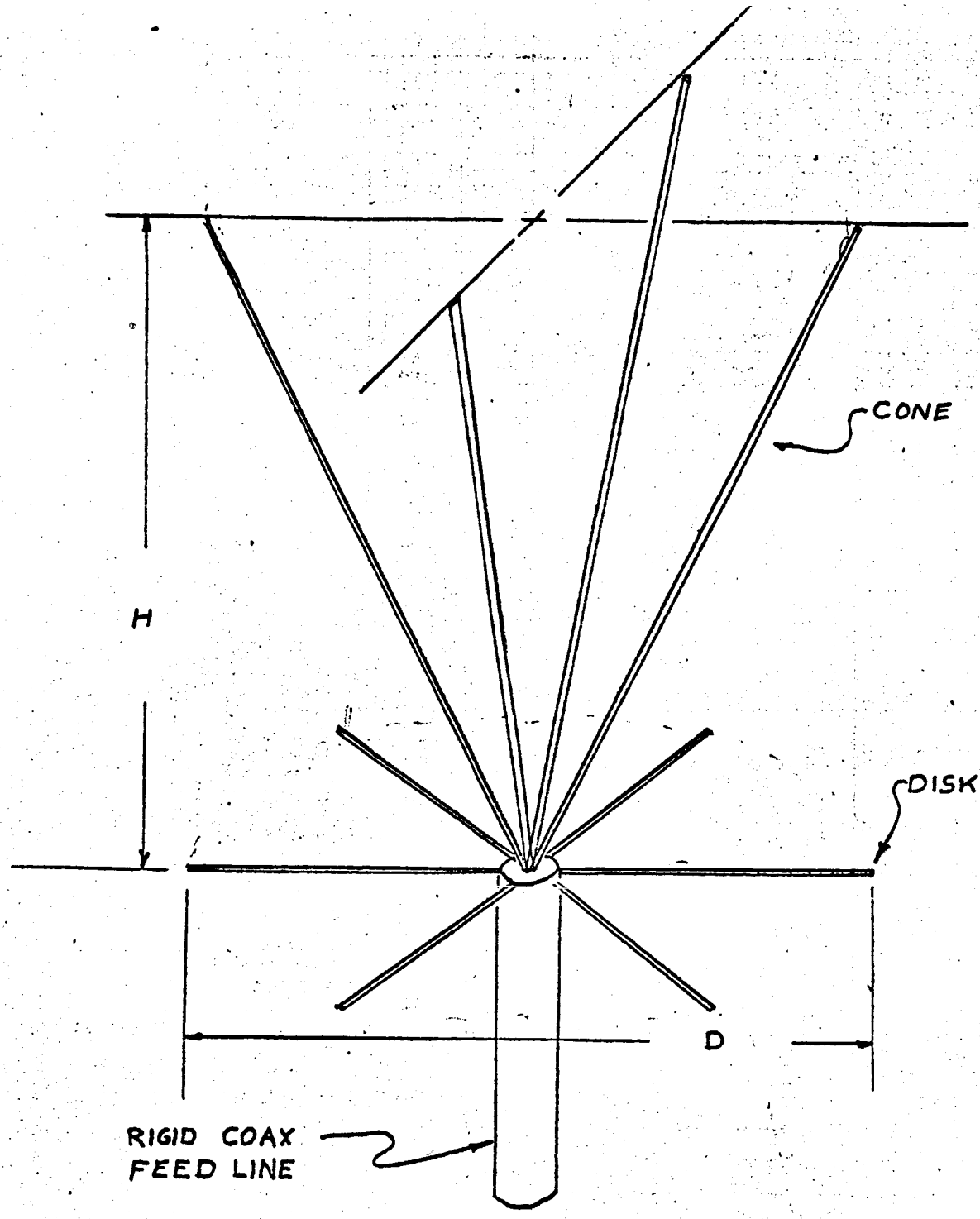

FIGURE 31. DISCONE ANTENNA

sults also exist. These show that for a cone angle of 60°, a good match to 50 ohms is obtained at all frequencies above a certain cutoff, determined by the diameter and height of the antenna.

3.3.7.1. Discone Antenna on PLSS

This antenna is an erectable/retractable type having the capability of being folded into a compact volume and stowed within a narrow well. Because of this mounting requirement, special consideration is given to the selection of materials to be used as the antenna elements. Early models used small cylindrical brass rods shaped into an inverted discone to demonstrate the electrical characteristics of a collapsible antenna. Patterns and impedance were measured at various PLSS locations.

In the prototype model, the brass rods were replaced with beryllium copper strips. Each of these is shaped so its cross section is an arc of a circle, and then heat treated. This gives them the required mechanical rigidity when the antenna is erected, yet sufficient flexibility to allow retraction. The antenna radiating element consists of six of these strips shaped into a cone measuring 16 inches long and having a 30 degree included angle. The cone is fed by the center conductor of a 10-inch section of rigid coxial line. Located at the feed point, the disc section is connected to the outer conductor of the coax.

Patterns taken with this antenna located at various PLSS locations indicated the presence of reactive currents on the feed line and on the space suit. These currents were removed by trimming the disc elements to a quarter-wavelength and bending them into a conical shape back over the coaxial section at a 32-degree angle. This changes the antenna from the classical discone to a nearly biconical configuration.

Patterns taken with the feed point 10 inches above the center of the back edge on the PLSS are shown in Figures 32 and 33. These patterns show a gain level well in excess of the minimum of -3dB allowd at 259.7 Mc and -5dB allowed for 296.8 Mc.

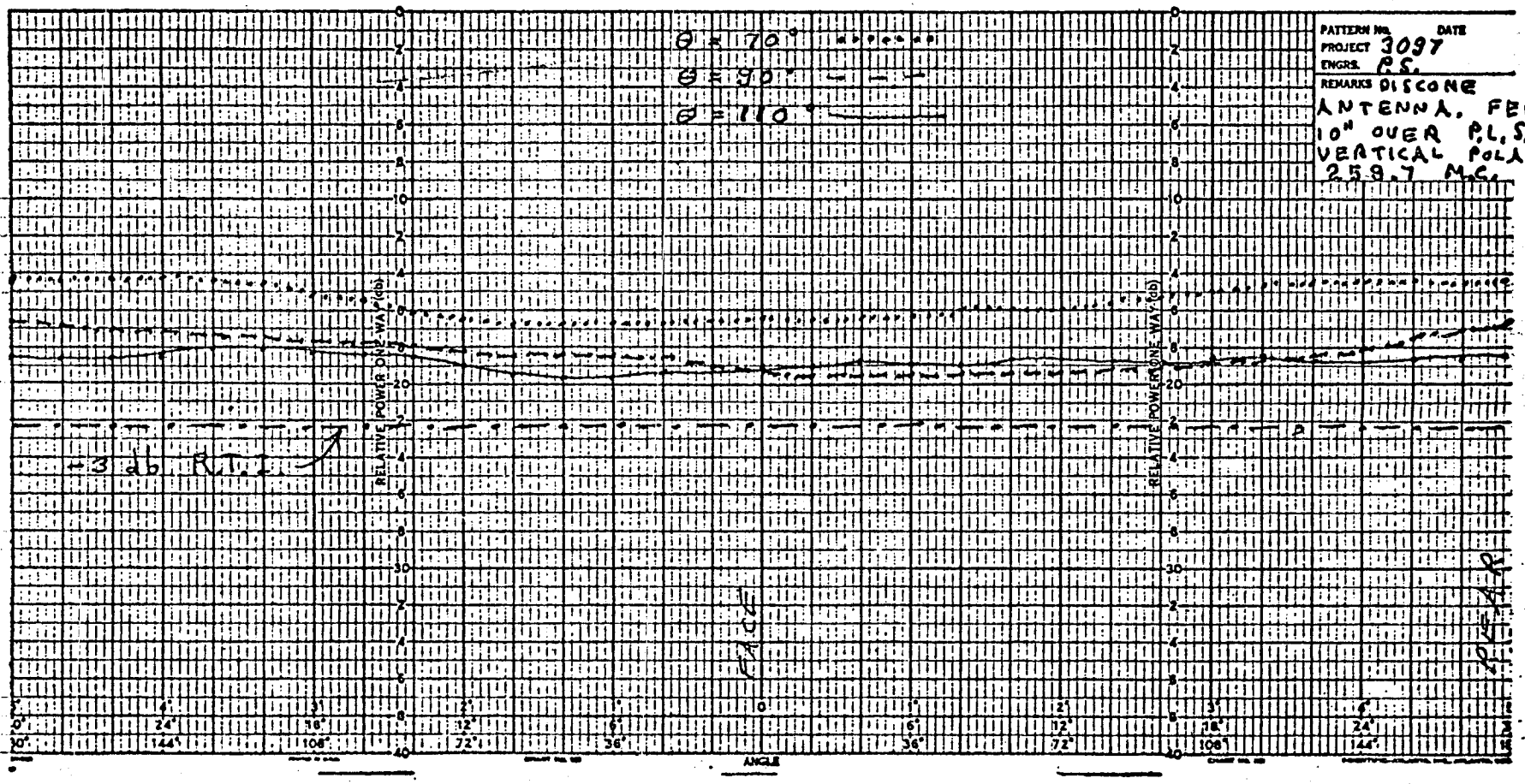

Figure 32. Radiation Patterns of Discone Antenna Mounted 10 Inches over Rear-Center of PLSS. Frequency = 259.7 mc

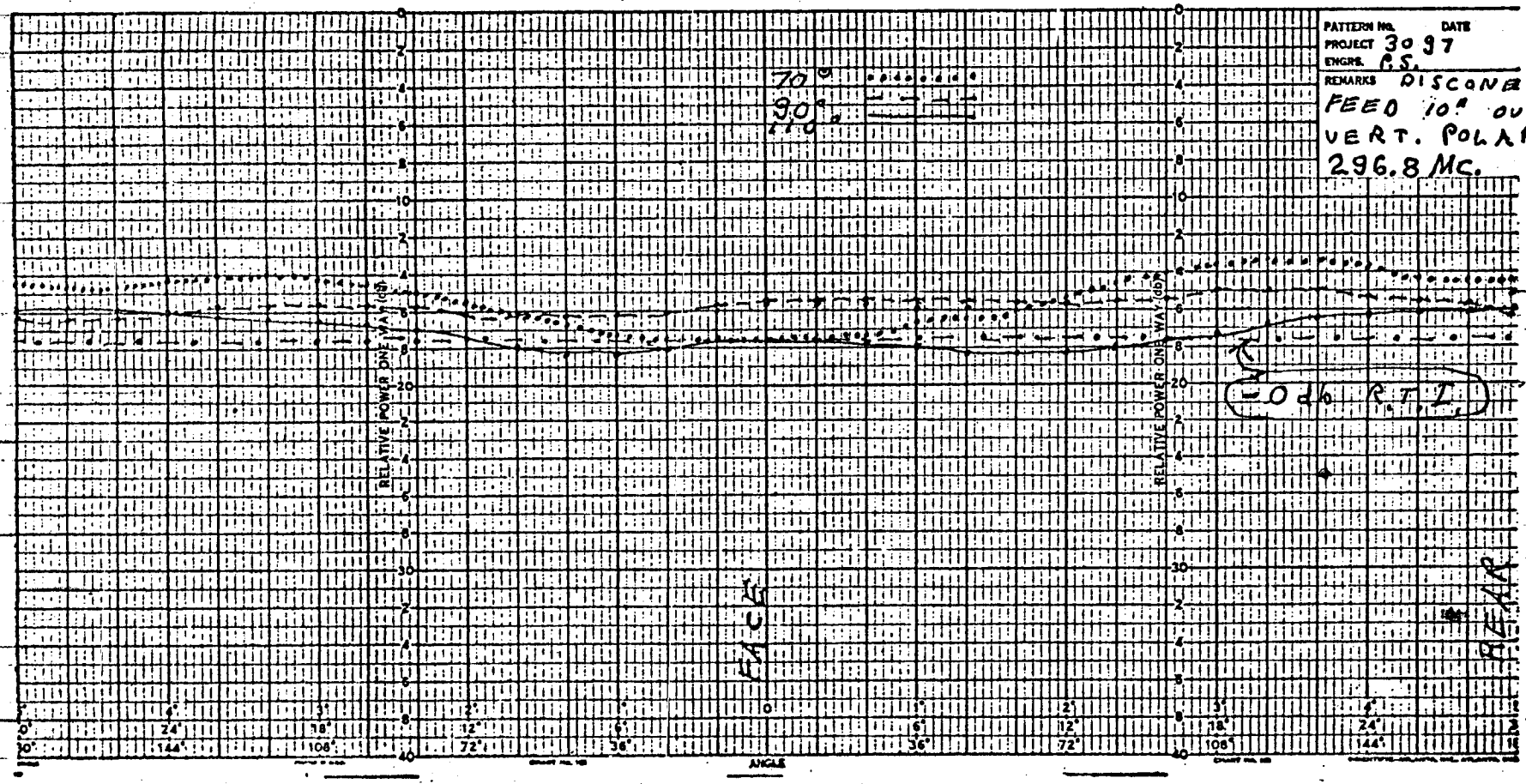

Figure 33. Radiation Patterns of Discone Antenna Mounted 10 Inches over Rear-Center of PLSS. Frequency = 296.8 mc

Measured VSWR is in excess of 3 at each frequency. However, a Smith chart impedance plot shows that the reactance falls within a symmetrical semi-circle about the chart's center. This inidicates that a simple reactive matching section may be inserted into the coaxial feed line to yield a well-matched system at the two frequencies of interest. This matching section will not add significantly to the size or weight of the unit. The main objection to this structure is its size: 1/3 wavelength long at the lowest frequency, of 13.9 inches, and a cone and disk of 7.4 inches (at the base) and 6 inches in diameter respectively. Even if the structure were composed of rods as shown in Figure 31, it would be much heavier than the antennas discussed so far.

3.3.8 Bow-Tie Antenna

A bow-tie antenna such as shown in Figure 34 can be considered to be a flattened biconical antenna, and most of its properties are similar to those of a biconical. It is very broadband, above a cutoff frequency (typically such that the length of each arm is about 1/6 wavelength), and its impedance depends on the vertex angle of the two triangles. (Impedance increases from 70 ohms to more than 150 ohms for large angles.) This antenna in free space should be fed from a high impedance balanced line. The broadband properties of the bow-tie antenna are compromised if it is located near to and parallel with a large conducting surface. The large mutual impedance between the antenna and its image in the conducting surface varies rapidly with frequency, causing the input impedance also to change rapidly with frequency. As a result, the antenna becomes a narrow band device.

3.3.8.1 Bent Bow-Tie Antenna on Helmet

The bent bow-tie is a fixed antenna located on the space suit helmet. This antenna was originally designed to operate over a dielectric helmet, some distance from any conducting objects. However, since on the SSC System helmet it must operate near the electrically conducting thermal garment more care must be taken with the design to prevent excessive currents on the ground

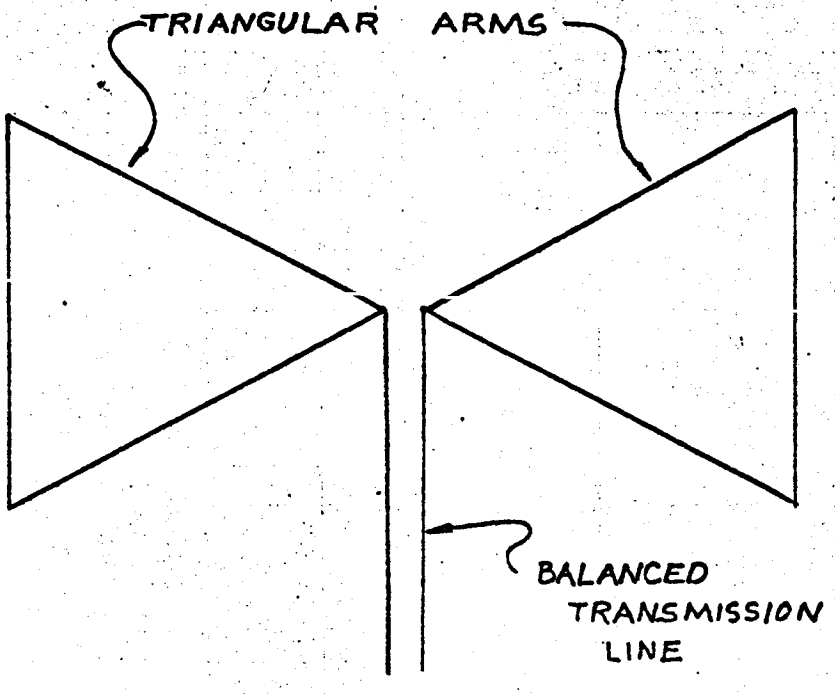

FIGURE 34.

BOW TIE DIPOLE ANTENNA

plane.

Several possible bow-tie configurations were studied (see Figure 35) which would help to alleviate these problems. However, most of these involved increasing the size of the helmet structure.

In order to obtain the best possible performance from a bow-tie antenna mounted under these conditions, a configuration using two identical bow-tie antennas is used. These are mounted on each side of the helmet, having their elements oriented as nearly vertical as possible. They are separated from the thermal garment ground plane by one inch of low loss foam. Their ends extend from the top center of the helmet to an area just over the ear position. Each element is center fed with a balanced line and connected to a coaxial line through a matching balun. These elements, their baluns, and connecting lines are identical units in their electrical design. They are driven in phase from a balanced tee power divider.

Radiation patterns are shown where the twin bow-tie antennas are placed on a simulated helmet and visor protector. Aluminized mylar separates the antenna from the helmet. The baluns are extended through the helmet interior to prevent their affecting the radiation field. In a final design, these baluns would be the coaxial type following the contour of the helmet. The patterns are shown in Figure 36. The minima observed in the azimuth patterns are caused by the array factor of the two antenna elements.

Placing the antenna on the space suit mockup results in further degradation of the pattern as shown by Figure 37. These patterns represent the antenna in its most optimum form when mounted in this configuration. The reason for the deep nulls is found by scanning the suit with a current probe and locating current maxima at various points. These currents result in spurious radiation sources. A great deal of effort was devoted to eliminating the suit currents by means of various chokes in and over the thermal garment and by chokes in the transmission line cable. However, this problem cannot be easily overcome, and thus this arrangment represents the best arrangement for

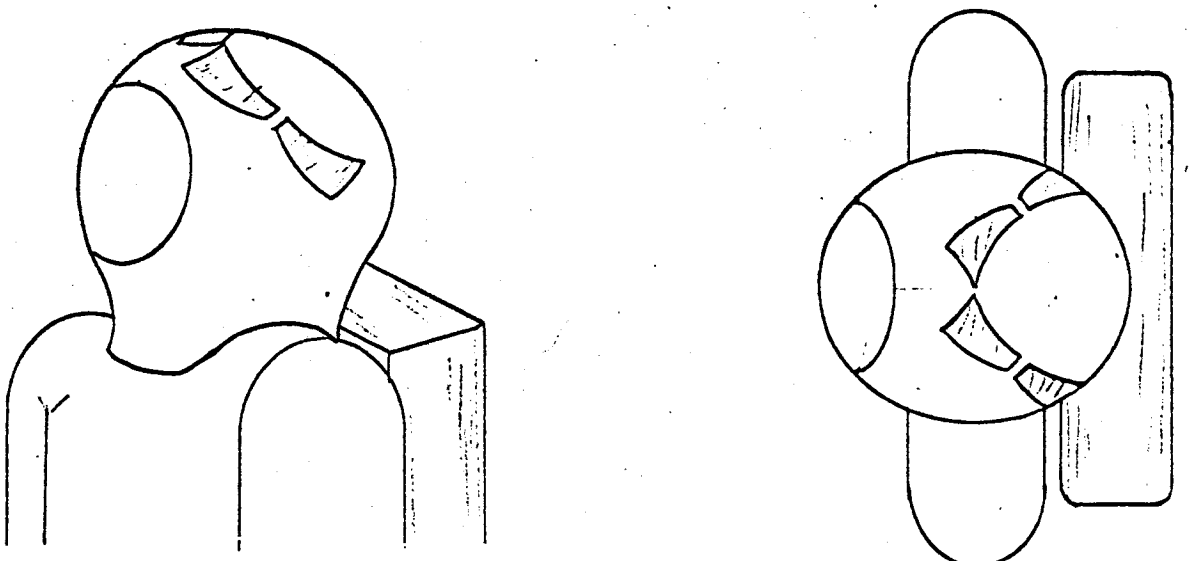

CROSSED BOW TIES FOR VERTICAL POLARIZATION

a.

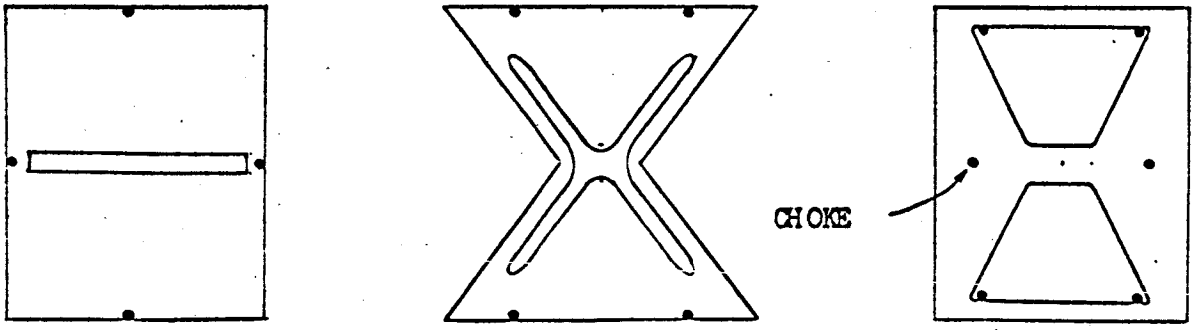

SLOT FED FOLDED SLOT FED CHOKE-MOUNTED

TYPES OF "BOW TIES" (DOTS INDICATE TIES TO GROUND)

b.

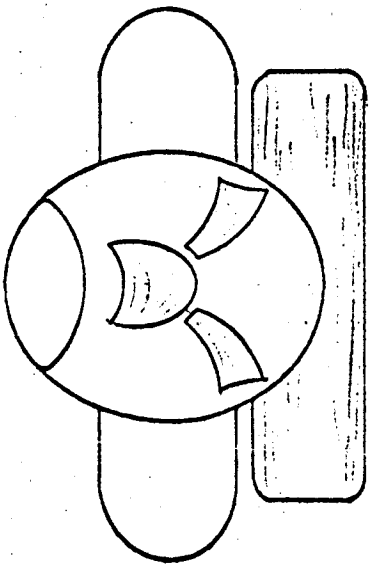

TWO CROSSED "BOW TIES" COMBINED

c.

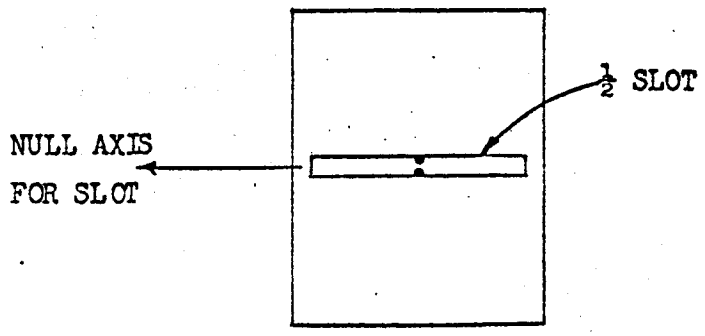

FAT BOW TIE, SLOT FED, MOUNTED ON SIDE OF HELMET

d.

FIGURE 35.

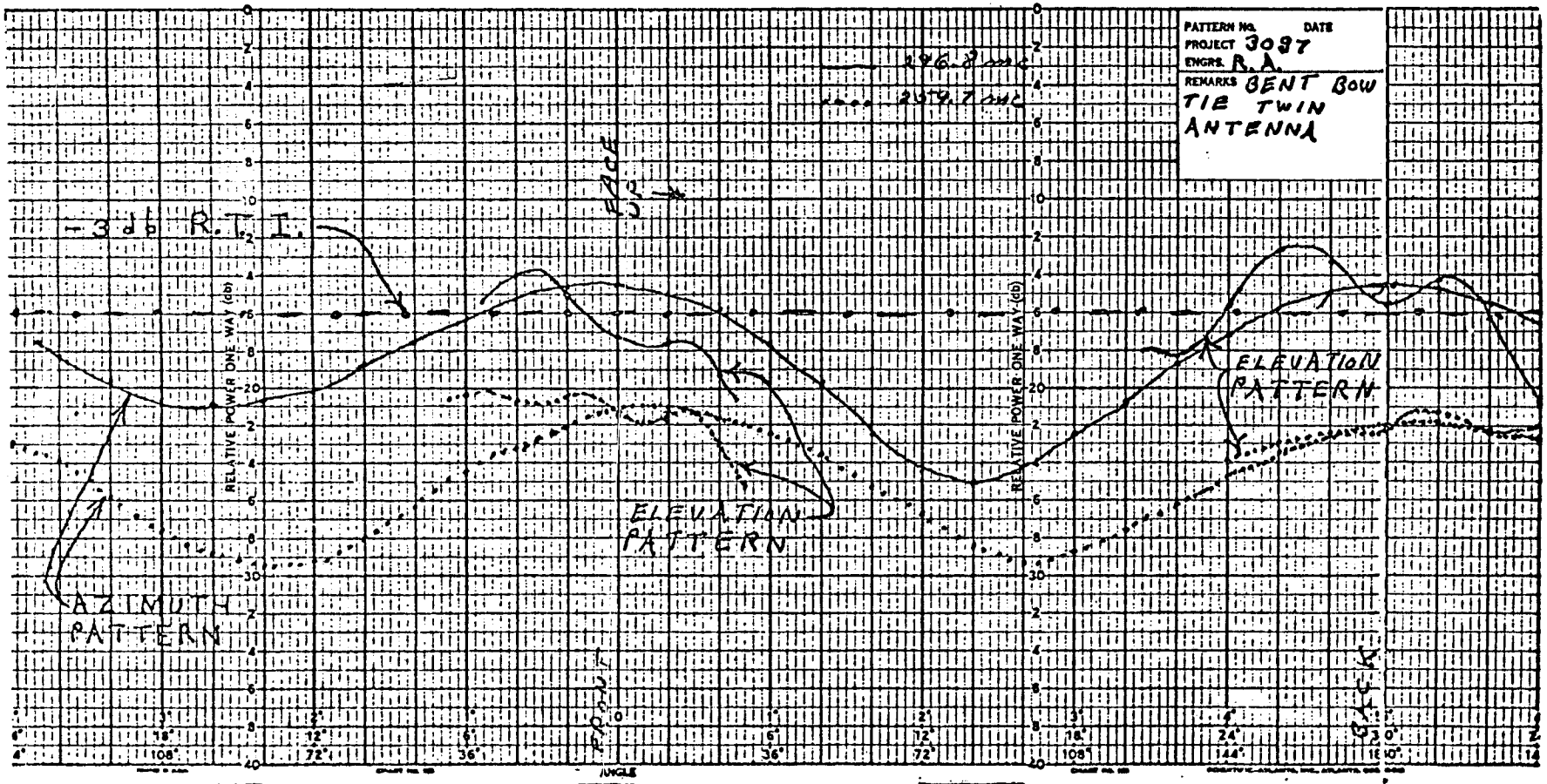

Figure 36. Radiation Patterns of Twin Bent Bow Tie Antennas Mounted on Helmet

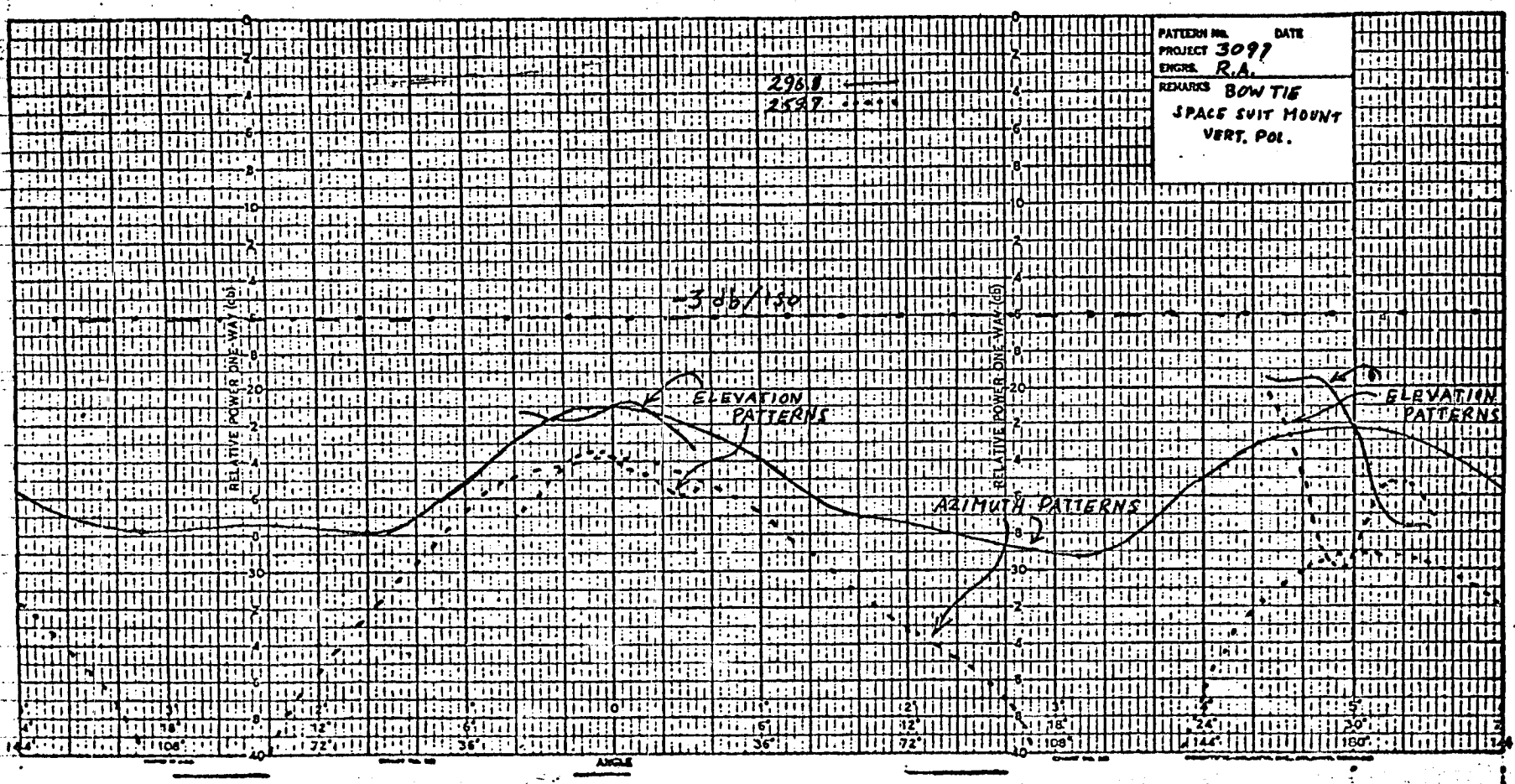

Figure 37. Radiation Patterns of Twin Bent Bow Tie Antennas Mounted on Space Suit Mockup

the bow-tie antenna without going to more elaborate arrays requiring complex feed systems.

3.3.9 Slot Antennas

Slot antennas offer a complete flush mounting capability and thus were given an evaluation for this study. To obtain vertical polarization requires that a slot antenna be mounted horizontally. The pattern of a slot antenna is omnidirectional in the plane normal to the long dimension of the slot with the E-field parallel to the plane, and nulls appear off each end of the slot. Thus, to obtain an omnidirectional vertically polarized pattern requires at least a pair of slot antennas in the horizontal plane and one slot 90 degrees (in the horizontal plane)from the other, that is "crossed slots." The slots also have 90 electrical degrees between them. An air filled resonant slot is approximately 20 inches long; and if this dimension was reduced by half by dielectric loading, it would still be large. For this loaded antenna, a depth of 5 inches would be desired; however, this could be reduced some with a corresponding degradation of input impedance (VSWR). In any event, a depth of 2 or more inches would be required. In view of the large volume required by a crossed slot pair to obtain the necessary radiation pattern, the slot antenna was not considered.

3.4 INVESTIGATION OF ERECTION-RETRACTION MECHANISMS

Erectable-retractable antennas will have inherently lower reliability because they must have movable mechanical and electrical components. By proper choice of materials and methods, the reliability can be maximized if this design should evolve as the mounting scheme yielding the optimum performance. The problem of material specifications is multiplied for erectable antennas. Problems such as flexing and shock at very low temperature, cold welding of similar materials at very low pressures, etc., compound the design problems. Another distinctive disadvantage of this type antenna is the larger volume required to accommodate it and its erection/retraction mechanism.

3.4.1 Helmet Systems

Several helmet mounted erectable antennas are considered. The type with the most merit mechanically is the simple spring mounted whip, as shown in Figure 38a which is restrained by a dielectric cord until the astronaut is outside his spacecraft, at which time he can release it by merely releasing the cord. When he wishes to re-enter the craft, he again pulls the cord and attaches it to a pin, hook, or other fastener. It may be possible that the antenna will not need to be retracted but can be left extended. As the astronaut dons his thermal garment and visor protector, the antenna will be in place and, being spring mounted, will not be damaged during impacts which may occur during missions out of and back into the craft. Both of these types have very high reliability because of their simplicity.

Another type employs the same flexible wire whip except that for storage it is pulled down into a tube mounted to the helmet (see Figure 38b). This would be erected and retracted by pulling on one or the other of the 2 cords. This design would require a sliding RF connection or a flexible cable attachment to the whip.

Figure 38c shows a monopole which consists of an aluminized mylar cylindrical envelope which would be extended by releasing a coiled spring

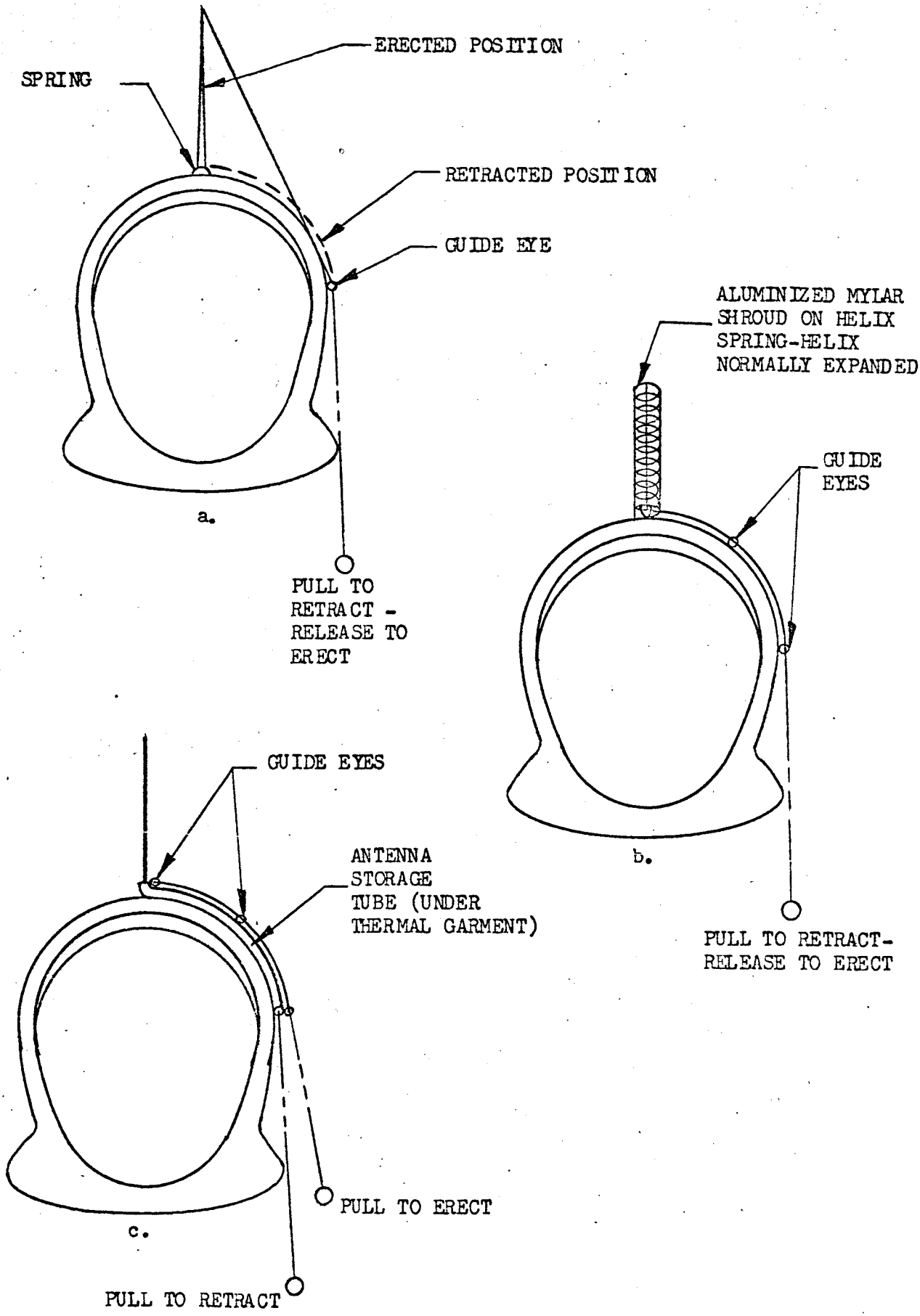

FIGURE 38
ERECTABLE-RETRACTABLE HELMET ANTENNAS

inside the envelope. Retraction is accomplished by pulling a cord which compresses the spring into a cylinder of minimum height. No movable RF connection is required. The mechanical design and implementation would be less difficult than the whip monopole, and the reliability would be high because of its relative simplicity.

A similar aluminized mylar envelope could use air pressure from the suit as the erection mechanism. (See Figure 39b). This method is not highly recommended because of the possibility of leakage, valve problems, and susceptibility to damage.

A spool of very thin heat treated beryllium copper which forms itself into a long cylinder when unrolled (see Figure 39a) is a consideration for this application. A similar type is used on the Canadian "Alouette" satellite which extends monopole arms to 75 feet.

The last type considered is a steel rule type which extends and retracts similar to its namesake (see Figure 39c). It could be extended or retracted by pulling on one or the other of the two cords, or possibly one depending on the design of this mechanism. This would require a movable RF connection which reduces its reliability.

Figure 40 is an example of a helmet erection-retraction system.

The antenna consists of a thin metal strip which is attached to an RF connector at its lower end and is operated by pulling a bead-chain. The radiating element is made from a 6 mil thick strip of beryllium copper, 0.4-inch wide, formed and heat-treated in a shape similar to a common flexible steel measuring tape. The tape is permanently attached to an RF connector and is wound around it approximately three times. In the retracted position, the tape is stowed inside a housing made from plexiglass. The antenna element is perforated at intervals along its center line to match a dielectric bead-chain, against which it is held tightly for a short interval. As the bead-chain is pulled, the antenna element is drawn out of its storage cavity and pushed upward into its operating position. To retract the element, the other

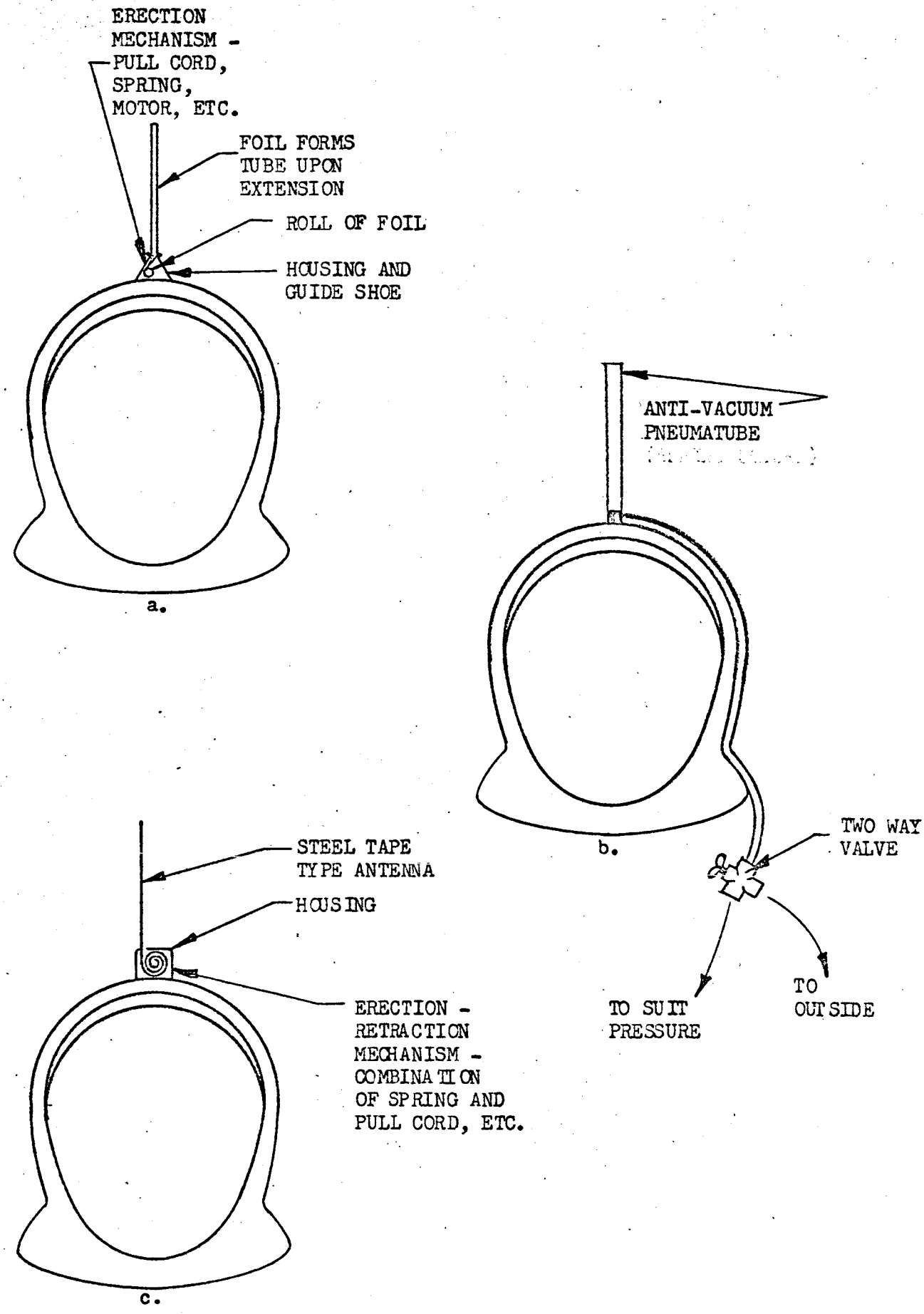

FIGURE 39
ERECTABLE-RETRACTABLE HELMET ANTENNAS

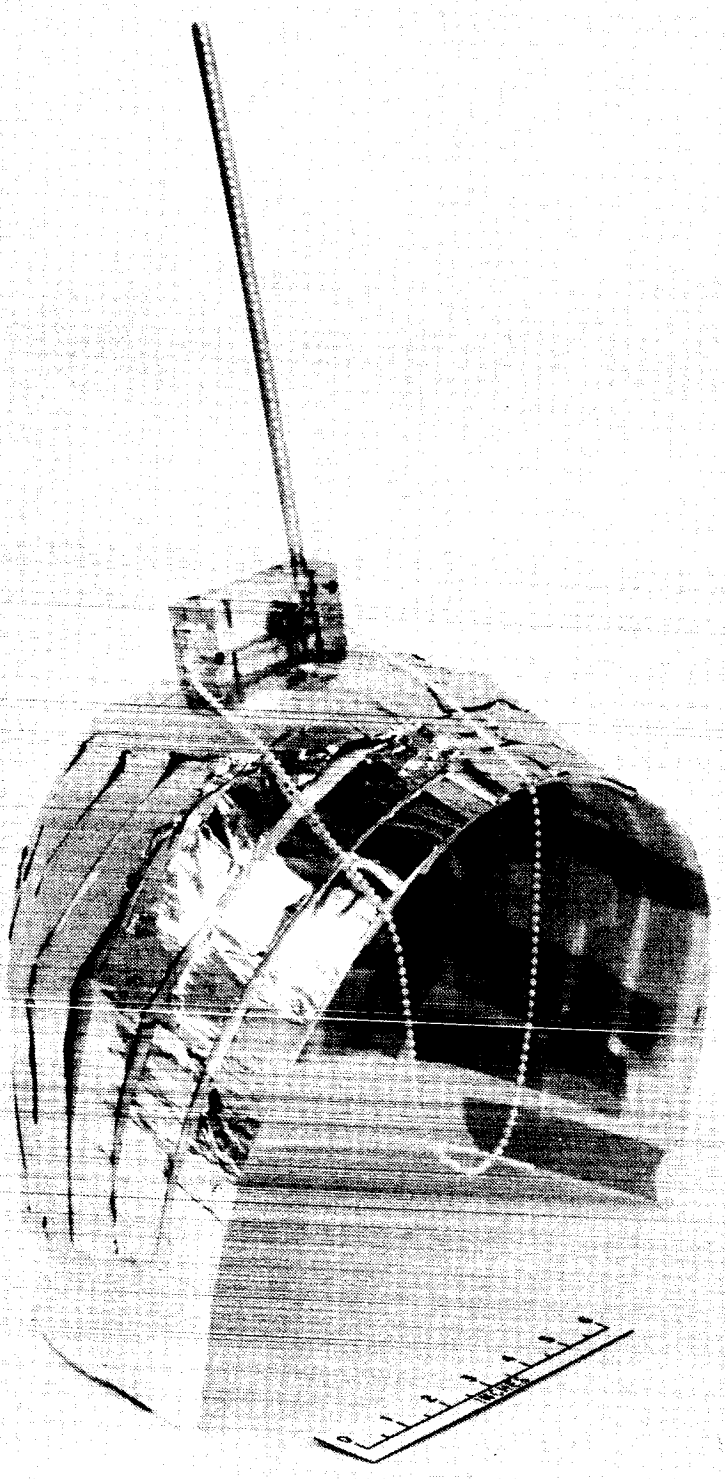

Quarter Wavelength Whip Antenna With
Erect-Retract Mechanism On Dielectric
Helmet Spacer

end of the chain is pulled until the element has been completely drawn into the cavity. The retraction device is contained in the plexiglass housing. The experimental model measures 3 x 1.25 x 1 inch; however, these dimensions can be significantly reduced in a prototype model.

Another helmet erection-retraction technique is shown in Figure 26.

The spring monopole antenna is made up from a flexible conductive envelope, a supporting spring, a cord for retracting, and a ground plane with provisions for RF connections. The conductive envelope is made from one mil aluminized mylar having a vacuum-deposited film of aluminum on each side. This mylar is formed into a cylinder and bonded with mylar tape. The spring is made from heat-treated beryllium copper. The spring has wires soldered across the inside which contain loops at the spring center through which the retraction cord is guided. The retraction cord is of woven nylon material. The conductive cylinder is applied around the spring and fastened top and bottom with thin aluminum caps. This assembly is fastened to the ground plane through teflon insulators. The RF cable is attached to the bottom of the ground plane and to a screw on the radiating element which projects through the ground plane. The operating cord is also run through this screw. The antenna is retracted by pulling the nylon cord, and is erected by releasing the cord. A spring-loaded locking device holds the cord and thus the antenna in the retracted position. The lock is released by pulling on a second cord.

3.4.2 PLSS Systems

The major reason for using an erectable type antenna system on the PLSS is to raise the radiator to the height above the helmet and its associated visors, shields, and thermal garment. The erected support mast will extend further above that height. Because of the high reliability requirements, a simple erection mechanism is desirable and it, too, must be implemented with controls in the chest area of the suit. The two major problems associated with this configuration are the erection mechanism itself and the RF connection to the movable antenna.

Figure 41 shows an arrangement of the system that requires a simple pulling motion to erect the antenna and a similar motion on another cord for retraction. The antenna slides up and down inside a tube which may be either inserted into the PLSS package proper or may be mounted external to it. The slack in the pull cords is taken up by winding on a spring-loaded wheel inside this tube. The system is completely manual so that reliability is at a maximum. If the antenna is slightly damaged during egress, it can still be operated by applying a greater than normal amount of force on the pull-cord. Construction will be of aluminum alloy with dielectric materials as required.

A variation of this design is shown in Figure 42. In this design, the erection is accomplished by releasing a coiled spring, again by pulling a cord. Retraction is manual as in the system above.

Several variations of these systems are possible, the difference being the method for erecting and retracting the antenna. This could be done with springs, electric motors, hand cranks, compressed gas cartridges, etc., but the reliability goes down as the complexity increases.

Another possible configuration (see Figure 43) consists of an antenna, completely external to the PLSS, which is folded along the side of it and swings either around to one side for the back and up to a vertical position. This, again, can be accomplished by either manual pull-cords, or a combination of mechanisms as noted above. This requires much more volume in which to erect the antenna.

The RF feed for these antennas may be any of those shown in Figure 44. Figure 44a is a plug-receptacle type which requires good alignment and complete extension of the antenna for operation. If volume is available, a slack cable would be the simplest and most reliable type of connection as shown in Figure 44b. The temperatures in which standard cables may be operated are within the temperatures expected within the PLSS. Either an RF rotary joint or a cable which bends or twists may be used for the antenna shown in Figure 44c.

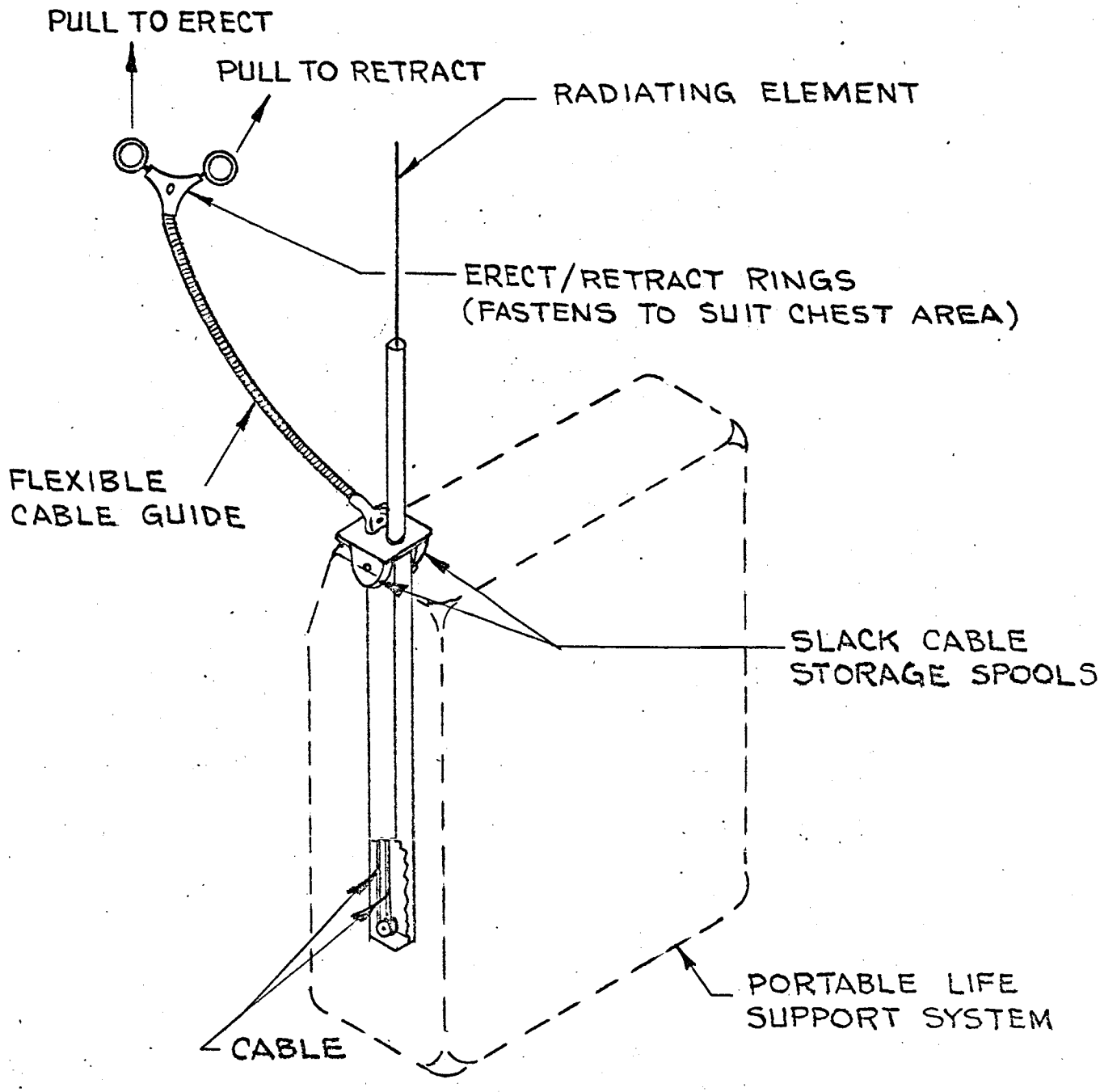

FIGURE 41 MANUAL ERECTION / RETRACTION.

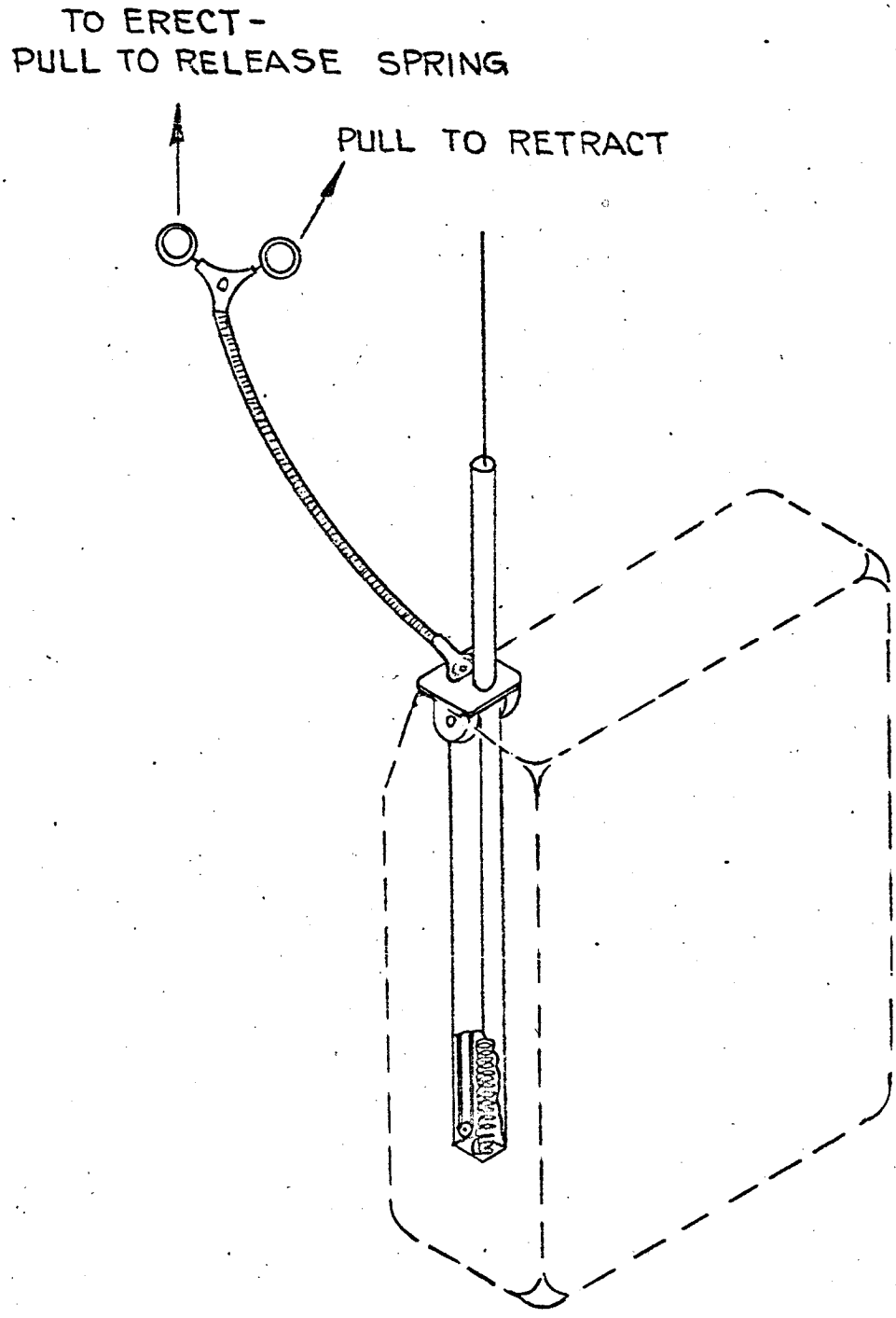

FIGURE 42. AUTOMATIC ERECTION, MANUAL RETRACTION SYSTEM.

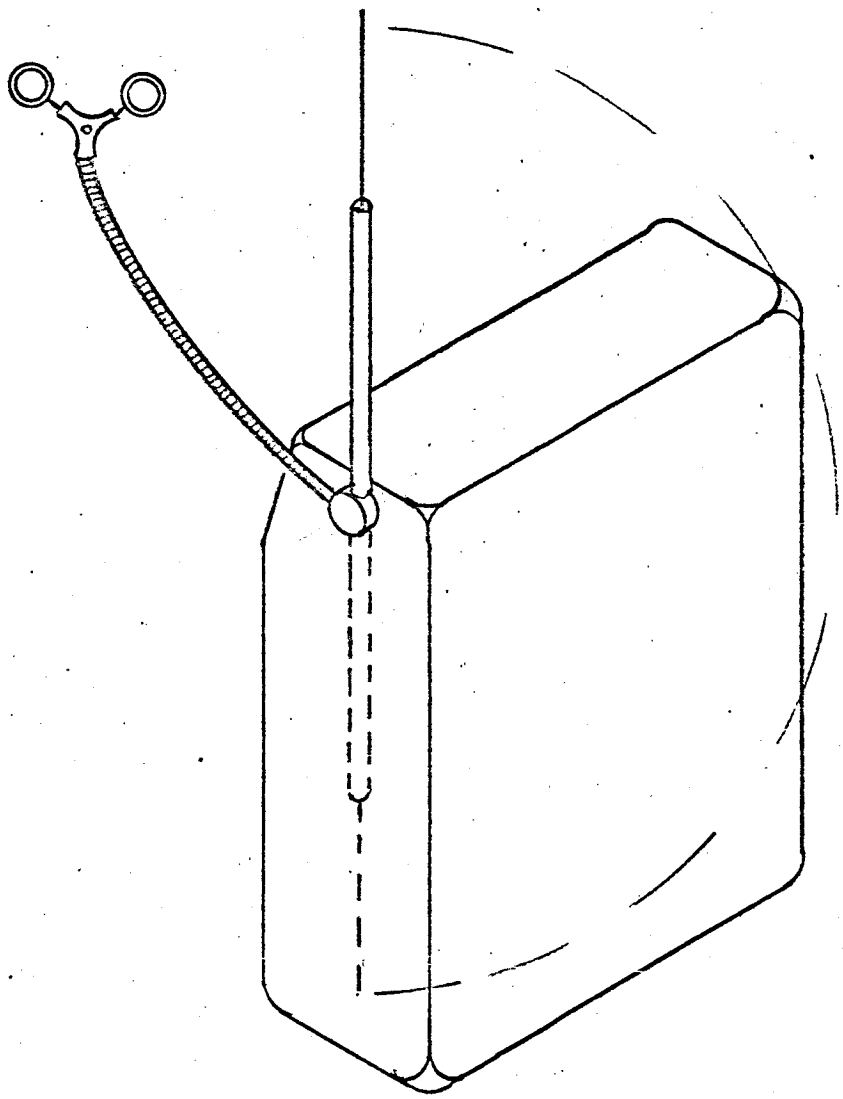

FIGURE 43
MANUAL ERECTION/RETRACTION SYSTEM
WITH PIVOTED ANTENNA

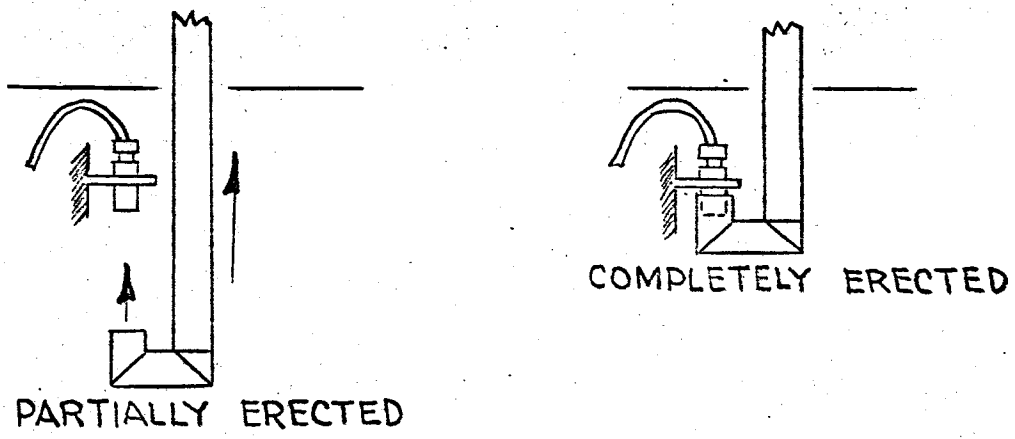

a-

b-

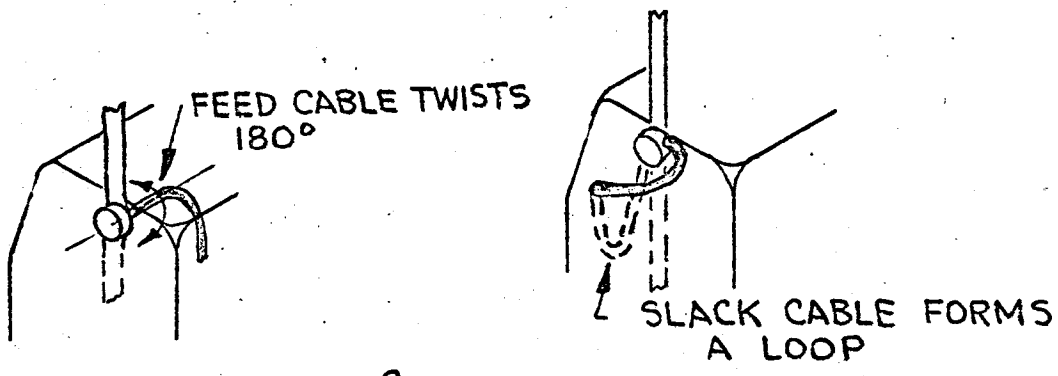

c-

FIGURE 44
PROPOSED FEED SYSTEMS

An example of a PLSS erection-retraction system is shown in Figure 45. Here a discone antenna is employed on a manual erection-retraction system similar to that shown in Figure 41.

The discone antenna is fabricated using 6 mil thick by 0.4-inch wide heat treated beryllium copper, formed on a 0.38-inch radius arc across the 0.4-inch width as the cone elements and 4 mil thick material for the radial disc elements. The elements are fastened at their bases to small machined cones and held in place by machine screws. The support/mast for this assembly is a section of rigid, teflon-insulated, coaxial line. The "disc" section is actually a cone with a 64° apex angle, with the apex upward, thus forming a biconical antenna, rather than a common discone.

The erection/retraction mechanism consists of a closed loop cable which runs through guides, around pulleys, around the neck of the astronaut and is fastened to the antenna. This arrangement is similar to that shown in Figure 41. The antenna retracts into an epoxy-bonded fiberglass tube 29-inches long. A positive lock has been incorporated into the design which locks the antenna at its upper and lower limits. To erect the antenna, the operator first pulls on both ends of the cable, which is located in the chest area. This pull retracts the locking pin and the antenna is free to move. He then pulls harder on the erecting cable and the antenna assembly will be raised in the tube. As the antenna reaches its erected position, the lock pin snaps into place. As the elements leave the tube, they automatically snap into place. To retract the antenna, the motions are repeated, pulling on the retraction cable until the lock pin snaps into place. On retracting, the elements hit the edge of the tube and are folded into place as they are further retracted.

The erection/retraction mechanism is now designed for the discone antenna model with horizontal disc elements. When the elements were changed to point 58° downward from their mounting point, the folding problem was compounded. The elements must bend through a greater angle and thus are subjected to greater stresses. A partial model has been made of a mechanism

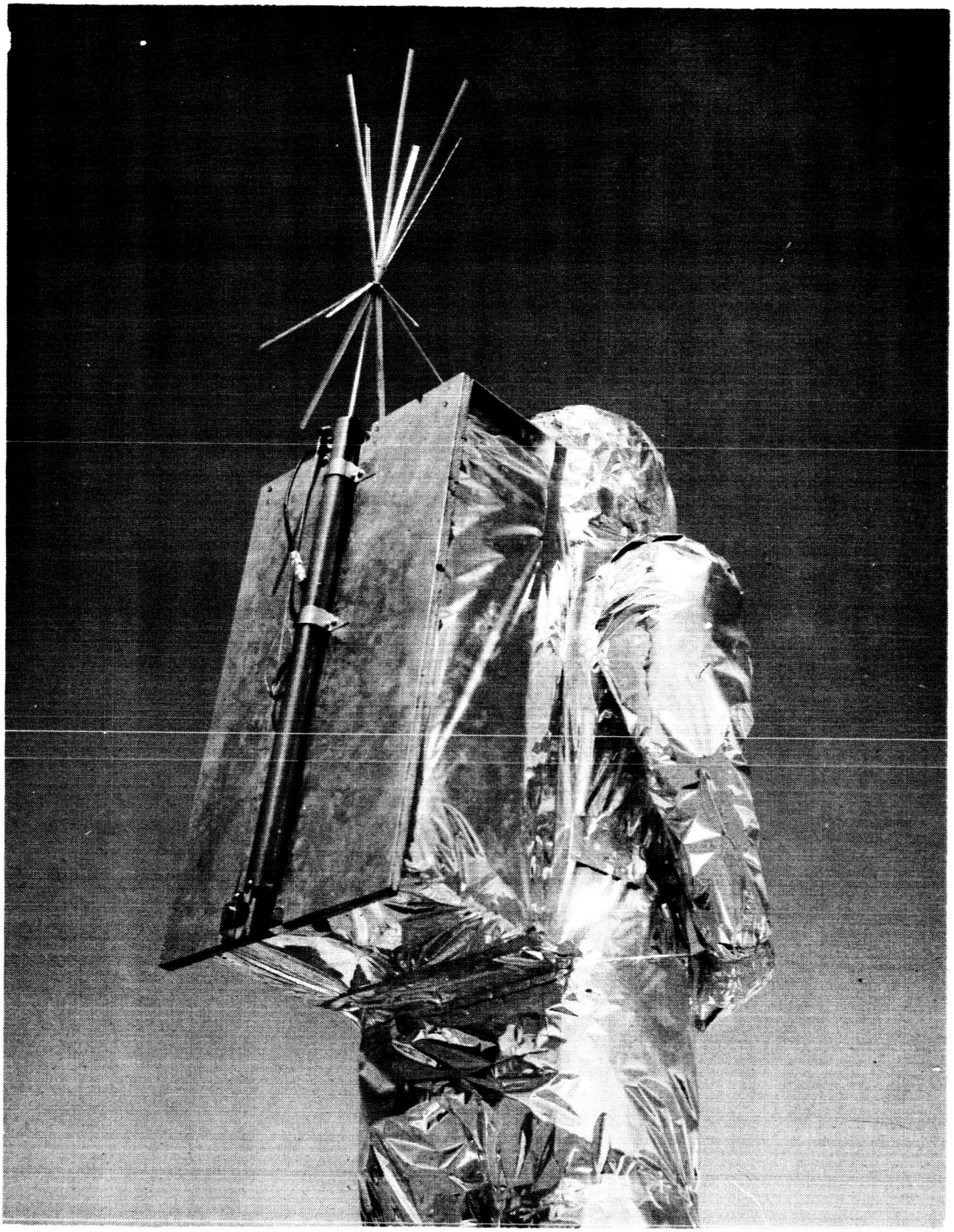

Discone Antenna System on PISS
Showing Erection/Retraction Mechanism

which demonstrates that these elements may be folded downward against the support before being retracted into the tube.

3.5 DETAILED EVALUATION OF THE TRANSMISSION LINE ANTENNA

The desirable mechanical and electrical properties of the dual frequency transmission line antenna defined earlier in the program and described in Section 3.3.1 dictated that a further evaluation of this antenna be made. Consequently the transmission line antenna was developed into an engineering prototype model. This effort consisted of designing the engineering model of the transmission line antenna described in Section 3.3.1 into an engineering prototype antenna. Specifically, the antenna ground plane size and shape were defined and a protective cover was provided. Also a method of attaching the antenna to the PLSS thermal garment was defined.

Measurements were made of the antenna's VSWR and radiation pattern using various fabrication and mounting techniques. These measurements indicated the antenna's ground plane size and shape have negligible effect on the overall performance. However, it was found that a positive RF coupling must be maintained between the antenna ground plane and the PLSS thermal garment. As a final design a four-inch diameter ground plane, 0.064 inch thick was used. The antenna was potted with a foam-in-place polyurethane material and an epoxy-fiberglass radome was provided. A small slit is placed in the PLSS thermal garment cover to allow protrusion of the antenna cable and connector.

Electrical performance tests were made on the completed antenna design. These tests included antenna radiation patterns and impedance. The tests were made with the antenna mounted on the top surface of the PLSS, located at its approximate center. Measurements were made at the Motorola Antenna Pattern Range Test Facility and were supplemented with anechoic chamber radiation pattern tests. The purpose of these tests was to verify the antenna design and to show its electrical performance for the specific mounting method.

Measurements of VSWR show the following results:

Frequency Mc	VSWR
258.08	1.3
296.80	1.5

To determine the antenna's radiation level over the volume of interest, radiation patterns were taken about the antenna's vertical (Z) and horizontal (X) axis. All measurements were made with the antenna/mockup oriented according to the coordinate system of Figure 46. The patterns taken about the Z axis were taken at values of θ = 70, 80, 90, 100 and 110°, while those taken about the X axis were taken at values of θ measuring from 0° through 360° at 45° increments. The data were reduced to a contour plot showing levels of radiated power relative to an isotropic radiator. Angles of θ are plotted along the ordinate and angles of ϕ are given on the abscissa. These data are shown in Figure 47 and 48 for frequencies 296.8 Mcs and 258.08 Mcs respectively. The contours shown are for radiation power levels lying between +2 and -10 dB at 2 dB increments. The percentage of the total area covered by the respective 2 dB increments are shown in the lower left hand corner of each figure.

Following a study of this data a study was undertaken to improve the performance of the transmission line antenna by relocating it on the PLSS. This relocation would attempt to decouple the antenna as much as possible from the thermal garment of the space suit. Following a brief empirical study of mounting methods, the antenna was raised from the thermal garment of the PLSS 2.5 inches. The 4-inch ground plane was supplemented with a separate ground plane extending out from the antenna 5.5 inches to either side and approximately 10 inches over the back of the PLSS, where it was separated from the PLSS thermal garment by a 1-inch layer of foam. The results of this relocation are shown by a contour plot of radiation power levels shown by Figure 49 and 50 for each of the respective frequencies. In each instance the relocation caused a slight change in the optimum frequency of operation.

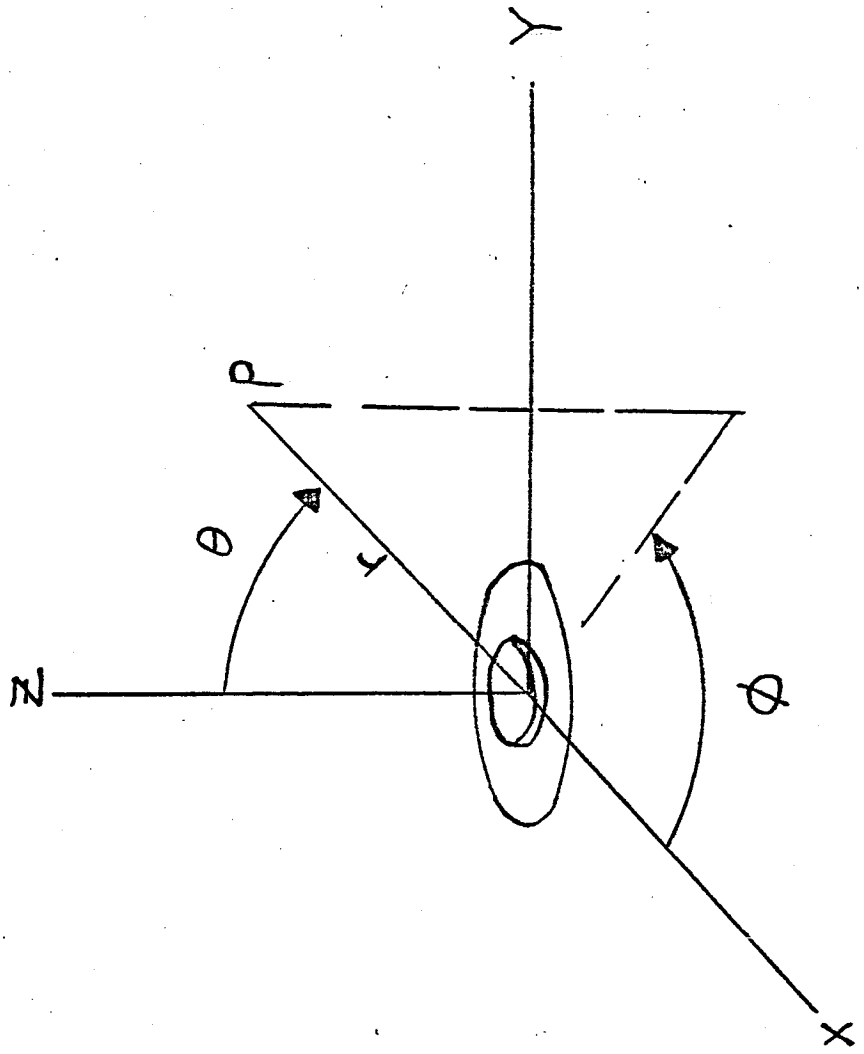

FIGURE 46.

Coordinate System

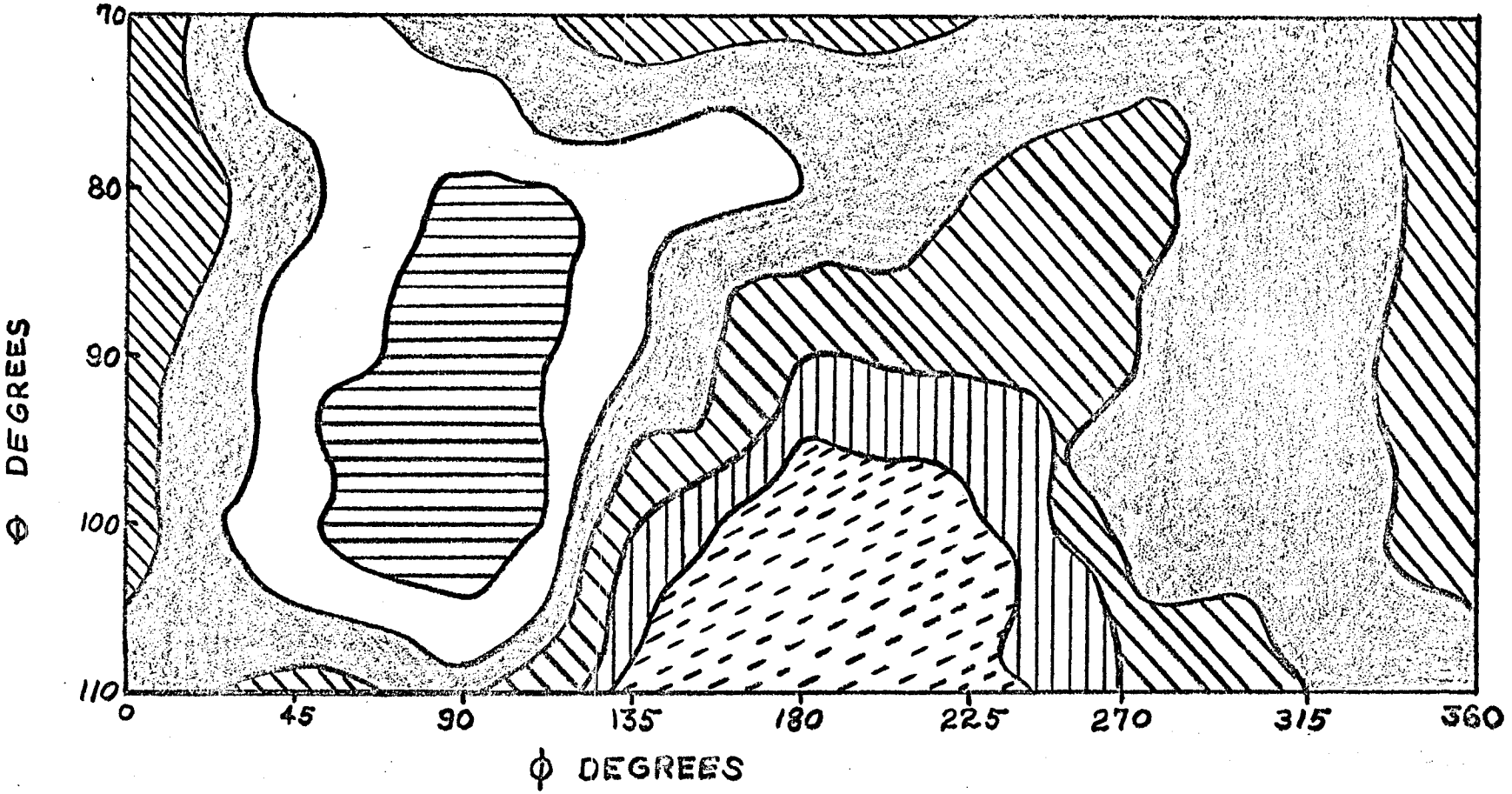

2 →	0	9.5%
0 →	-2	6.8%
-2 →	-4	23.0%
-4 →	-6	40.5%
-6 →	-8	13.7%
-8		6.4%

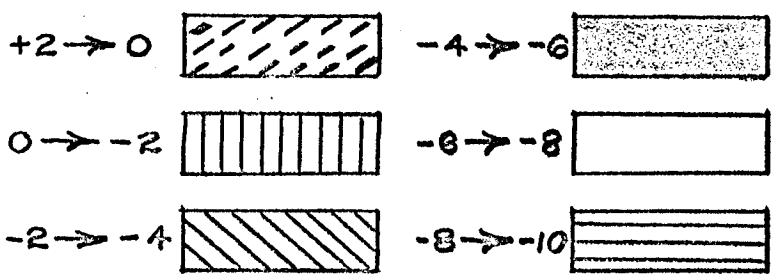

Figure 47. Contour plot showing radiation power levels (in dB) of transmission line antenna over ± 20° of the horizon for all angles of azimuth. Frequency = 296.8 Mc.

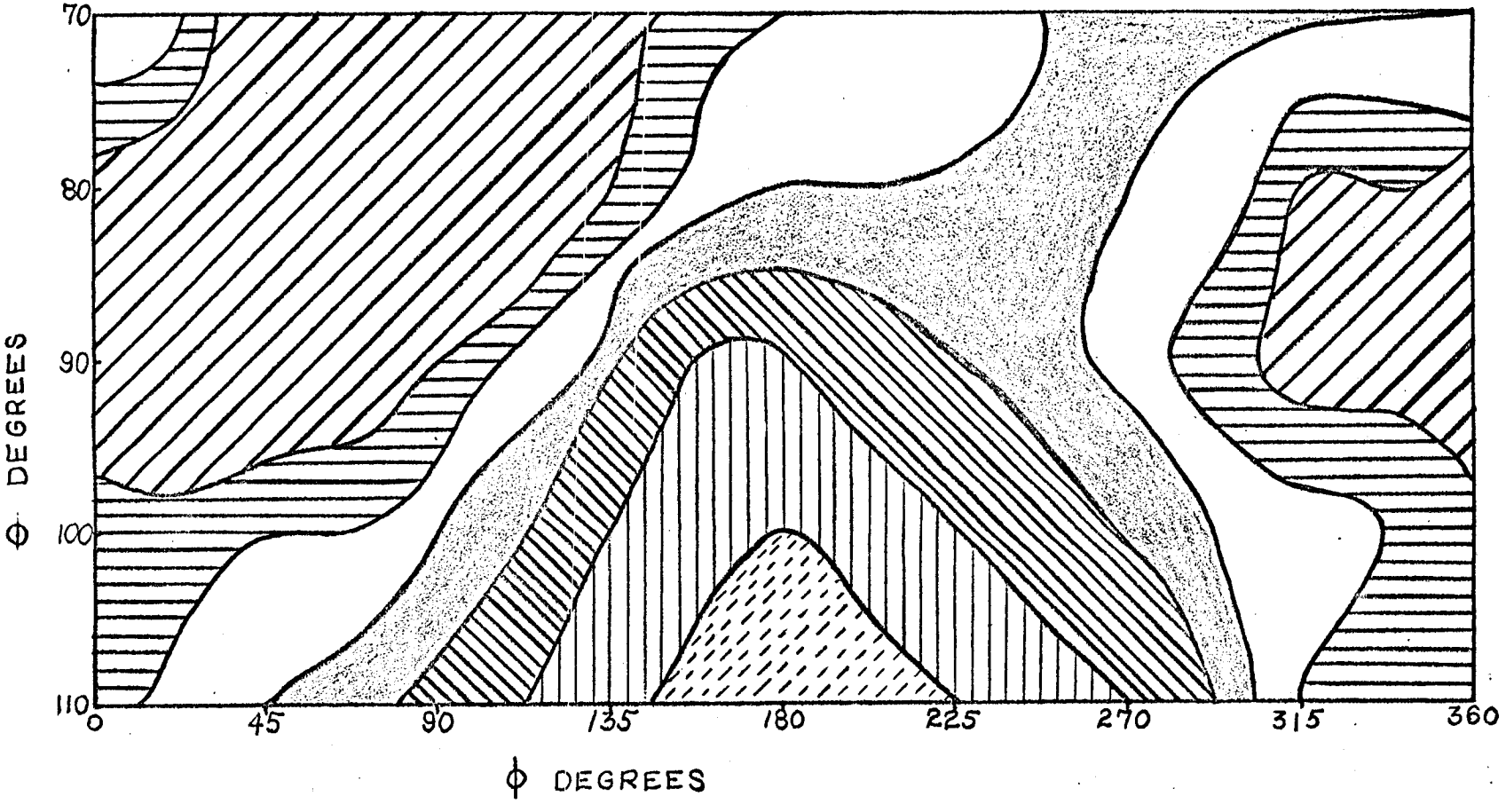

2 → 0	2.8%
0 → -2	9.8%
-2 → -4	11.0%
-4 → -6	15.3%
-6 → -8	20.3%
-8 → -10	16.4%
-10	24.4%

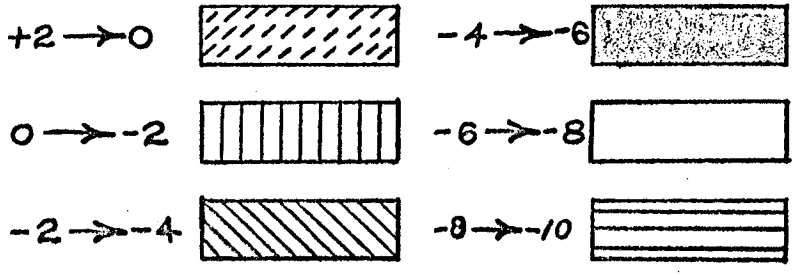

Figure 48. Contour plot showing radiation power levels (in dB) of transmission line antenna over ± 20° of the horizon for all angles of azimuth. Frequency = 258.08 Mc.

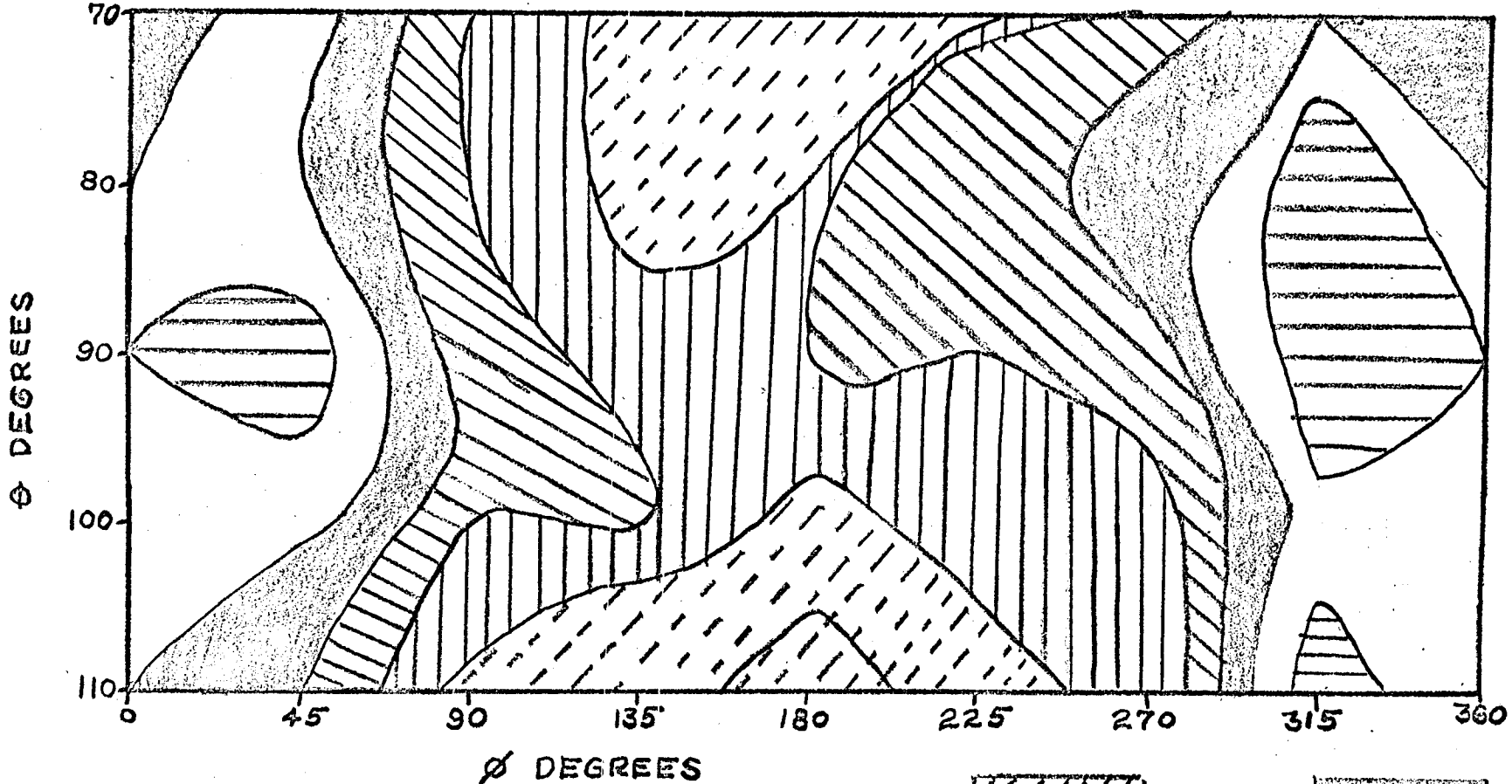

+2→0	8.8%
0→-2	24.0%
-2→-4	20.5%
-4→-6	13.3%
-6→-8	24.9%
-8→-10	8.4%

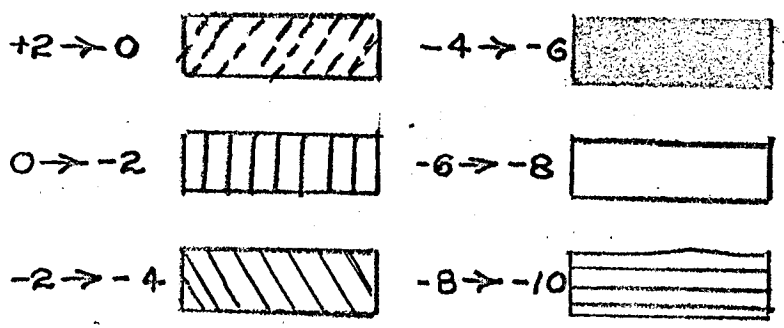

Figure 49. Contour plot showing radiation power levels (in dB) of transmission line antenna relocated 2½ inches over thermal garment. Data shows measurement over ± 20° of the horizon for all angles of azimuth. Frequency = 294.5 Mc.

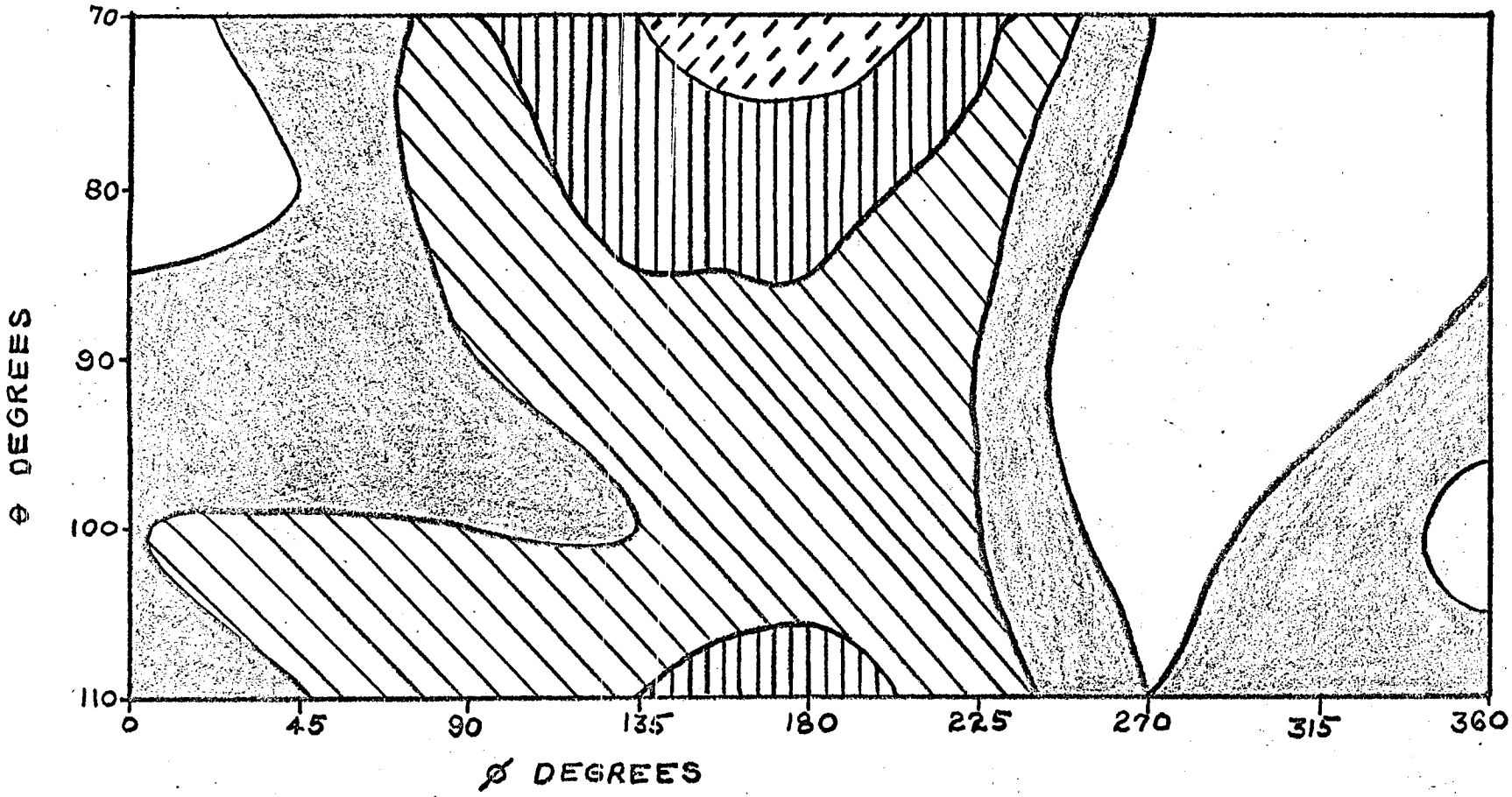

2→0	1.9%
0→-2	10.0%
-2→-4	32.7%
-4→-6	32.0%
-6→-8	23.3%

Figure 50. Contour plot showing radiation power levels (in dB) of transmission line antenna relocated $2\frac{1}{2}$ inches over thermal garment. Data shows measurement over ± 20° of the horizon for all angles of azimuth. Frequency = 257.1 Mc.

Of particular significance, however, is the noted improvement in the operation at 257.1 mcs.

As the antenna development continued the performance of the antennas improved. A later, modified engineering prototype model gave significantly improved performance. This antenna is shown in Figure 51.

This antenna was mounted on the space suit mockup PLSS and tuned for an optimum impedance match at 259.7 Mcs and 296.8 Mcs. Results from this test show the antenna has a VSWR of 1.3 and 1.6 at each of these frequencies.

VSWR tests were also made of the antenna mounted on a 36-inch diameter metallic ground plane. This test shows a high VSWR at the original resonant frequencies. This is to be expected since the antenna was originally tuned on the PLSS. The transmission line antenna is closely coupled to surrounding objects with strong ground currents and for this reason it is reasonable to expect changes in the frequency of operation and impedance as it is moved from one ground plane condition to another. The VSWR test shows the antenna has a VSWR of 1.85 at 259.7 Mcs and 3.0 at 296.8 Mcs. The VSWR at the new resonant frequencies are 1.68 at 259.830 Mcs and 1.36 at 296.032 Mcs.

The modified antenna was tested in an RF anechoic chamber for its radiation pattern. Data from these tests were compiled and reduced to contour plots showing levels of radiated power over the sector of interest relative to an isotropic radiator. These data are shown in Figures 52 and 53 for frequencies 259.7 Mc and 296.8 Mc respectively with the antenna mounted on the PLSS. The contours shown are for radiation power levels lying between +3 and -12 dB at 3 dB intervals. The percentage of the total area covered by the respective 3 dB levels are shown in the lower left hand corner of each figure. For comparison with the performance of a whip antenna, compare the contour plots of Figures 52 and 53 with those for the whip, Figure 16 and 17 of Section 3.3.2. Data taken while the antenna was mounted on a 36-inch

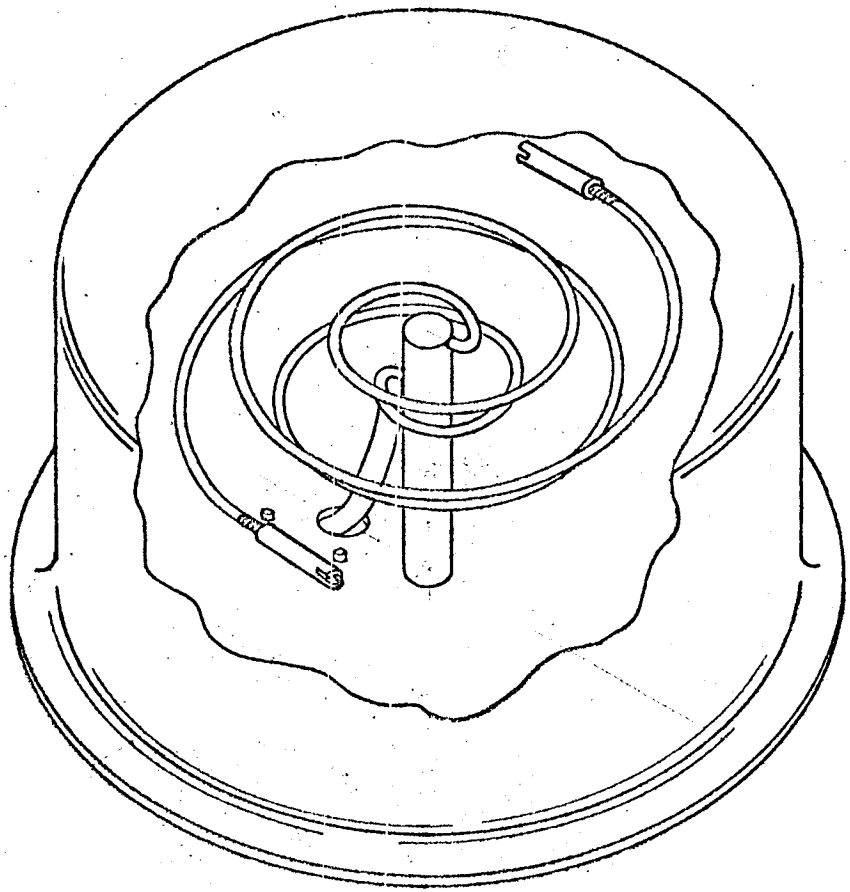

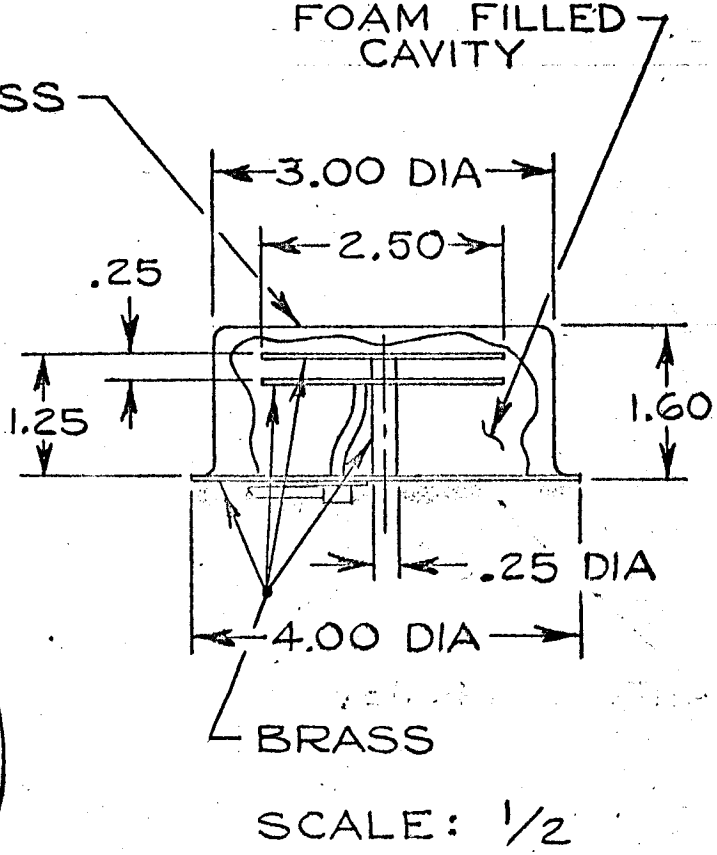

VHF DUAL FREQUENCY TRANSMISSION LINE ANTENNA

FIGURE 51

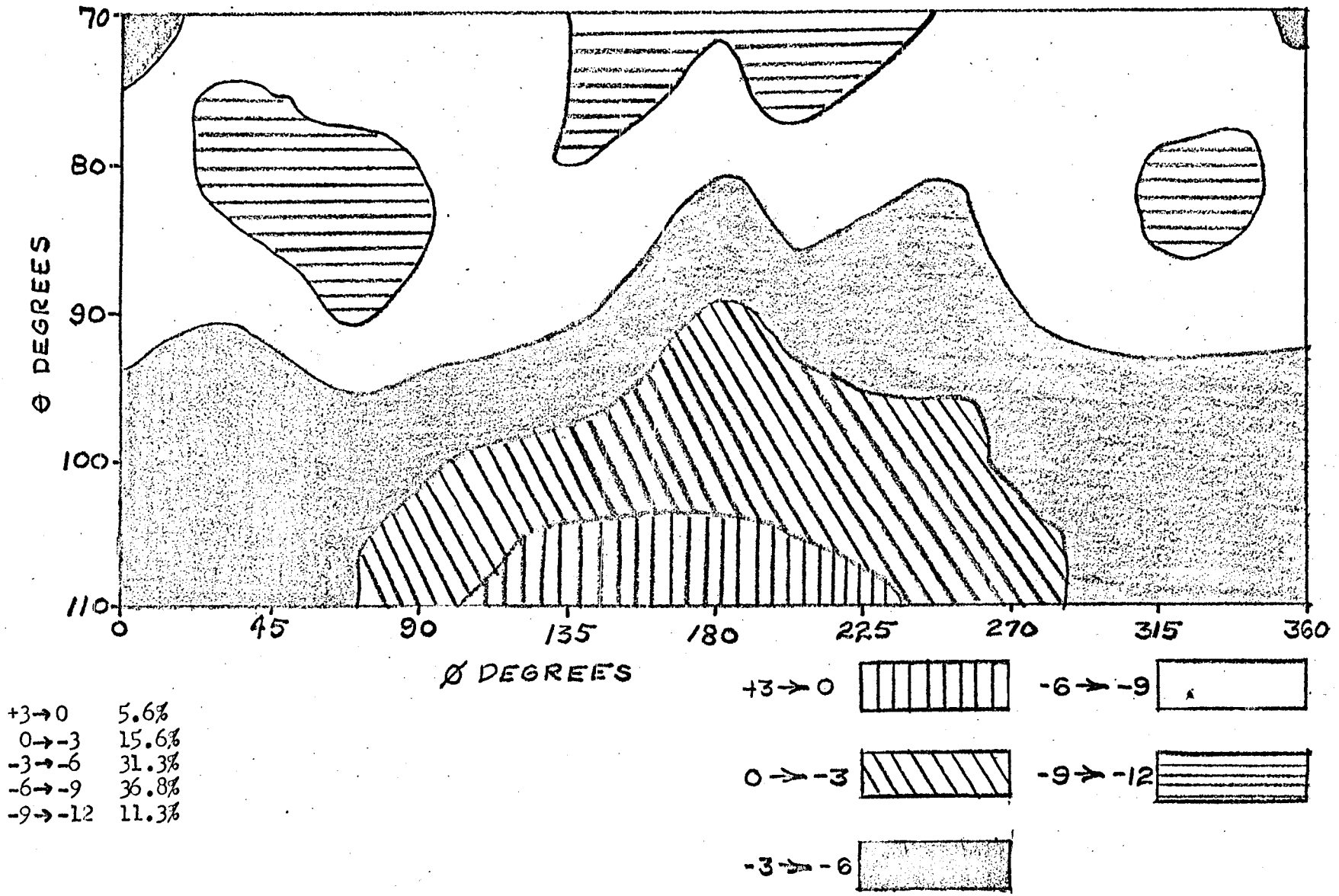

+3→0	5.6%
0→-3	15.6%
-3→-6	31.3%
-6→-9	36.8%
-9→-12	11.3%

Figure 52. Contour plot showing radiation levels (in dB) of transmission line antenna mounted on Space Suit Mockup over ± 20° of the horizon for all angles of azimuth. Frequency = 259.7 Mc.

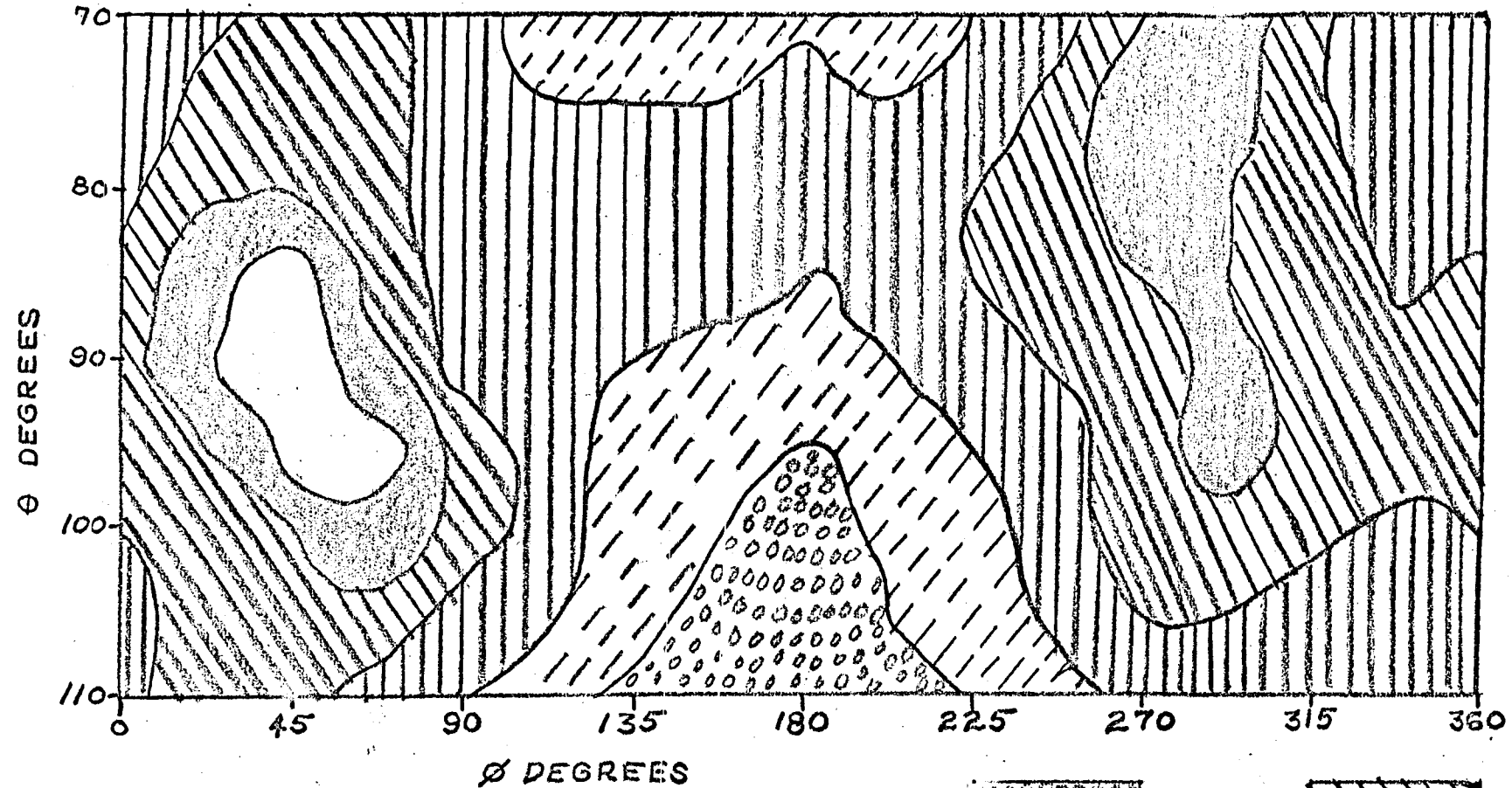

+9 → +6	4.5%
+6 → +3	17.1%
+3 → 0	37.7%
0 → -3	28.8%
-3 → -6	10.0%
-6 → -9	2.2%

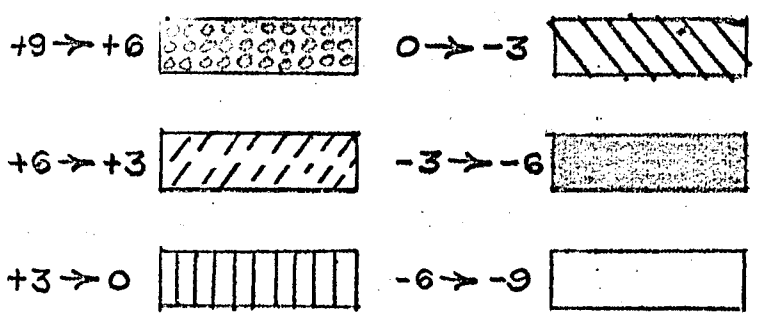

Figure 53. Contour plot showing radiation levels (in dB) of transmission line antenna mounted on Space Suit Mockup over ± 20° of the horizon for all angles of azimuth. Frequency = 296.8 Mc.

diameter ground plane are shown in Figures 54 and 55 for frequencies of 260.92 Mcs and 296.032 Mcs respectively.

In addition to the contour plots individual radiation patterns are also included. These show the in-plane polarization and cross polarized patterns for the antenna as it is mounted on the PLSS and on the 36-inch ground plane at the above frequencies. These data are shown in Figures 56 through 67. Each figure is labeled for its respective sector of interest, polarization, frequency, and method of antenna mounting.

To determine the performance of the antenna under conditions most closely simulating those in actual use, measurements were made with the antenna and the mockup PLSS mounted on a person outfitted with an actual space suit and helmet. For comparison, patterns were also taken with the transmission line antenna replaced by a quarter wavelength whip. The tests were performed in an anechoic chamber. The results are shown in Figures 68 through 73. Data was limited to 0 = 90 degrees $\pm$ 10 degrees due to the difficulty of the subject to remain in position at 20 degrees of elevation or depression. Examination of this data results in two conslusions.

1. Patterns on the mockup space suit and with a person wearing an actual space suit are in relatively close agreement; minimums are within 2 db.
2. The whip performance and the transmission line antenna performance are very similar when mounted on a person wearing an actual space suit; at 260.0 Mc the patterns and gains are almost identical and at 295.82 Mc the patterns are again almost identical with the whip averaging approximately 1 to 2 dB higher than the transmission line antenna.

3.6 FLIGHT QUALIFIABLE ANTENNA FABRICATION

Following completion of the antenna development program Motorola was asked to fabricate and test three flight qualifiable antennas for NASA. The design is based upon the results obtained in Section 3.5, Detailed Evaluation.

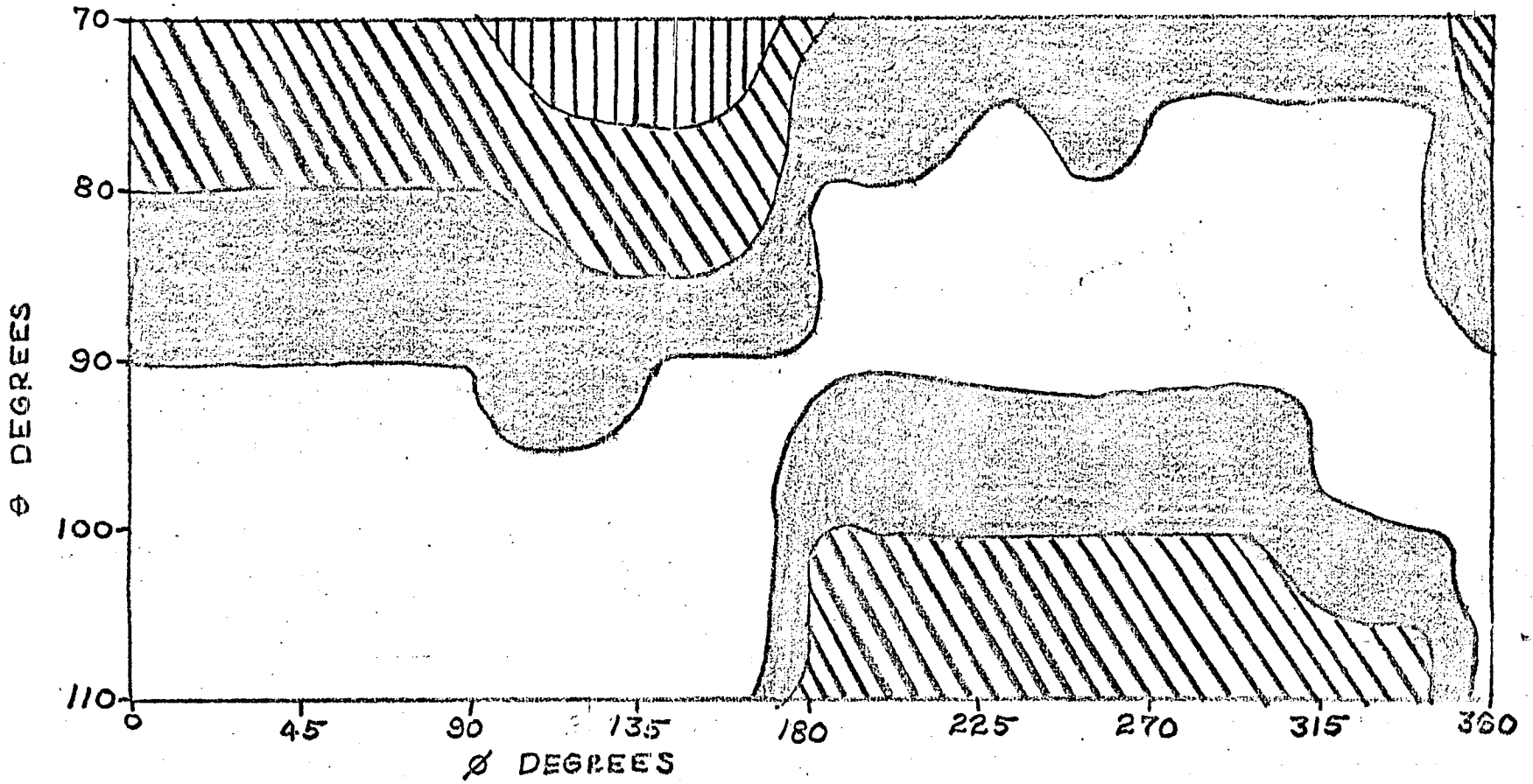

+1 → 0 = 2.5
0 → -1 = 20.6
-1 → -2 = 31.6
< -2 = 46.1

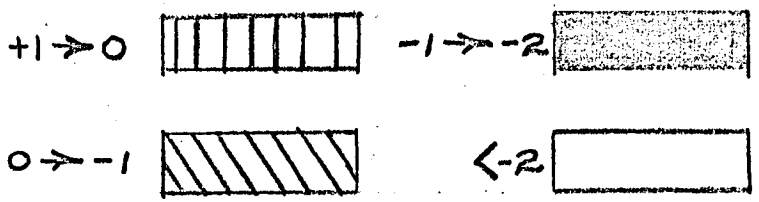

Figure 54

Contour plot showing radiation levels (in dB) of transmission line antenna mounted on 36" diameter ground plane over ± 20° of the horizon for all angles of azimuth. Frequency = 260.92

Contour Interval = 1 dB
Datum Relative to Isotropic

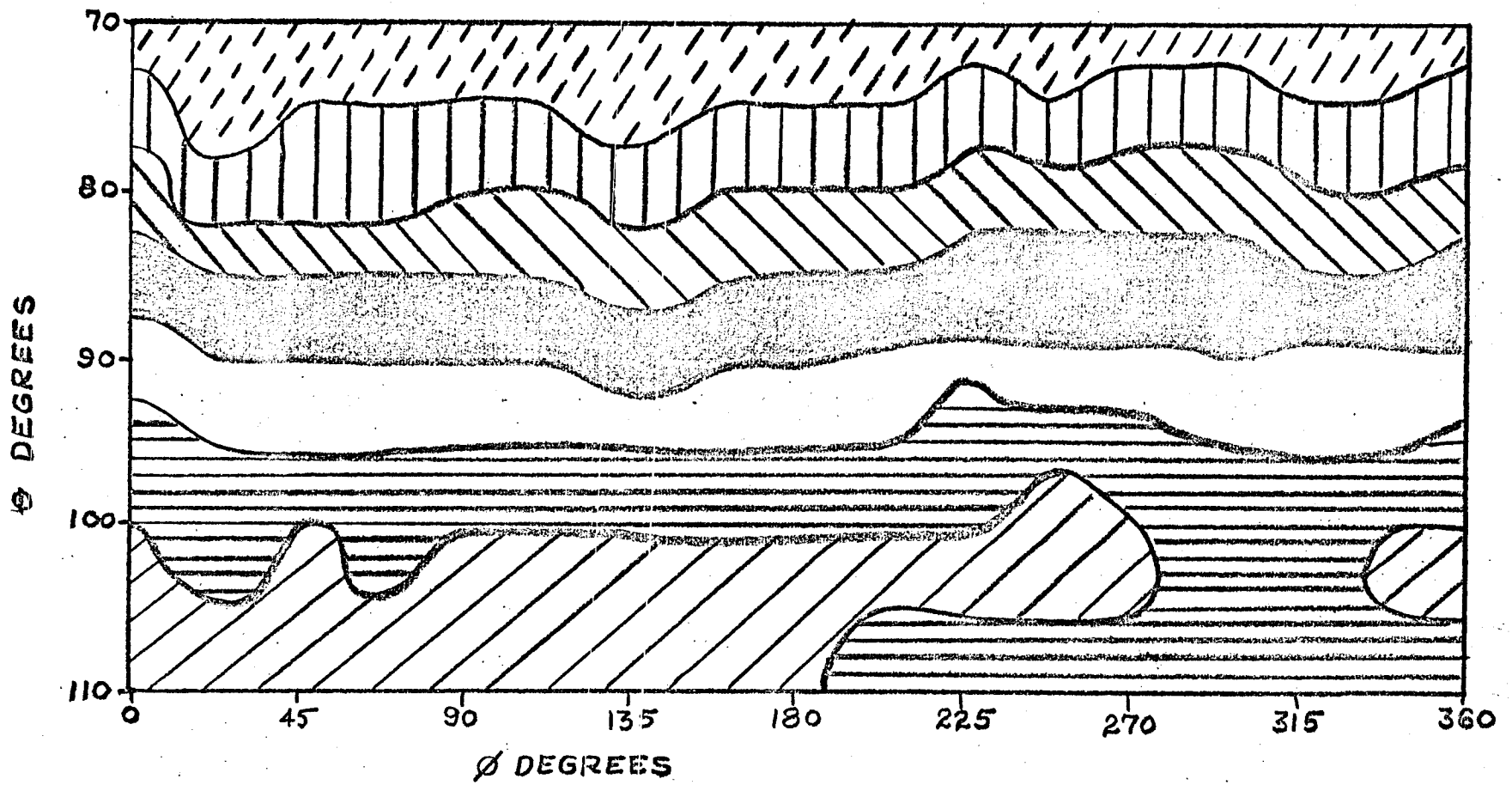

+1 → 0 = 11.5%
0 → -1 = 12.7%
-1 → -2 = 11.1%
-2 → -3 = 13.3%
-3 → -4 = 12.7%
-4 → -5 = 22.7%
-5 → -6 = 15.9%

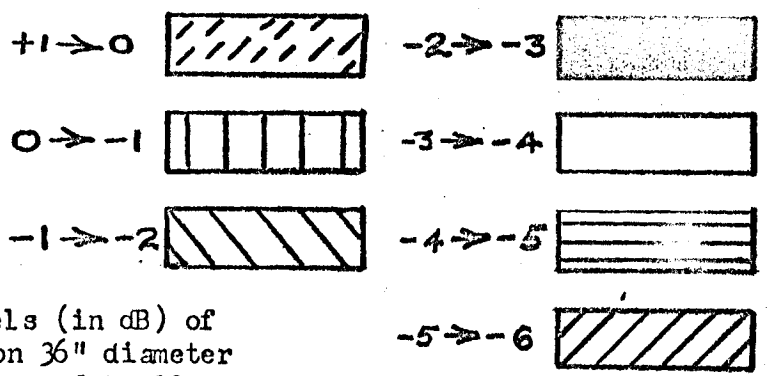

FIGURE 55

Contour plot showing radiation levels (in dB) of transmission line antenna mounted on 36" diameter ground plane over ± 20° of the horizon for all angles of azimuth. Frequency = 296.032 Mc.

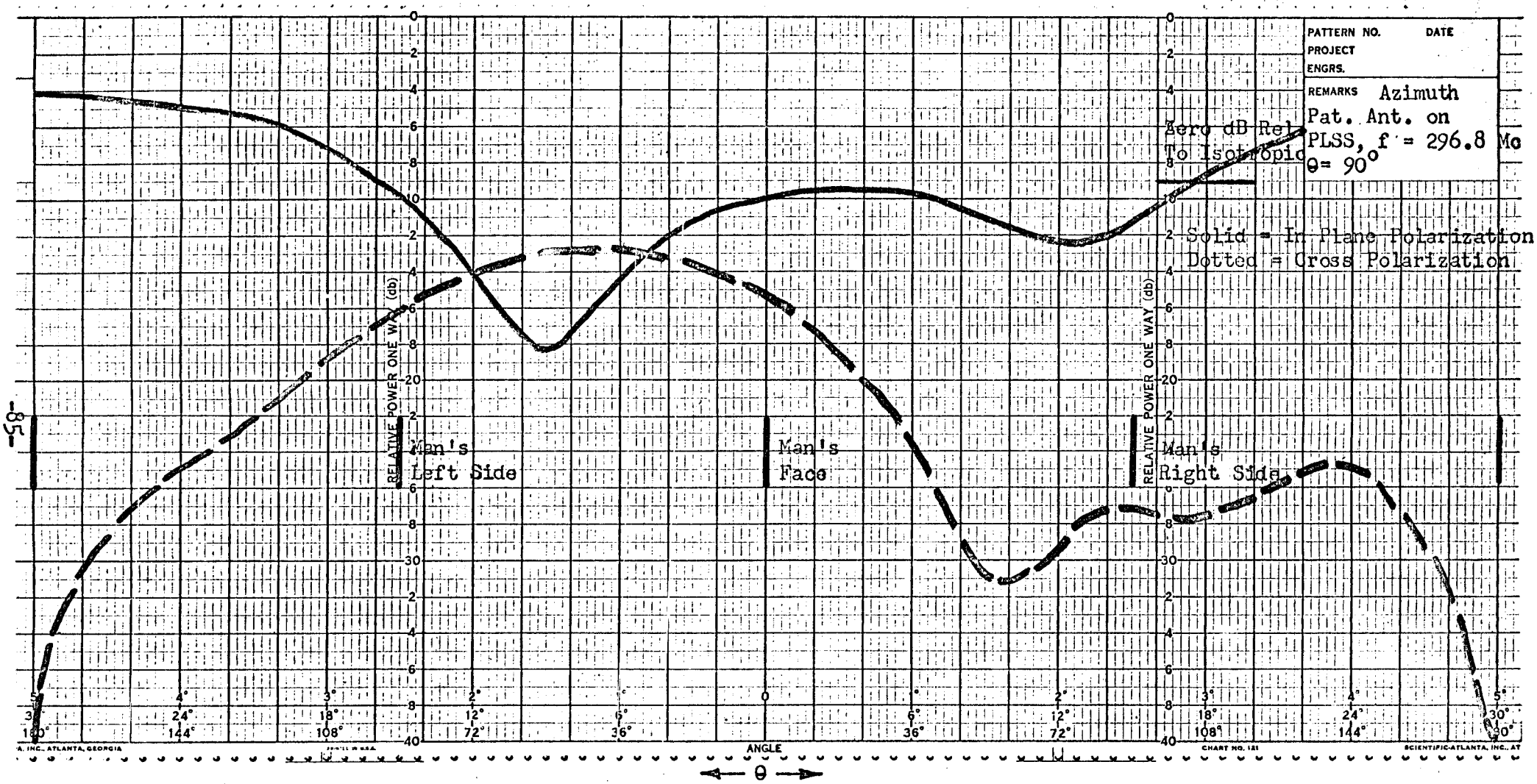

Figure 56.
Azimuth Pattern of Prototype Antenna
Mounted on Space Suit Mockup

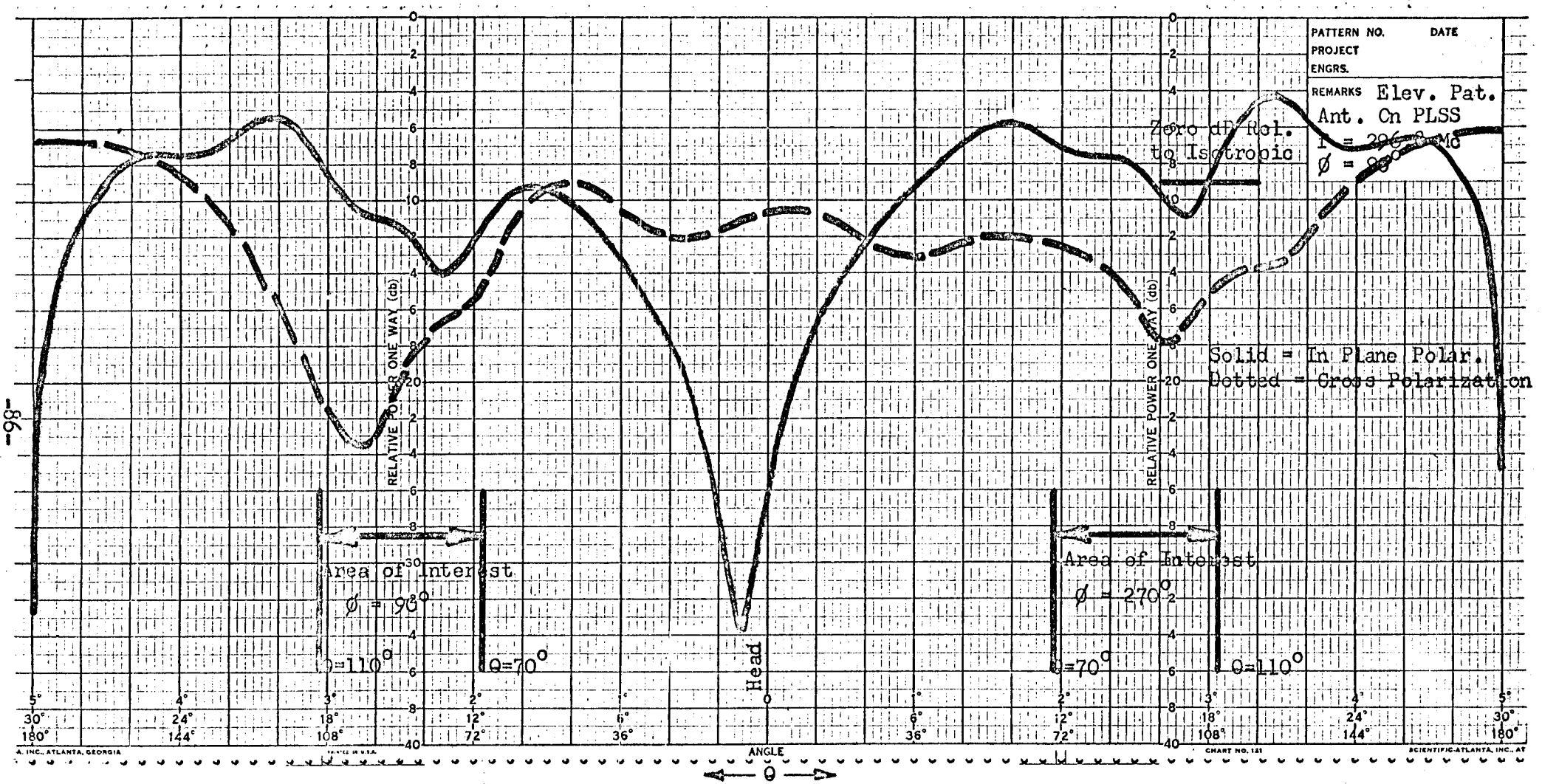

Figure 57.
Elevation Pattern of Prototype Antenna
Mounted on Space Suit Mockup

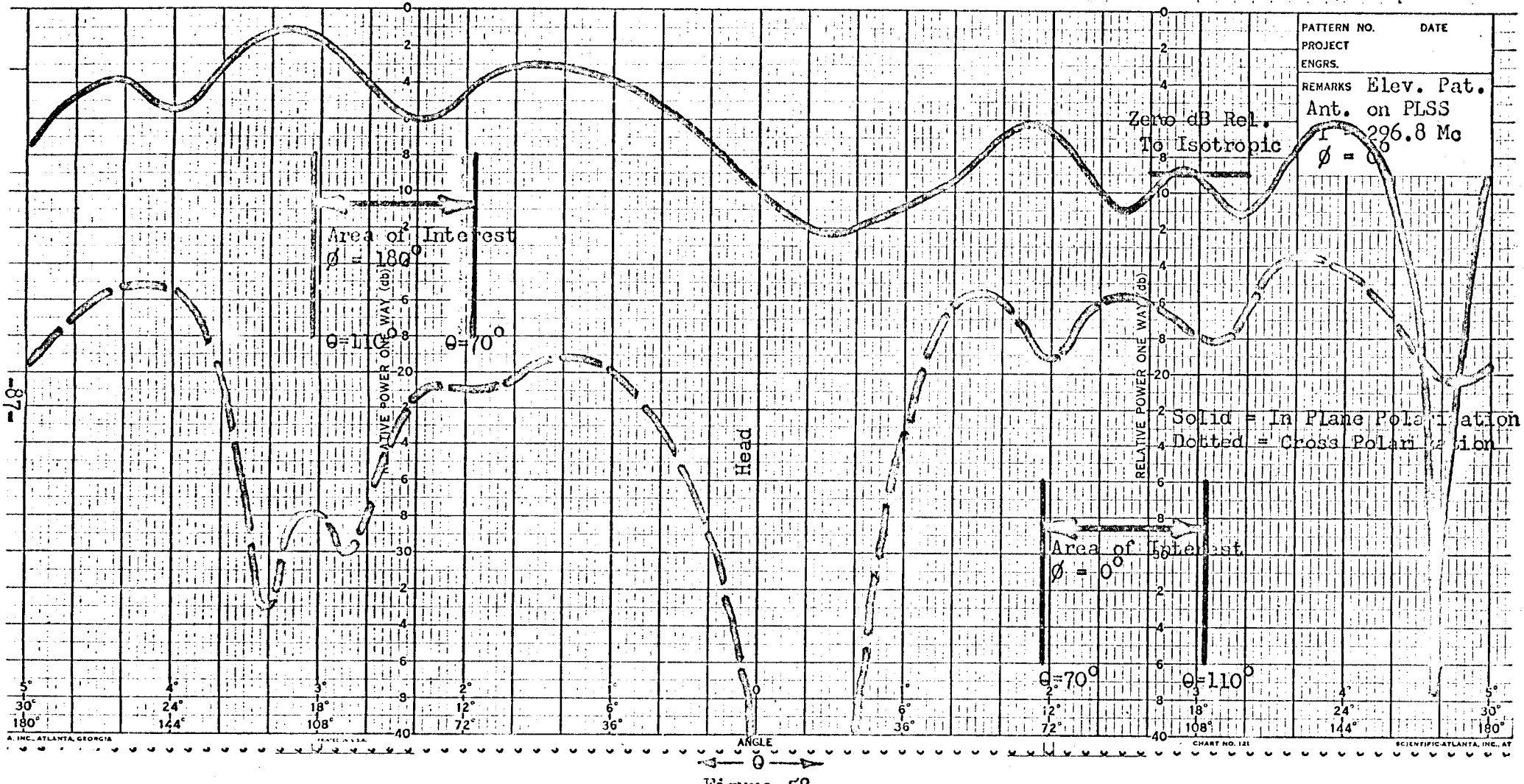

Figure 58
Elevation Pattern of Prototype Antenna
Mounted on Space Suit Mockup

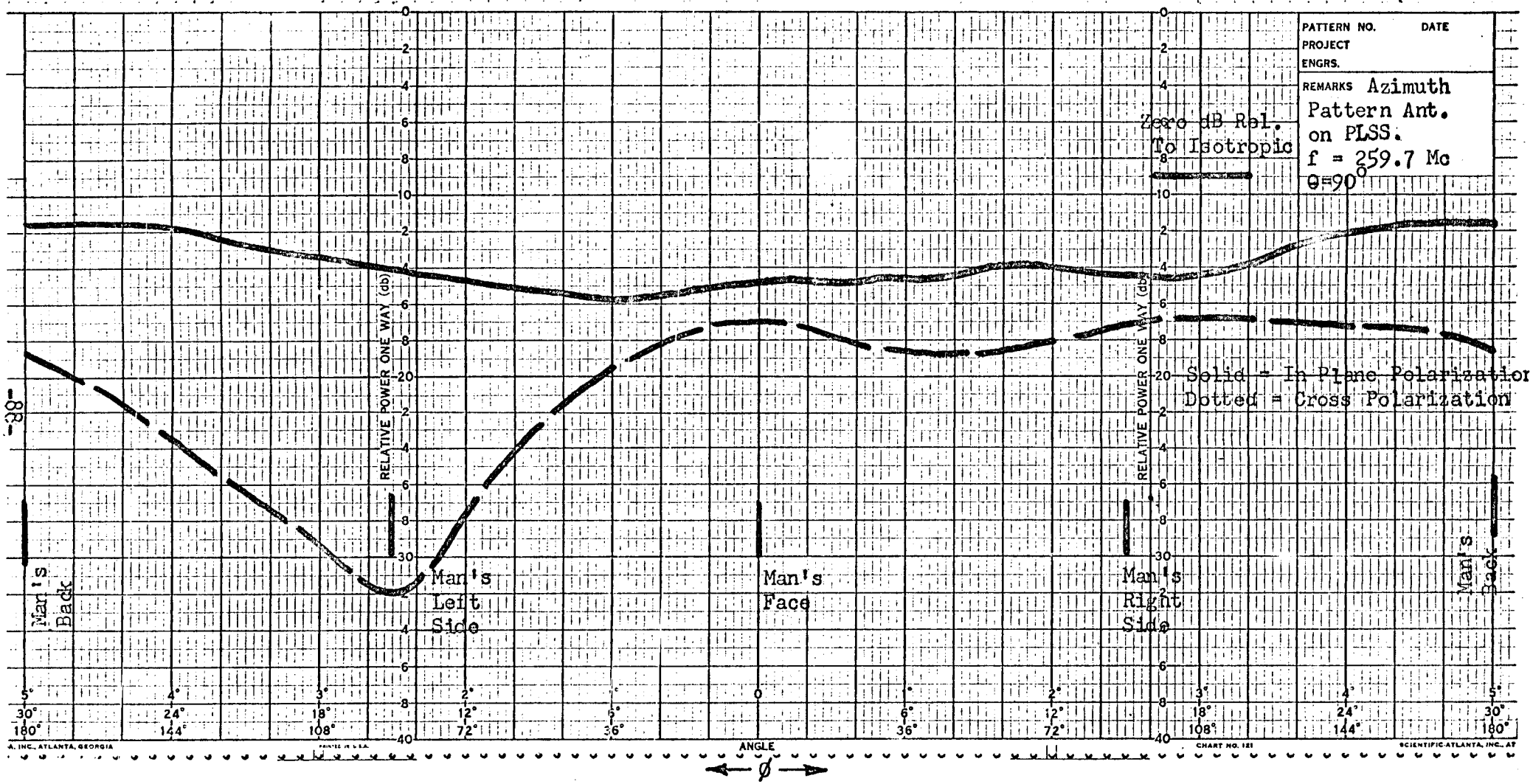

Figure 59
Azimuth Pattern of Prototype Antenna
Mounted on Space Suit Mockup

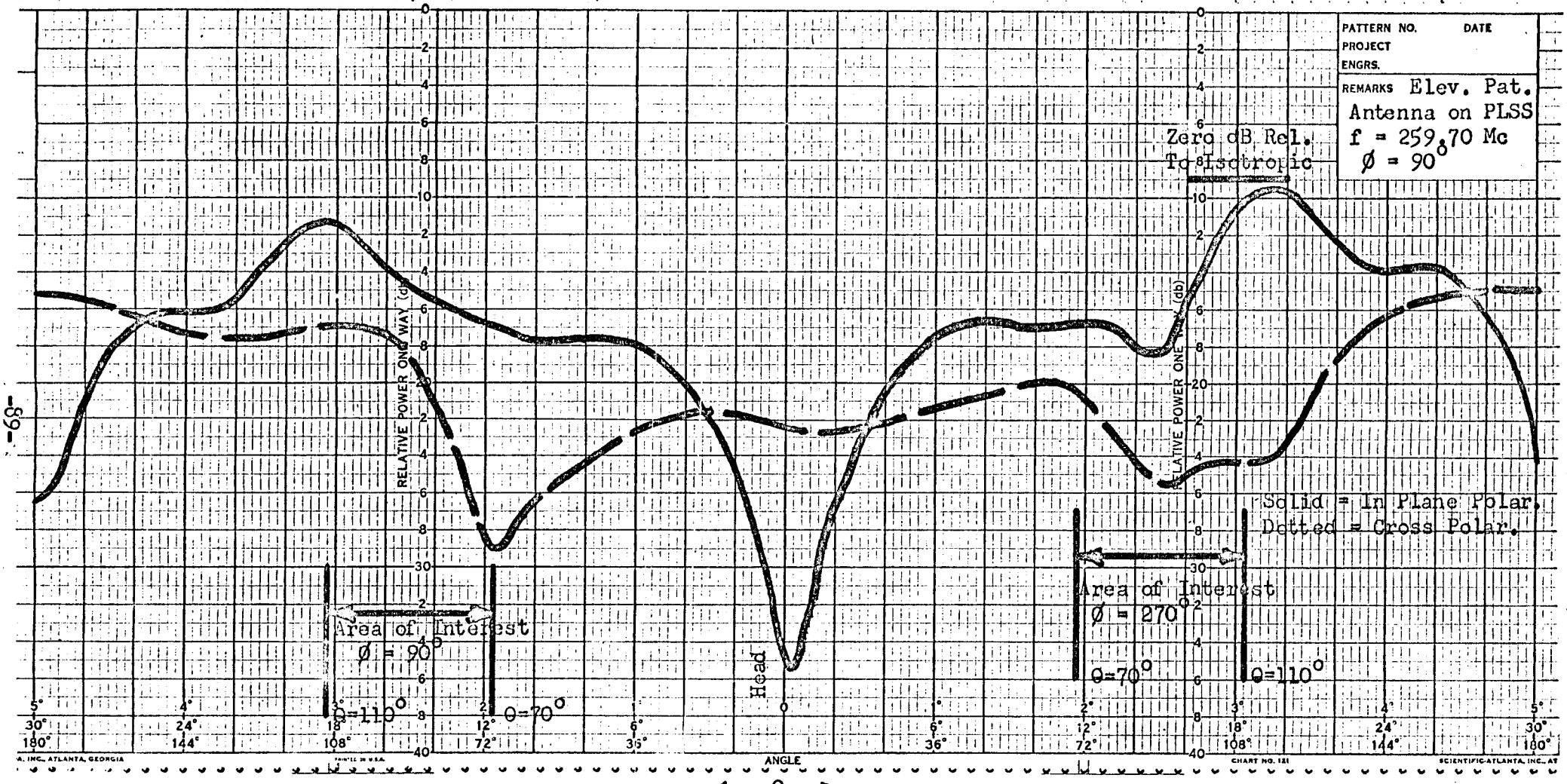

Figure 60
Elevation Pattern of Prototype Antenna
Mounted on Space Suit Mockup

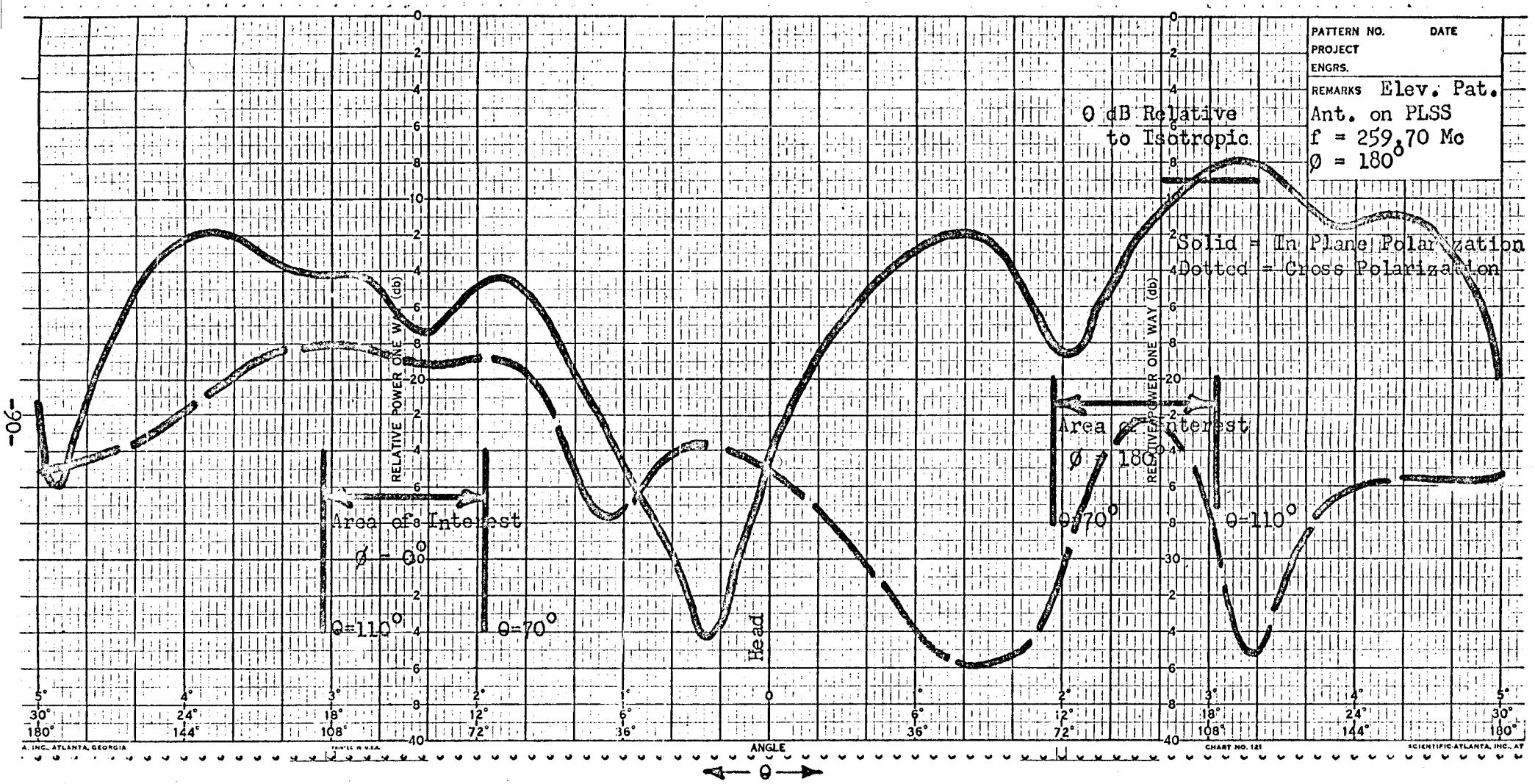

Figure 61
Elevation Pattern of Prototype Antenna
Mounted on Space Suit Mockup

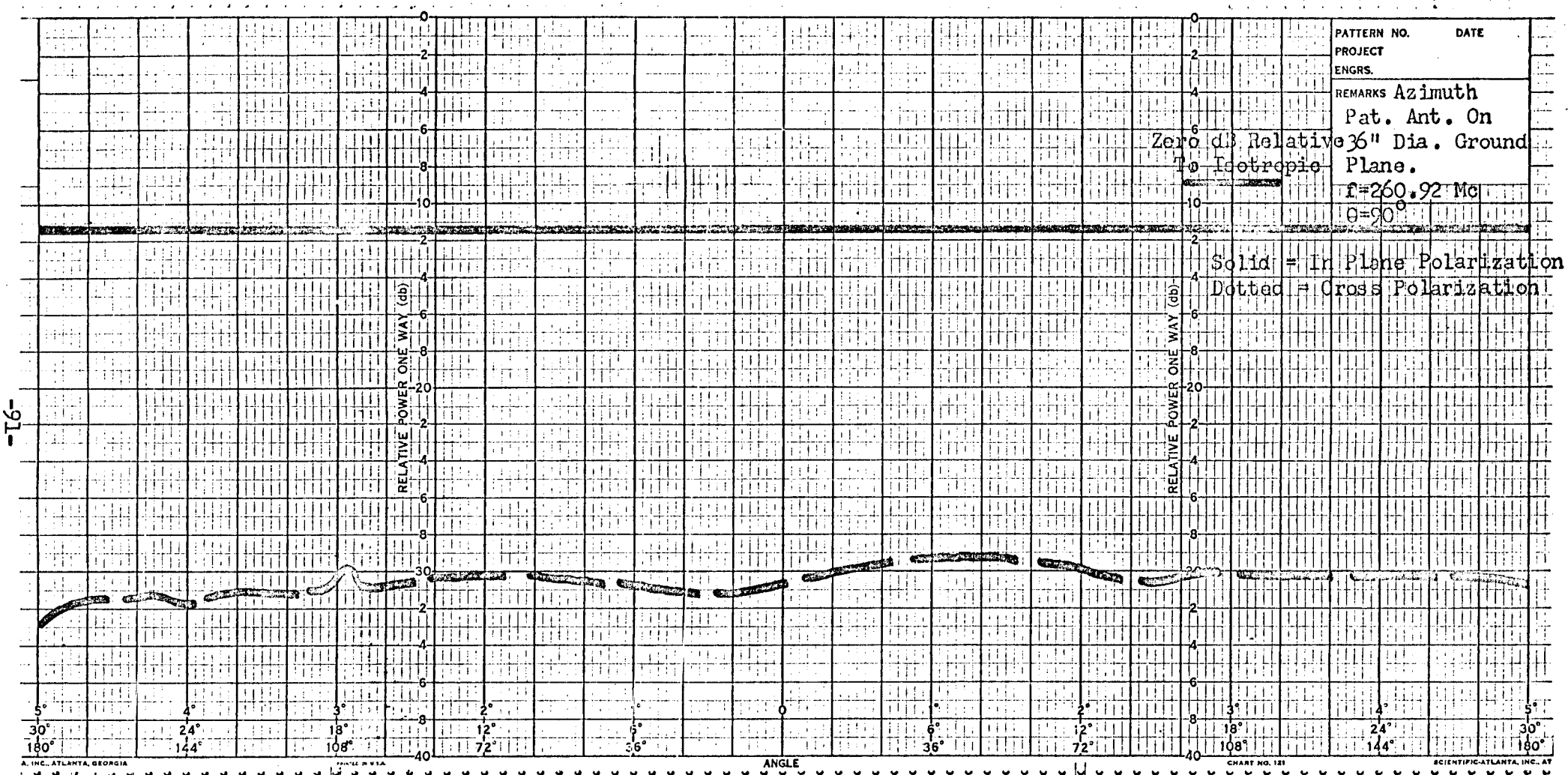

Figure 62
Azimuth Pattern of Prototype Antenna
Mounted on 36 Inch Ground Plane

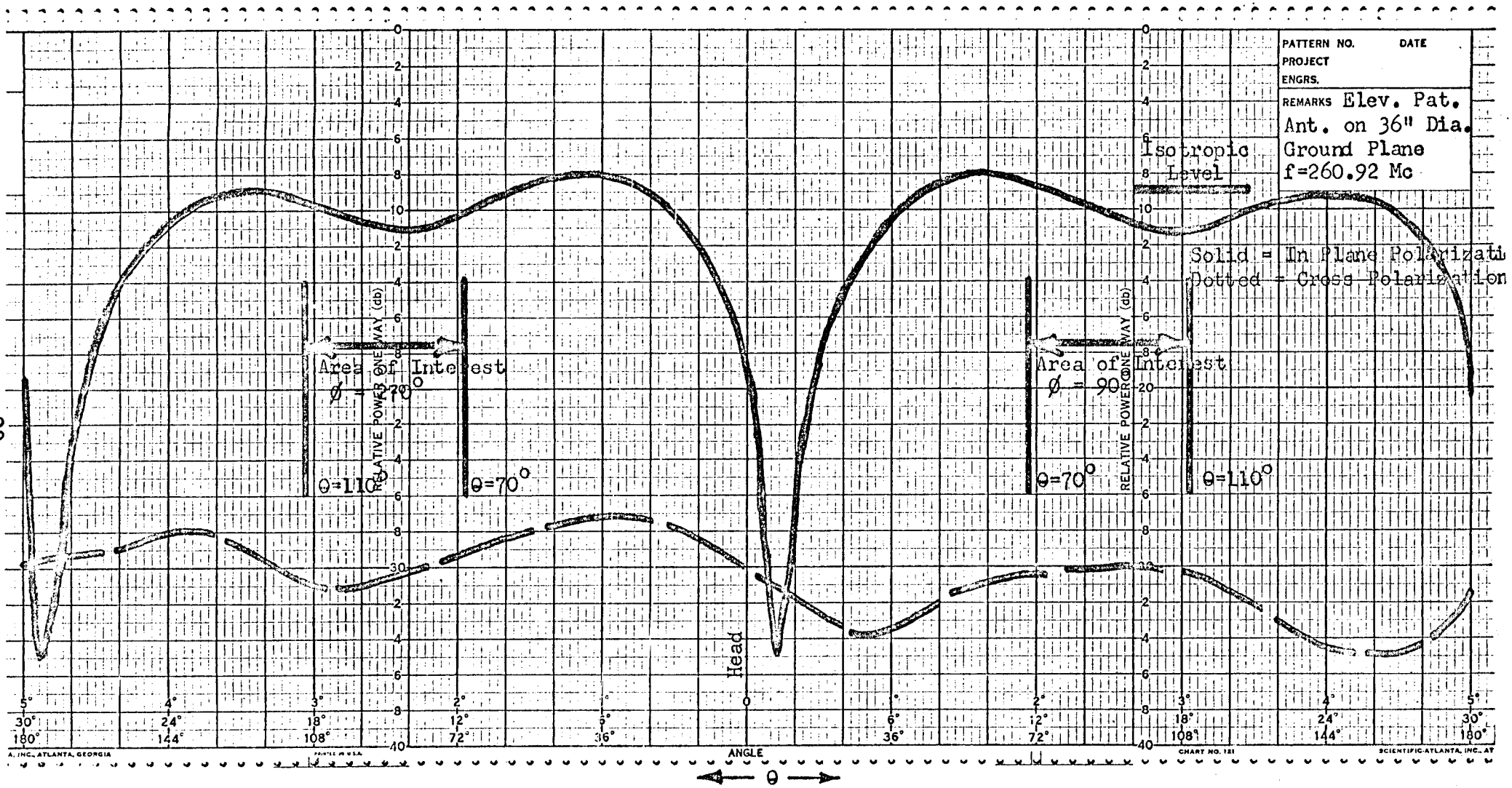

Figure 63
Elevation Pattern of Prototype Antenna
Mounted on 36" Ground Plane

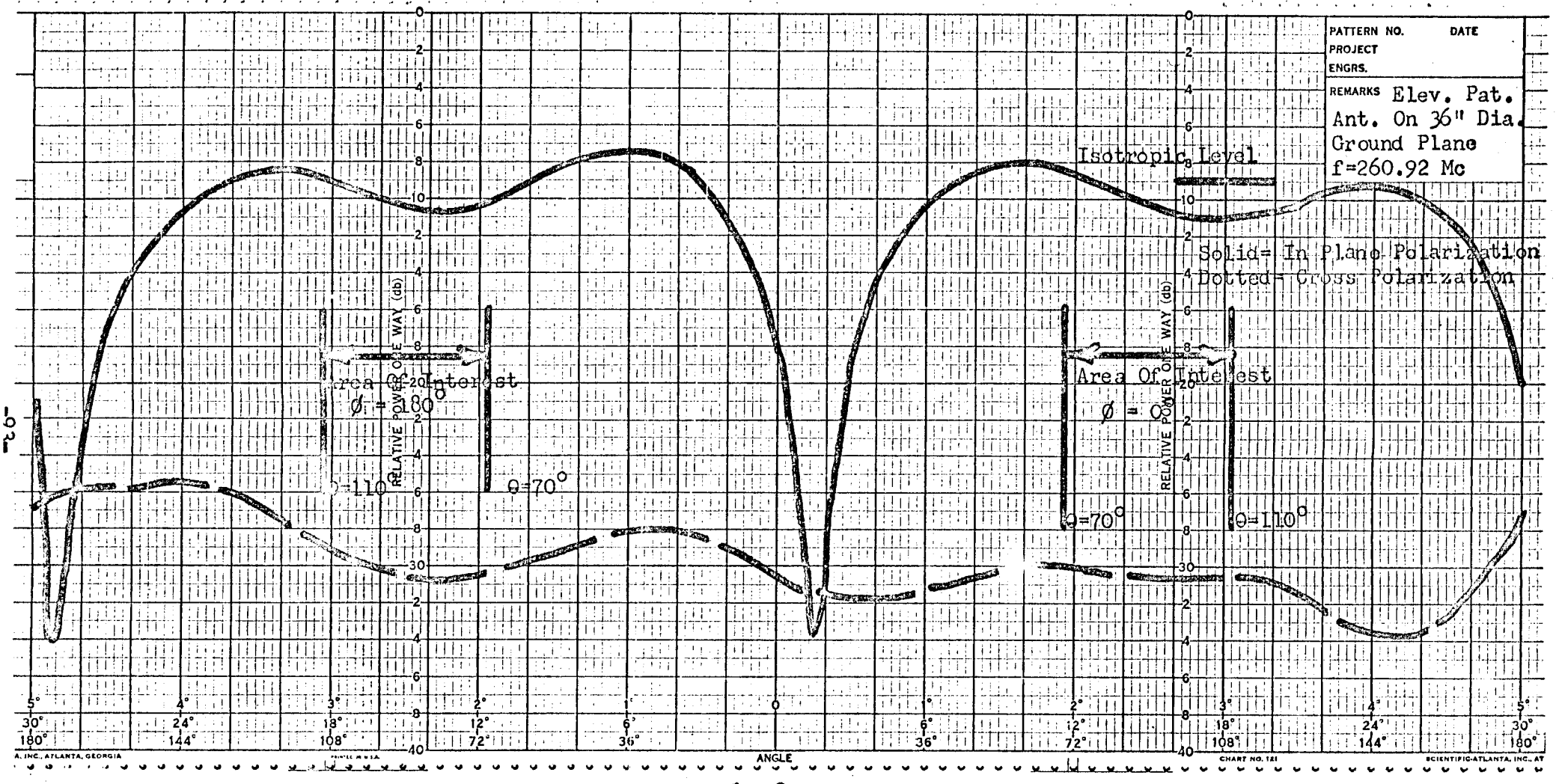

Figure 64
Elevation Pattern of Prototype Antenna
Mounted on 36" Ground Plane

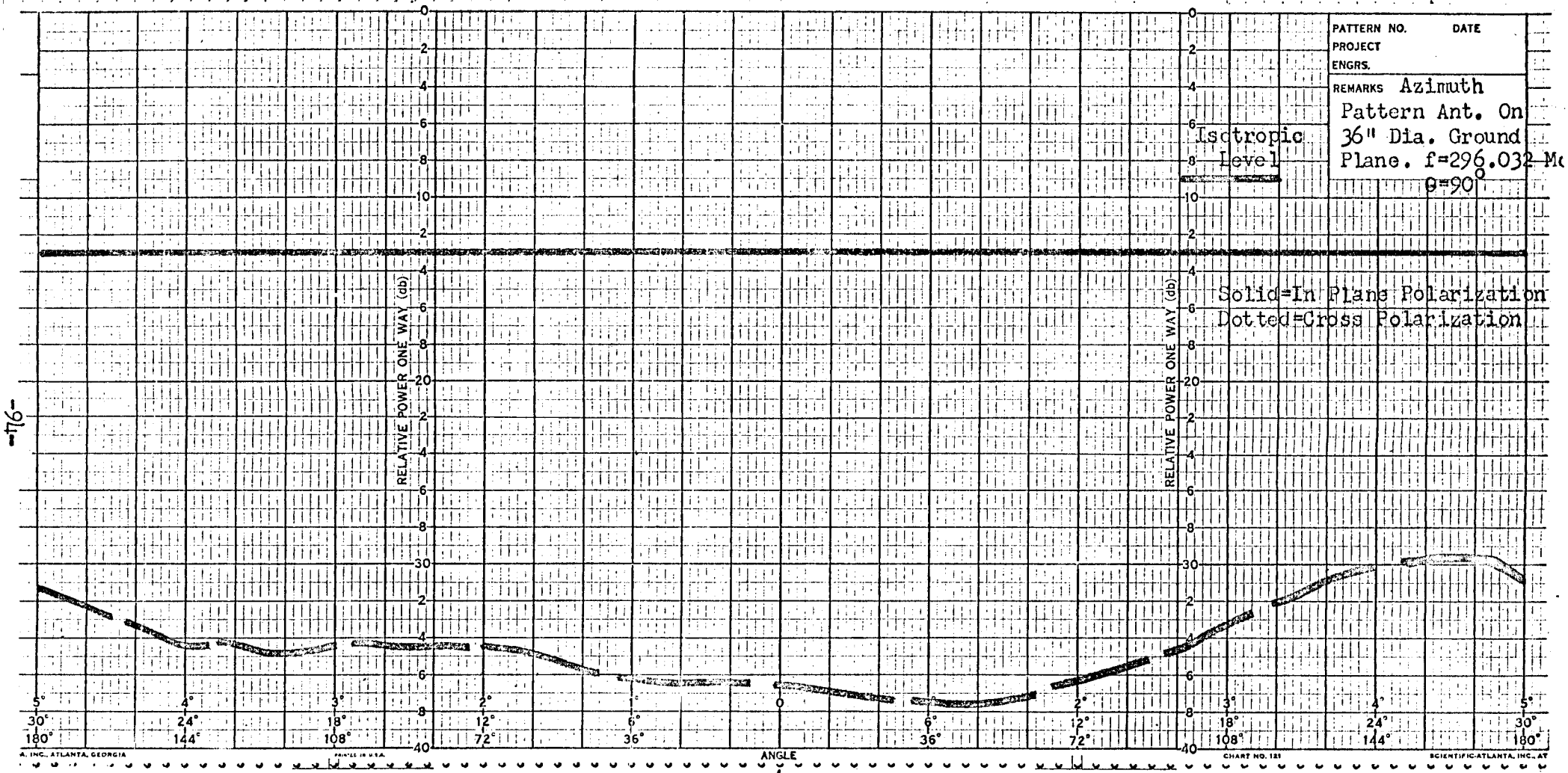

Figure 65
Azimuth Pattern of Prototype Antenna
Mounted On 36" Ground Plane

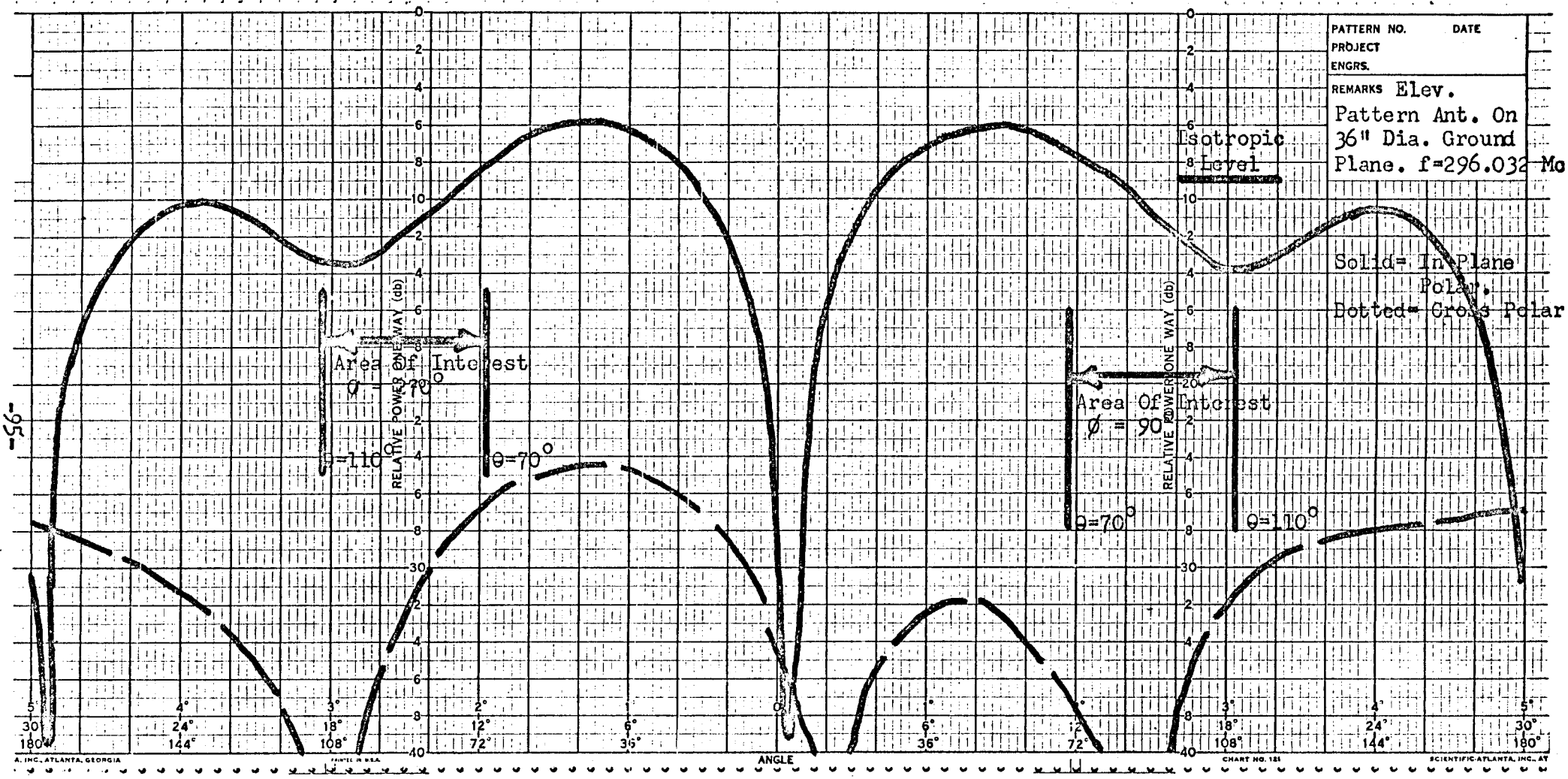

Figure 66

Elevation Pattern of Prototype Antenna
Mounted on 36" Ground Plane

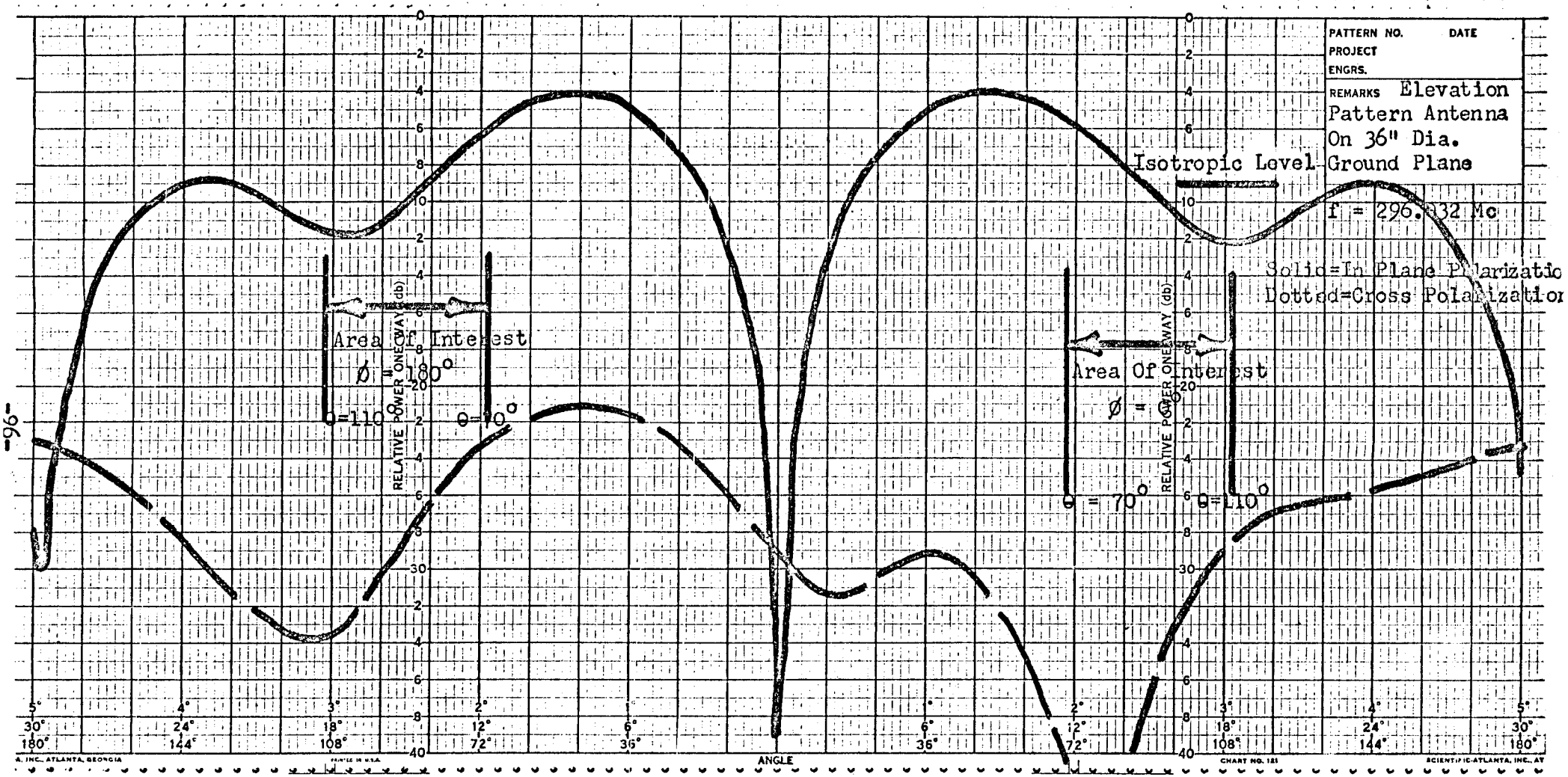

FIGURE 67

← θ →

Elevation Pattern of Prototype Antenna
Mounted on 36" Ground Plane

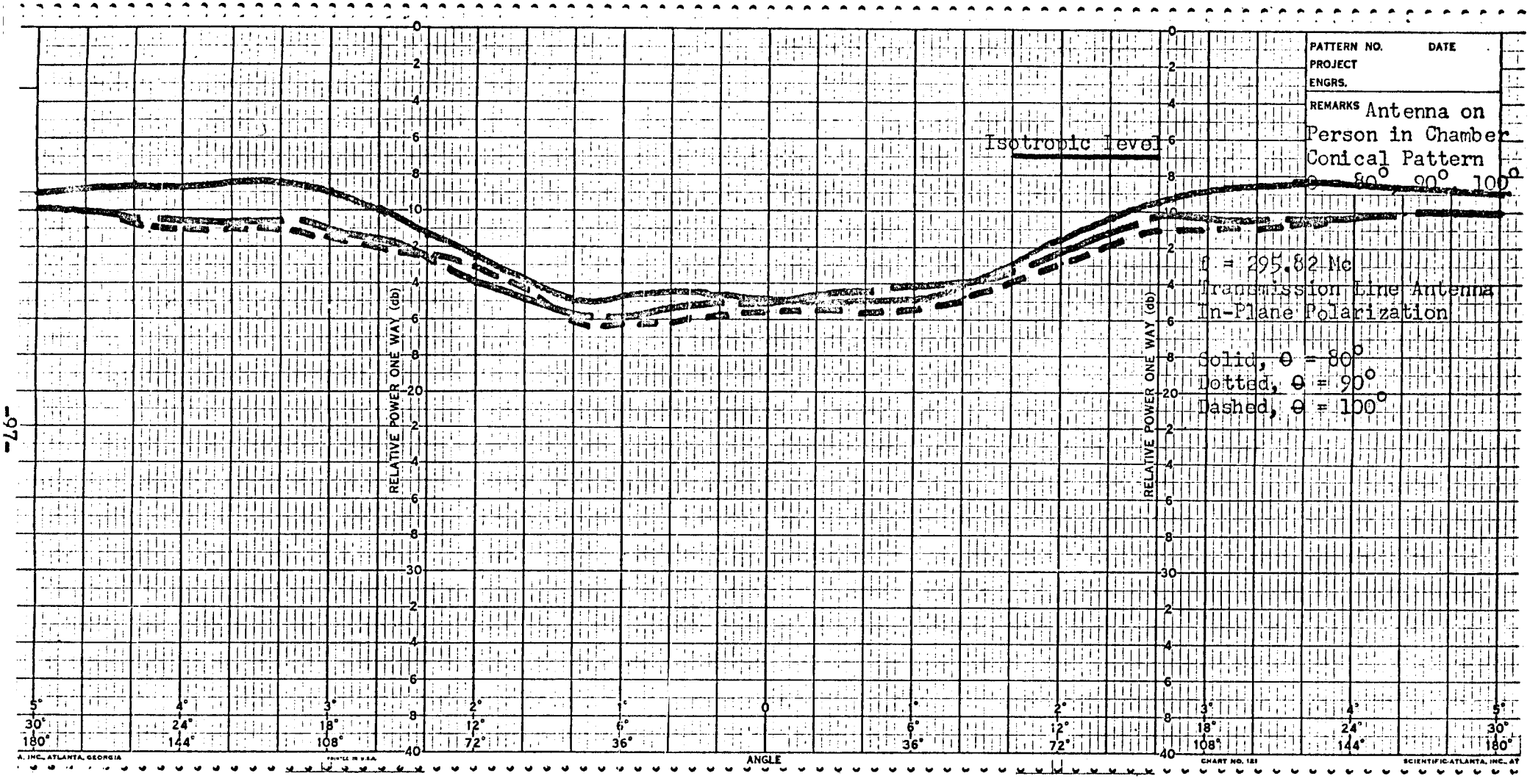

FIGURE 68

Azimuth pattern at f = 295.82 Mc, of transmission line antenna showing horizon ($\theta = 90^{\circ}$) and $\pm 10^{\circ}$ from the horizon ($\theta = 80^{\circ}, 90^{\circ}$).

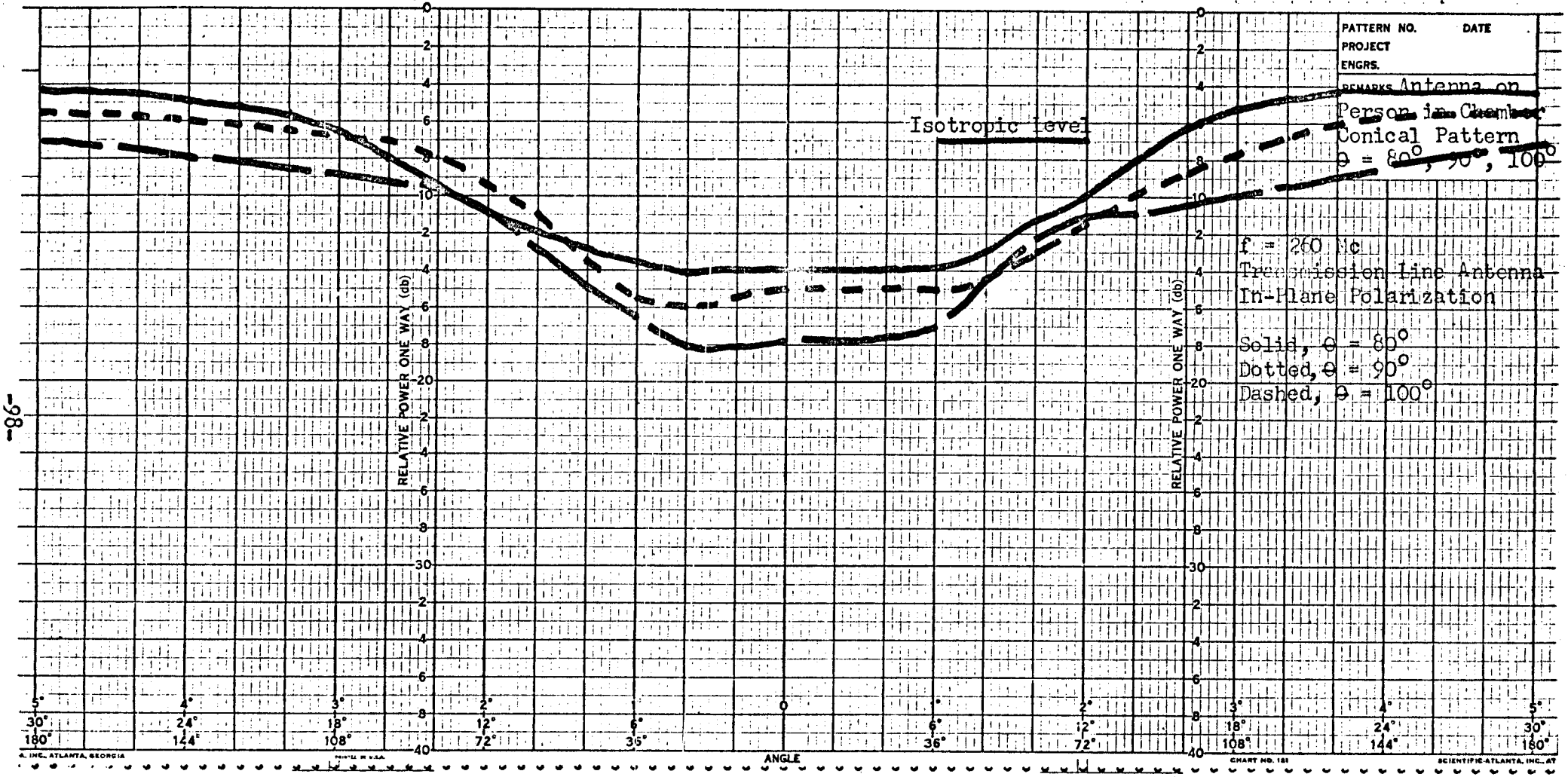

FIGURE 69

Azimuth pattern at f = 260.0 Mc, of transmission line antenna showing $\theta = 80^{\circ}$, 90°, and 100°

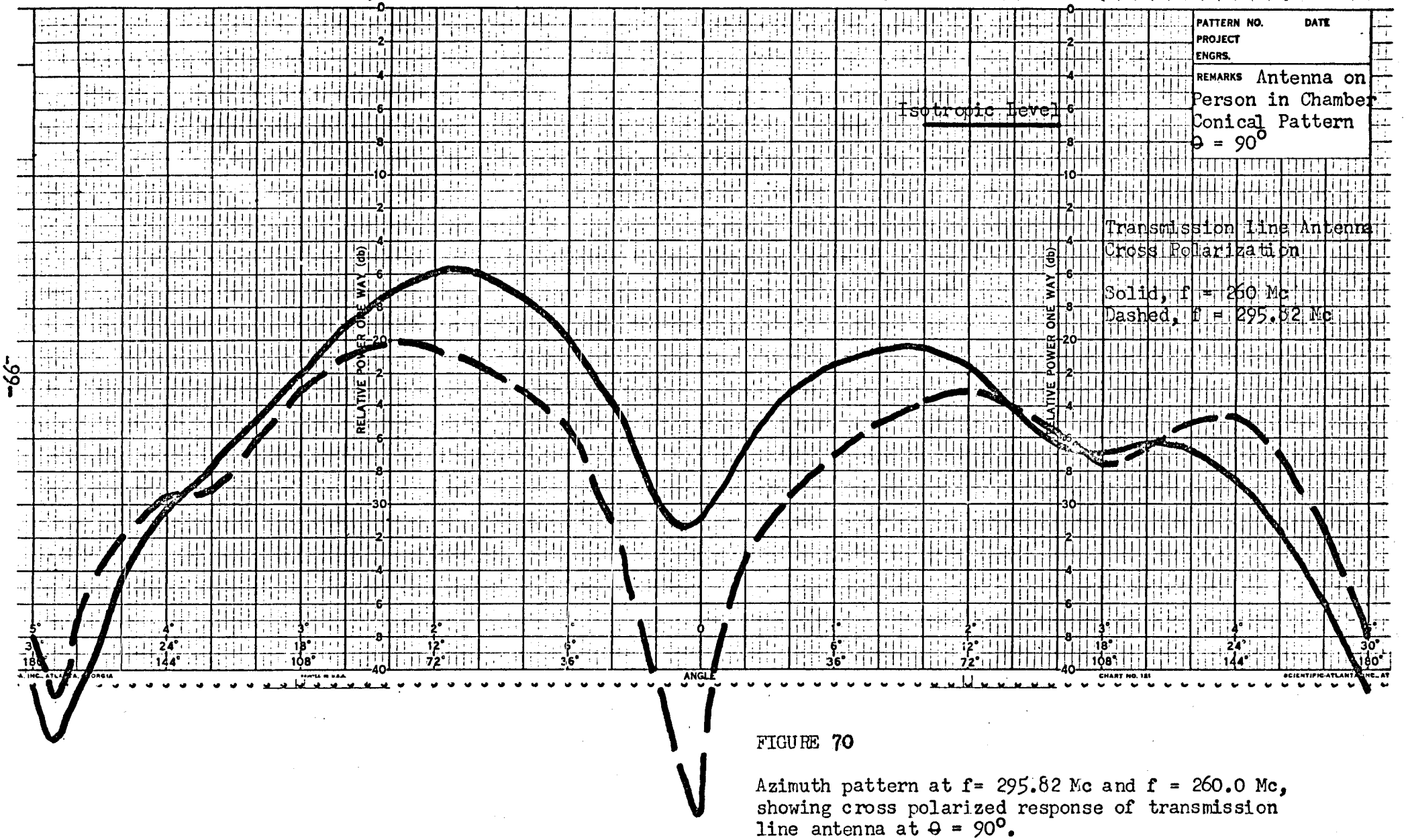

FIGURE 70

Azimuth pattern at f= 295.82 Mc and f = 260.0 Mc, showing cross polarized response of transmission line antenna at $\theta = 90^{\circ}$.

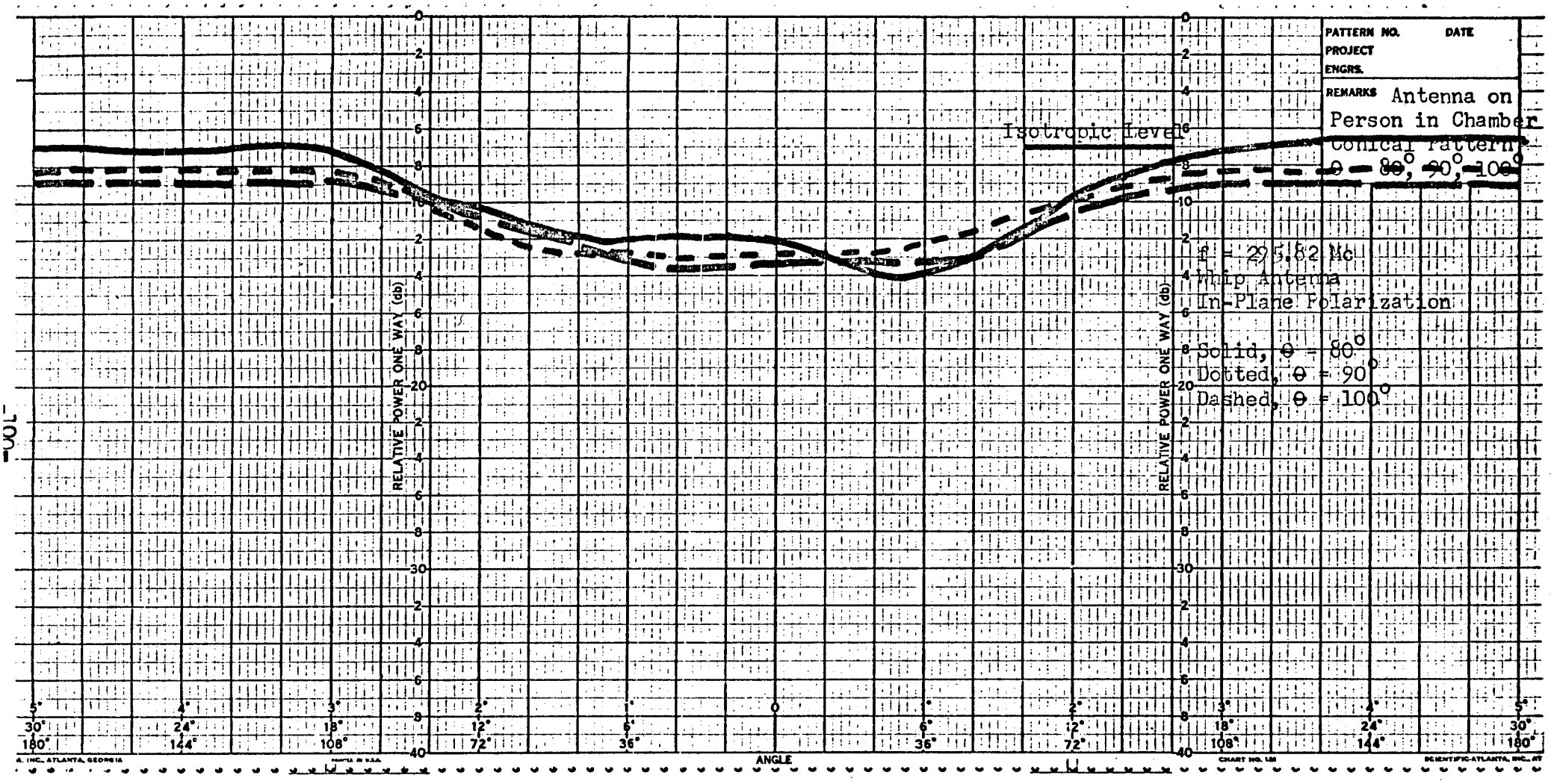

FIGURE 71

Azimuth pattern at f = 295.82 Mc of quarter-wave whip antenna showing 80°, 90°, and 100°.

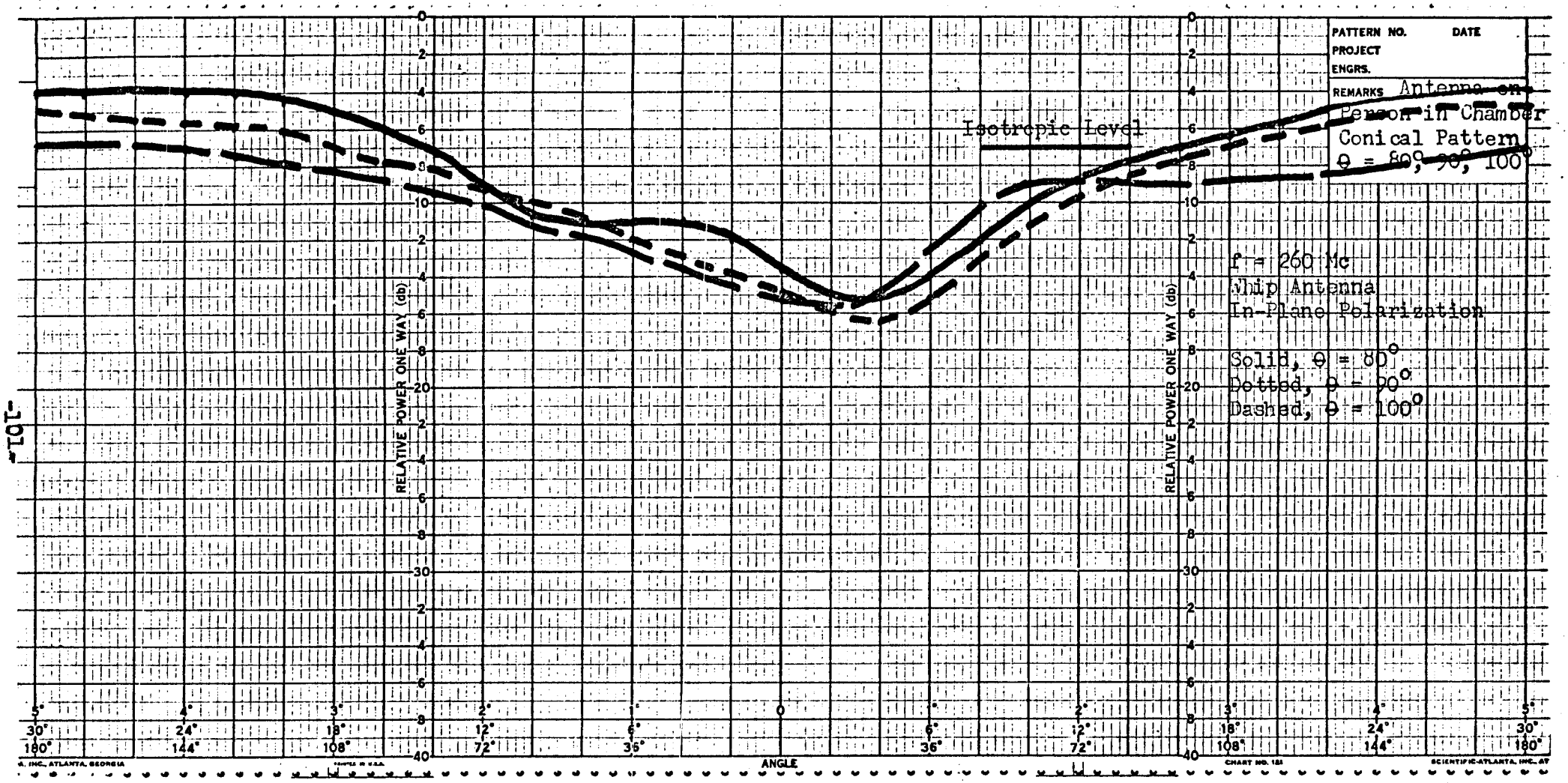

FIGURE 72

Azimuth pattern at f = 260.0 Mc, of quarter-wave whip antenna showing $\theta = 80^{\circ}$, 90°, and 100°.

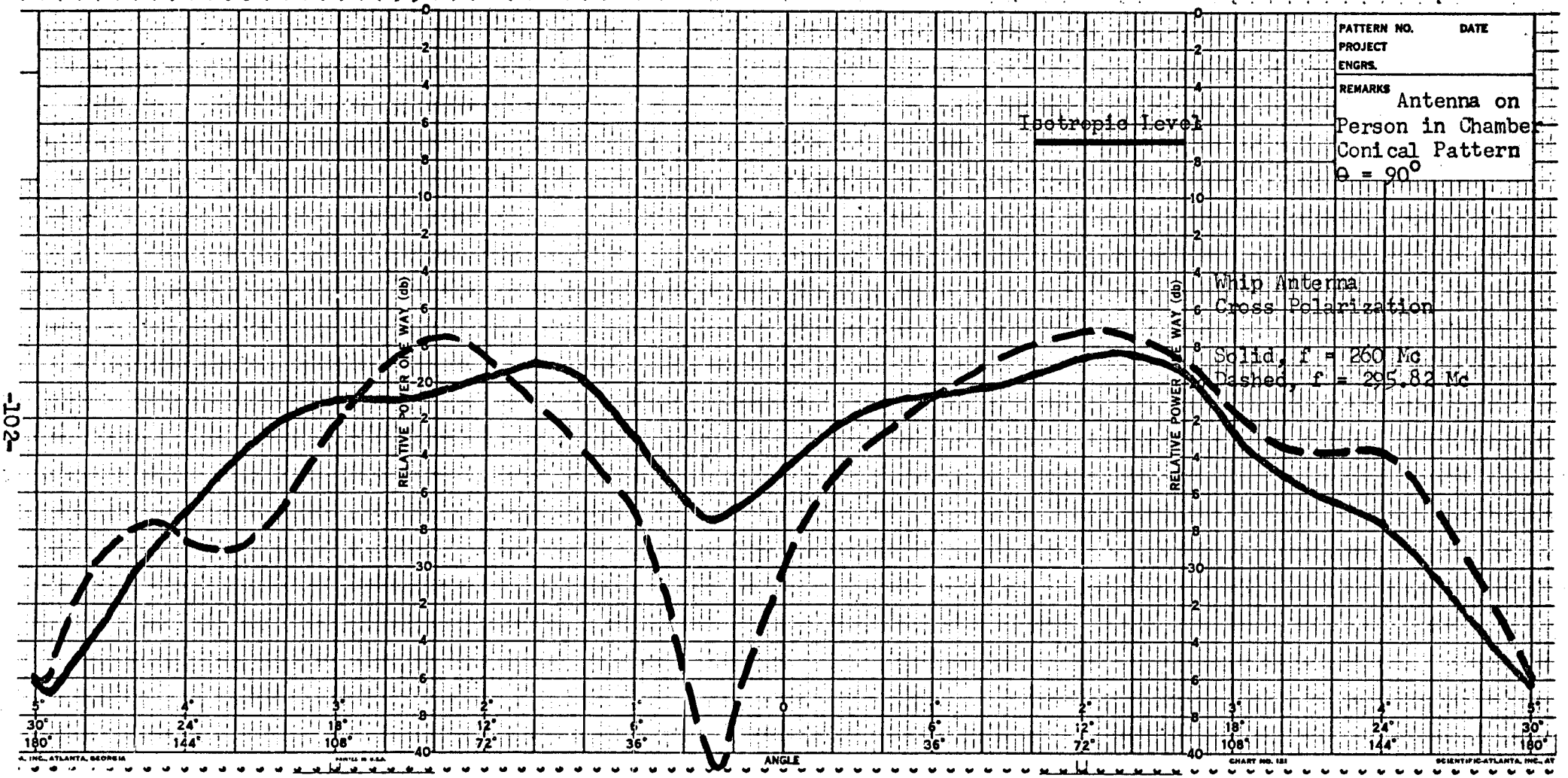

FIGURE 73

Azimuth pattern at f = 295.82 Mc and f = 260.0 Mc, showing cross polarized response of quarter-wave whip antenna at $\theta = 90^{\circ}$.

of the Transmission Line Antenna. This design was to be a dual frequency transmission line antenna for use on the PLSS.

To preserve the interface between the antenna and the PLSS and their stowage in the space vehicle certain additional ground rules and constraints were identified for the flight qualifiable models. Following is an itemization of each of these:

1. The PLSS thermal garment must maintain an intimate contact with the antenna ground plane.
2. The envelope of the PLSS shall not be increased by modifications on the transmission line antenna.
3. Holes or slits placed in the PLSS thermal garment for the purpose of running cables and placing the antenna mounting feet shall be kept in a nominal size and when possible shall be placed beneath the antenna ground plane.
4. The coaxial cable leading from the antenna should remain beneath the PLSS thermal garment at all times.
5. Mounting feet which are to be placed beneath the antenna ground plane should be located beneath the fiberglass cover of the antenna radome.

The antenna is packaged in a configuration which will ensure that it will withstand all of the rigorous environmental conditions to which it would be subjected during a typical Apollo mission, and also with a weight which is consistant with the mission requirements. Its design encompasses each of the ground rules as set forth above. The antenna consists of 4 basic parts: the base plate, cable assembly, spiral radiators, and the radome. Figure 74 is a view of the antenna showing the basic antenna structure. The base plate which contributed most of the structural integrity of the unit is made from gold plated aluminum alloy. The base plate shell is made from 0.031 inch thick aluminum alloy and dip-brazed together. This forms a rigid, but very light structure. The 0.25 inch base plate thickness is imposed by mounting considerations; and, therefore, the plate is necessarily hollow. This

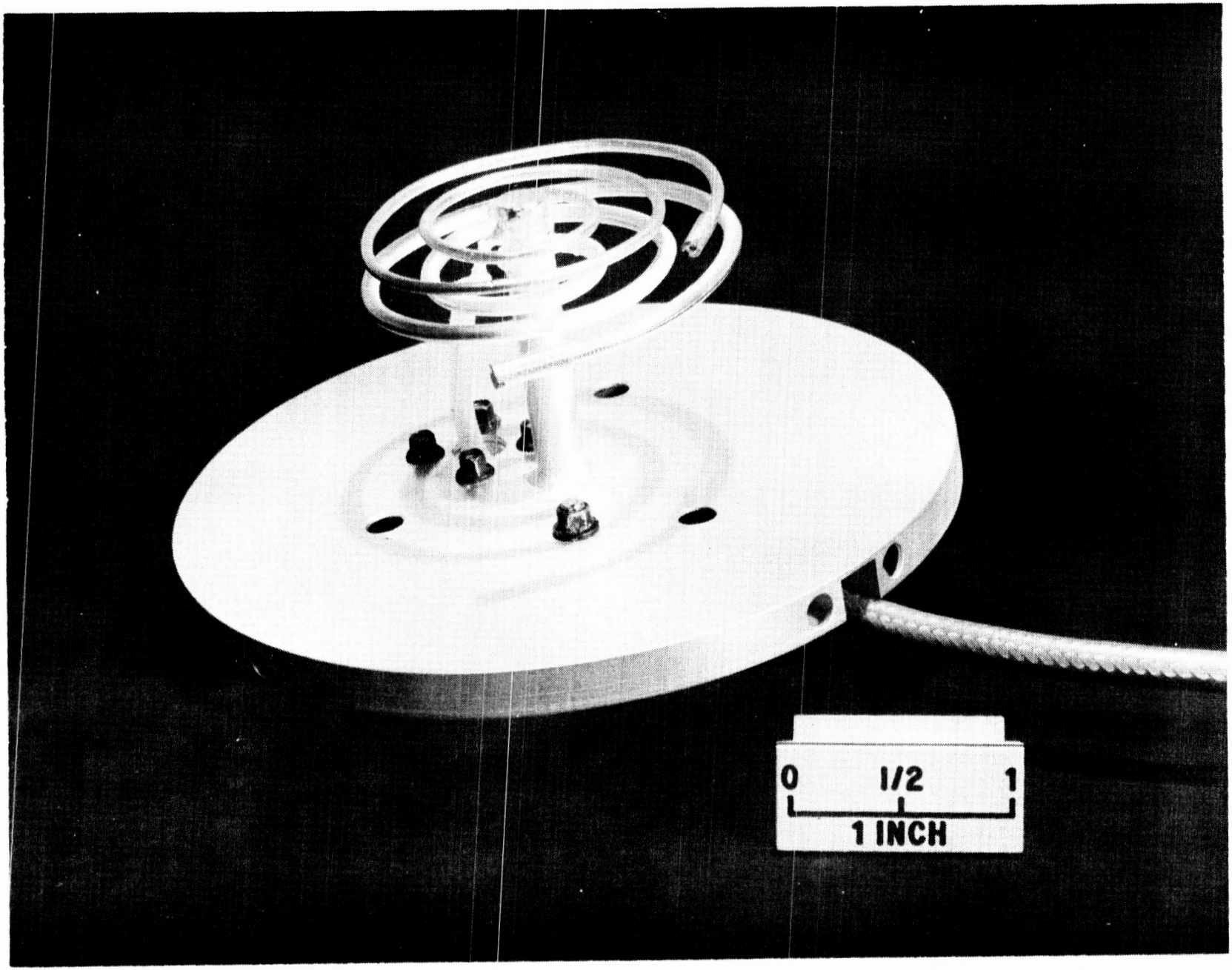

VHF Dual Frequency
Transmission Line Antenna On
Modified Ground Plane.

base plate also contains the three plated aluminum mounting feet (which will plug into the PLSS), the connector assembly mount, tuning access holes, and the post for the radiating elements. The cable assembly has a Deutsch type DC3-500005 connection, a section of RF 142B/U RF cable and a plated brass connector which is attached to the base plate with (4) screws. The stripped end of this cable is then fed through a hole in the base plate and is soldered to the appropriate place on the post which is determined by electrical tests. The spiral radiating elements are silver plated invar wire and are soldered into holes in the mounting post. Tuning elements are screwed onto the free end of these elements and used for adjusting the resonant frequency of the elements. This tuning mechanism, shown in Figure 75 provides a screwdriver adjustment of the antenna frequency ± 1 Mc about the optimum frequencies of 259.7 Mc and 296.8 Mc. Access to the tuning mechanism is located beneath the antenna ground plane through two holes. These holes are sealed with removable screw-in plugs and silicon rubber discs. The radome is made of epoxy-bonded glass cloth with a thickness of 0.015 inch. At assembly, the volume inside the radome and above the base plate, which are bonded together, is filled with a rigid low density unicellular polyurethane foam. This foam gives support to the radiating elements, holding them rigidly in position and also supporting the radome which in turn protects the elements from damage. The exposed surface of the radome and the outer edge of the base plate is covered with a white silicon thermal-control coating to keep the heat flux of the antenna at an acceptable level. Figure 76 shows Motorola assembly drawing 85-24486E giving the antenna's design features. Figure 77 is a photograph of the completed antenna unit.

3.7 FINAL ANTENNA PERFORMANCE

Prior to delivery of the flight qualifiable antennas, measurements of VSWR and radiation patterns were made for each antenna. This data was measured with the antenna mounted on 1) the space suit mockup and, 2) on a 36-inch diameter ground plane. The measured VSWR for each case and each

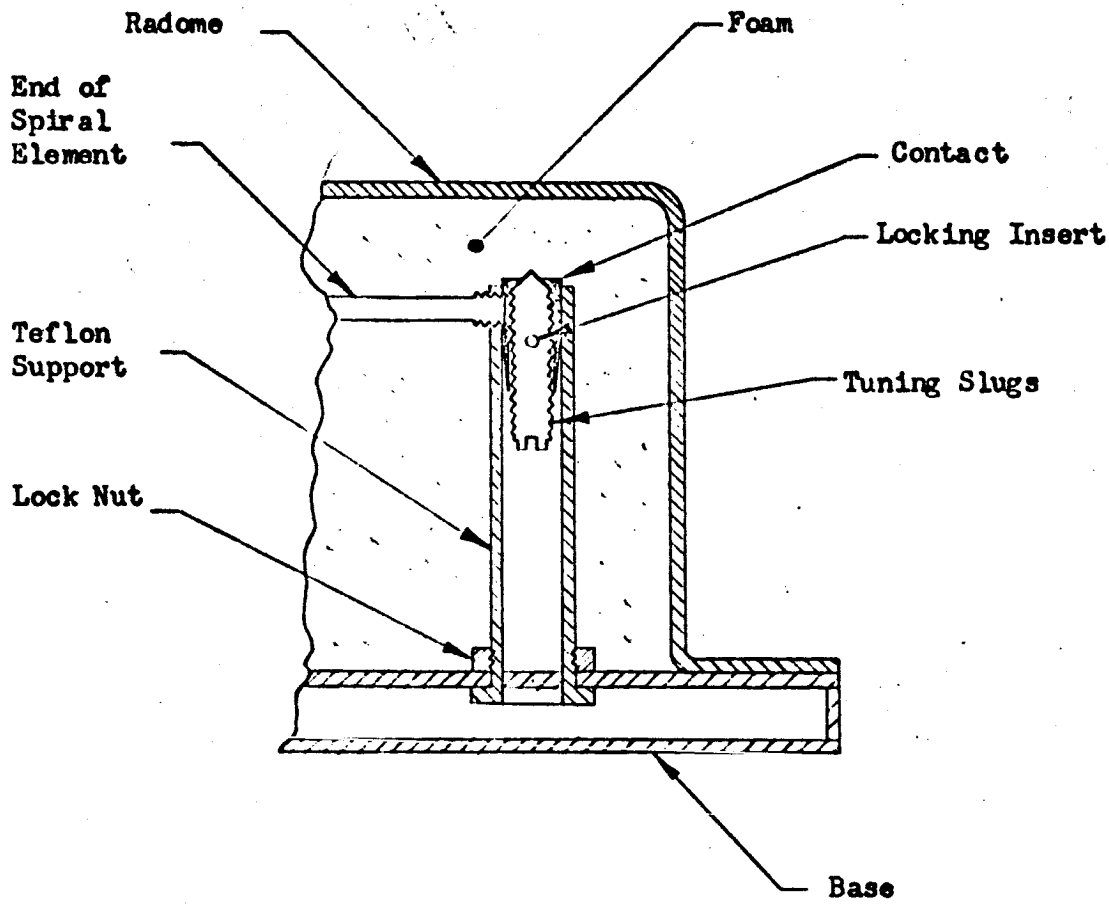

FIGURE 75

TRANSMISSION LINE ANTENNA TUNING DEVICE

ASTERISK INDICATES DATA WHICH IS NONMANDATORY — FOR INFORMATION ONLY

NOTES:

1. AS SUPPLIED BY DEUTSCH COMPANY, BANNING, CALIFORNIA, FED CODE IDENT. NO. 11139, OR APPROVED EQUIVALENT.
2. ALL SOLDERING TO BE DONE PER MIL-S-6872, USING SOLDER, ITEM 16.
3. INSTALL CABLE, ITEM 7 INTO HOUSING, ITEM 4 ALLOWING 3.0 ± .12 INCHES OF TEFLON INSULATED WIRE TO PROJECT THROUGH ITEM 4. SOLDER BRAID OF ITEM 7 TO OUTSIDE OF ITEM 4 PER NOTE 2. INSTALL SLEEVING, ITEM 23. (SHRINK)
4. ASSEMBLE ELECTRICAL PLUG, ITEM 8, TO CABLE, ITEM 7.
5. ALIGN SUPPORT, ITEM 21 AS REQUIRED AND SOLDER TO BASE PLATE, ITEM .
6. AFTER SOLDERING ITEM 21, SILVER PLATE, TYPE II, GRADE B, .0003-.0005 THICK PER SPEC QQ-S-365. THEN MASK ITEM 21 AND ALL OF ITEM 1 THAT WILL BE COVERED BY RADOME, ITEM 2. GOLD PLATE, TYPE II, CLASS 3, BRIGHT, PER SPEC MIL-G-45204, AND INSTALL SCREW, ITEM 22.
7. SOLDER ANTENNA ELEMENTS, ITEMS 19 AND 20 TO ITEM 21.
8. ATTACH CABLE SUBASSEMBLY (ITEMS 4, 7, 8, 23) TO BASE PLATE, ITEM 1, USING ITEMS 5, 6, 9, 10, 11, 12, 13 RUNNING TEFLON INSULATED WIRE THRU HOLE IN ITEM 1.
9. AFTER CUTTING TO LENGTH, SOLDER STRIPPED END OF CABLE, ITEM 7 INTO HOLE IN ITEM 21 OR TO ITEMS 19 OR 20 AS REQUIRED FOR ELECTRICAL PARAMETERS.
10. SOLDER JOINTS AND ADJACENT AREAS, AS REQUIRED, TO BE SILVER PLATE, TYPE II, GRADE B, .0003-.0005 THICK PER SPEC QQ-S-365.
11. INSTALL CONTACT, ITEM 3, 2 PLACES, ADJUST AS REQUIRED, AND SOLDER TO ITEMS 19 AND 20.
12. FOAM USING ITEM 14. AS SUPPLIED BY CPR DIVISION OF UPJOHN CO., TORRANCE, CALIFORNIA, FED CODE IDENT NO. 18975.
13. ADJUST ITEMS 24 AND 25, FOR MINIMUM INPUT VSWR AT THE REQUIRED FREQUENCIES AFTER FOAMING.
14. EPOXY RESIN, ITEM 18 PER MIL-R-9300, TYPE II, CLASS 2,
15. BOND ITEMS 28 AND 29 TO ITEM 1 USING ITEM 18.
16. BOND RADOME, ITEM 2 TO ANTENNA BASE PLATE, ITEM 1 USING ITEM 18.
17. MASK ENTIRE BOTTOM SURFACE AND CABLE. FINISH THE EXTERNAL SURFACE WITH TWO COAT PRIMER, NO. 4097, AND 2 COATS AERO SPACE SEALANT NO. 92-007, AS SUPPLIED BY DOW CORNING CORP., SAGINAW ROAD, MIDLAND, MICHIGAN. FED. CODE IDENT. NO. 71984.
18. MARKING TO BE LOCATED APPROXIMATELY AS SHOWN. MARK IN PERMANENT BLACK CHARACTERS .12 HIGH OF CONDENSED GOTHIC TYPE USING INK, M-O-M W/CATALYST A, CODE 79436.

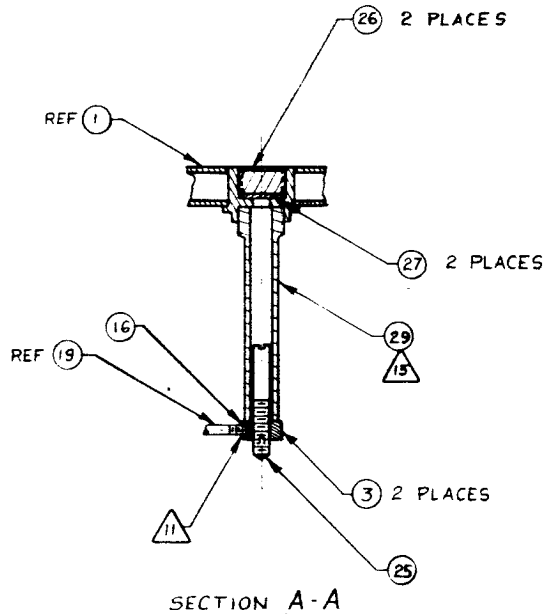

SECTION A-A
SCALE 2/1

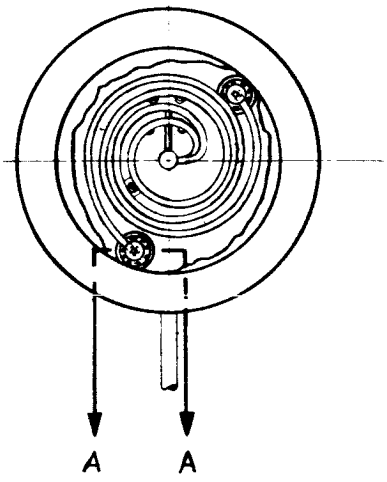

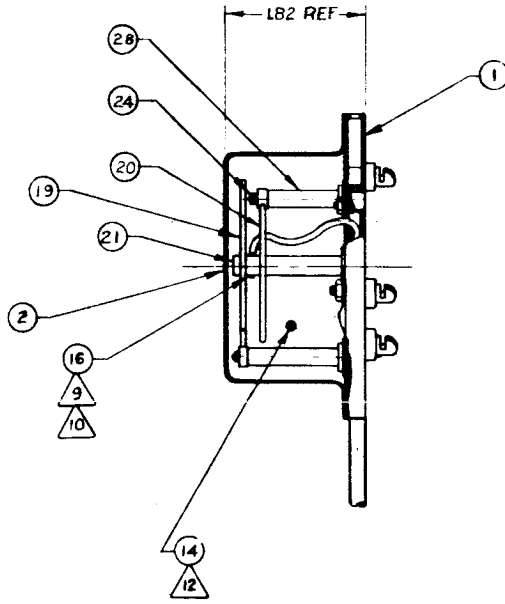

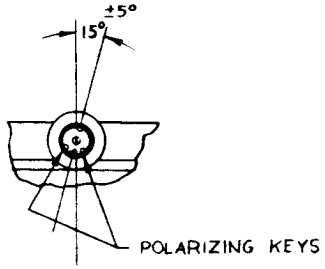

VIEW B B
SCALE 2/1

1071-1

SYM	SIZE	QTY
HOLE LIST		

REVISIONS				
ZONE	LTR	DESCRIPTION	DATE	APPROVED
	X1	PRELIMINARY RELEASE	6-9-66	

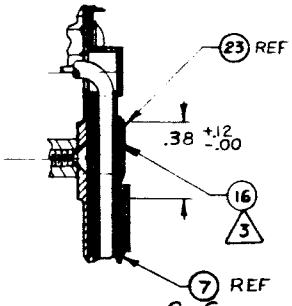

SECTION C-C
SCALE 2/1

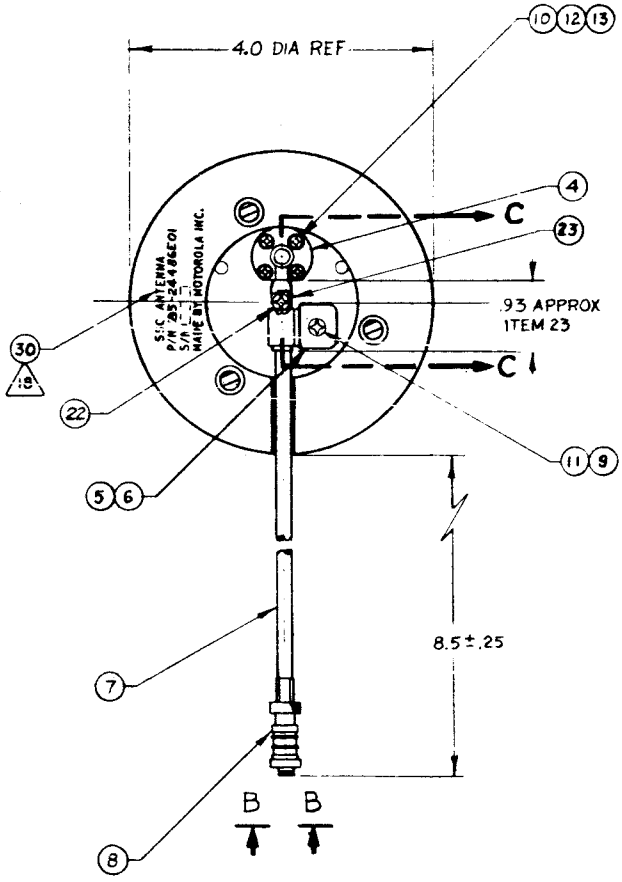

107-2

85-24486E01 MOTOROLA PART NUMBER	NEXT ASSEMBLY / USED ON: ★ APPLICATION	INTERPRET DRAWING IN ACCORDANCE WITH STANDARDS PRESCRIBED BY. UNLESS OTHERWISE SPECIFIED: DIMENSIONS ARE IN INCHES; SURFACE FINISH ✓; TOLERANCES: TWO PLACE DEC ±, THREE PLACE DEC ±, ANGLES ±, HOLE DIA +/−; MATERIAL; FINISH 17 10 6	APPROVALS: DR BY R.I. DAGLE 28 JUN 66; CHK BY; ENG; PROJ NO.; CONTRACT NO; RELEASE NUMBER, DIRECTIVE & DATE; APPROVED NAME DATE 6/29/66; APPROVED NAME DATE	FOR LIST OF MATERIAL SEE LM 85-24486E	MOTOROLA INC. Military Electronics Division / WESTERN CENTER 8201 EAST McDOWELL ROAD SCOTTSDALE, ARIZONA
				VHF DUAL FREQ TRANSMISSION LINE ANTENNA, TUNABLE	
				SIZE F; CODE IDENT NO. 94990; 85-24486E	
				SCALE 1/1; WEIGHT; SHEET	

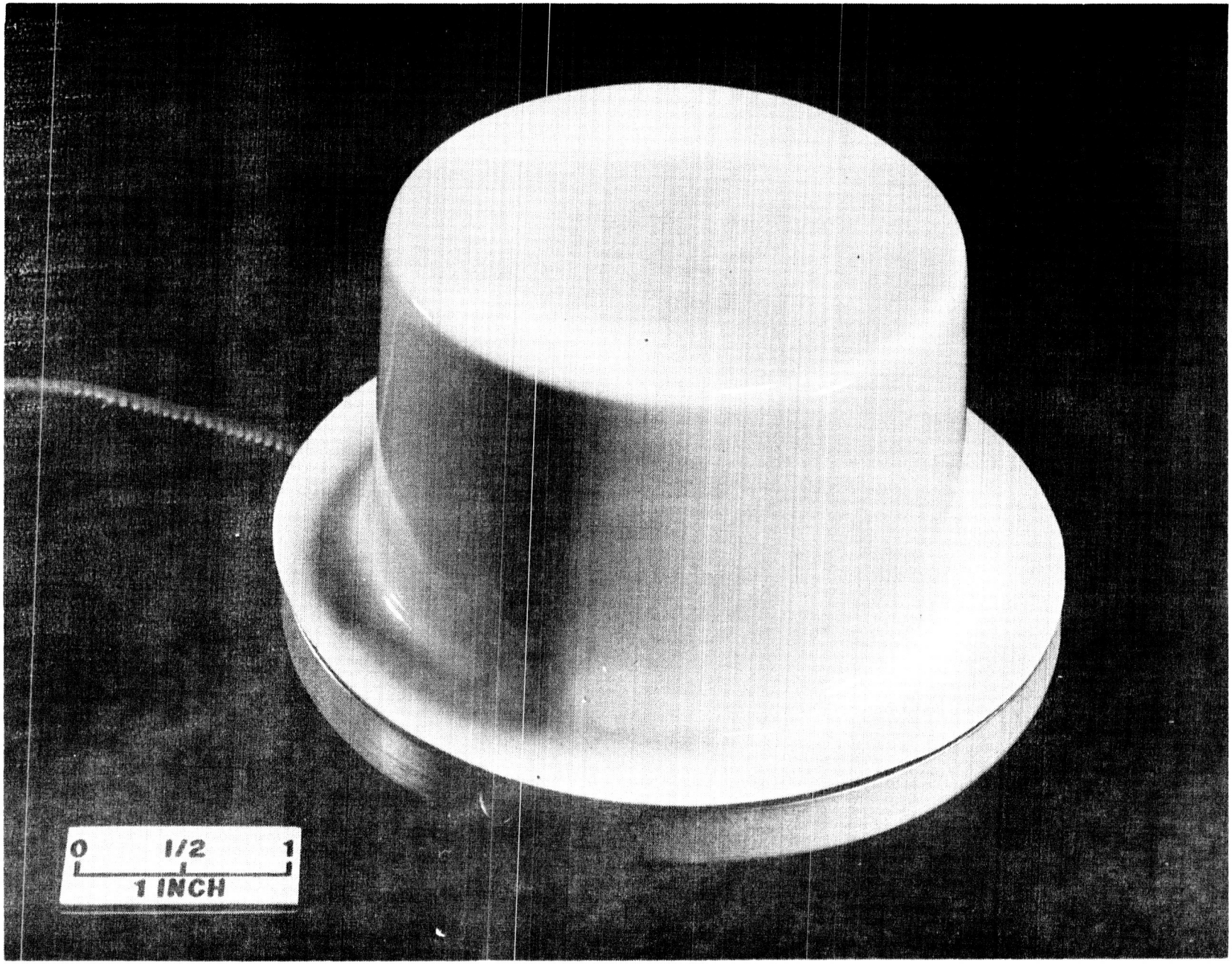

LOW PROFILE VHF DUAL FREQUENCY
TRANSMISSION LINE ANTENNA

unit is tabulated as a function of frequency as follows:

Space Suit Mockup Test

Frequency Mc	VSWR Unit Number		
	1	2	3
258.7	1.08	1.13	1.12
259.7	1.07	1.10	1.09
260.7	1.08	1.10	1.06
295.8	1.13	1.08	1.40
296.8	1.09	1.06	1.40
297.8	1.07	1.09	1.40

36-inch Ground Plane Test

Frequency Mc	VSWR Unit Number		
	1	2	3
259.7	2.2	2.10	4.1
f_1	2.1	1.98	2.3
296.8	1.82	2.9	3.3
f_2	1.75	2.1	3.2

The 36 inch ground plane test shows high VSWR's at the original resonate frequencies of 259.7 and 296.8. This is to be expected as the antennas were originally tuned on the space suit mockup. VSWR was also measured at the new resonate frequencies f_1 and f_2.

In addition, impedance plots versus frequency were made for unit number one. These data are shown in Figures 78 and 79 for the space suit mockup test and Figure 80 for the 36 inch ground plane test. Units two and three have similar impedance characteristics.

Radiation patterns were measured at each center frequency for each antenna in each mounting condition. These are shown in Figures 81 to 90 for the mockup test and Figures 91 to 93 for the ground plane test. Each pattern is marked to show sector of interest. In addition, the data for unit number one was reduced to contour plots and are shown in Figures 94 and 95.

NAME	TITLE	DWG. NO.
		DATE
SMITH CHART FORM 82BSPR (2-49)	KAY ELECTRIC COMPANY, PINE BROOK, N.J. ©1949 PRINTED IN U.S.A.	

IMPEDANCE [redacted] COORDINATES

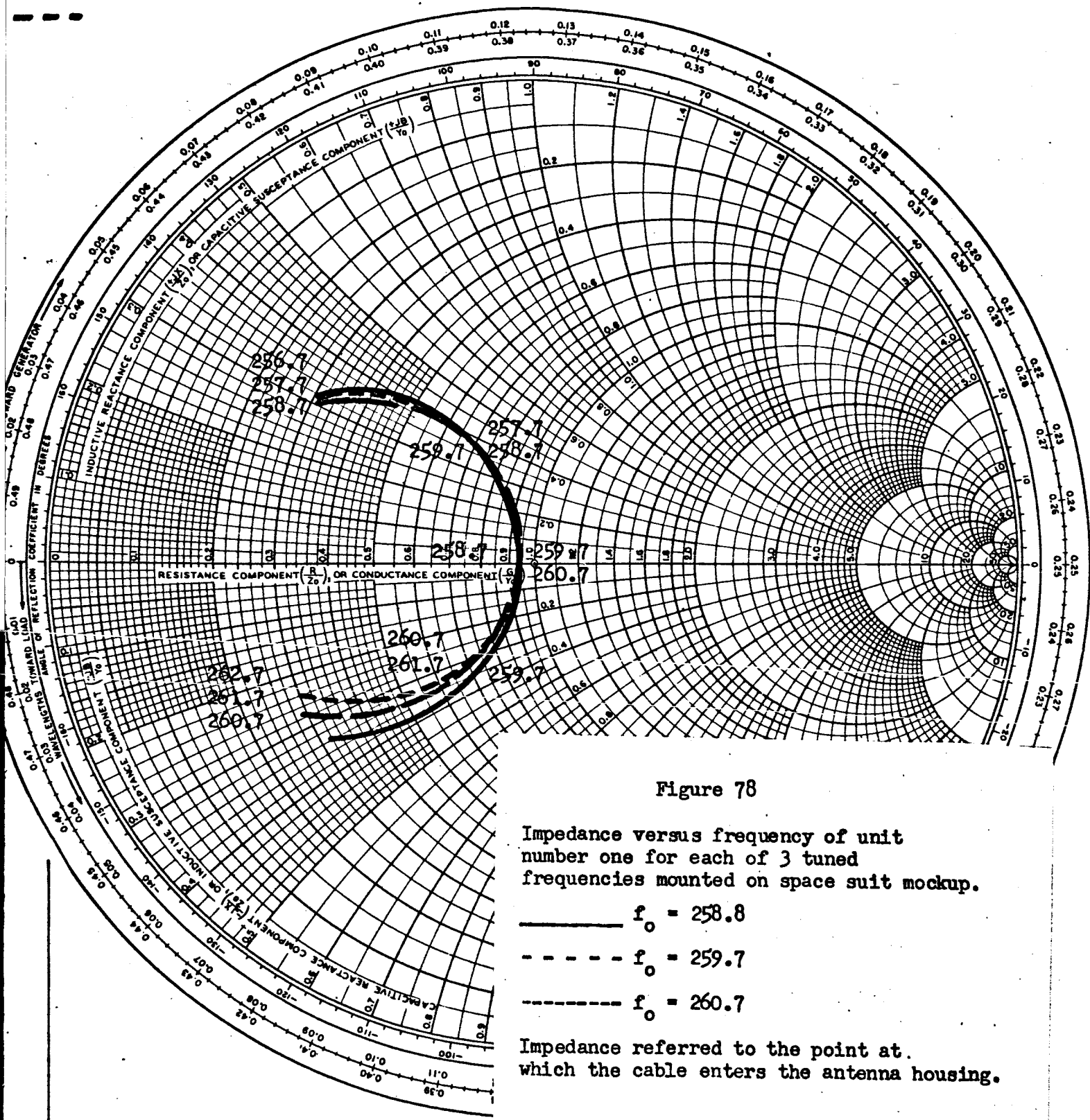

Figure 78

Impedance versus frequency of unit number one for each of 3 tuned frequencies mounted on space suit mockup.

———— f_o = 258.8

- - - - - f_o = 259.7

-------- f_o = 260.7

Impedance referred to the point at which the cable enters the antenna housing.

NAME	TITLE	DWG. NO.
SMITH CHART FORM 82BSPR (2-48)	KAY ELECTRIC COMPANY, PINE BROOK, N.J. ©1948 PRINTED IN U.S.A.	DATE

IMPEDANCE [redacted] COORDINATES

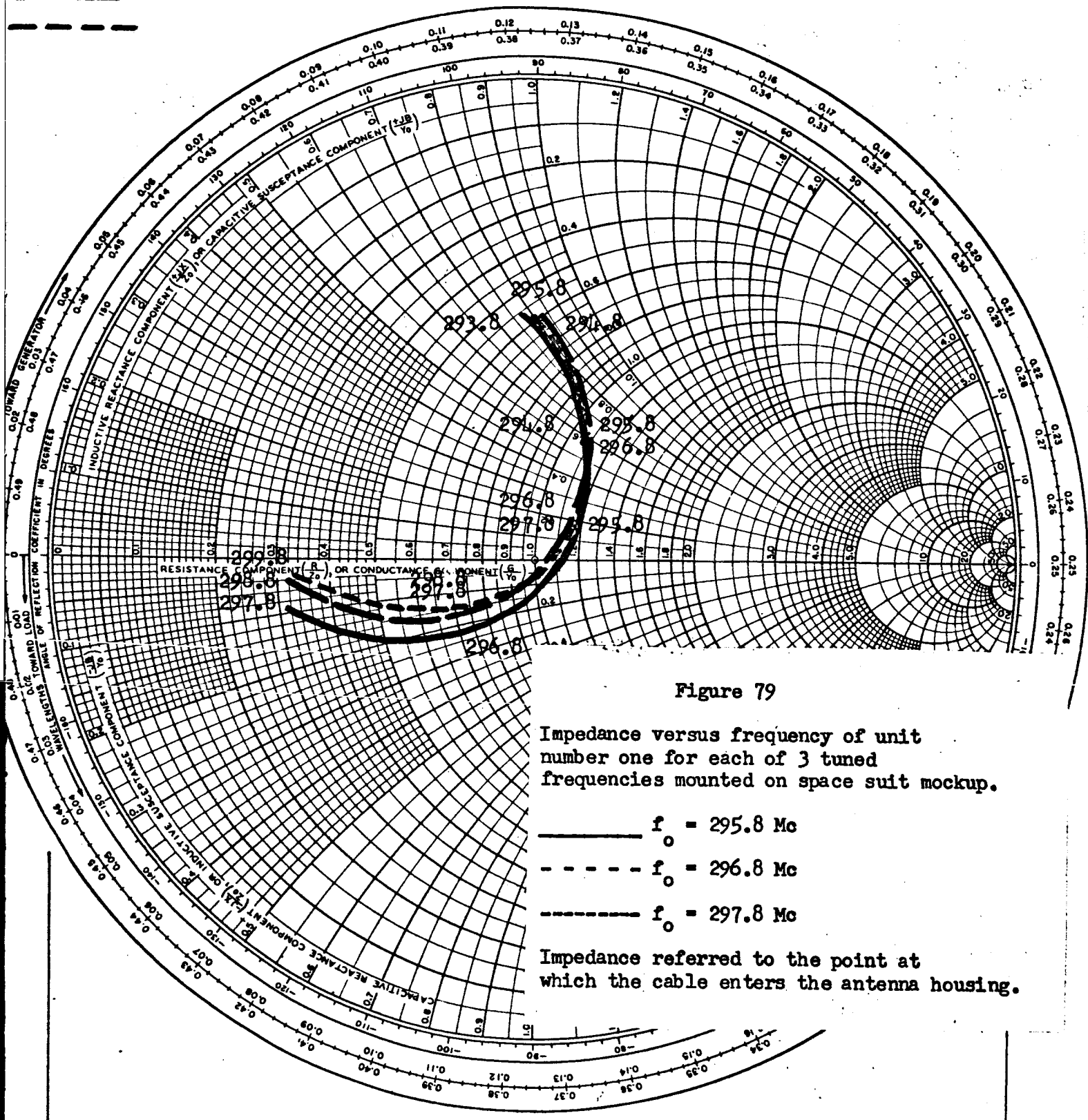

Figure 79

Impedance versus frequency of unit number one for each of 3 tuned frequencies mounted on space suit mockup.

——— f_o = 295.8 Mc

- - - - - f_o = 296.8 Mc

-------- f_o = 297.8 Mc

Impedance referred to the point at which the cable enters the antenna housing.

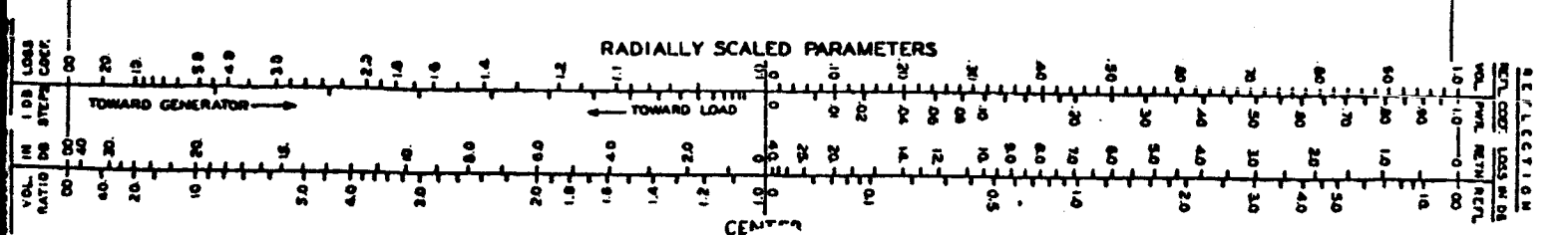

NAME	TITLE	DWG. NO.
		DATE
SMITH CHART FORM 82BSPR (2-49)	KAY ELECTRIC COMPANY, PINE BROOK, N.J. ©1949 PRINTED IN U.S.A.	

IMPEDANCE [redacted] COORDINATES

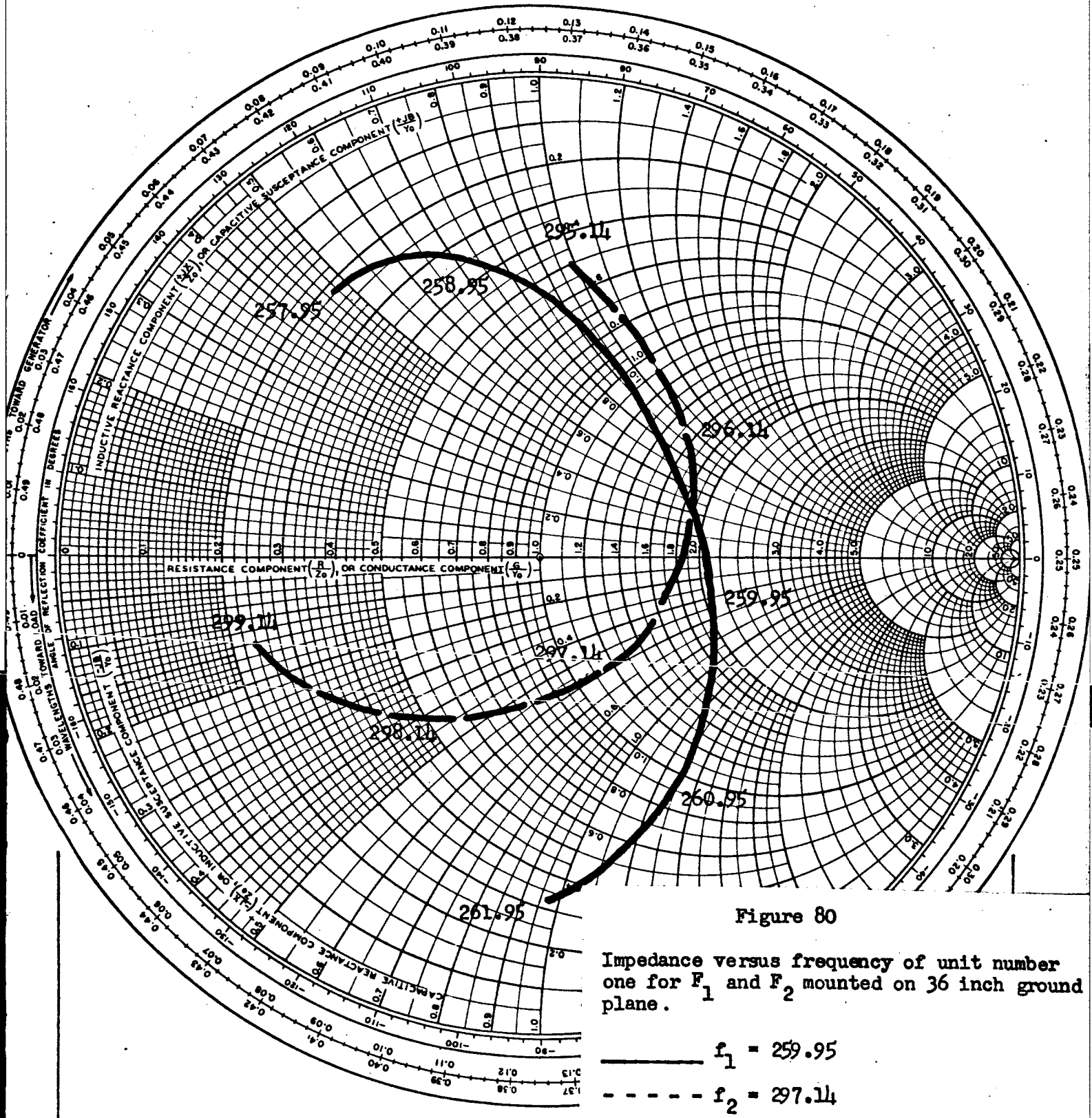

Figure 80

Impedance versus frequency of unit number one for F_1 and F_2 mounted on 36 inch ground plane.

——— $f_1 = 259.95$

- - - - - $f_2 = 297.14$

Impedance referred to the point at which the cable enters the antenna housing.

Electronics- Vol. 17, No. 1, PP. 130–133, 318–325, Jan. 1944

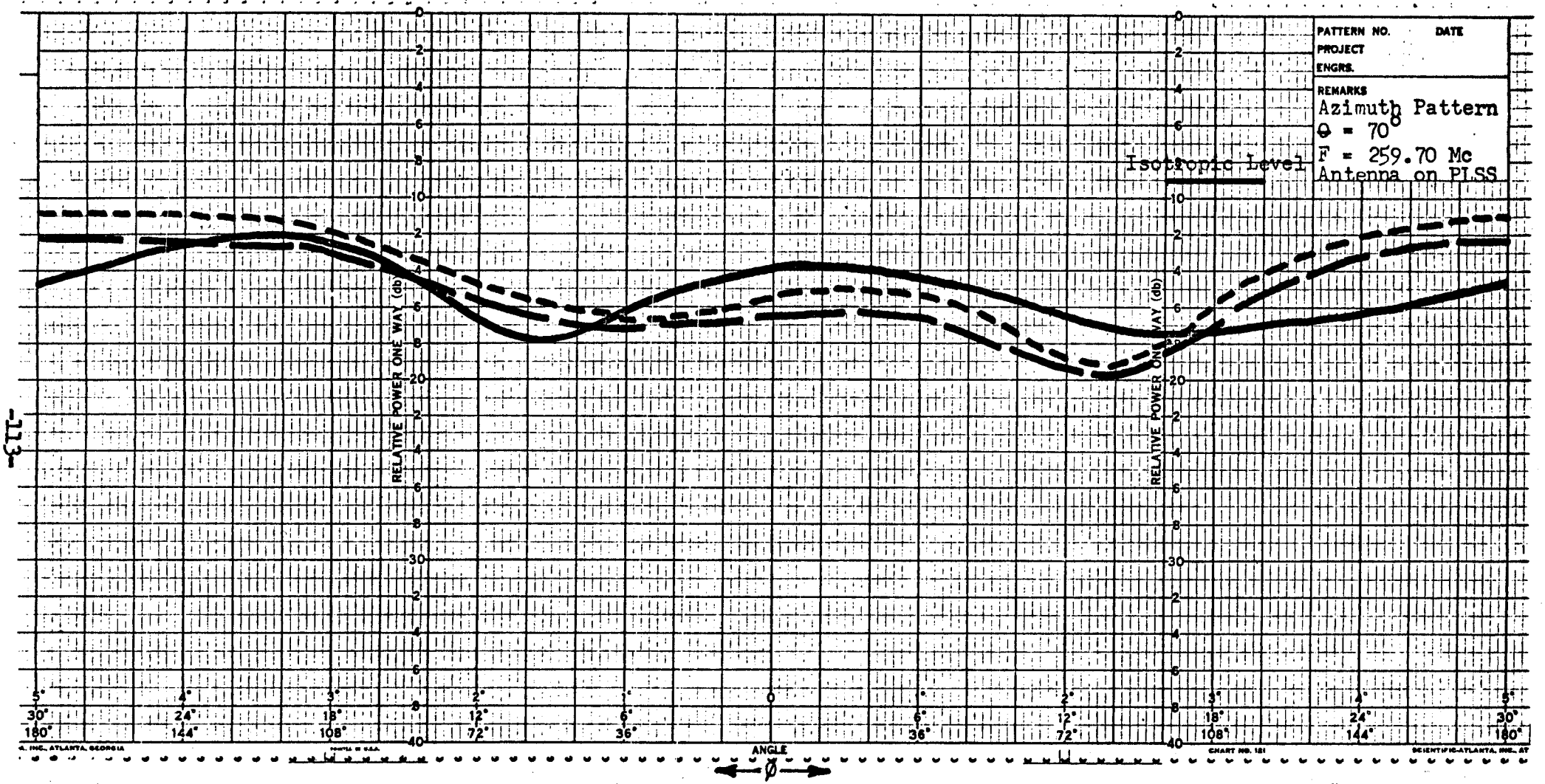

FIGURE 81

Azimuth Radiation Pattern of Flight Qualifiable Models
Mounted on Space Suit Mockup

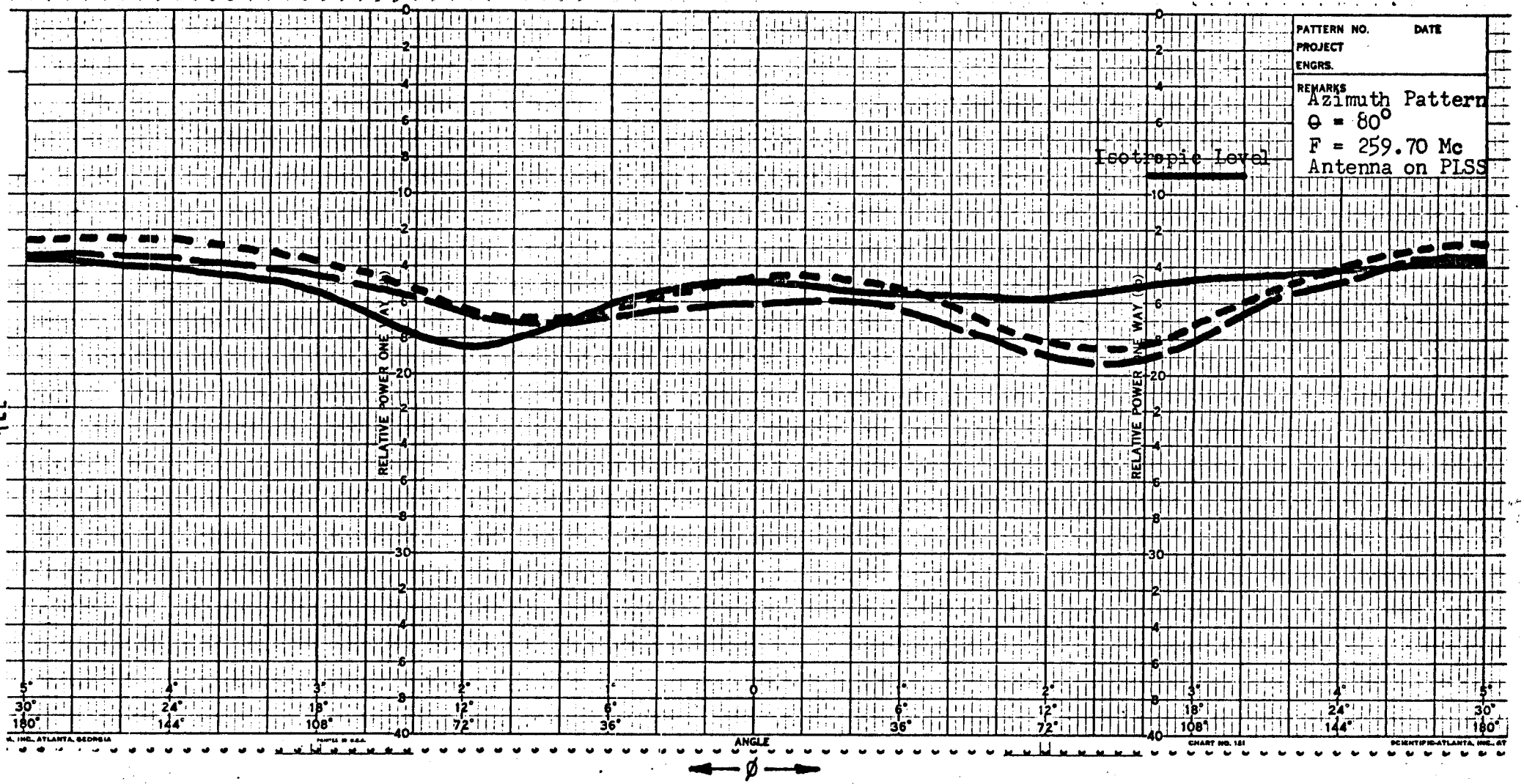

FIGURE 82

Azimuth Radiation Pattern of Flight Qualifiable Models Mounted on Space Suit Mockup

——— Unit #1
— — Unit #2
– – – – Unit #3

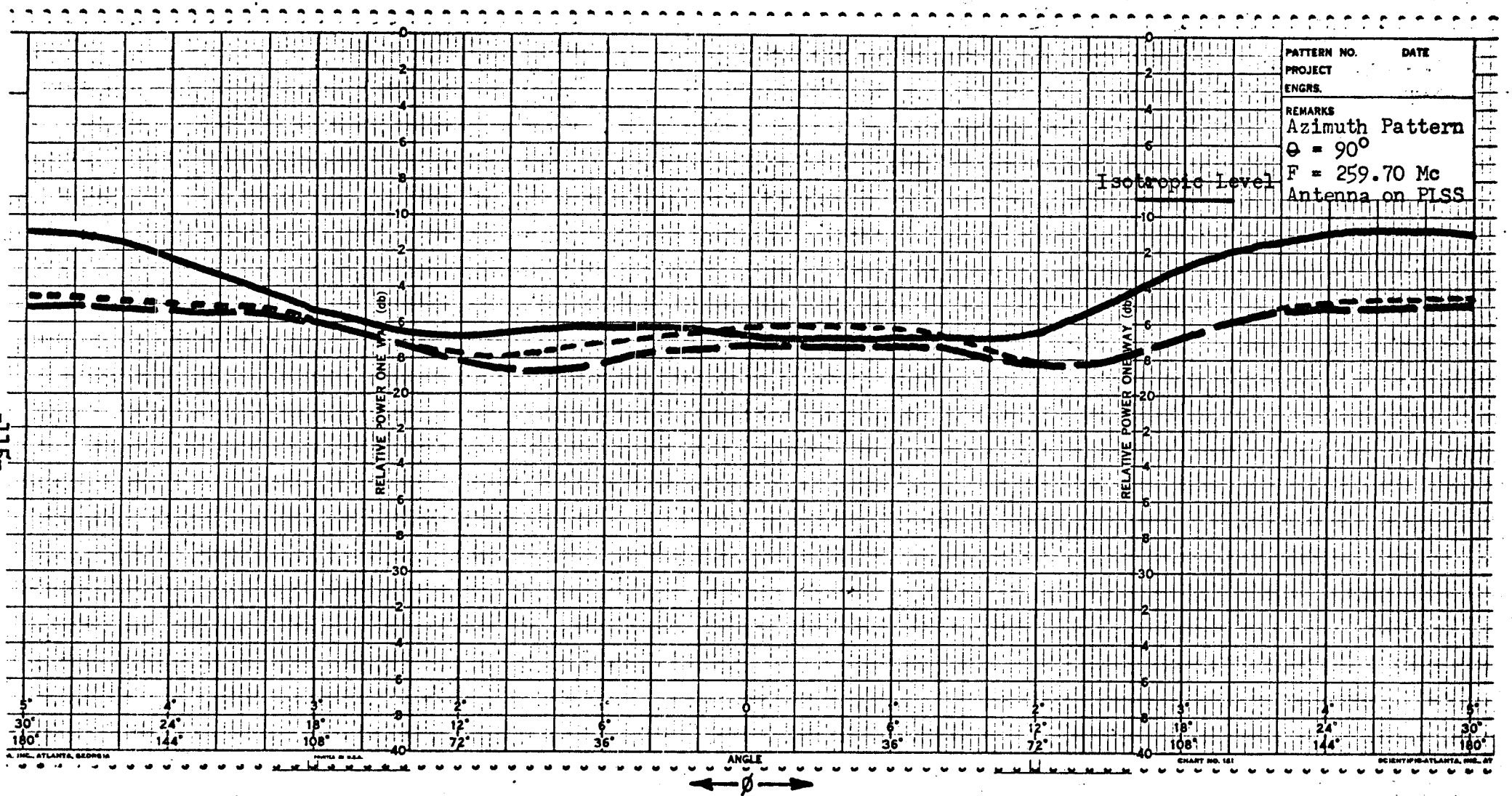

FIGURE 83

Azimuth Radiation Pattern of Flight Qualifiable Models
Mounted on Space Suit Mockup

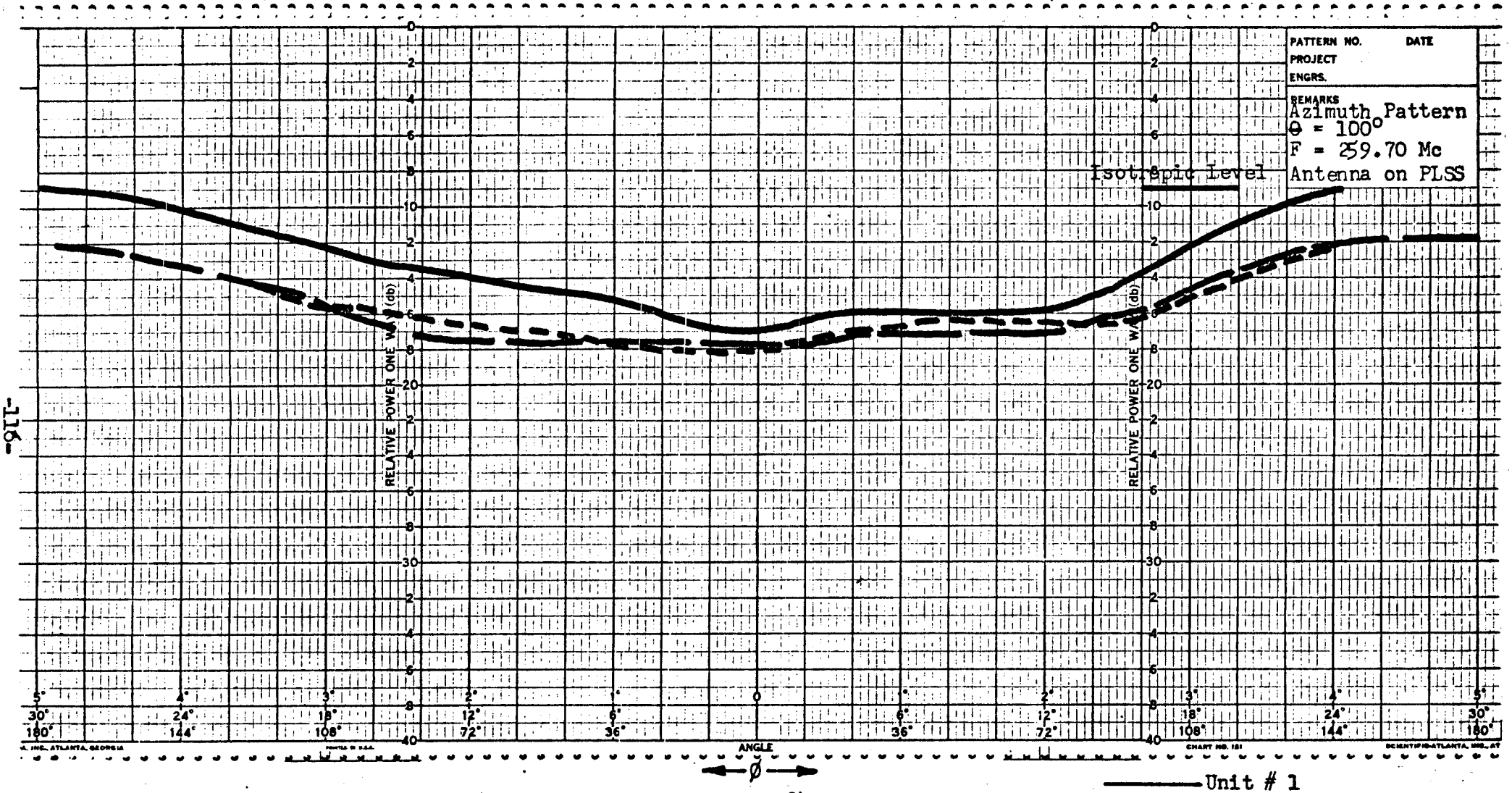

FIGURE 84

Azimuth Radiation Pattern of Flight Qualifiable Models
Mounted on Space Suit Mockup

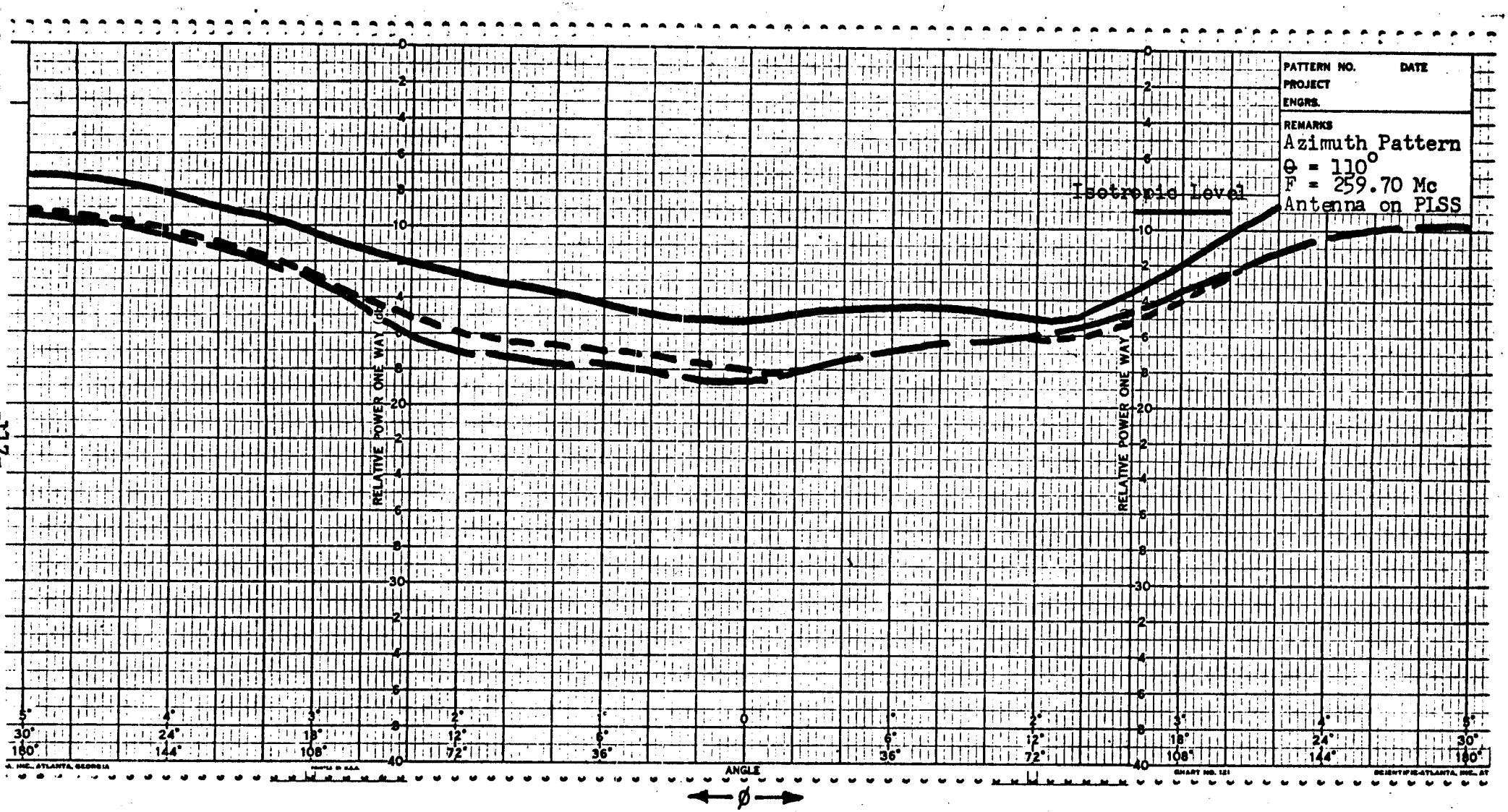

FIGURE 85

Azimuth Radiation Pattern of Flight Qualifiable Models Mounted on Space Suit Mockup

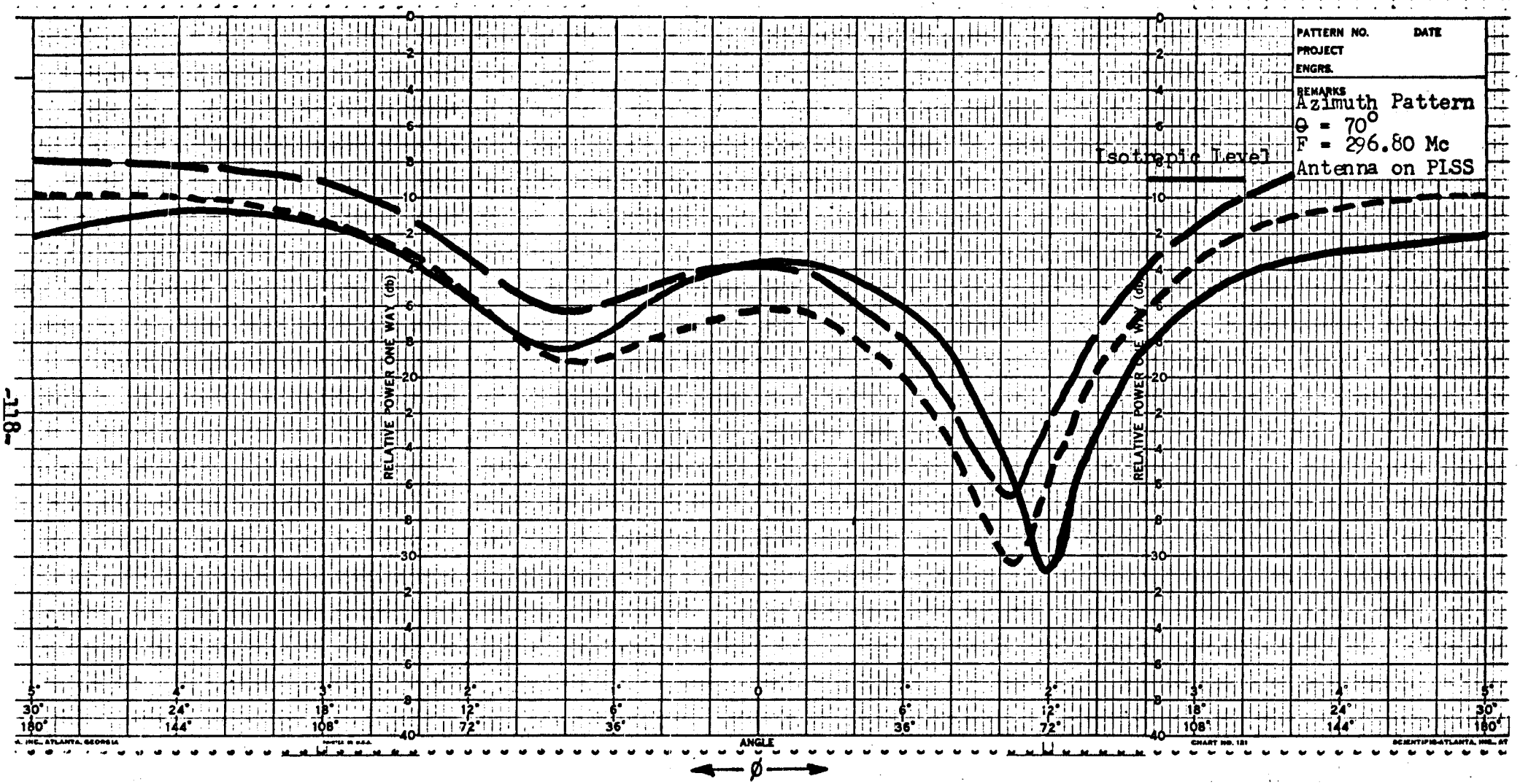

FIGURE 86

Azimuth Radiation Pattern of Flight Qualifiable Models
Mounted on Space Suit Mockup

——— Unit # 1
— — — Unit # 2
– – – – Unit # 3

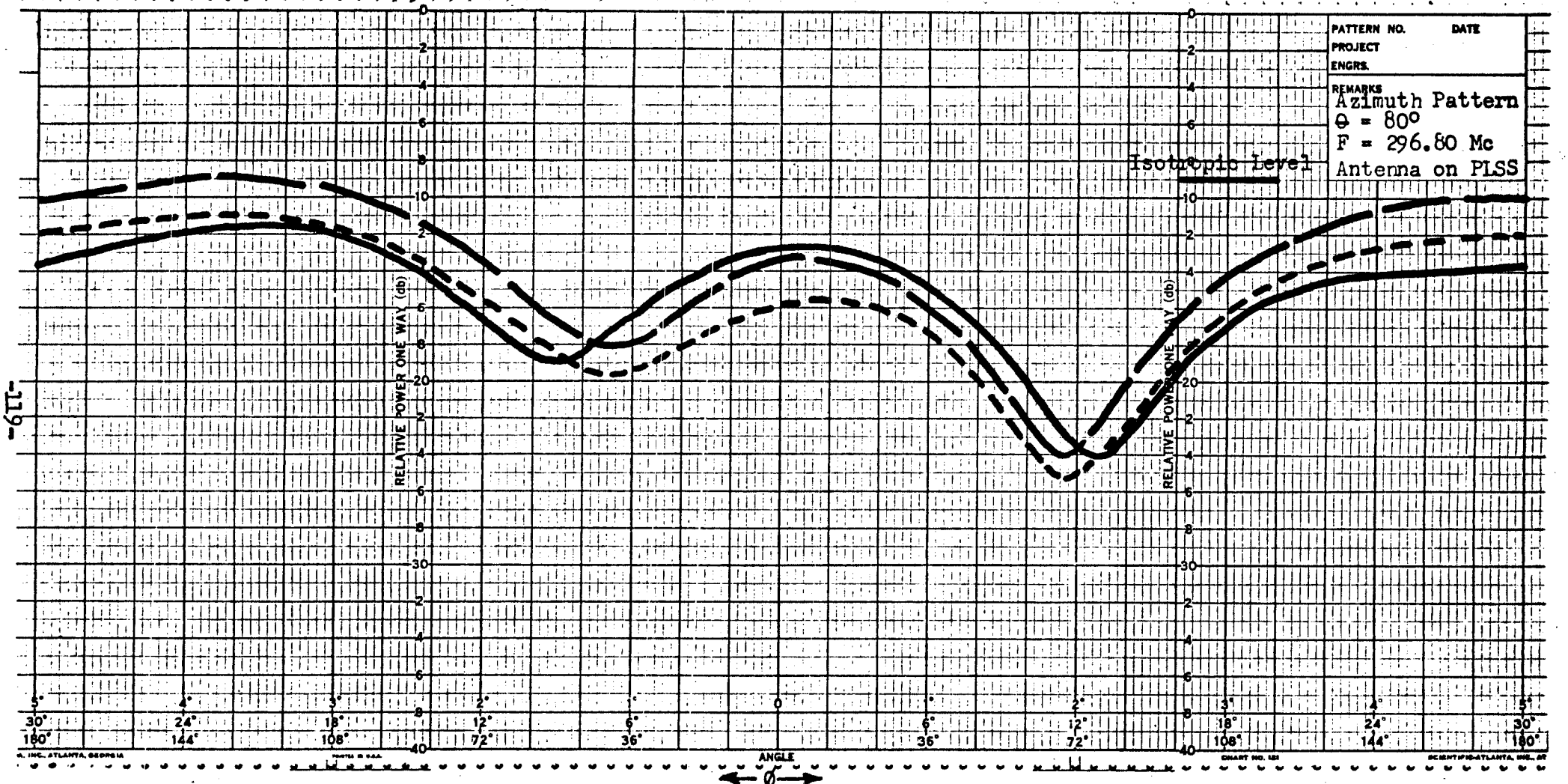

FIGURE 87

Azimuth Radiation Pattern of Flight Qualifiable Models Mounted on Space Suit Mockup

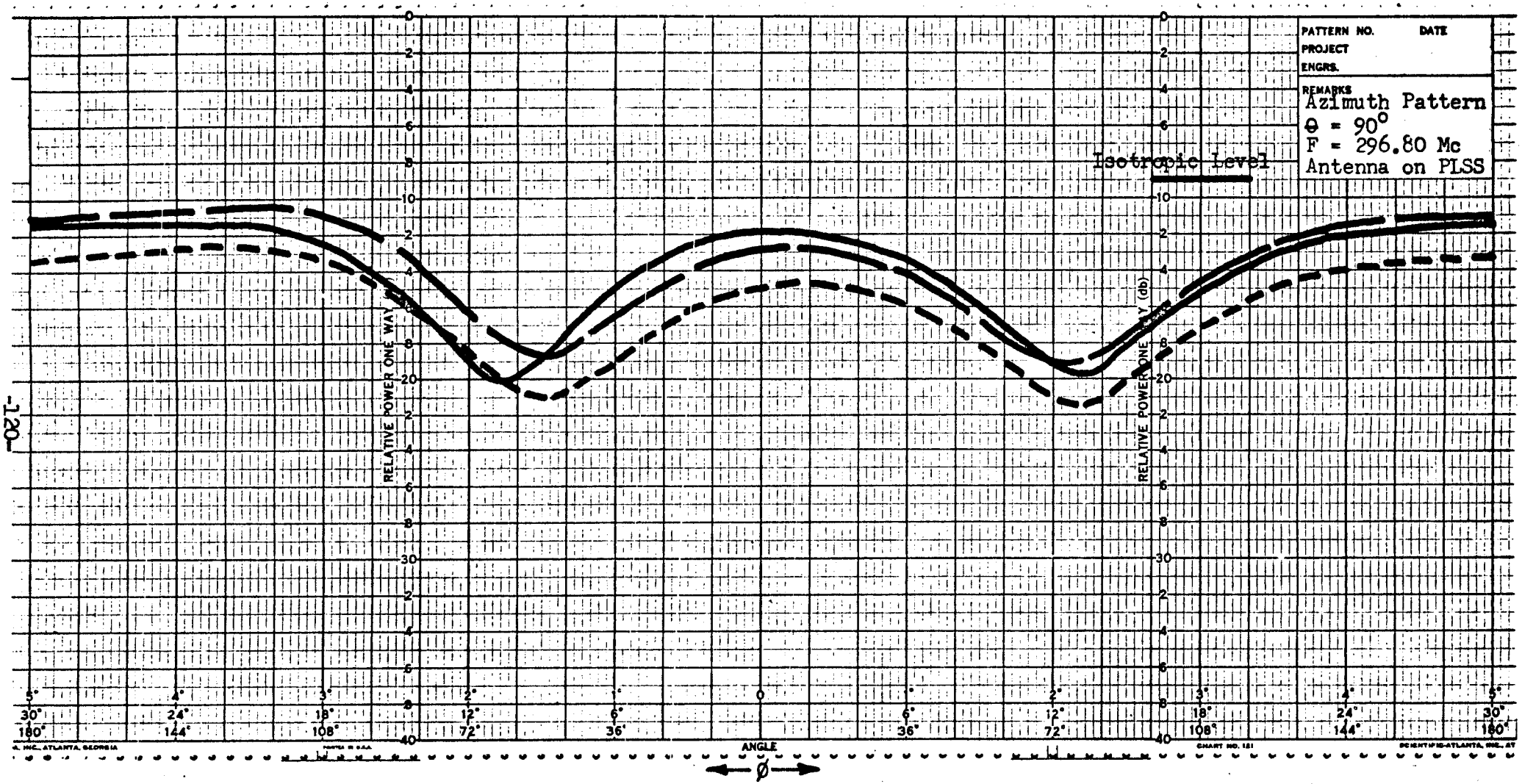

FIGURE 88

Azimuth Radiation Pattern of Flight Qualifiable Models
Mounted on Space Suit Mockup

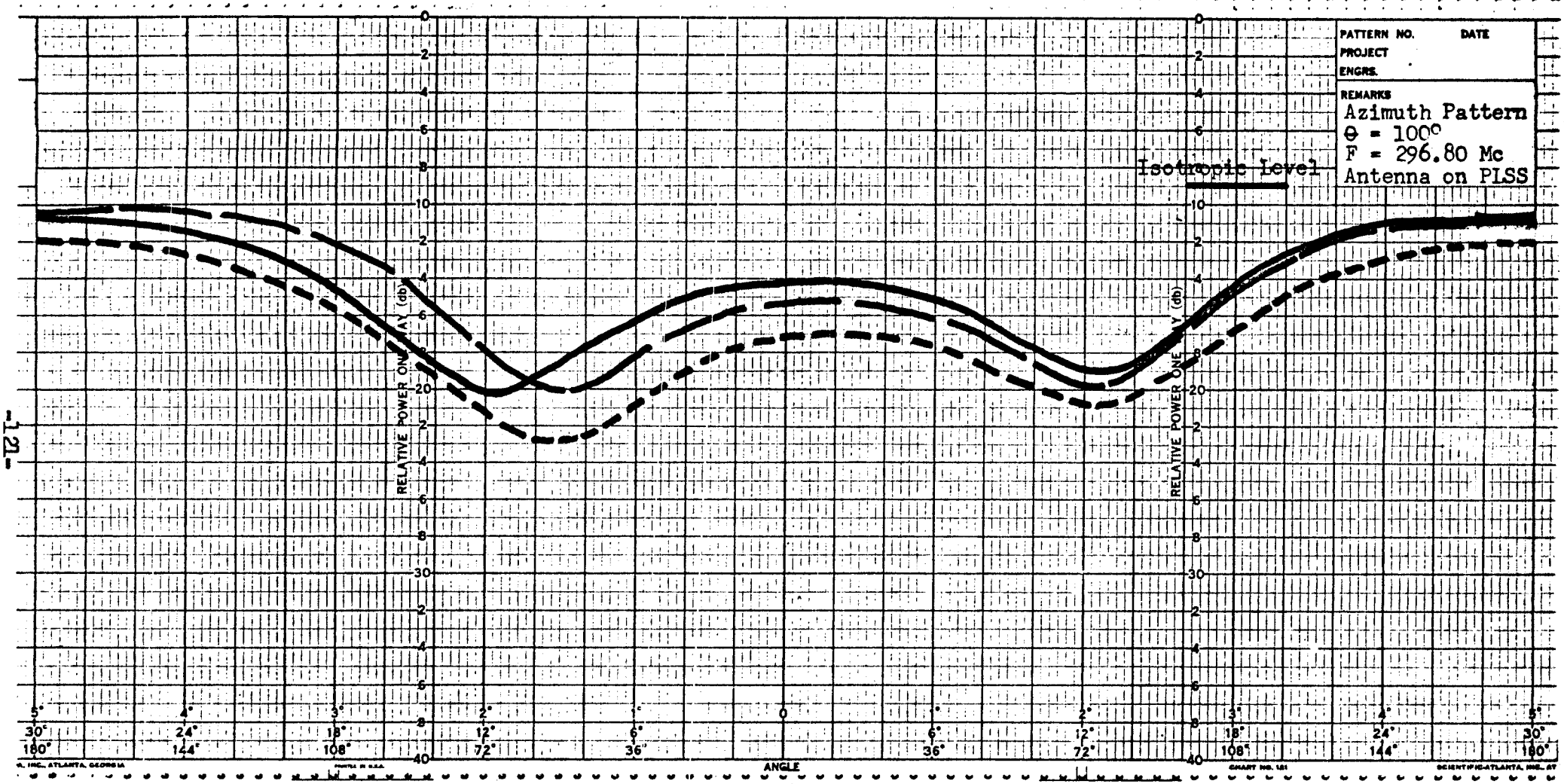

FIGURE 89

Azimuth Radiation Pattern of Flight Qualifiable Model Mounted Space Suit Mockup

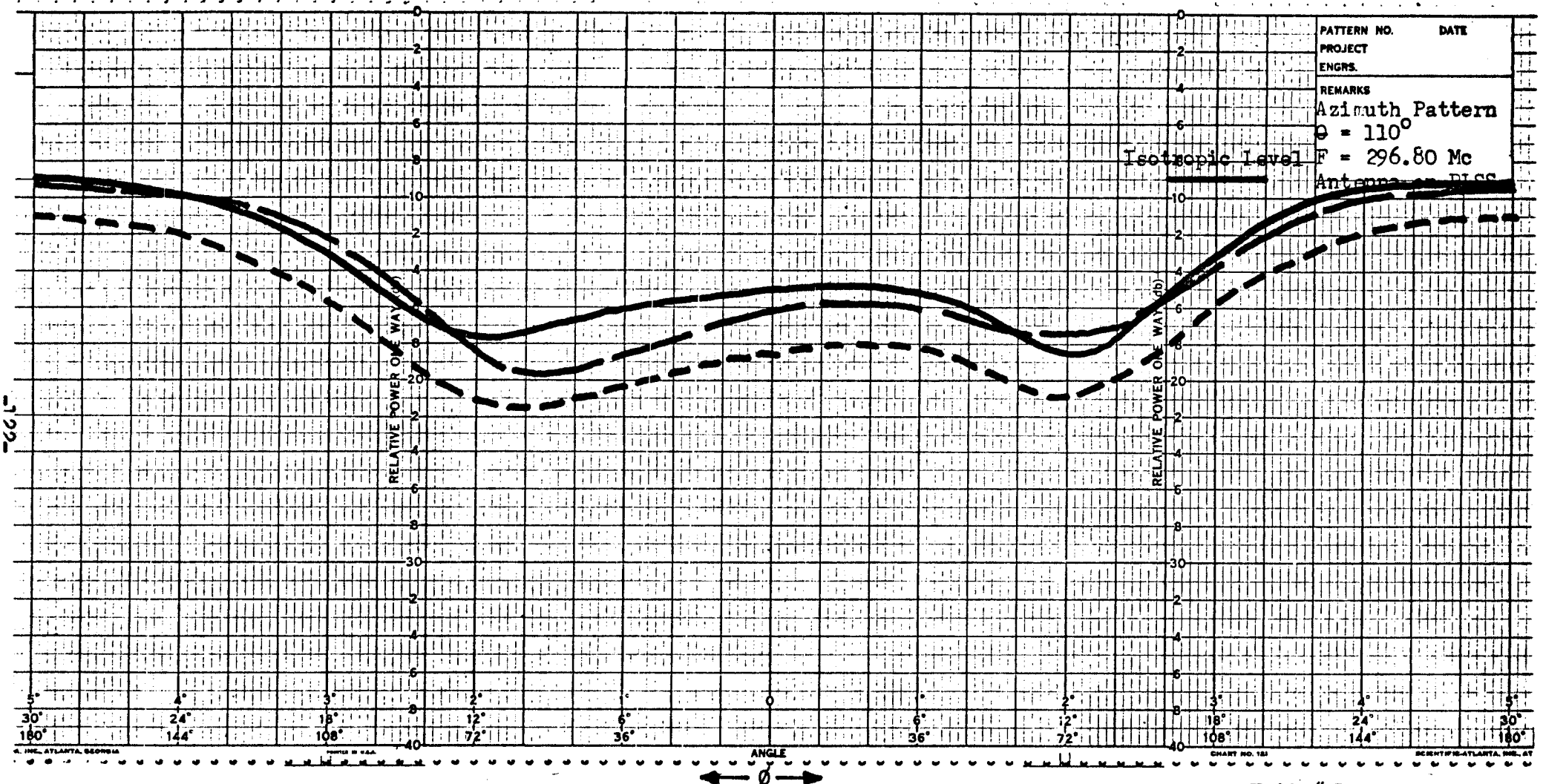

FIGURE 90

Azimuth Radiation Pattern of Flight Qualifiable
Mounted on Space Suit Mockup

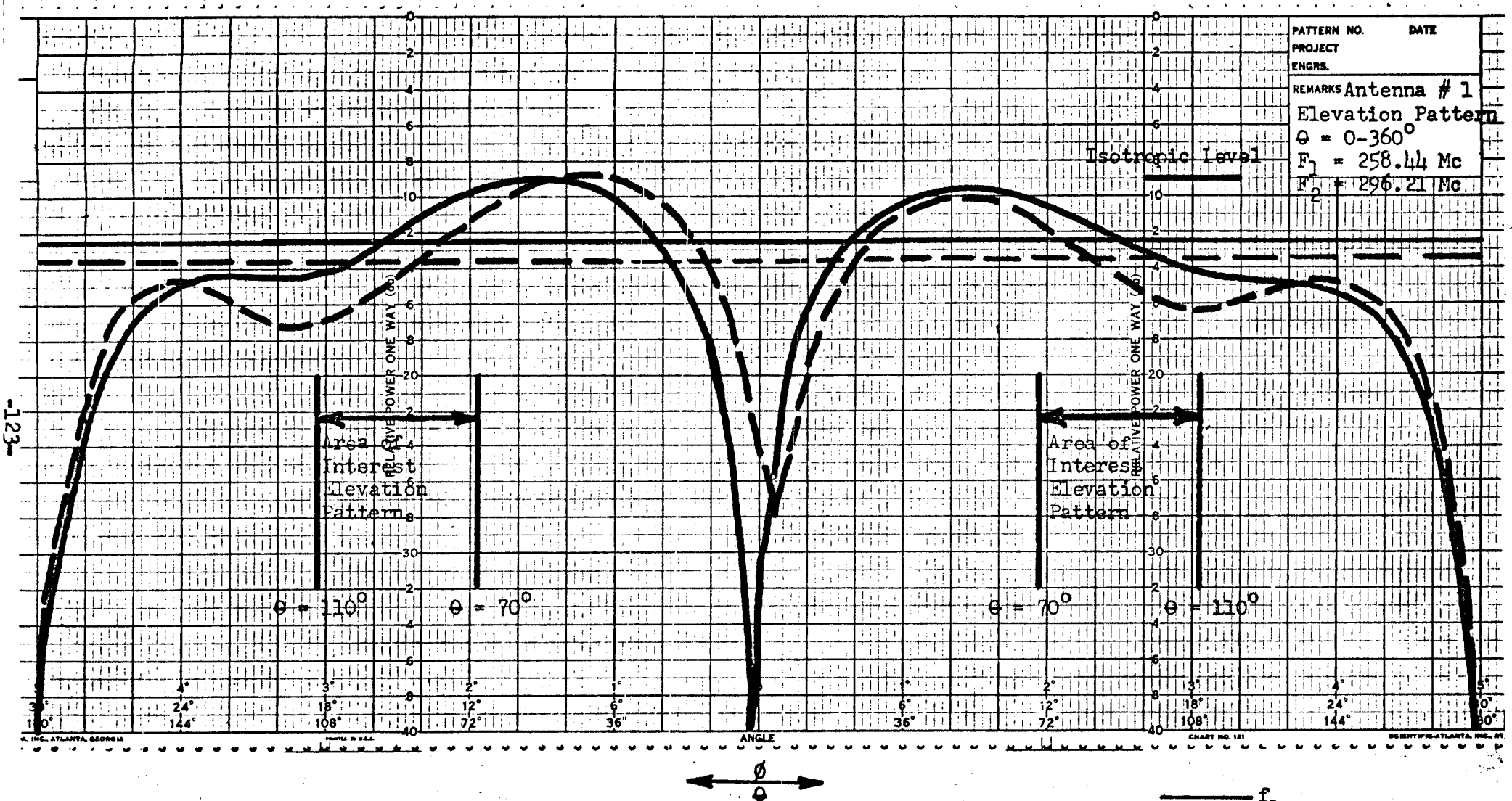

FIGURE 91

Azimuth and Elevation Radiation Pattern of Unit Number 1
Mounted on 36-Inch Ground Plane

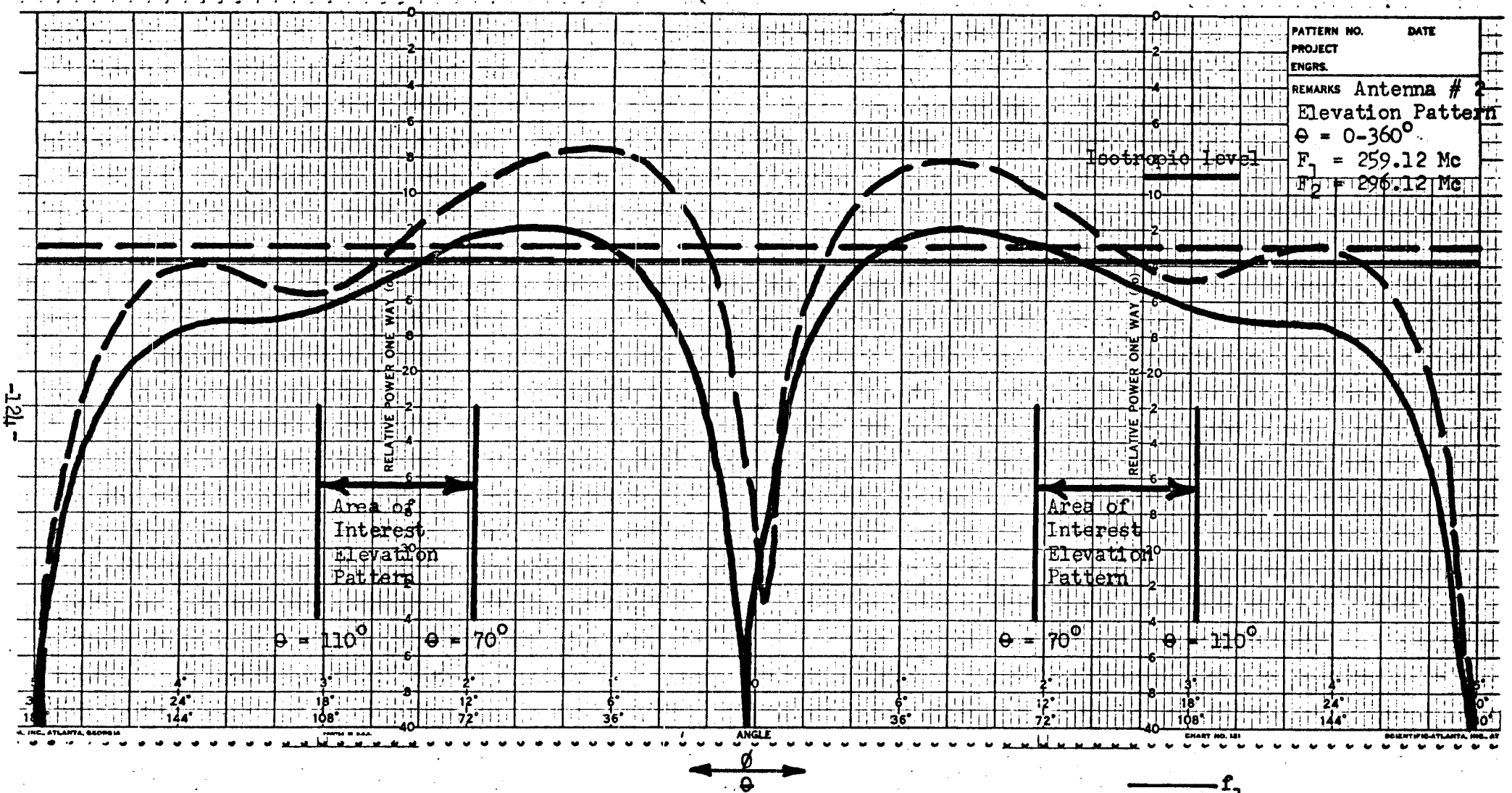

FIGURE 92

Azimuth and Elevation Radiation Pattern of Unit Number 2
Mounted on 36-Inch Ground Plane

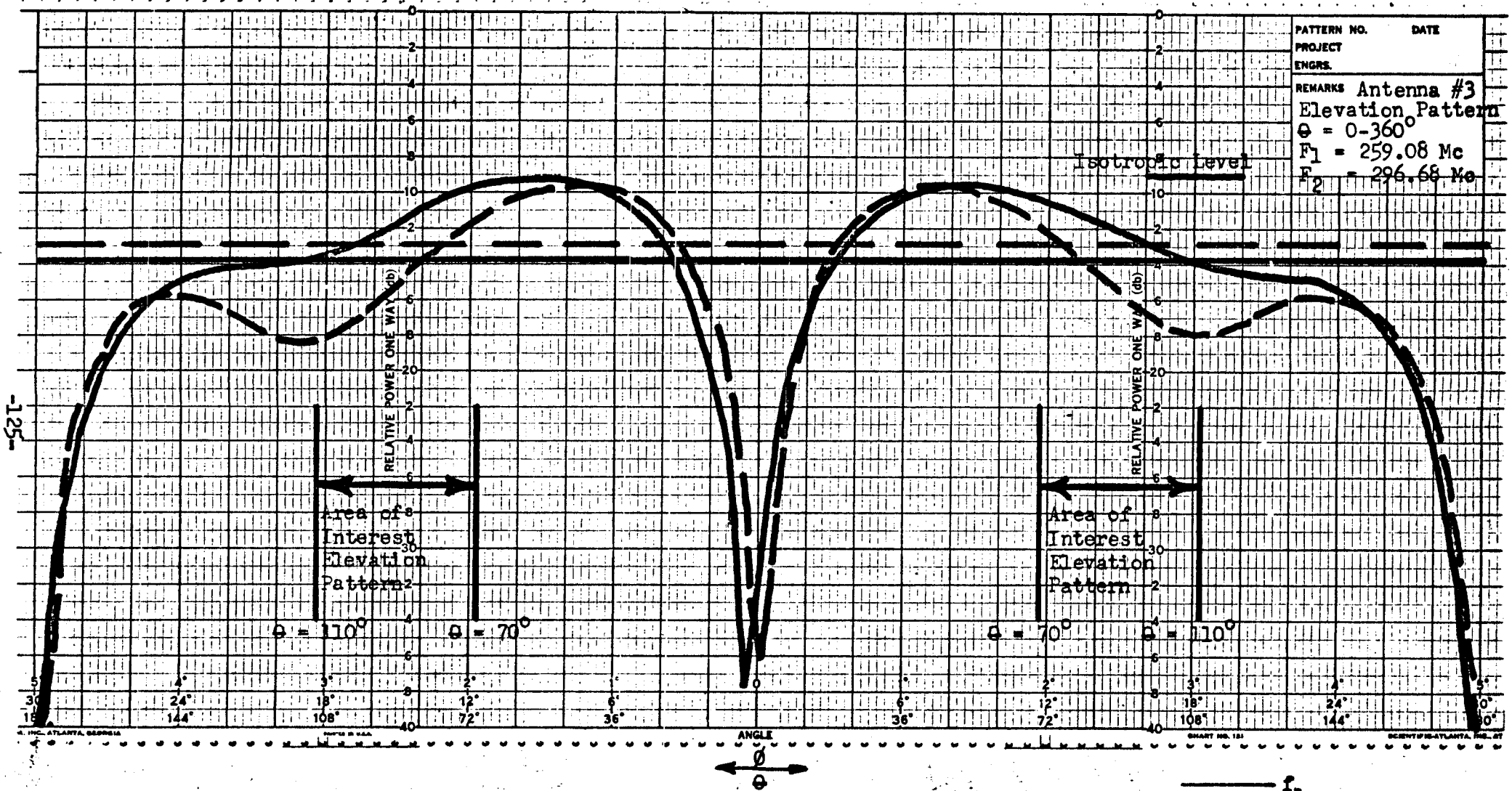

FIGURE 93

Azimuth and Elevation Radiation Pattern of Unit Number 3
Mounted on 36-Inch Ground Plane

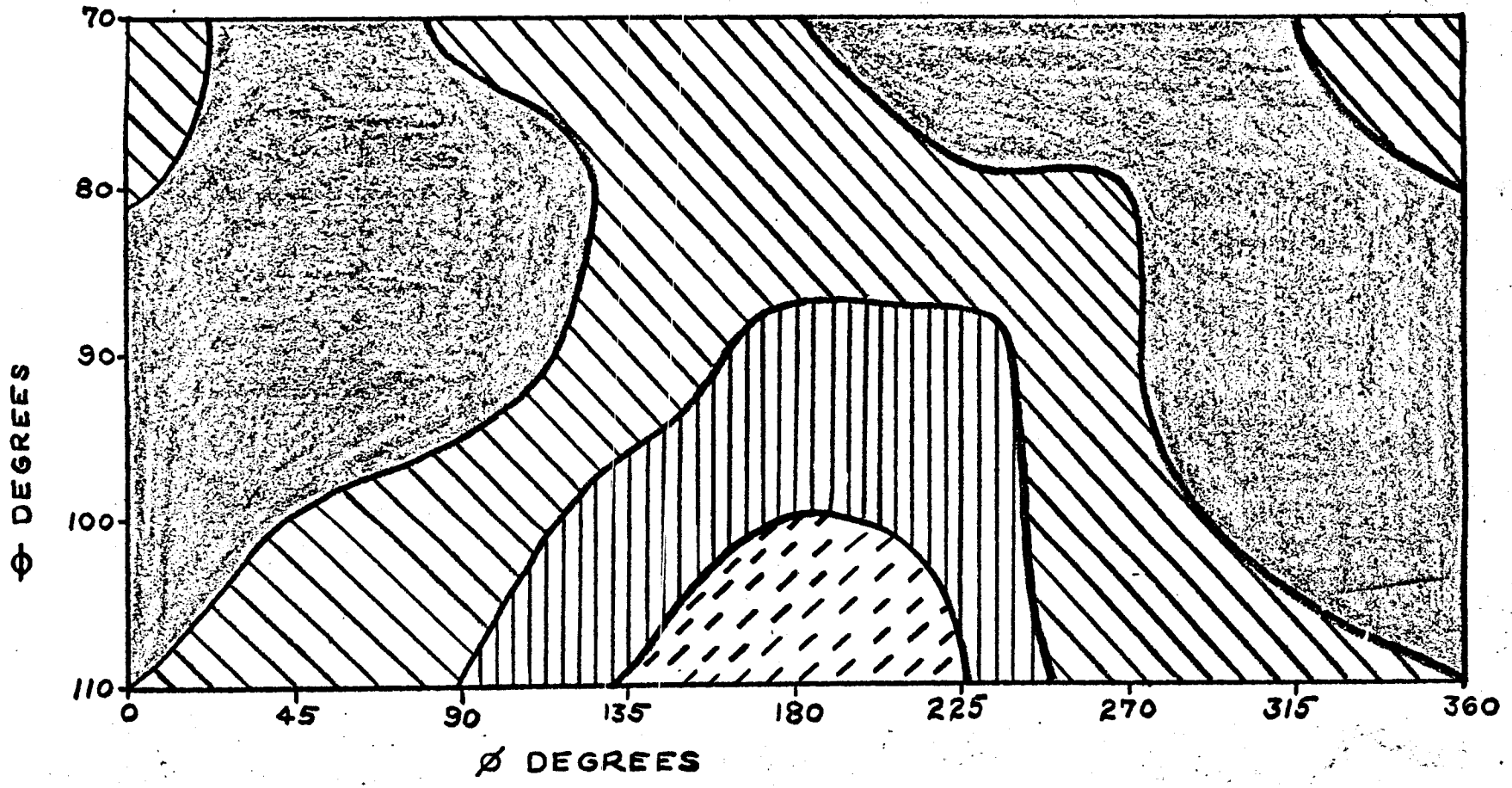

+3 → +0 = 4.8%
0 → 3 = 17.3%
-3 → -6 = 29.2%
-6 → -9 = 48.7%

+3→0 -3→-6

0→-3 -6→-9

Figure 94

Contour plot showing radiation levels (in dB) for unit number one mounted on space suit mockup over ±20° of the horizon for all angles of azimuth. Frequency = 259.7 Mc

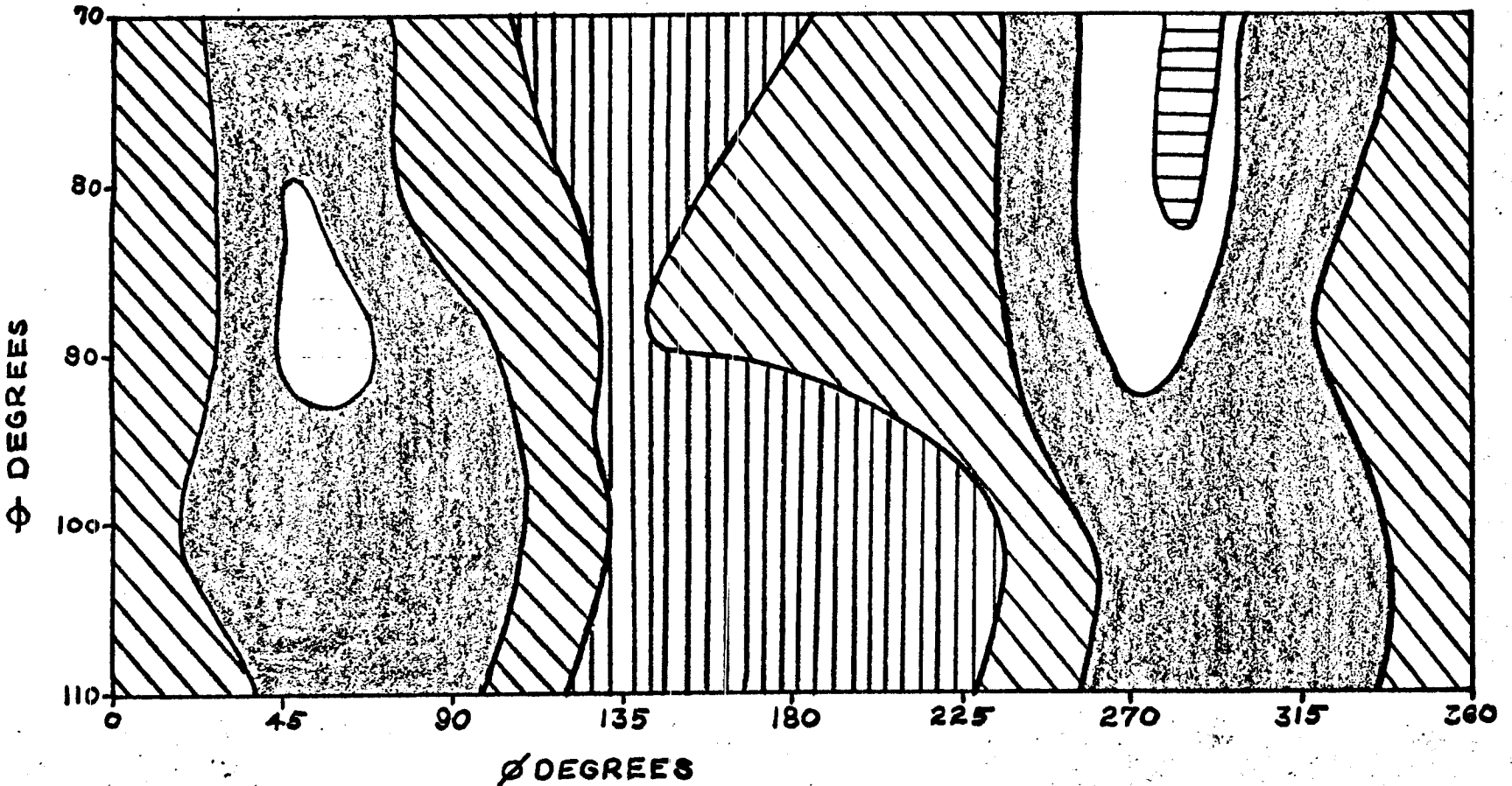

0 → -3 = 17.5%
-3 → -6 = 39.5%
-6 → -9 = 37.1%
-9 → -12 = 5.0%
< -12 = 1.0%

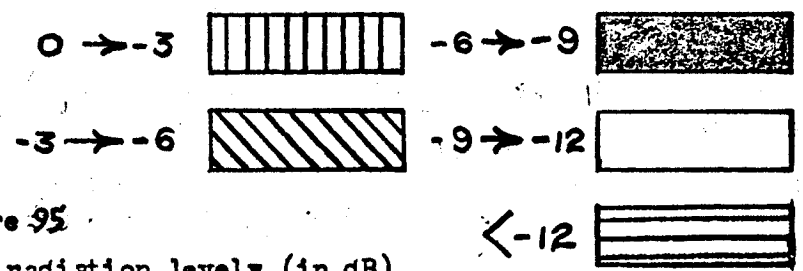

Figure 95

Contour plot showing radiation levels (in dB) of unit no. 1 mounted on space suit mockup over ± 20° of the horizon for all angles of azimuth. Frequency = 296.8 Mc.

4. CONCLUSIONS

The purpose of this report has been to describe the activities, antenna design considerations, tests, and test results achieved during the course of the Space Suit Communications Antenna System study. The data presented herein shows the performance of each antenna under specific mounting conditions and is the basis for the following conclusions:

1. The performance of any of the radiating systems studied in this investigation was improved by elevating the system. In particular, the helmet location is far superior to the PLSS location and the PLSS mounted antennas improved if they were raised above the normal flush mounting condition on the surface of the PLSS.
2. Currents on the conductive thermal garment generated fields that caused nulls to appear in the antenna patterns. This cannot be avoided without properly treating the thermal garment to reduce its conductivity.
3. Erection-retraction mechanisms can be made to function satisfactorily, however they add considerable weight and complexity to the system. For these reasons a fixed antenna system is more desirable.
4. Visor position does not affect the radiation patterns.
5. The transmission line antenna has excellent impedance matches at both frequencies of interest, has satisfactory radiation patterns on the PLSS and has excellent patterns on the helmet.
6. The whip exhibits generally poorer impedance matches compared to the transmission line antenna; however, it has a slight gain improvement at the higher frequency for the PLSS mounting.

5. RECOMMENDATIONS

The following recommendations are made based upon the experience gained and the information derived from the performance of this investigation:

1. Based upon the electrical, mechanical, and environmental requirements imposed upon the antenna system, it is recommended that the dual frequency transmission line antenna be employed with the Apollo astronaut communication system. This selection is based upon the mechanical characteristics, low profile configuration, and electrical performance demonstrated during the program.
2. The whip should be considered as a back-up, or alternate antenna system. Its radiation patterns and gain when mounted in the PLSS location are approximately equal to those of the transmission line antenna, however its input impedance and configuration are less desirable.
3. Future efforts to improve the radiating system should include the reconsideration of the helmet as an antenna location.
4. Significant changes in the space suit and/or PLSS, in size, relative position, composition, or configuration should be accompanied by a reconfirmation of the antenna system performance and a consideration of possible variations of antenna design or location to improve the antenna system performance.

6. BIBLIOGRAPHY

1. King, R., Harrison, C.W., and Denton, D.H., "Transmission Line Missile Antennas," IRE Trans. on Antennas and Propagation, AP-8, January 1960.

2. Norgorden, O., and Walters, A.W., "Experimentally Determined Characteristics of Cylindrical Sleeve Antennas," J. of Amer. Naval Engineers: 1 May 1950.

3. Brown, G.H., and Woodward, O.M., "Experimentally Determined Impedance Characteristics of Cylindrical Antennas," Proc. IRE, Vol. 33, pp. 257-262.

APPENDIX A

REVISION TO

PROPAGATION EFFECTS STUDY FOR ASTRONAUT-LEM COMMUNICATION LINK

23 February 1966

SUPERSEDING APPENDIX TO CONTRACT

SEMIMONTHLY PROGRESS REPORT ON

SPACE SUIT COMMUNICATIONS ANTENNA

SYSTEM dated 10 December 1965

Prepared for NASA/MSC

under Motorola Project 3097

Contract NAS 9-4174

TABLE OF CONTENTS

1.0 INTRODUCTION

The purpose of this Technical Memorandum is to clarify the Propagation Effects Study submitted as the Appendix to Contract Semimonthly Progress Report on Space Suit Communication Antenna System dated 10 December 1965. The results of the above document (Free Space Path Loss = 96 dB, Multipath Loss = 32 dB, Total Loss = 128 dB) are essentially correct for the worst case conditions of propagation over a perfectly flat surface. However, some of the terminology used in that document is subject to misinterpretation and therefore warrants clarification. Also, it can be shown that long range undulations in the surface, such as the natural curvature corresponding to the lunar radius can significantly reduce the multipath loss to a value on the order of 10 dB. This Technical Memorandum is completely self contained, and may be employed without the necessity of referring to the previous document.

The objective of this analysis is to evaluate the effects of the lunar surface on the link loss of the astronaut-LEM communications link. In accordance with the specified system geometry, it is assumed that an unobstructed line of sight exists between the two terminals. Under this condition the primary effect of the lunar surface is multipath fading. Nevertheless, a rudimentary analysis of obstacle effects is included in order to establish broad limitations on the tolerable dimensions of intervening ridges and to facilitate a preliminary appreciation of the magnitude of the resulting diffraction loss.

At the present time, no reliable data is available on localized rf characteristics of the pertinent region of the lunar surface. Therefore, to permit a systematic analysis, it is necessary to assume a model of the

lunar surface that is as realistic as possible. In this case, the assumption of a smooth, lossless dielectric surface yields a conservative estimate of the link loss.

The following sections discuss system geometry, relations between intrinsic surface parameters and reflection characteristics, multipath effects, obstacle diffraction and polarization loss.

2.0 TECHNICAL DISCUSSION

This section discusses factors affecting propagation in the astronaut-LEM communication system and presents calculations of the various contributions to the total loss.

2.1 SYSTEM PARAMETERS

The system geometry is shown schematically in Figure 1. It is assumed that an unobstructed line of sight path exists between the two terminals of the link. However, the effects of large obstacles are discussed in Section 2.4. The parameters of the communications link are tabulated in Table I.

This memorandum is concerned only with evaluation of the link loss and does not consider internal system parameters such as transmitter power, signal-noise ratio, receiver sensitivity, etc.

2.2 FREE SPACE PATH LOSS

When propagation through free space is considered, the ratio of received to transmitted power is

$$\frac{P_R}{P_T} = \frac{G_1 G_2 \lambda^2}{16\pi^2 D^2} \quad , \tag{1}$$

where λ is the wavelength. The free space path loss is designated by

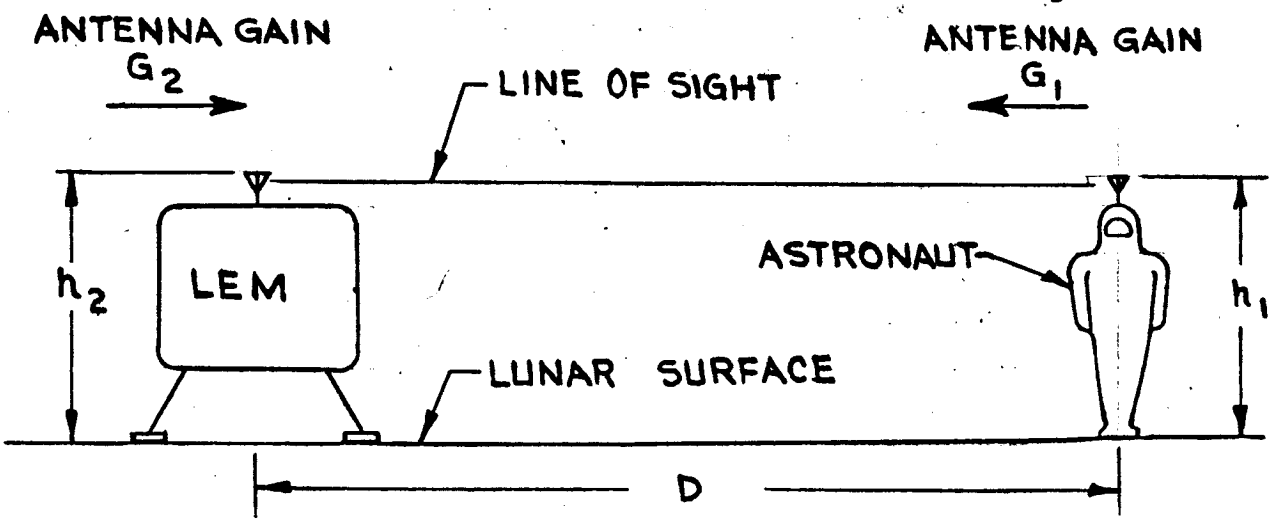

Figure 1. System Geometry

Table I. Link Parameters

Astronaut Antenna Height:	h_1 = 6 ft.
LEM Antenna Height:	h_2 = 24 ft.
Maximum Range:	D_{max} = 18,000 ft.
Operating Frequency:	f_o = 259.7 MHz*
Worst Case Astronaut Antenna Gain:	G_1 = -14 dB
LEM Antenna Gain:	G_2 = -3 dB

*Some calculations are also carried out for 296.8 MHz.

$$L_{FS} = \frac{\lambda^2}{16\pi^2 D^2} \quad . \qquad (2)$$

Nomographs of equation (2) are available in several sources.[1] For this system the free space path loss at the maximum range of 18,000 ft. is

Frequency = 259.7 MHz L(dB) = 95.5 dB

Frequency = 296.8 MHz L(dB) = 96.6 dB,

At the receive terminal the signal power is reduced by the product of the free space path loss and any additional loss occurring in the system, such as multipath.

2.3 MULTIPATH EFFECTS

Multipath is caused by interference between the signal directly radiated along the line of sight and signals that are reflected from objects or terrain in the vicinity of the communications link. The magnitude of the resultant received signal is determined both by the path length differences or phase shifts introduced by the system geometry and by the reflecting properties of the terrain.

In particular, if the reflecting terrain is rough, or if there are many randomly spaced scattering objects, the total reflected field will generally consist of a superposition of many reflected fields of random amplitude and phase, and the total field can then be interpreted as the sum of a constant vector and a Rayleigh distributed vector. On the other hand, if the surface is smooth there will be only one reflected ray, with a unique phase and amplitude. The net result is that a truly rough surface displays an irregular or random interference pattern, with fade depths of greater than 30 dB occurring with a probability of less than 5×10^{-4} and fade depths of 10 dB occurring with about 5% probability, when a line of sight path exists. However, a truly smooth surface with a reflection coefficient of -1 will result in a well defined interference pattern with relatively deep nulls. Thus, the assumption of a

smooth surface leads to a worst case analysis. The following subsections examine the factors that determine whether or not specular reflection occurs, the effect of material parameters and system geometry on the effective reflection coefficient, and the resulting multipath loss. It is shown that finite curvature of the lunar surface or long range undulations greatly affect the loss.

2.3.1 Surface Roughness

The Rayleigh criterion provides the most widely accepted and successful approach for determining the relative specular or diffuse scattering properties of a surface. This criterion is ordinarily applied to determine the vertical dimensions of surface irregularities that are required to produce specular reflection at a given wavelength and angle of incidence. However, it also can be, and in this case should be extended to determine the lateral dimensions as well.

First, considering the effect of the vertical dimensions of the surface irregularities, a cross section of an idealized rough surface, taken in the plane of incidence, would be as shown in Figure 2.

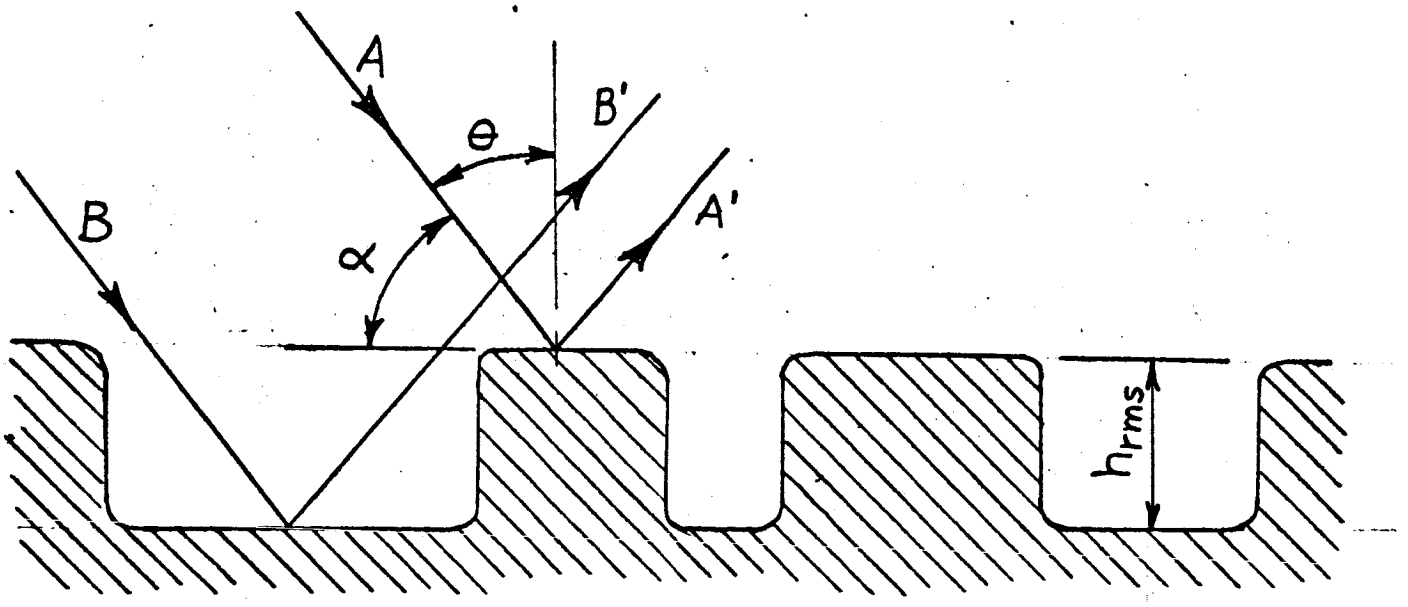

Figure 2. Vertical Cross Section through an Idealized Rough Surface

The distance h_{rms} is taken as the rms value of the vertical dimensions of the surface disturbance. Hence, the rms value of the phase shift between the reflected waves A' and B' is

$$\Delta\phi_{rms} = \frac{4\pi h_{rms}}{\lambda} \sin \alpha \qquad (3)$$

$$= \frac{4\pi h_{rms}}{\lambda} \cos \theta \ ,$$

where α is the grazing angle and θ the angle of incidence. The criterion of $\Delta\phi = \frac{\pi}{2}$ was originally specified as the dividing line between specular and diffuse reflection. Other values, namely $\frac{\pi}{4}$ and $\frac{\pi}{8}$, have more recently been suggested as more realistic.[2,3] However specular reflection represents the worse condition for this system, so in keeping with a worst case analysis, the critical value is assumed to be $\frac{\pi}{2}$. Hence the condition that the surface behave as a specular scatterer is

$$\frac{h_{rms}}{\lambda} \cos \theta = \frac{h_{rms}}{\lambda} \sin \alpha < \frac{1}{8} \ . \qquad (4)$$

At the longest range, the grazing angle will be less than $\frac{1}{600}$ radian. Hence, with a wavelength of 3.8 feet at 260 Mc, the Rayleigh criterion implies that the surface would behave as a specular, or smooth, scatterer if the vertical dimensions of the surface irregularities were less than 260 feet. This is considerably greater than the antenna heights and therefore does not give a realistic appreciation of the effects of roughness.

It is also necessary to consider the lateral scattering which can occur from irregularities and obstacles in the vicinity of the communications system. A second elementary principle states that the scattering properties of a surface are determined principally by the region of the surface that lies within the first Fresnel Zone.[4] The boundary of the first Fresnel zone is the locus of scattering points for which the difference between direct and reflected ray

paths is one half wavelength. A discussion of this principle is beyond the scope of this analysis. For antenna heights much less than the range, the first Fresnel zone is an ellipse with foci at the transmitting and receiving terminals as shown in Figure 3.

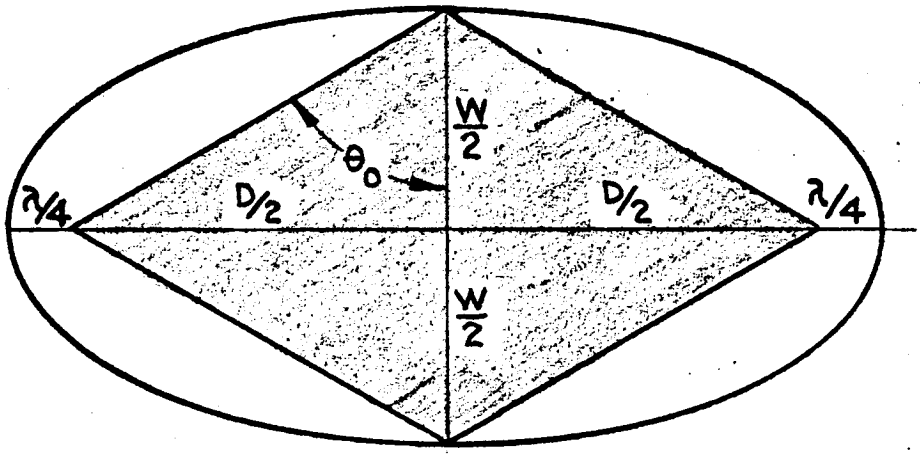

Figure 3. First Fresnel Zone for Low Antennas

The minor axis of the ellipse is given by $W = \sqrt{\lambda D}$ for $\lambda \ll D$, or W = 260 ft. at the maximum range of this system.

This principle thus states that for the surface to behave as a specular scatterer it must be smooth over the first Fresnel zone. This means that for small antenna heights the Rayleigh criterion must be satisfied for all points of reflection within the ellipse of Figure 3, where the angle of incidence, θ_o, is now defined as half of the angle between the direct and reflected rays, and h_{rms} is interpreted as a lateral dimension of the surface irregularities. It can be seen that the shaded area of Figure 3 is about 64% of the total area of the ellipse. Hence, applying the Rayleigh criterion with the "angle of incidence" given by θ_o of Figure 3, will determine reasonable limitations on the lateral dimensions of the surface irregularities.

It can be shown that for $\lambda \ll D$

$$\cos \theta_o \approx \sqrt{\frac{\lambda}{D}}, \qquad (5)$$

and thus with low antennas the Rayleigh criterion for the lateral dimensions of surface irregularities becomes

$$h_{rms} \leq \frac{\sqrt{D\lambda}}{8} = \frac{W}{8} \quad . \tag{6}$$

Thus at 260 Mc if the lateral dimensions of all surface irregularities lying within ± 130 feet of the line of sight are less than about 30 ft., the surface can be considered a specular scatterer. (Note if $\Delta\phi = \frac{\pi}{4}$ or $\Delta\phi = \frac{\pi}{8}$ had been taken as the critical values in the Rayleigh criterion, the critical dimensions would have been 16 ft. and 8 ft., respectively.)

Present information on local statistical characteristics of the lunar surface are limited to interferences from radar astronomy data and photographs taken by Rangers 7 & 8 and the Russian Luna 9. Radar astronomy measurements taken from earth based sites are naturally limited to measuring the average characteristics of relatively large (>> 3 miles) regions of the lunar surface. However, measurements of the frequency dependence of the directional scattering properties of the moon, and measurements of the libration-induced power spectrum of reflected signals have provided semi-quantitative information on the statistical characteristics of the lunar surface irregularities.[4] These measurements indicate that a large percentage of lunar surface irregularities exist either as large undulations with dimensions of at least tens of meters, or as small inhomogeneities smaller than 1 cm. This would be consistent with a model of the lunar surface consisting of large undulations made up of very porous rock or covered with a layer of small particulate matter. This is also consistent with the close-in photographs transmitted from Ranger 8 and Luna 9.

Therefore, with an unobstructed line of sight, and with the geometry characteristic of this system, the assumption of a smooth, specularly reflecting surface is not unrealistic. Furthermore, this assumption is conservative and provides the basis for a worst case multipath analysis.

It will be shown in Sections 2.3.3 and 2.3.4 that even for a surface which is locally smooth in the Rayleigh sense, the presence of long undulations, or variations from planarity, can considerably reduce the amount of multipath loss.

2.3.2 Reflection Coefficient

For a perfectly smooth surface it is necessary to determine the dependence of the reflection coefficient upon the grazing angle and upon the surface material parameters. For vertical polarization at small grazing angles, the amplitude reflection coefficient can be written[3]

$$R_v = \frac{|Y|^2\alpha - \sqrt{|Y|^2 - 1 + \alpha^2/2}}{|Y|^2\alpha + \sqrt{|Y|^2 - 1 + \alpha^2/2}} \quad , \tag{7}$$

where α is the grazing angle and Y is the normalized characteristic admittance of the reflecting medium, given by

$$|Y|^2 = \frac{1}{\epsilon_o}\left(\epsilon - j\frac{\sigma}{\omega}\right) \quad . \tag{8}$$

For dry earth, values of σ range from 10^{-3} to $10^{-4}\,\Omega^{-1}\,M^{-1}$. It is reasonable to expect that the lunar surface is at least as poor a conductor as dry earth, and hence at 260 MHz it can be assumed that $\omega\epsilon \gg \sigma$, i.e., that the lunar surface material consists of a pure dielectric. For $\epsilon/\epsilon_o > 2$ and for grazing angles less than 1^o, equation (7) can be rewritten

$$R = -1 + \frac{2(\epsilon/\epsilon_o)\alpha}{\sqrt{\left(\frac{\epsilon}{\epsilon_o}\right) - 1}} \quad . \tag{9}$$

For multipath calculations it is convenient to rewrite (9) as

$$R = -1 + \beta \quad ,$$

where

$$\beta = \frac{2\left(\frac{\epsilon}{\epsilon_o}\right)\alpha}{\sqrt{\left(\frac{\epsilon}{\epsilon_o}\right) - 1}} \quad . \tag{10}$$

It can be shown that β reaches a minimum for $\frac{\epsilon}{\epsilon_o} = 2$. Also, it is unlikely that the relative dielectric constant of the lunar surface would exceed 10, because of its porous nature, and a value of $\epsilon/\epsilon_o < 5$ would be much more realistic. For the geometry of this system at maximum range, the grazing angle is $\frac{1}{600}$ radian. Thus for $\epsilon/\epsilon_o = 2$, β will be $\frac{1}{150}$ and for $\frac{\epsilon}{\epsilon_o} = 10$, β will be $\frac{1}{90}$. It will be shown in Section 2.3.4 this difference is insignificant and that the intrinsic reflection coefficient can be taken as -1 in the flat surface multipath calculations.

It should be noted that if the surface were a good conductor, the reflection coefficient for vertical polarization would be +1 rather than -1.

2.3.3 System Geometry

In this subsection it is first assumed that the surface is flat, with the effects of the finite lunar radius and surface curvature taken into account later. The geometry pertinent to the multipath analysis for a flat surface is shown in Figure 4.

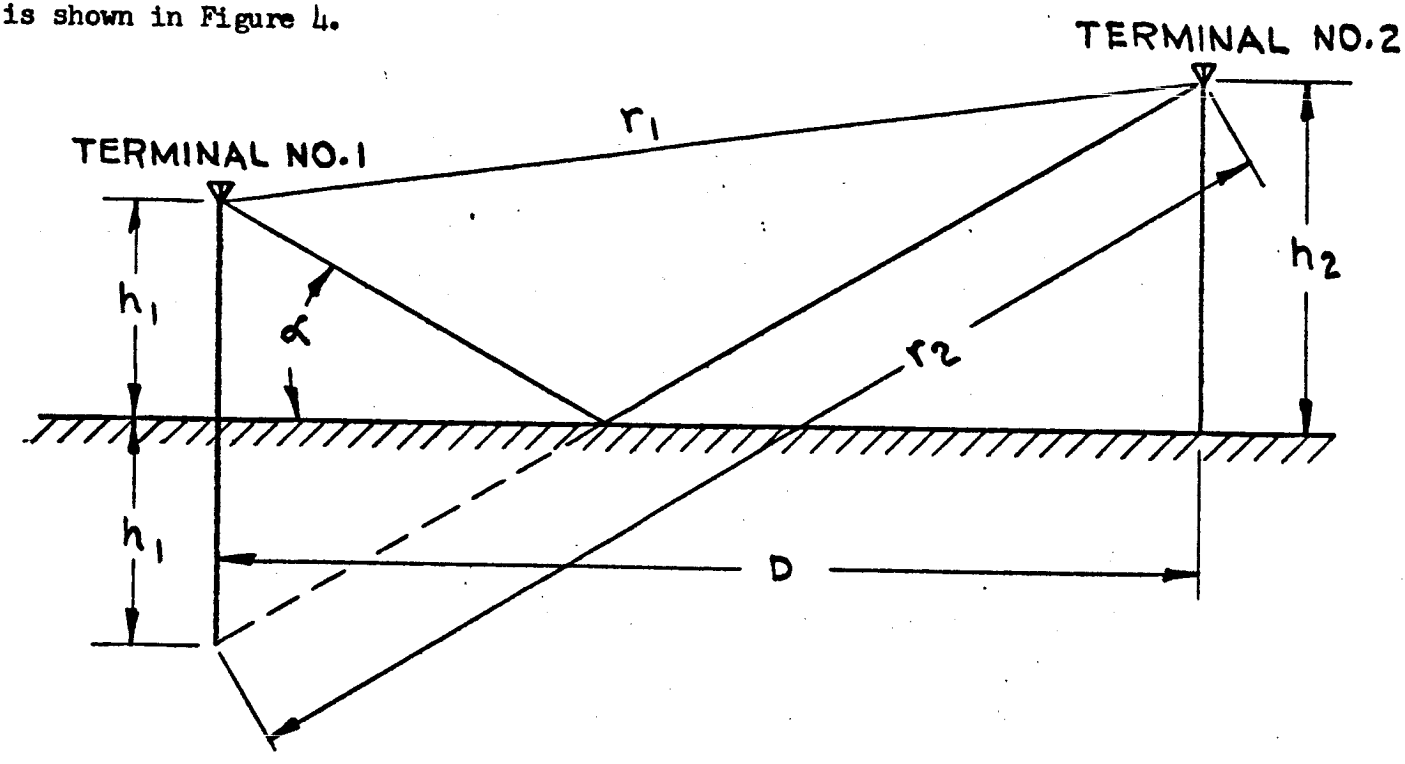

Figure 4. Flat Surface Geometry

The grazing angle is given by

$$\text{Tan } \alpha = \frac{h_1 + h_2}{D} \quad , \tag{11}$$

and the path length difference is

$$\Delta = r_2 - r_1 \simeq \frac{2h_1 h_2}{D} \qquad \text{for } h_1, h_2 \ll D \; . \tag{12}$$

The corresponding phase difference between the two paths is

$$\phi = \frac{4\pi h_1 h_2}{\lambda D} \quad . \tag{13}$$

It is not feasible to conduct a general analysis of the case where long range ($\approx$ D) undulations occur in a specularly reflecting surface. However, an analysis of propagation with a surface curvature corresponding to the lunar radius provides a good example of such effects.

Although a derivation of the geometrical relationships for a curved surface is too involved to present here, several nomographs have been published that permit rapid computation of the significant quantities.[4,5] The principal effect of curvature in this system is to cause divergence of the reflected rays and thus reduce the effective reflection coefficient. The divergence factor gives the reduction of the effective reflection coefficient due to divergence of the scattered rays, i.e.,

$$R_{curved} = dR_{flat}.$$

Curvature also reduces the grazing angle and path length difference.

Taking the lunar radius as 0.273 of the earth's radius, or 5.72×10^6 feet, the following quantities are computed:

Reduction of Grazing Angle: $\alpha_{curved} = 0.44\, \alpha_{flat}$

Reduction of Path Difference: $\Delta_{curved} = 0.17\, \Delta_{flat}$

Divergence Factor: $d = 0.6$

For undulations having a radius of curvature of 2.2×10^7 ft., the divergence factor would be d = 0.9. It will be seen in Section 2.3.4 that the curvature and the attendant divergence lead to considerable reduction of the multipath loss.

2.3.4 Calculation of Multipath Loss

In this section the multipath loss is first calculated for a flat surface and then for a surface with a curvature corresponding to the lunar radius. For specular reflection, the ratio of the total received field strength to the component in the direct ray is

$$\frac{E}{E_o} = 1 + Re^{j\phi}, \tag{14}$$

where R = reflection coefficient

ϕ = phase difference between paths

$$= \frac{2\pi\Delta}{\lambda}$$

where Δ = path length difference.

The power loss is given by

$$\left|\frac{E}{E_o}\right|^2 = 1 + R^2 + 2R\cos\phi. \tag{15}$$

For $\phi \ll 1$ it can be shown that the minimum value of $\left|\frac{E}{E_o}\right|^2$ occurs for

$$R_{min} = -1 + \frac{\phi^2}{2} \tag{16}$$

(i.e., magnitude of the reflection coefficient slightly less than unity), and that the minimum value is

$$\left|\frac{E}{E_o}\right|^2_{min} = \phi^2. \tag{17}$$

If the reflection coefficient does not take on the value given by (16), but is given by

$$R = -1 + \beta, \tag{18}$$

where $\phi \neq \beta \ll 1$, then the loss is approximately

$$\left|\frac{E}{E_o}\right|^2 = \beta^2 + \phi^2. \qquad (19)$$

The multipath power loss will now be calculated for both flat and curved surfaces, and a discussion of the range dependence of the total loss will be given.

a. Flat Surface

At maximum range, D = 18,000 ft. and with h_1 = 6 ft., h_2 = 24 ft., λ = 3.8 ft. at 260 Mc, Equation (13) shows that

$$\phi^2 = 7 \times 10^{-4}.$$

In Section 2.3.2, it was shown that

$$\beta^2_{min} = 0.44 \times 10^{-4} \qquad \text{for } \frac{\epsilon}{\epsilon_o} = 2$$

and

$$\beta^2 = 1.2 \times 10^{-4} \qquad \text{for } \frac{\epsilon}{\epsilon_o} = 10.$$

Hence from Equation (18), the multipath loss in dB is

$$L(dB) = 10 \log_{10} \frac{\epsilon_o}{\epsilon}^2 = 31.3 \text{ dB} \qquad \text{for } \frac{\epsilon}{\epsilon_o} = 2$$

$$= 30.8 \text{ dB} \qquad \text{for } \frac{\epsilon}{\epsilon_o} = 10 .$$

It is seen that variation of the relative dielectric constant of the surface from 2.0 to 10 has little effect on the multipath loss, and a value of 31 dB can be taken as a worst case figure for propagation over a flat surface.

b. Curved Surface

As discussed in Section 2.3.3, if a curvature corresponding to the lunar radius is assumed, the effective reflection coefficient due to divergence is about 0.6, (d = 0.6, R_{eff} = dR). Thus, equation (14) becomes

$$\frac{E}{E_o} = 1 - 0.6 \quad [\text{Cos } \phi + j \text{ Sin } \phi]$$

and for $\phi \ll 1$, the loss is

$$\frac{E}{E_o}^2 = (1 - 0.6)^2 = 0.16$$

or the multipath loss is 8 dB.

The value of the divergence factor, d, is based upon the laws of geometrical optics and if the curvature of the earth is sufficient to affect the reflection coefficient to this great a degree, then additional loss due to diffraction by the spherical surface may be significant even though a line of sight exists. However, the diffraction loss for this system will not be more than about 2 dB so that the total of the multipath loss and the diffraction will be 8 to 10 dB. Similarly, it can be shown that for undulations having a radius of curvature of 2.2×10^7 ft., the divergence factor would be about 0.9, and the resulting multipath loss would be 20 dB.

It is noteworthy that the tremendous difference in multipath loss between the flat surface and curved surface cases results from a seemingly insignificant deviation of the surface. At a distance of 18,000 feet, the deviation between a flat surface and a curved surface corresponding to the lunar radius is only 28 feet. A deviation of only 4 feet would correspond to a radius of curvature of 2.2×10^7 feet. Furthermore, it should be noted that there can exist many localities where the full surface curvature would not be realized. For example, in the vicinity of a mountain range or crater, the ground could easily rise by as much, or even more than 28 feet in 3 miles, thus cancelling the surface curvature, or even leading to a negative curvature.

The effect of a negative curvature would be to cause convergence of the reflected rays thus increasing the magnitude of effective reflection coefficient

to a value greater than unity. However, it was pointed out above (Equations (16) and (17)) that the maximum multipath loss occurs with the magnitude of the reflection coefficient slightly less than unity, and that the maximum loss in dB is 10 $\text{Log}_{10} \frac{1}{\phi^2}$. Hence, there is no value of curvature, either positive or negative, that will cause the multipath loss to exceed the flat surface value.

c. Range Dependence of Total Loss

The quantity $\left|\frac{E}{E_o}\right|^2$ in equation (19) gives the ratio of total received power to the power that would be received under free space conditions. The total loss, including both multipath and free space loss, for a flat surface, with $\delta = 0$, can be found by combining equations (2), (13), and (19)

$$L_{TOT} = \frac{h_1^2 h_2^2}{D^4} \quad , \tag{20}$$

which is seen to vary inversely with the fourth power of the range, and is independent of frequency. To compensate for the worst case loss of 32 dB, would thus require reduction of the range by 8 dB or a factor of 0.16. Thus, resulting range would be (0.16) (18,000) = 2900 ft. or less than 1/2 mile.

2.4 OBSTACLE DIFFRACTION LOSS

The ground rules for this study state that a clear line of sight shall be maintained between the two terminals. However, to provide a preliminary appreciation of possible obstacle effects, this subsection presents typical examples of knife edge diffraction loss for the frequency and typical ranges of this system. The geometry to be considered is shown in Figure 5.

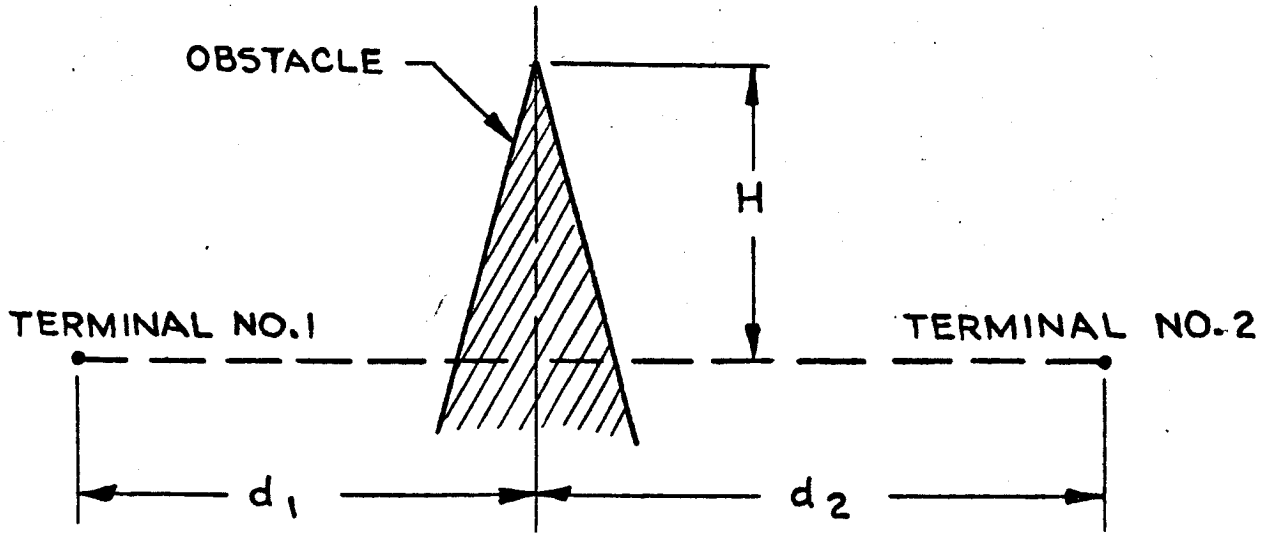

Figure 5. Obstacle Diffraction Geometry

H is the height of the obstacle above the line connecting the terminals. The obstacle diffraction loss and total of the obstacle loss plus free space path loss is shown in Figures 6 and 7 for the special case of equal separations, d_1 and d_2, of the two terminals from the obstacle. The curves are valid only for $d_1, d_2 \gg H$, and therefore should not be relied upon in the regions shown by the dashed lines. Also, the obstacle must be relatively sharp to approximate a knife edge. These curves also neglect possible multipath loss due to reflections between the obstacle and either terminal. Of course it is unlikely that flat surface conditions would prevail in the vicinity of a large obstacle, and therefore, multipath should account for more than 10 dB additional loss.

Obviously, it is not possible to give a systematic treatment of diffraction loss for all possible combinations of terminal to obstacle distances, or for various combinations of multiple obstacles, and such cases must be treated individually.

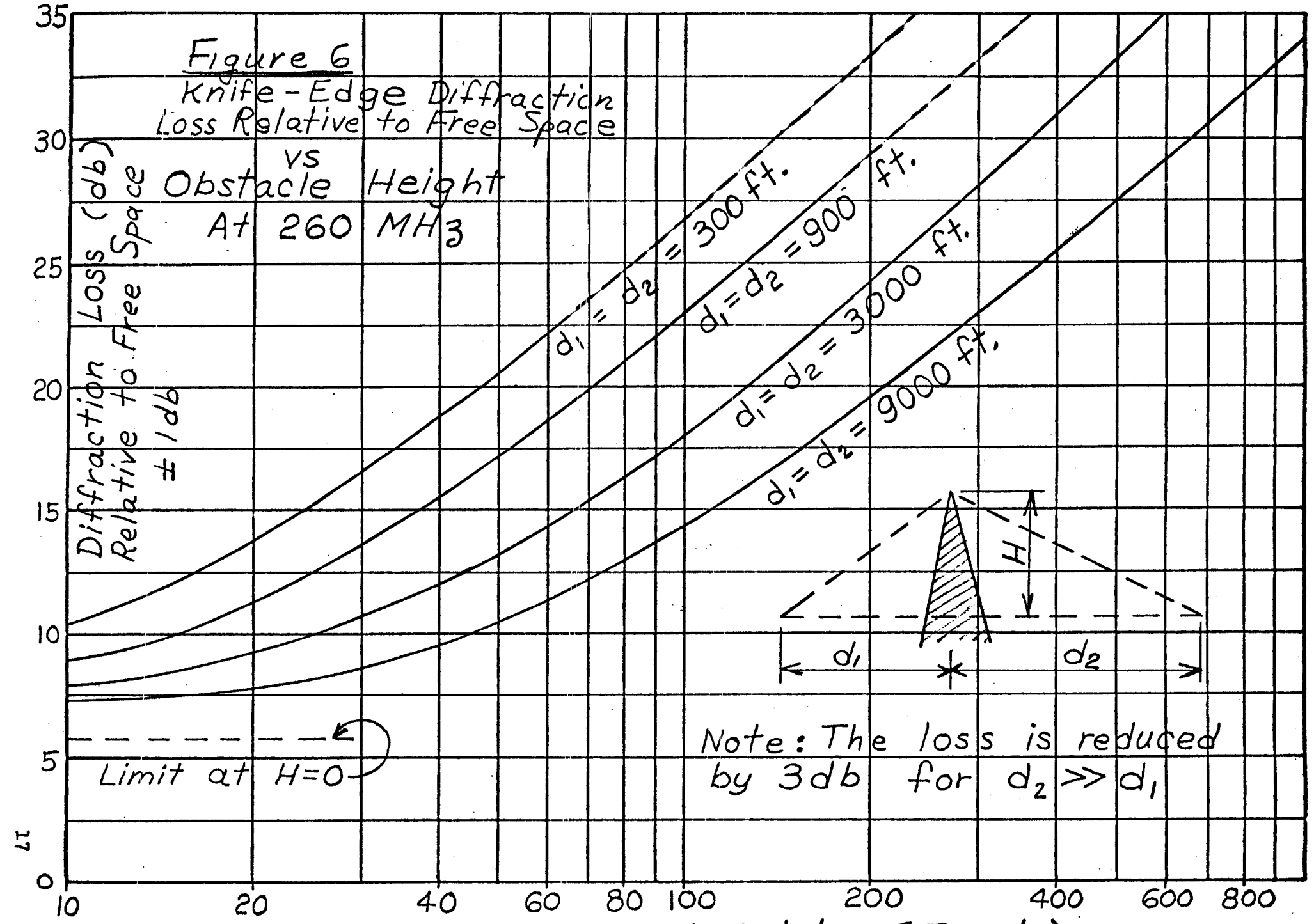

Fig. 6

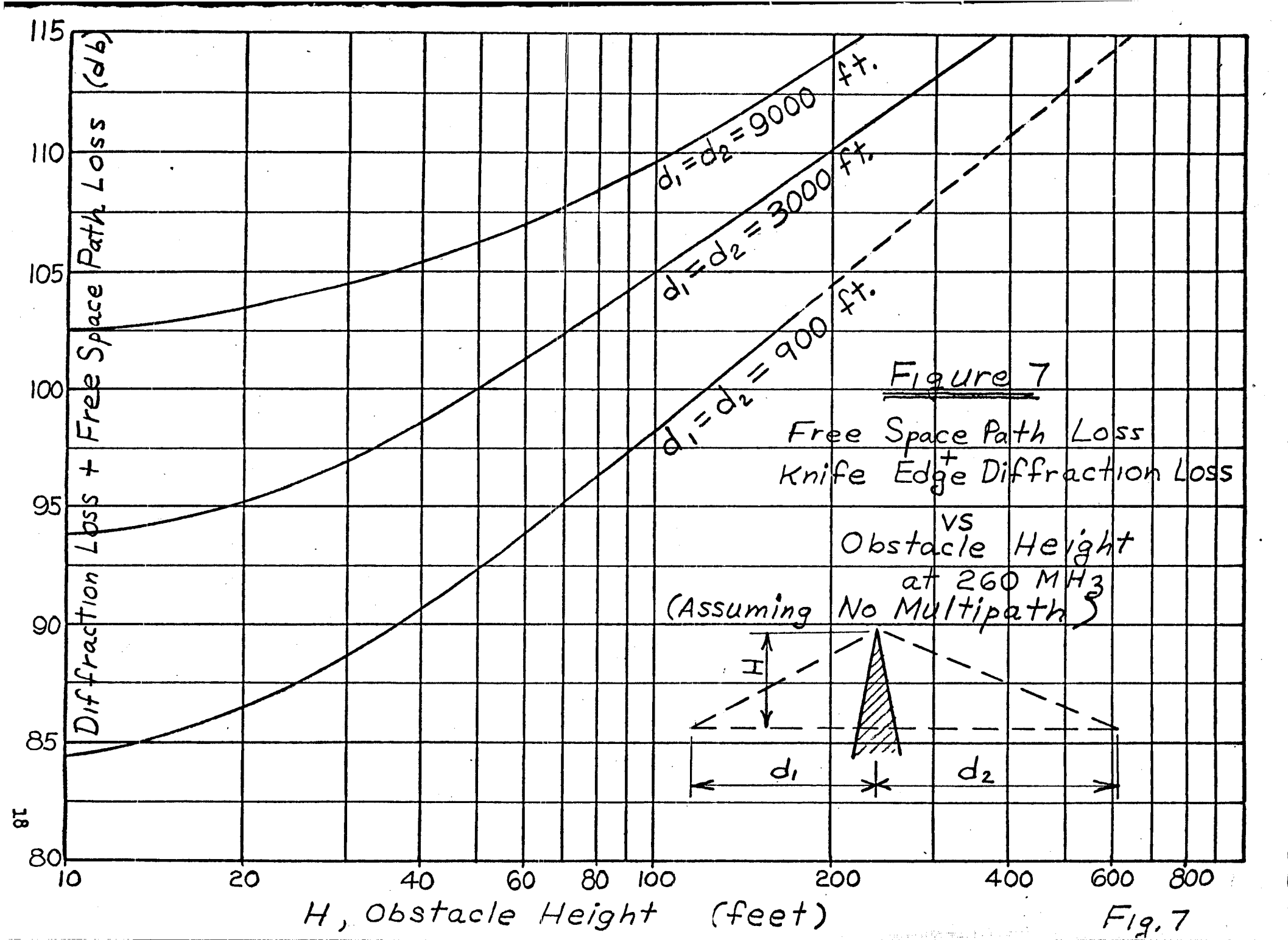
115
110
105
100
95
90
85
80
Diffraction Loss + Free Space Path Loss (dB)
$d_1 = d_2 = 9000$ ft.
$d_1 = d_2 = 3000$ ft.
$d_1 = d_2 = 900$ ft.
Figure 7
Free Space Path Loss + Knife Edge Diffraction Loss vs Obstacle Height at 260 MHz
(Assuming No Multipath)
H
d_1
d_2
10
20
40
60
80
100
200
400
600
800
H, Obstacle Height (feet)

Fig. 7

2.5 POLARIZATION LOSS

Assuming that the LEM antenna is vertical, the loss due to misorientation of the astronaut antenna is given by

$$L_{pol}\ (dB) = 20\ Log_{10} \frac{1}{Cos\ \gamma}\ , \qquad (21)$$

where γ is the tilt angle of the astronaut antenna away from vertical. Hence for a 45° tilt the loss is 3 dB, etc.

Since the reflection coefficient of the lunar surface is approximately -1 for both vertical and horizontal polarization, the multipath loss will be practically unaffected by antenna misalignment.

3.0 SUMMARY AND RECOMMENDATIONS

This memorandum has pointed out that the dominant effect of the lunar surface on line-of-sight propagation in the Astronaut-LEM communications system will be multipath loss due to interference between the directly transmitted ray and reflections from the lunar surface. Detail data on lunar rf surface characteristics is presently not available. However, for the frequencies and geometry involved in this system, it is very likely that the lunar surface will behave as a specular, or electrically smooth scatterer, particularly if a relatively level, unbroken plain is chosen as the landing site.

On this basis, the worst case multipath loss would occur for a perfectly flat surface and would amount to approximately 31 dB. However, the presence of relatively gradual, long range undulations, comparable for example with the mean spherical curvature of the lunar surface, will cause divergence of the reflected waves, with a corresponding change of the effective surface reflection coefficient, resulting in a significant reduction of the multipath loss.

If the surface in the vicinity of the communications link were to appear rough for the geometry and frequencies of interest, the multipath

interference pattern would be "randomized." In this case, 30 dB nulls would occur with very low ($< 5 \times 10^{-4}$) probability and with very small spatial extent, while 10 dB nulls would occur with probability of about 5%. However, rough surface, or diffuse, scattering would be realized only if a statistically large number of surface irregularities were present with rms dimensions on the order of tens of feet, or if antenna heights of hundreds of feet were employed, and such conditions cannot be realistically assumed for this system.

Assuming then, that the surface behaves as a specular reflector, the following values are obtained for the free space and multipath loss of this system at 260 MHz and a range of 18,000 feet:

Free Space Path Loss: $\frac{\lambda^2}{16\pi^2 D^2}$: 96 dB

Flat Surface Multipath Loss (Worst Case) $\frac{16\pi^2 h_1 h_2}{\lambda^2 D^2}$: 31 dB

Curved Surface Multipath Loss, Radius of Curvature $= 5.7 \times 10^6$ ft. (Lunar Radius) (28 ft. deviation from flat surface) : 8-10 dB

Curved Surface Multipath Loss, Radius of Curvature $= 2.2 \times 10^7$ ft. (4 ft. deviation from flat surface) : 20 dB

Since the occurrence of a surface which is perfectly flat, i.e., within 4 ft. or 28 ft., would be a rather rare topographical phenomenon, the 32 dB multipath loss figure should be considered as representative of a case which is definitely worst. It appears that a more realistic value of the multipath loss margin would be 10 to 15 dB.

The total path loss, including both free space and multipath loss, increases approximately as the fourth (4th) power of the range. Thus, if a multipath loss

of 12 dB is assumed for the maximum range of 18,000 feet, it would be necessary to reduce the range by 3 dB, or a factor of two, in order to compensate for the multipath loss.

In order to provide a preliminary appreciation of tolerable limitations on the effects of intervening obstacles, such as ridges or crater rims, data on knife edge diffraction loss has been presented for a few realistic values of the system geometry. Specific cases, involving other geometries or multiple obstacles, would require individual treatment.

Because of the limited extent of this study, it has been necessary to assume a rather idealized model of the surface scattering process. This has involved simplifying assumptions with regard to both the electrical and topographical characteristics of the lunar surface. However, it is seen that the assumptions regarding the electrical parameters are not nearly so critical nor restrictive as those of the topographical features. Therefore, even if no further data on the lunar rf surface characteristics were to become available, consideration should be given to the possibility of refining the propagation loss calculations by taking topographical details into account. Such an investigation could follow two approaches: one directed toward obtaining statistical characteristics of the multipath loss, based upon the statistical characteristics of the topography, and the other directed toward deriving specific loss figures for individual propagation paths with specified topographical parameters. The latter approach would require data on elevation deviations accurate to within about ± 5 ft. or ± 10 ft. Thus, if only inaccurate topographical data were available from such sources as astronomical, Ranger or Lunar Orbiter photographs, this investigation would be limited to the former approach.

REFERENCES

1. Jasik, H., "Antenna Engineering Handbook," McGraw-Hill Book Co., Inc, (1961). Ch. 33.

2. Norton, K. A. and Omberg, A.C., "Maximum Range of a Radar Set," Proc. IRE 45, 4 (1947).

3. Kerr, D.E., "The Propagation of Short Radio Waves," MIT Rad. Lab. Series #13, McGraw Hill, New York (1951).

4. Beckman, P. and Spizzichino, Andre', "The Scattering of Electromagnetic Waves From Rough Surfaces," The MacMillan Co., New York (1963).

5. Summary Tech. Rept. of the Committee on Propagation, NDRC, Vol. 3, "The Propagation of Radio Waves Through the Standard Atmosphere," (1946).